DEVELOPMENT OF A DUAL POLYMER HYDRAULIC FRACTURING FLUID

A Dissertation

by

TARIQ ABDULSATTAR A ALMUBARAK

Submitted to the Graduate and Professional School of
Texas A&M University
in partial fulfillment of the requirements for the degree of

DOCTOR OF PHILOSOPHY

Chair of Committee,	Nobuo Morita
Committee Members,	Hadi Nasrabadi
	Jerome Schubert
	Mahmoud El-Halwagi
Head of Department,	Jeff Spath

December 2020

Major Subject: Petroleum Engineering

ABSTRACT

As exploration for oil and gas continues, it becomes necessary to produce from deeper formations that have low permeability and higher temperature. Unconventional shale formations utilize slickwater fracturing fluids due to the shale's unique geomechanical properties. On the other hand, conventional formations require crosslinked fracturing fluids to properly enhance productivity.

Guar and its derivatives have a history of success in crosslinked hydraulic fracturing fluids. However, they require higher polymer loading to withstand higher temperature environments. This leads to an increase in mixing time and additive requirements. Most importantly, due to the high polymer loading, they do not break completely and generate residual polymer fragments that can plug the formation and reduce fracture conductivity significantly.

In this work, a new hybrid dual polymer hydraulic fracturing fluid is developed. The fluid will consist of a guar derivative and a polyacrylamide-based synthetic polymer. The polymer mixture solutions is prepared at a total polymer concentration of 20 to 40 lb/1,000 gal and at a volume ratio of 2:1, 1:1, and 1:2. The fluids are crosslinked with a metallic crosslinker and broken with an oxidizer at temperatures up to 400°F. Testing focuses on crosslinker to polymer ratio analysis to effectively lower loading while maintaining sufficient performance to carry proppant at this temperature. HP/HT rheometer will also be used to measure viscosity, storage modulus, and fluid breaking performance. HP/HT aging cell and HP/HT see-through cell will be utilized for proppant

settling. FTIR, Cryo-SEM, and HP/HT rheometer will also be utilized to understand the polymer interactions.

Results indicate that this new system is easily hydrated, requires fewer additives, can be mixed on the fly, and maintains excellent rheological performance at low polymer loadings.

Extensive experiments are conducted to evaluate the new dual polymer system. This system exhibits a positive interaction between polysaccharide and polyacrylamide families and generates excellent rheological properties. The major benefit of using a mixed polymer system is to reduce polymer loading. Lower loading is highly desirable because it reduces material cost, eases mixing and fluid preparation during the field operation, and potentially lowers damage to the fracture face, proppant pack, and formation.

DEDICATION

This work is dedicated to my parents, sisters, brother, friends, loved ones, and my late advisor Dr. Hisham Nasr-El-Din -may god have mercy on his soul.

ACKNOWLEDGEMENTS

I would like to thank my committee chair, Dr. Morita for accepting me and welcoming me to his research group. I would also like to thank my committee members, Dr. El-Halwagi, Dr. Nasrabadi, and Dr. Schubert for their continuous support.

Sincere thanks and appreciation go to my late advisor Dr. Hisham Nasr-El-Din. He gave me freedom to conduct research that I am most passionate about, it is through his support and guidance that I became the person I am today. May Allah bless his soul and award him the highest level of heaven.

None of this would be possible without the support of my family and friends. I would like to thank my parents, my sisters Sama and Yara, and my brother Majed for their endless love and patience with me. Special thanks go to Jun Hong Ng, Majid Rafie, Khalid Aldhayee, and Kenta Nakajima for their encouragement throughout the years.

CONTRIBUTORS AND FUNDING SOURCES

This project was supervised by a dissertation committee consisting of Dr. Nobuo Morita, Dr. Hadi Nasrabadi, and Dr. Jerome Schubert of the Department of Petroleum Engineering Department and Dr. Mahmoud El-Halwagi of the Department of Chemical Engineering Department.

Jun Hong Ng helped with monitoring some of the experiments. All other work for the thesis was completed by the student independently.

There are no outside funding contributions to acknowledge related to the research and compilation of this document.

NOMENCLATURE

#	lb/1,000 gal
AA	Acrylic acid
AM	Acrylamide
AMPS	2-Acrylamido-2-methylpropane sulfonic acid
ATMP	aminotrimethylenephosphonic acid
Bpm	barrels per minute
$CdSO_4$	Cadmium sulfate
CFA	closure fracture acidizing
CMHPG	Carboxymethyl hydroxypropyl guar
CON	conventional formation
DI	Distilled water
DTPMP	diethylenetriaminepentamethylenephosphonic acid
DW	distilled water
EDS	energy dispersive X-ray spectrometry
EDS	Energy dispersive x-ray spectroscopy
EDTMP	ethylenediaminetetramethylenephosphonic acid
ESEM	Environmentally scanning electron microscope.
FB	formation brine
FeS	Iron sulfide
G’	Elastic/storage modulus

G’’	Viscous/loss modulus
GPC	Gel permeation chromatography
gpt	Gallons per thousand gallons
H_2S	Hydrogen sulfide
HEDP	1-hydroxyethane-1,1-diphosphonic acid
HMDTMP	hexamethylenediaminetetramethylenephosphonic acid
HMP	hexametaphosphate
HPG	Hydroxypropyl guar.
HT/HP	High-temperature/high-pressure
MBI	Monoborate ions
MIC	minimum inhibition concentration
MMSCFD	million standard cubic feet per day
Mp	Peak molecular weight
MW	Molecular weight
PAA	polyacrylic acid
PBTCA	2-phosphonobutane-1,2,4-tricarboxylic acid
PDI	Polydispersity index
pKa	Acidity constant/ acid ionization constant
PMA	polymaleic acid
PPCA	polyphosphinocarboxylic acid
ppg	pounds per gal
ppm	Parts per million

ppt/pptg	pounds per thousand gallons
PSC1	Polymeric clay stabilizer 1
PSC2	Polymeric clay stabilizer 2
PV	pore volume
QA/QC	quality assurance/quality control
Room temperature	77°F.
SI	scale inhibitor
SW	seawater
TDS	Total dissolved solid
UNC 1	Permeability: < 0.2 md, Porosity: 4-10%
UNC 2	Permeability: < 2 md, Porosity: 7-15%
UNC 3	Permeability: < 0.1 md, Porosity: 8-10%
UNC	Unconventional formation
USGS	United States Geological Survey
XRD	X-ray diffraction
Zr-La	Zirconium lactate
Zr-La-PG	Zirconium lactate and propylene glycol
Zr-La-TEA	Zirconium lactate and triethanol amine
Zr-TEA-La	Zirconium triethanol amine and lactate

TABLE OF CONTENTS

Page

LIST OF FIGURES

Page

LIST OF TABLES

Page

1. INTRODUCTION

The goal of this dissertation is to develop solutions to current industry problems associated with crosslinked hydraulic fracturing fluid treatments. The industry problems revolve around issues related to high polymer loading, high concentration of additives used, high temperature stability, and high salt tolerance.

This dissertation consists of five research studies from Chapter 2 to Chapter 6. Although they are related to each other, each of them has a specific objective that requires them to be independently described in separate chapters.

Chapter 1 – Introduction of overall research objectives.

Chapter 2 – Dual Polymer Hydraulic Fracturing Fluids: A Synergy Between Polysaccharides and Polyacrylamides: This chapter covers aspects regarding the development of a new dual polymer hydraulic fracturing fluid that can be used at high temperature with a significantly lower loading.

Chapter 3 – New Insights into Hydraulic Fracturing Fluids used for High-Temperature Wells: This chapter evaluates different high temperature stabilizers used in hydraulic fracturing fluids and proposes combinations to generate a fluid that is stable up to 400°F at low polymer loading.

Chapter 4 – Zirconium Crosslinkers: Understanding Performance Variations in Crosslinked Fracturing Fluids: This chapter studies different compositions of zirconium crosslinkers used during hydraulic fracturing applications and proposes choices to improve the temperature and shear tolerance limits.

Chapter 5 – Insights on Potential Formation Damage Mechanisms Associated with the use of Gel Breakers in Hydraulic Fracturing: This chapter studies the interactions between gelling polymers and breakers used in hydraulic fracturing fluids, evaluates the residual polymer fragments, and studies the interactions between the breakers and other polymeric fracturing fluid additives.

Chapter 6 – Design and Application of High-Temperature Raw Seawater-Based Fracturing Fluid: This chapter shows the process of successfully developing a salt tolerant fracturing fluid for high temperature conditions and upscaling it from lab testing conditions to field application.

2. DUAL POLYMER HYDRAULIC FRACTURING FLUIDS: A SYNERGY BETWEEN POLYSACCHARIDES AND POLYACRYLAMIDES*

2.1. Introduction

The Hugoton gas field was the first application of a hydraulic fracturing treatment to stimulate and enhance well productivity. Since then fracturing techniques and additives have evolved significantly. To conduct a successful hydraulic fracturing treatment, fluids are pumped higher than fracture pressure to initiate the fracture, following that, pumping is maintained above fracture closure pressure, and the fluid's rheological characteristics must enable proppant transport inside the fracture (Gidley et al. 1989, Constien et al. 2000, Harris et al. 2005; Loveless et al. 2011).

At the end of the hydraulic fracturing treatment, it is necessary to break the polymer solution to reduce formation damage and allow maximum flow back of the pumped fluids. This can be achieved using breakers such as oxidizers, acids, or enzymes. Effective oxidizers include ammonium persulfate, sodium bromate, and sodium hypochlorite (Funkhouser and Norman 2003; Almubarak et al. 2015).

These oxidizers break polymers by cleaving the polymer acetyl linkage or the crosslinking bond (Economides and Nolte 2000). Persulfates are used at low temperature (< 250°F), and bromate oxidizers are used at higher temperatures (> 250°F) (Gall and Raible 1985; Al-Muntasheri 2014).

*Part of this chapter is modified with permission from "Dual Polymer Hydraulic Fracturing Fluids: A Synergy between Polysaccharides and Polyacrylamides" by Almubarak, T., Ng, J., Nasr-El-Din, H.A. et al. 2019. SPE J **24** (6): 2635-2652. Copyright 2019 by Society of Petroleum Engineers.

Polymers are the main additive in fracturing fluids, and they can be divided into two main types: biopolymers and synthetic polymers. Guar is the most common biopolymer used. However, it falls short regarding thermal stability and produces significant polymer residue, thus, reduces productivity. At harsher conditions, higher polymer loading is typically used, and the influence of the impurities becomes significant. To resolve these issues, guar is typically processed to biopolymers that can withstand higher temperatures and produce less residue; namely HPG (hydroxypropyl guar) and CMHPG (carboxymethyl hydroxypropyl guar) (Lei and Clark 2007; Guo et al. 2012).

There have been many efforts in the industry to reduce polymer loading used in fracturing fluids. Legemah et al. (2015) showed a CMC based system crosslinked with a Zr-crosslinker at 30 lb/1,000 gal and 200°F. Malik et al. (2013) tested fracturing fluids incorporating CMHPG and Zr-based crosslinkers at an optimum pH of 10.2. The lowest polymer loading they achieved was 35 lb/1,000 gal at 250°F. Legemah et al. (2014) stated that by increasing the length of crosslinkers, polymers could be used at a concentration below their critical overlap concentration, C* (Lei and Clark 2007). Loveless et al. (2014) developed a polymeric multifunctional boronic acid crosslinker to crosslink guar below its C*. The crosslinker was capable of generating the same viscosity as a conventional borate-guar fluid system while using 30-50% less guar loading. Also, a new class of boron crosslinkers was developed which reduced the guar polymer loading typically needed. However, these systems were limited to temperatures < 250°F (Williams et al. 2012). Polyaminoborates were developed as an efficient crosslinker to form multiple bonds with polymers at 25 lb/1,000 gal, and the results showed that the viscosity using these new

crosslinkers is higher than its conventional counterpart. The reason for the viscosity improvement was attributed to the large size of the crosslinker as well as the higher number of available crosslinker cites to form bonds with guar chains (Sun and Qu 2011). Holtsclaw et al. (2017) introduced a multifunctional crosslinker (MXL) to crosslink 10 lb/1,000 gal HPG polymers for applications below 200°F. Unlike previous reports that showed a loss of almost 90% of borate crosslinked fluid viscosity at 10,000 psi (Parris et al. 2008), the HPG/MXL system only lost 25% of its viscosity at these high pressures.

Recently, nanoparticles have been utilized to decrease polymer loading and increase the thermal stability of fracturing fluids. For instance, a synthetic polymer-based fracturing fluid was improved with the use of silica-based/amine-functionalized nanocrosslinkers (Liang et al. 2017). Wang et al. (2017) developed nano-borate-crosslinkers (NBC) through a two-step surface modification approach. They crosslinked 30 lb/1,000 gal HPG through NBC and the maximum temperature tested was 212°F. The authors showed that pH had a significant effect on rheological properties of crosslinked HPG with NBC through its impact on dispersion characteristics and the concentration of borate ions, and the best performance regarding thermal stability and sand carrying capacity was observed at pH 10.

Moreover, research has been conducted toward synergy applications to address challenges existing in the industry. Yang et al. (2016) showed synergetic behavior between associative polymers and VES, and they were able to improve thermal stability, conductivity, and differential pressure through this mixture. Huang (2015), Simeoni (2016), and Habibpour and Clark (2017) studied the friction reduction properties of both

hydrolyzed polyacrylamides and xanthan gum and proposed the use of hydrolyzed polyacrylamide/xanthan gum and polyacrylamide/carboxymethylcellulose (CMC) as friction reducers. Haque et al. (2012) introduced a double network gel using poly-2-acrylamido-2-methylpropane sulfonic acid (PAMPS) and polyacrylamide (PAAm).

Synergistic rheological improvements were mentioned throughout the literature between PHPA and chitosan (a biopolymer), CMHPG and anionic surfactant, guar and non-acetylated xanthan gum, locust bean gum and xanthan gum, xanthan gum and HPG, guar and polyacrylamide, polyethylene oxide and sulfonated surfactant, polyacrylamide and xanthan gum, and xanthan gum and konjac glucomannan (Pettitt 1970; Hornof et al. 1983; Clark et al. 1985; Copetti et al. 1997; Fischer et al. 2001; Paradossi et al. 2002; Vidal et al. 2005; Khouryieh 2006; Agoub et al. 2007; Alquraishi and Alsewailem 2011; Das et al. 2017; Cai et al. 2017).

To target higher temperature applications, there is a need for cleaner fracturing fluids with acceptable rheological properties. This work introduces the rheological synergy between biopolymers and synthetic polymers and their use in fracturing fluids. The tests discuss the synergetic interactions between CMHPG and polyacrylamide showing the improvements in rheological performance compared to the individual polymers and its capability to transport proppant effectively.

2.2. Experimental Procedures

2.2.1. Materials

The synthetic polymer used is in an emulsion form (30 wt% active) and is composed of acrylamide (AM), acrylic acid (AA), and 2-acrylamido-2-methylpropane

sulfonic acid (AMPS), **Fig. 2-1**. Sodium bromate breaker, CMHPG, and zirconium lactate and propylene glycol crosslinker (5.7 wt% ZrO_2) were provided by a service company and were used as received. Tetraethylenepentamine (TEPA) and acetic acid were provided at 99 wt% and used as received. Houston tap water (< 500 ppm) was used to prepare all the systems.

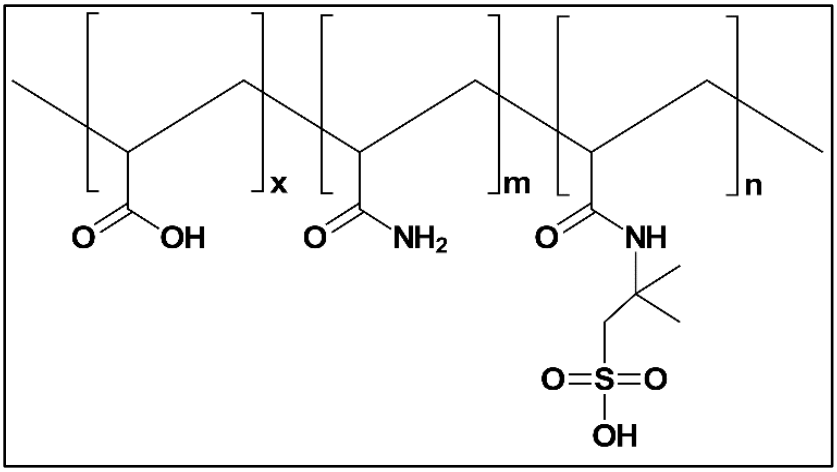

Fig. 2-1 Synthetic polymer chemical structure (AA-AM-AMPS).

2.2.2. Mixing Procedure

The fluids were prepared and mixed the same day, for that reason no biocide was used. Also, no surfactants, HT stabilizers, or crosslinking delay agents were used. This was to enable direct evaluation of the polymer to polymer interactions in the mixture without the influence of the additives.

A solution of 20 lb/1,000 gal synthetic polymer was prepared by adding 3.2 $cm^3$of the synthetic polymer to 400 cm^3 of tap water (8 gpt) in a Waring blender under rapid agitation (800+ RPM) for 15 s. Subsequently, the mixer speed was reduced to 200-400 RPM to generate a vortex and mixed for 15 minutes. 20 lb/1,000 gal CMHPG base gel

was prepared by adding 1.92 g of polymer to 800 cm^3 of tap water in a Waring blender maintaining a visible vortex for 15 minutes (200-800 RPM).

To prepare the 20 lb/1,000 gal dual polymer fluid, a total of 250 cm^3 of the hydrated polymer fluids were measured using a graduated cylinder at 1:1, 1:2, and 2:1 (volume ratio of CMHPG: Synthetic to maintain the same final total polymer loading). They were transferred to the blender and mixed at a low shear (200-400 RPM) for 5 minutes. The pH of the solution was then adjusted by adding an appropriate amount of TEPA for the pH 10 tests, and acetic acid for the pH 5 tests. The sodium bromate breaker was then added as required at this stage for the breaker related tests. Crosslinker was added last and mixed thoroughly for 30 s. The 30 and 40 lb/1,000 gal dual polymer fluids were prepared in a similar manner.

2.2.3. HP/HT Rheometer

HP/HT rheometer was used to measure the apparent viscosity of the fracturing fluids at 300°F. The rheometer utilized R1/B5 bob and rotor combinations, which required a sample volume of 52 cm^3. The rheometer had an electric jacket for heating; a temperature sensor was mounted on the stator/bob to control sample temperature. A pressure of 350-500 psi was applied with nitrogen gas to prevent boiling of the sample.

Viscosity measurements were performed under different shear rates to simulate the flow of the fracturing fluid through production tubular, perforations, and inside the created fracture. ISO13503-1 was followed, where the shear rate schedule was set to 100 s^{-1} with short shear ramp spikes between 25 and 100 s^{-1}. The heater temperature was preheated to

150°F before running the tests. This was done to ensure quick and consistent heating profiles. The fluid took 10-15 minutes to reach the testing temperature.

The dynamic viscoelastic properties of the fluid were measured using a hollow B5 bob in an oscillatory testing mode. Samples of 60 cm^3 were used in these tests. Amplitude and strain sweeps were conducted, and both values were determined to be appropriate at 5% to remain in the linear viscoelastic regime. The samples were pressurized and preheated for 1 hour at 300°F before testing to ensure full crosslinking. Storage modulus measurements were conducted at 300°F and 350-500 psi. The schedule included a frequency sweep from 1-5 Hz. No higher frequencies were tested because the concern with proppant settling was limited to static or low-frequency conditions when the pumping rate cannot assist in proppant transport.

2.2.4. HP/HT Aging Cell

Fracture fluid pre-heating to crosslinking conditions was conducted in the HP/HT aging cell. Each sample was prepared following the mixing procedure and was placed in 200 cm^3 glass bottles in the HP/HT aging cell. Glass bottles were used to prevent direct contact with metal in the aging cell. The aging cell was pressurized to 500 psi using nitrogen and heated to 200°F in an oven for 1 hour to crosslink the fluid samples.

2.2.5. HP/HT See-Through Cell

After heating and crosslinking the samples in the aging cell, the samples were removed and tilted to ensure the formation of a lip. Following that, 100 cm^3 of the sample was transferred to a graduated cylinder, and 4 ppg of 40/70 Ottawa sand was thoroughly stirred and mixed in the sample. The cylinder was then transferred into the HP/HT see-

through cell. The cell was pressurized to 500 psi using nitrogen, heated to 300°F, and observed for 2 hours. A similar procedure was conducted in a graduated cylinder at room temperature (77°F). Data was recorded at the end of the test to show the proppant suspension level at both room temperature and HP/HT conditions.

2.2.6. FTIR

Solutions of the individual polymers, as well as the mixture of CMHPG and synthetic polymers, were freeze-dried. The samples were frozen at -80°C for 2 days and dried under vacuum for 4 days to ensure the extraction of all water to acquire more accurate spectra. The freeze-dried samples were crushed into powder for FTIR analysis. IR spectra of the samples were recorded using a VARIAN FTS-800 FTIR spectrometer utilizing an ATR setup. The significance of this test is to study the interactions between the polymers.

2.2.7. Cryo-SEM

Samples of the individual and dual polymer crosslinked fracturing fluid were prepared. Each of the samples was transferred to a TEM grid using a syringe. An ethane bath was prepared by cooling it with liquid nitrogen to the freezing point (-188°C). As soon as the ethane started to melt the TEM grid samples were blotted and plunge frozen for 30 s (Thompson et al. 2016). Samples were then immediately transferred to the cryo-SEM stage immersed in liquid nitrogen. Following the successful freezing of 3-4 TEM grids, the cryo-SEM stage was covered with an aluminum foil to prevent contact with air and minimize frosting of the sample. After that, they were transferred within seconds to the etching/fracturing station using a container filled with liquid nitrogen. The samples

were then vacuumed, and the temperature was adjusted to -100°C to sublimate the outer surface. Following the sublimation, the temperature was reduced to -150°C and coated with platinum. Finally, the samples were transferred to the cryo-SEM under vacuum where images were taken.

2.3. Results

2.3.1. Hydration and Dual Polymer Ratios

Polymer solutions were prepared at concentrations of 20, 30 and 40 lb/1,000 gal to evaluate polymer hydration time. If the polymers do not hydrate fast enough, the fluids will not meet the expected viscosity and can cause delays in treatments. **Fig. 2-2** shows that both CMHPG and synthetic polymer achieve full hydration within 5 minutes.

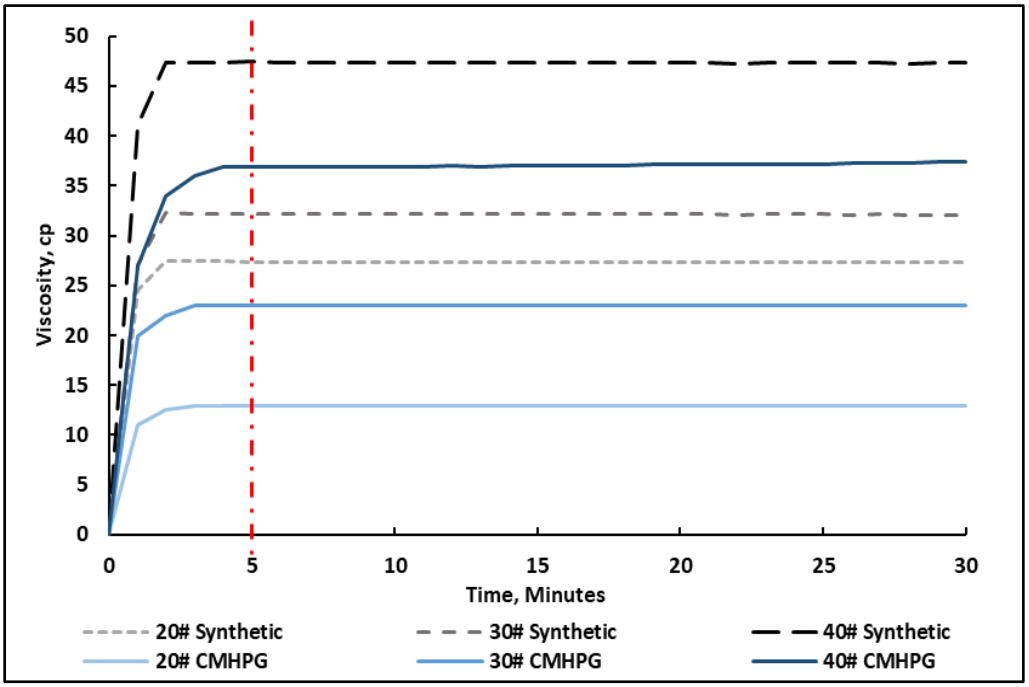

Fig. 2-2 Viscosity of 20, 30 and 40 lb/1,000 gal CMHPG and synthetic polymer at 300 RPM and 77°F.

Following hydration evaluation, dual polymer linear viscosity is measured. **Fig. 2-3** shows 40 lb/1,000 gal hydrated dual polymer solution viscosity at 77°F, at 100 and 300 RPM. The graph illustrates synergy with mixture ratios of 1:2 and 1:1 (CMHPG:Synthetic). The fluids prepared as a dual polymer mixture were able to achieve hydrated viscosities higher than the fluids prepared as an individual polymer system.

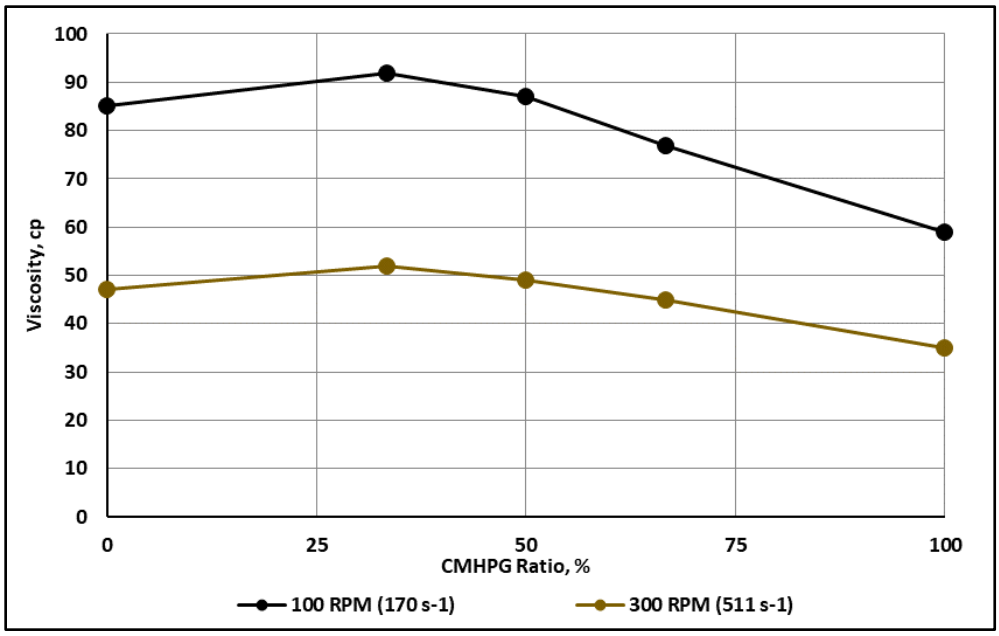

Fig. 2-3 Viscosity of 40 lb/1,000 gal CMHPG/ synthetic hydrated dual polymer fluid at all ratios, 77°F

2.3.2. Crosslinking pH

Each polymer has a proper crosslinking pH that depends on the chemistry of the crosslinker and the structure of the polymer. **Fig. 2-4** shows that CMHPG can crosslink at pH 5, 7, and 10. The results also indicate that CMHPG generates a stable viscosity when crosslinked at pH 10. **Fig. 2-5** shows that the synthetic polymer is unable to generate significant viscosity at a pH of 7 and 10. On the other hand, at a pH of 5, the synthetic polymer can crosslink and exhibits a stable viscosity. For this reason and because pH 5 is

a less damaging pH environment for clays this pH was chosen to develop the fracturing fluid (Gdanski 2001, 2002).

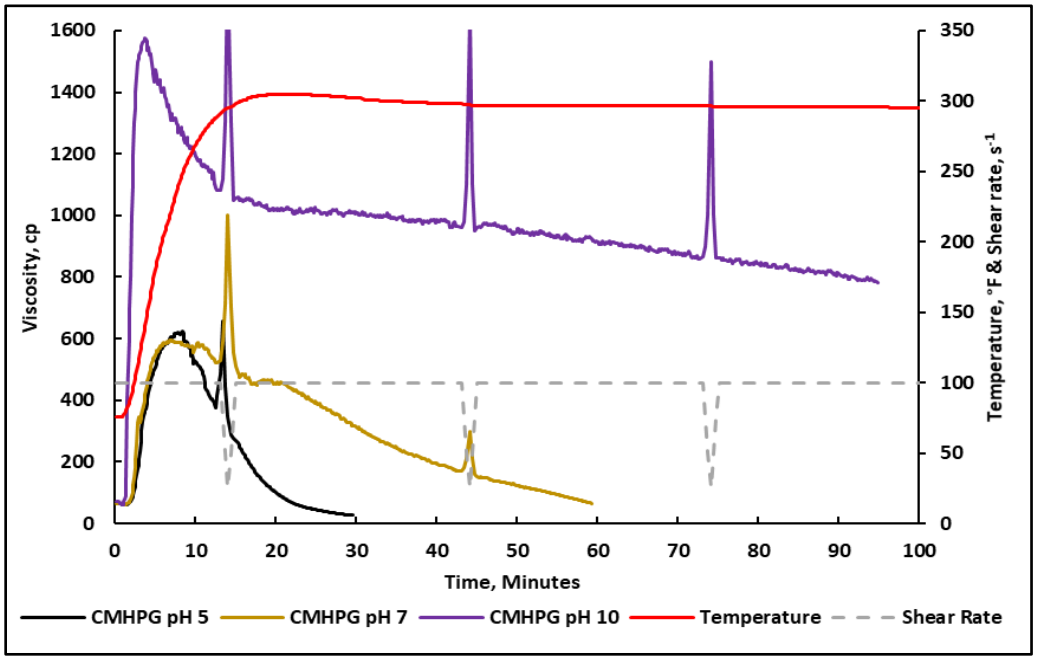

Fig. 2-4 Viscosity at 40 lb/1,000 gal CMHPG, 2 gpt crosslinker, pH 5-10 and 300°F.

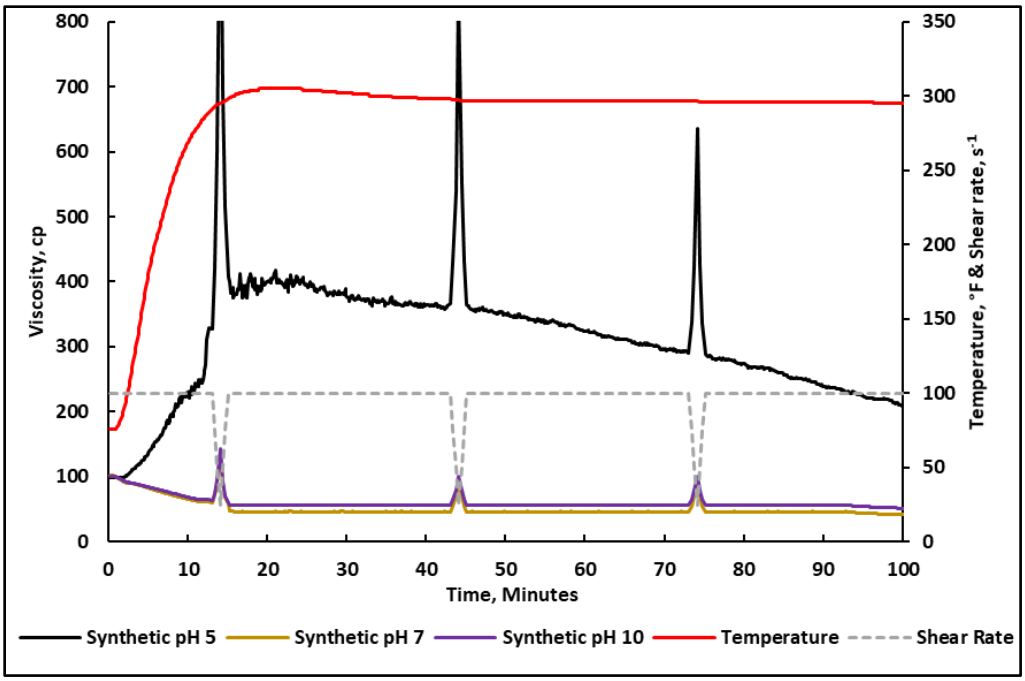

Fig. 2-5 Viscosity at 40 lb/1,000 gal synthetic polymer, 4 gpt crosslinker, pH 5-10 and 300°F.

2.3.3. Performance of Individual Polymer Crosslinking

Crosslinker concentration is studied to determine the concentration at which over-crosslinking occurs for each polymer. **Fig. 2-6** shows the results at 40 lb/1,000 gal CMHPG crosslinked with 1-5 gpt crosslinker. CMHPG crosslinked viscosity improved as the crosslinker concentration increased from 1 to 4 gpt. However, it decreased at 5 gpt. The decrease in viscosity at 5 gpt is due to over-crosslinking the polymer under these conditions. At pH 5 CMHPG is partially deprotonated (Janson 1998; Dogsa et al. 2014; Nová et al. 2017), generating an unstable polymer conformity that can't handle higher crosslinker concentrations.

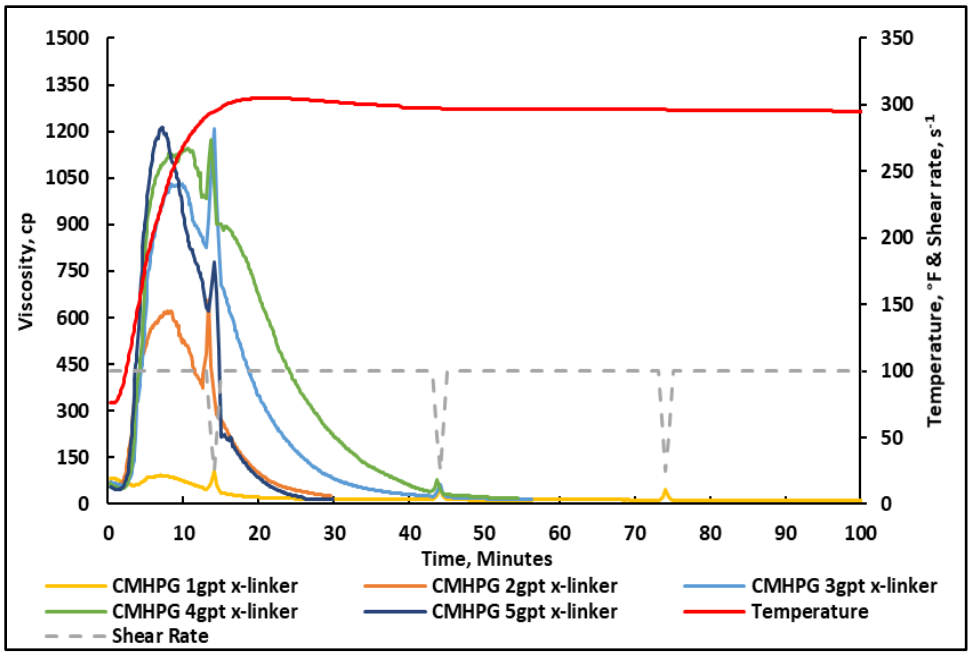

Fig. 2-6 Viscosity at 40 lb/1,000 gal CMHPG, 1-5 gpt crosslinker, pH 5 and 300°F.

Fig. 2-7 evaluates the crosslinking at 40 lb/1,000 gal synthetic polymer crosslinked with 1-6 gpt crosslinker. The synthetic polymer exhibits very weak crosslinking at concentrations below 3 gpt crosslinker. On the other hand, the crosslinking improves at 4 gpt and is best at 6 gpt. Over-crosslinking was not observed when crosslinking the synthetic polymer at the tested crosslinker concentrations. Based on the CMHPG and synthetic polymer crosslinking trends, the polymer mixture crosslinker concentration is limited by CMHPG's crosslinking ability. A conservative 4 gpt crosslinker concentration is chosen to carry out the dual polymer fracturing fluid tests.

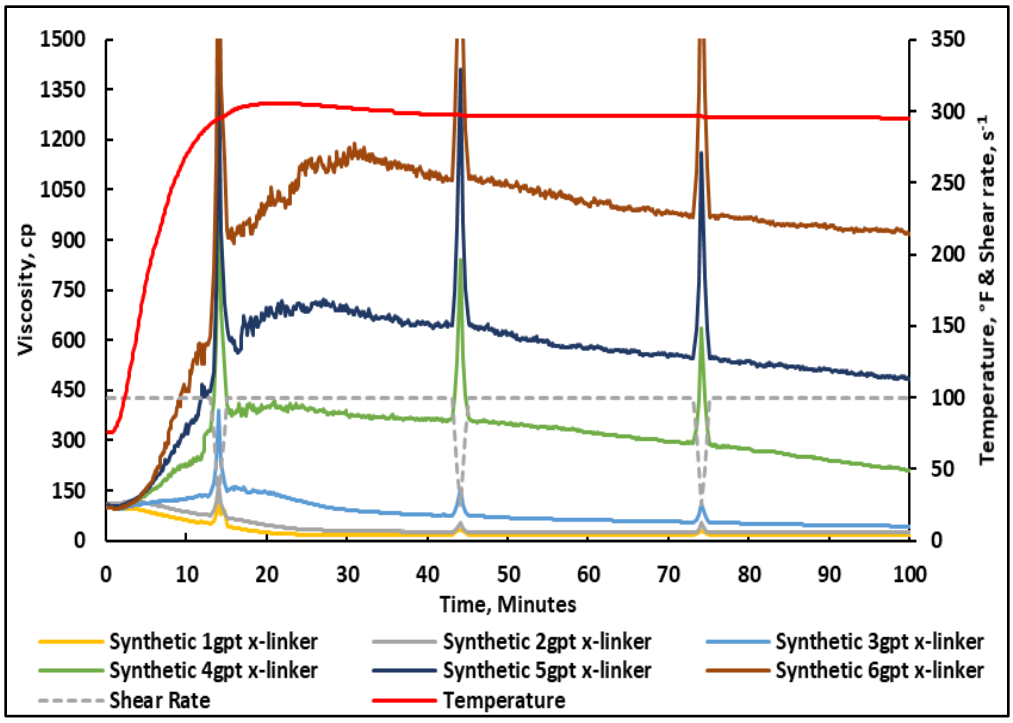

Fig. 2-7 Measured viscosity at 40 lb/1,000 gal synthetic polymer, 1-6 gpt crosslinker at pH 5 and 300°F.

2.3.4. Dual Polymer Crosslinking Viscosity

Fig. 2-8 presents 40 lb/1,000 gal dual polymer fracturing fluid viscosity results. All polymer mixtures surpass the performance of the individual polymer fracturing fluid with the 2:1 (CMHPG:Synthetic) fluids exhibiting the highest viscosity.

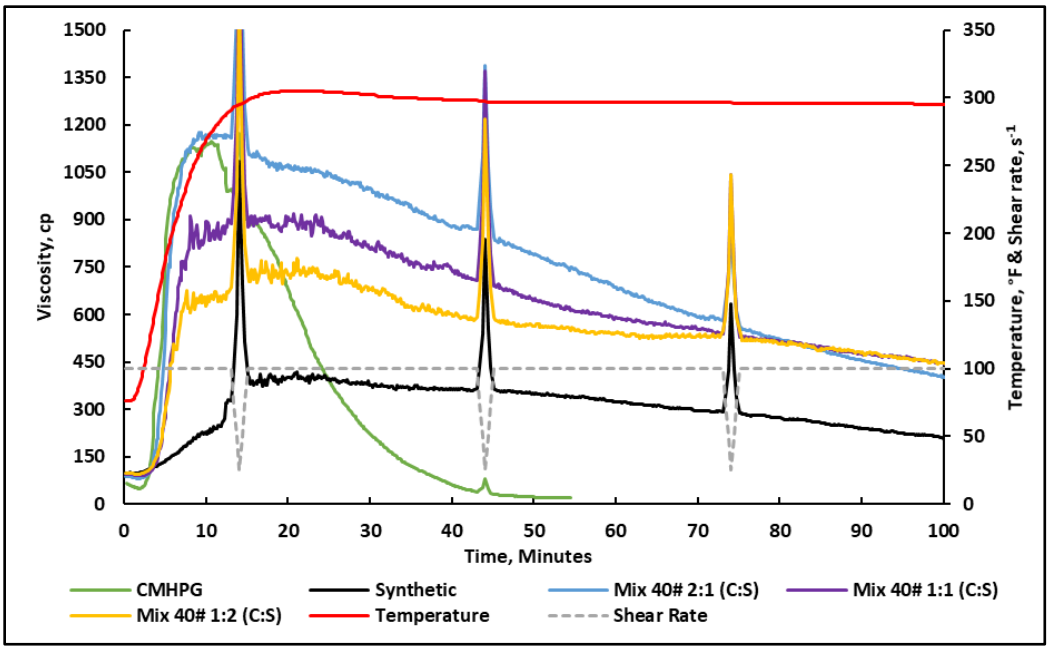

Fig. 2-8 Measured viscosity at 40 lb/1,000 gal dual polymer, 4 gpt crosslinker, pH 5 and 300°F.

Fig. 2-9 shows 30 lb/1,000 gal dual polymer fracturing fluid viscosity. Similar to the 40 lb/1,000 gal dual polymer results, the 30 lb/1,000 gal dual polymer fluids outperform the individual crosslinked polymer fracturing fluid viscosity. At 30 lb/1,000 gal, 1:1 (CMHPG:Synthetic) crosslinked dual polymer fluid shows the highest viscosity.

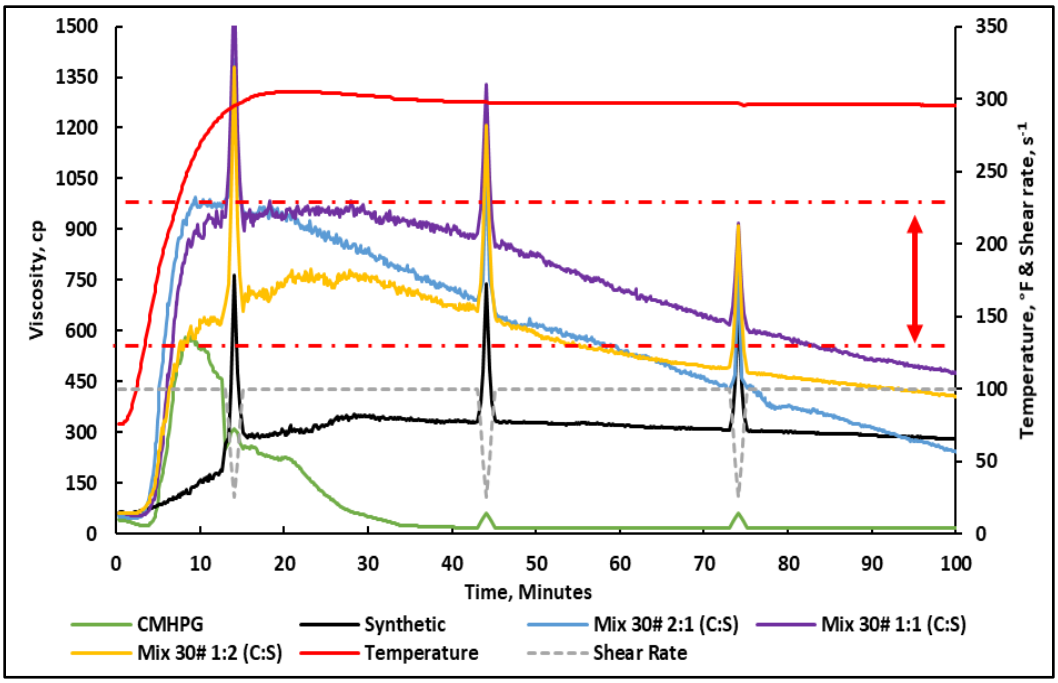

Fig. 2-9 Measured viscosity at 30 lb/1,000 gal dual polymer, 4 gpt crosslinker, pH 5 and 300°F.

Fig. 2-10 shows 20 lb/1,000 gal dual polymer fracturing fluid viscosity. At 20 lb/1,000 gal, 1:2 (CMHPG:Synthetic) crosslinked dual polymer solution shows the highest performance, surpassing the peak viscosity of the individual base fracturing fluid.

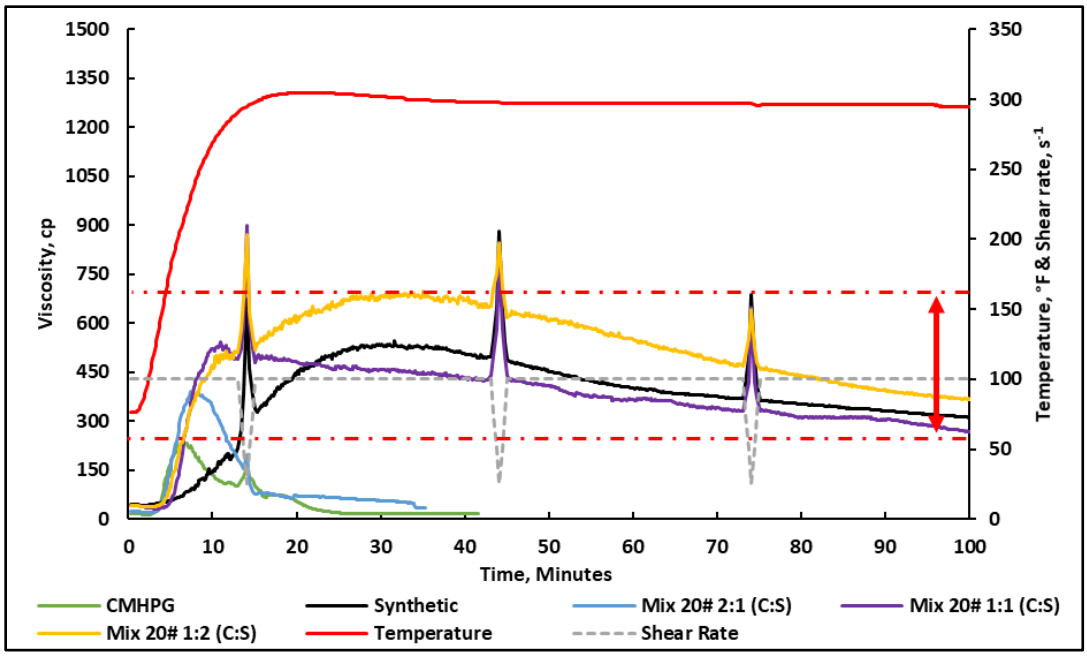

Fig. 2-10 Measured viscosity at 20 lb/1,000 gal dual polymer, 4 gpt crosslinker, pH 5 and 300°F.

2.3.5. Proppant Settling

Fig. 2-11 shows HP/HT see-through cell proppant settling results for the best ratios at 20, 30, and 40 lb/1,000 gal dual polymer fracturing fluids. The results show that all tested systems can suspend proppant at static conditions and 300°F. The polymer mixtures show good proppant suspension properties with minimal loss in proppant suspension level for 2 hours.

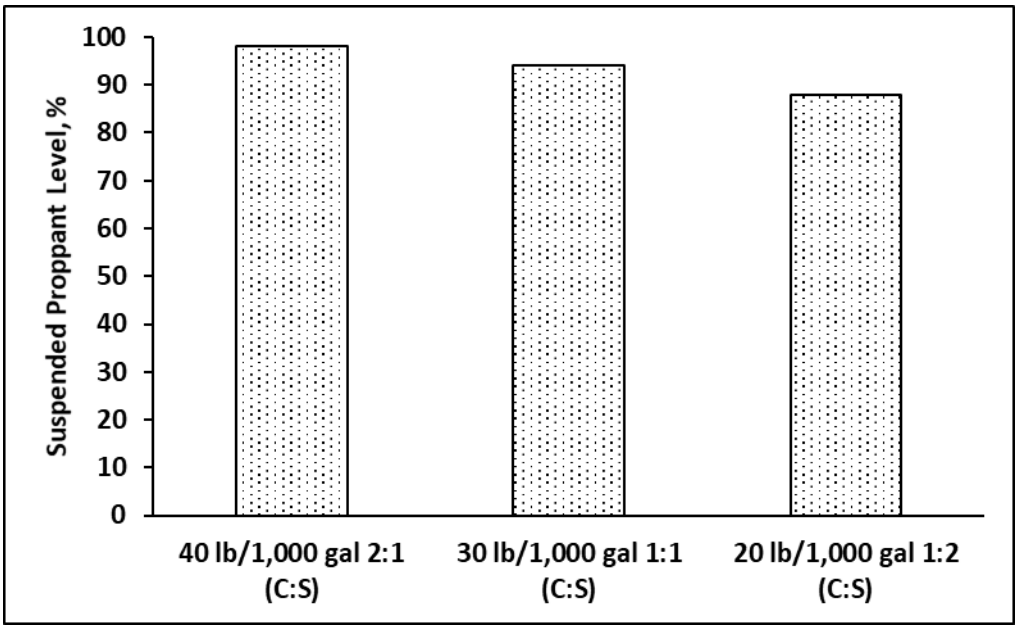

Fig. 2-11 Proppant settling (4 ppg) HP/HT see-through cell tests at 20, 30, and 40 lb/1,000 gal dual polymer, 4 gpt crosslinker, pH 5 and 300°F for 2 hours.

2.3.6. Breaker Tests

Figs. 2-12 to **2-14** share the results of breaking the best ratios of the 20, 30 and 40 lb/1,000 gal dual polymer fracturing fluids. Sodium bromate was able to break the dual polymer fracturing fluid and in appropriate concentrations the fluid were able to achieve a low broken fracturing fluid viscosity (< 20 cp) at the end of the 100 minute test. The effluent after the breaker test was collected from the rheometer and exhibited a water-like viscosity with no re-gelling characteristics at room temperature.

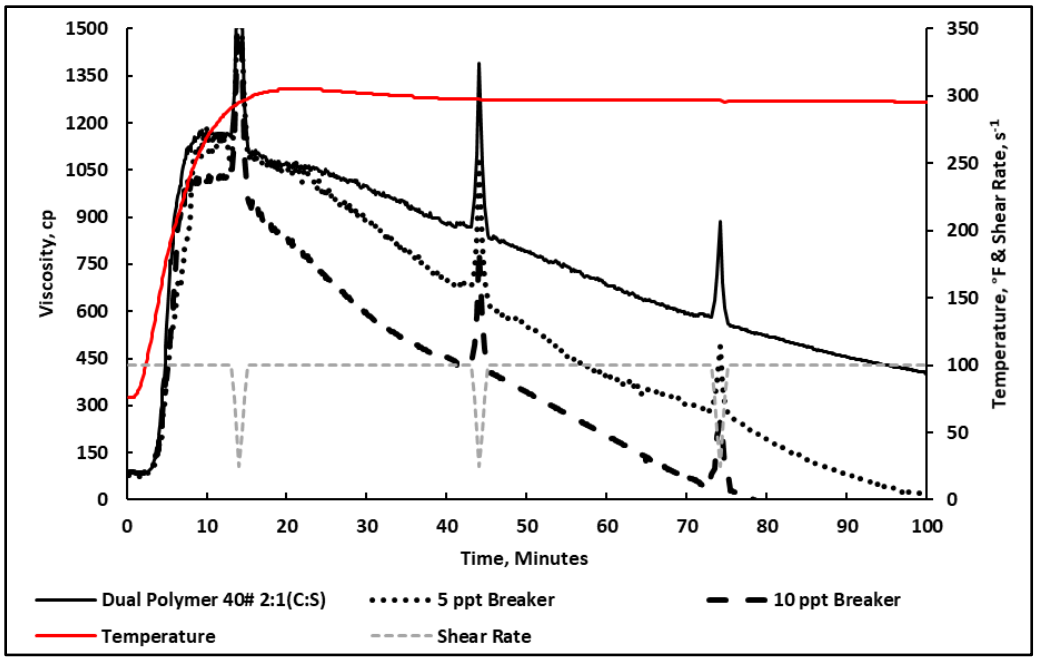

Fig. 2-12 Viscosity at 40 lb/1,000 gal dual polymer with sodium bromate oxidizer, 4 gpt crosslinker, pH 5 and 300°F.

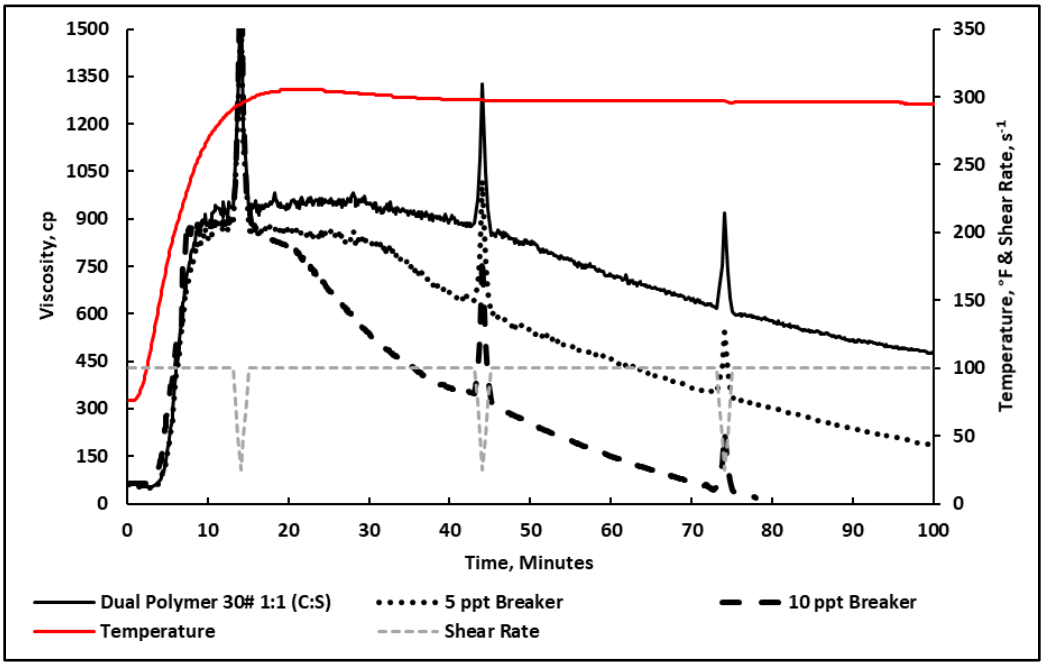

Fig. 2-13 Viscosity at 30 lb/1,000 gal dual polymer with sodium bromate oxidizer, 4 gpt crosslinker, pH 5 and 300°F.

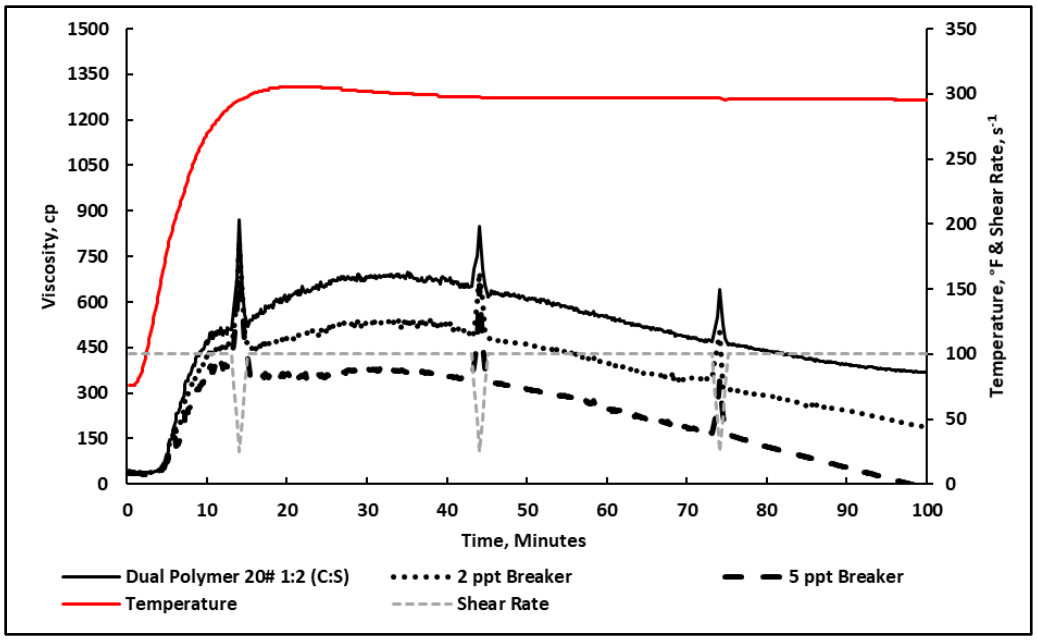

Fig. 2-14 Viscosity at 20 lb/1,000 gal dual polymer with sodium bromate oxidizer, 4 gpt crosslinker, pH 5 and 300°F.

2.4. Discussion

To understand the interaction between the two polymers in the system FTIR, cryo-SEM, and the rheometer were utilized. **Fig. 2-15** shows the IR spectrum of CMHPG at neutral pH. The broad band around 3,350 cm-1 is ascribed to OH stretching vibration. CH2 symmetrical stretching vibration is observed at 2,912 cm-1. The 1,4 glycosidic band stretch is seen at 1,152 cm-1 (Nikonenko et al. 2000). The 1,6 glycosidic linkage is seen at 1,005 cm-1 (Wiercigroch et a. 2017). The band at 868 and 1,051 cm-1 is indicative of skeletal stretching vibrations of CMHPG. The characteristic peak at 1,648 cm-1 is attributed to the intramolecular hydrogen bonded C=O stretching vibration of COO- (Zhang et al. 2005; Todica et al. 2015).

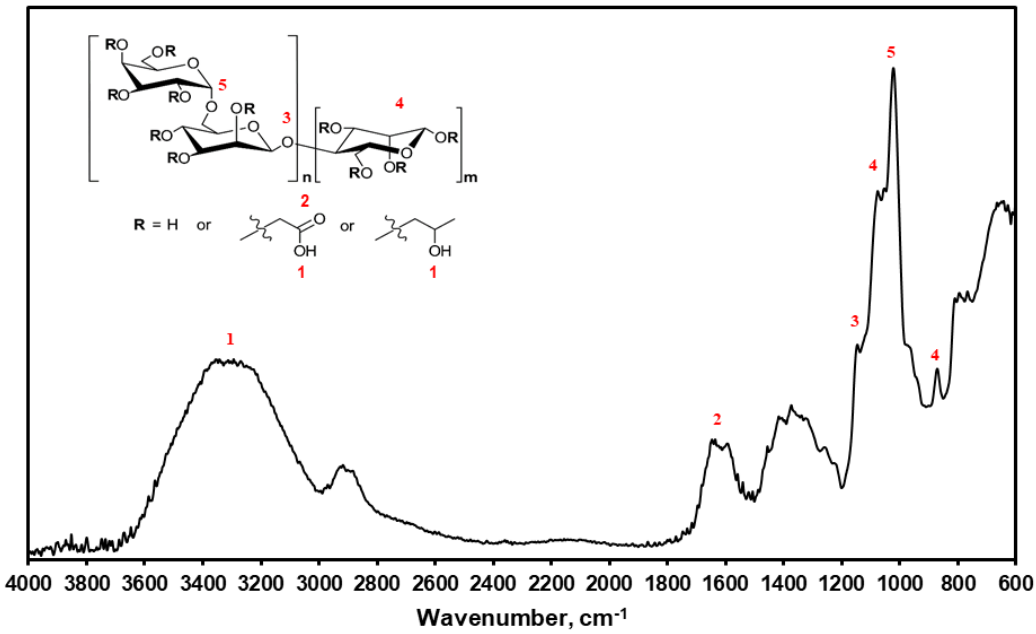

Fig. 2-15 FTIR spectrum of CMHPG.

Fig. 2-16 depicts the IR spectrum of the synthetic polymer at neutral pH. The backbone CH_2 symmetrical stretching vibration is seen at 2,919 cm^{-1}. The carboxylic OH and C=O stretching vibrations are attributed to the 3,350 cm^{-1} and 1,651 cm^{-1} peaks, respectively. The peak at 3,200 cm^{-1} represents one of the two characteristic stretches of the amide group. The second characteristic peak likely overlaps with the carboxylic acid –OH stretch at 3,350. The amide N-H deformation and C-N stretching vibration overlap with the C=O stretch vibrations at the area of 1,600-1,650 cm^{-1}. The AMPS group S=O asymmetric, symmetric stretches, and OH stretch can be found at 1,183 cm^{-1}, 1,041 cm^{-1}, 2,870 cm^{-1}, respectively (Dumaz and Okay 2000, Rosa et al. 2003, Jamshidi and Rabiee 2014) .

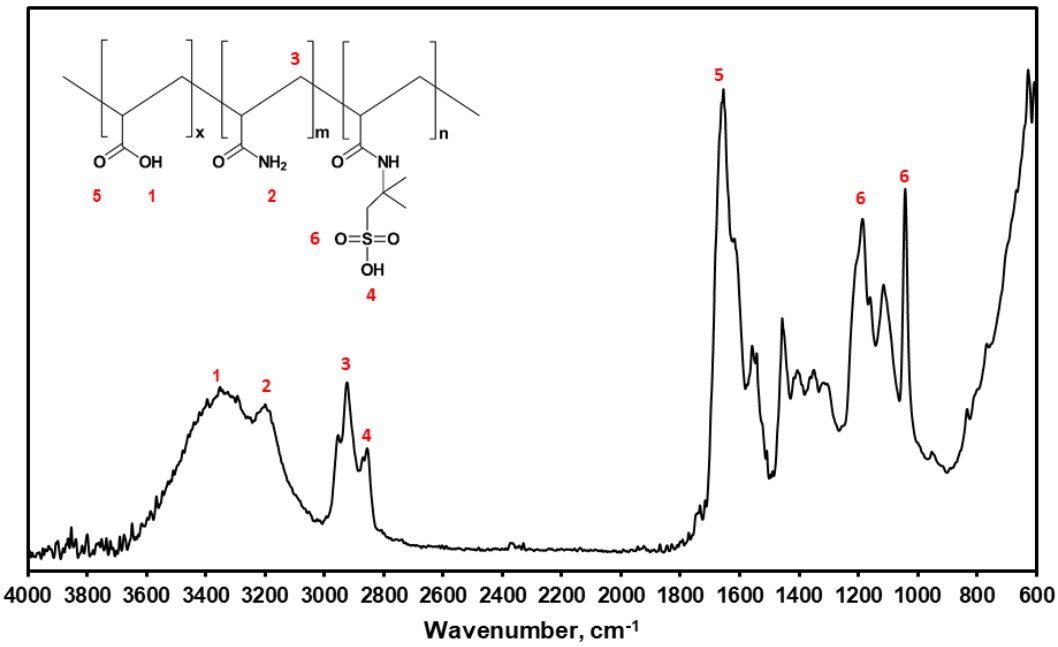

Fig. 2-16 FTIR spectrum of the synthetic polymer.

The IR spectrum of the mixture of CMHPG and synthetic polymers are presented in **Fig. 2-17**. There are no new peaks that are generated from mixing the two polymers; this indicates that no covalent chemical bonding occurred. However, the observed minor shifts in the IR spectra of the mix are representative of changes in hydrogen-bonded configurations of the polymers in solution. The first minor shift observed is the shift in the N-H band from 3,200 cm^{-1} to 3,221 cm^{-1} in the spectrum of the mixture compared to the spectrum of the synthetic polymer. The second minor shift is seen in the carboxylic acid C=O bonds from 1648 cm^{-1} to 1662 cm^{-1} in CMHPG and from 1,651 to 1,662 cm^{-1} in synthetic polymer. The expected hydrogen bonds are a combination of NH···O between amide group of synthetic and the carboxylic groups of CMHPG and COO···H hydrogen bonding between the carboxylic group of synthetic polymer and the OH side groups in

CMHPG. In addition, various changes in intramolecular hydrogen bonding are expected. Band widening and shifting was also observed for the S=O symmetric stretch, and adjacent OH around 1,041 and 2,870 cm^{-1} indicating that the polymer mixture likely exhibits a different hydrogen bonding orientation compared to individual synthetic polymer fluid (Behera and Das 2018).

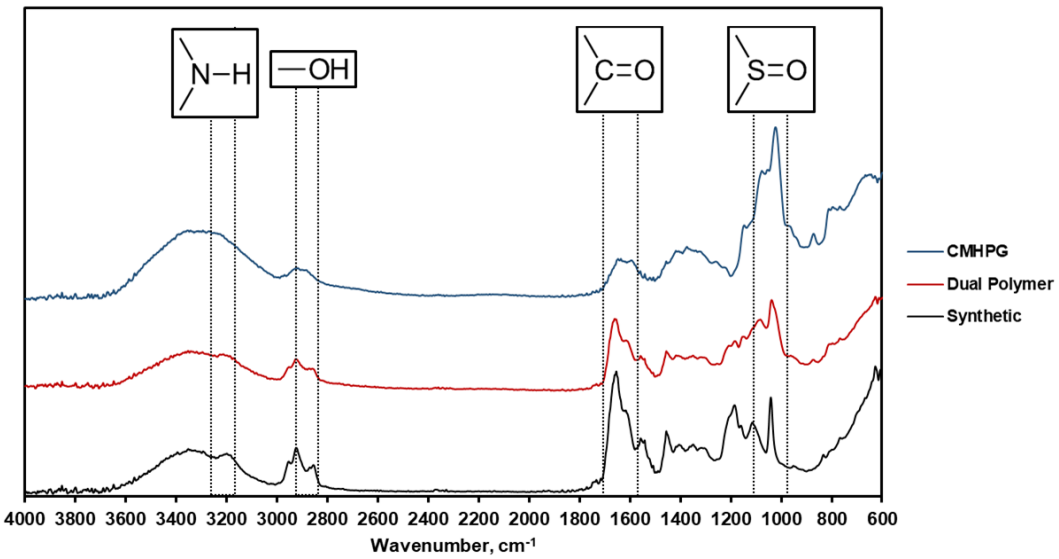

Fig. 2-17 Compiled FTIR spectrum of CMHPG (Top-blue), synthetic (Bottom-black), and the dual polymer mixture (Middle-red).

To visualize the magnitude of the interactions between the two polymers, three samples (CMHPG, synthetic polymer, and mixed polymer (1:1, CMHPG: Synthetic) were prepared at 1 wt% in 20 cm^3 bottles. The polymers were dissolved thoroughly and hydrated for an hour at room temperature. The individual polymer solution were viscous but able to flow when the bottle was flipped upside down. On the contrary, the mixed polymer solution at the same concentration could not flow and acted similarly to a solid,

Fig. 2-18. This is indicative of strong intermolecular interactions between the polymers when mixed.

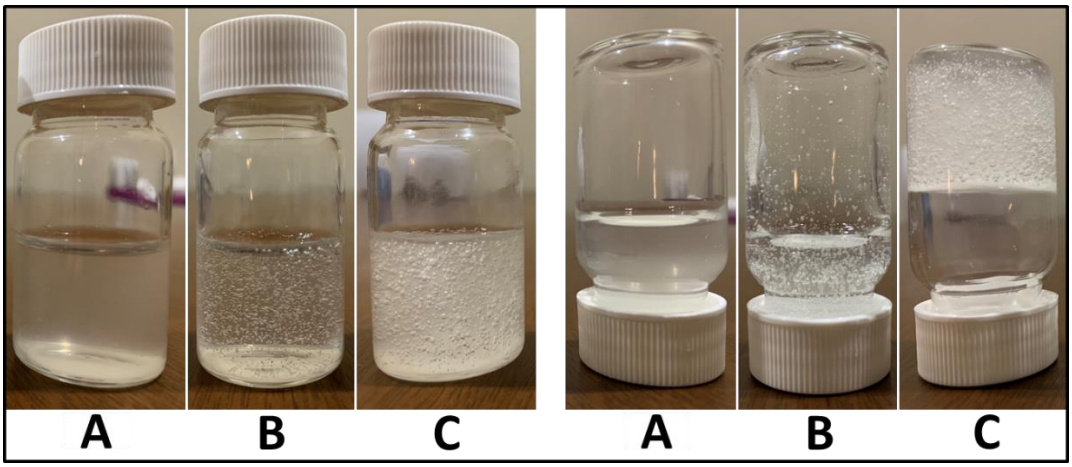

Fig. 2-18 Solution of (A) Individual CMHPG, (B) Individual Synthetic, and (C) Dual polymer CMHPG/ Synthetic 1:1, all at 1 wt% (~83 lb/1,000 gal) polymer concentration, hydrated (non-crosslinked), room temperature.

Cryo-SEM was also utilized to study the surface network properties of the crosslinked fluids. The Cryo-SEM images are seen in **Fig. 2-19**. The results show the differences between the individually crosslinked fracturing fluids and the dual polymer crosslinked fracturing fluid at the same preparation and testing conditions. The synthetic polymer fracturing fluid structure indicates a less crosslinked and a more flexible network compared to CMHPG based fracturing fluid, which looks tightly crosslinked. The dual polymer's surface structure shows a highly complex network formed by the combination of both polymers.

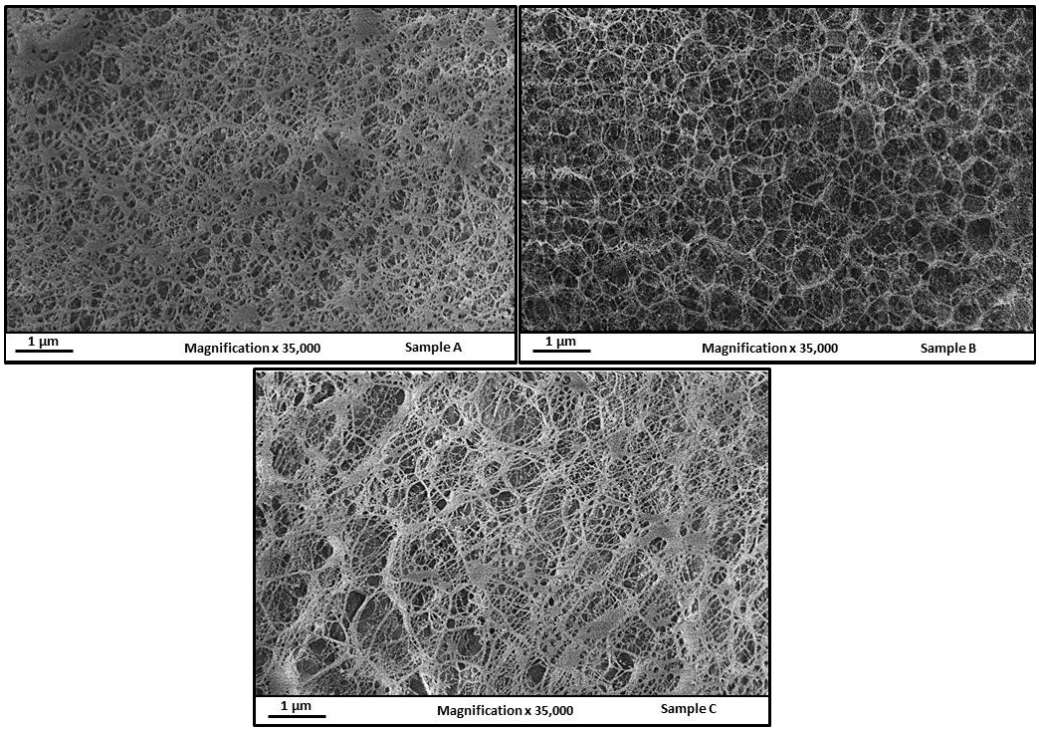

Fig. 2-19 Cryo-SEM images of (Sample A) crosslinked CMHPG, (Sample B) crosslinked Synthetic polymer, and (Sample C) crosslinked dual polymer.

A series of rheometer tests are run to investigate the influence of crosslinker to polymer ratio on the performance of the dual polymer system. **Figs. 2-20** to **2-22** show the effect of increasing the crosslinker concentration from 4 to 5 gpt at 40 lb/1,000 gal at 2:1, 1:1, and 1:2 (CMHPG:Synthetic) dual polymer system, respectively. The results show that the crosslinking viscosity performance is enhanced in all ratios for the 40 lb/1,000 gal dual-polymer fluid. As seen previously (Figs. 2-6 and 2-7), CMHPG can handle lower crosslinker concentration compared to synthetic polymer before it overcrosslinks. Consequently, the higher the CMHPG content in the ratio, the sooner the network reaches maximum viscosity and becomes susceptible to overcrosslinking.

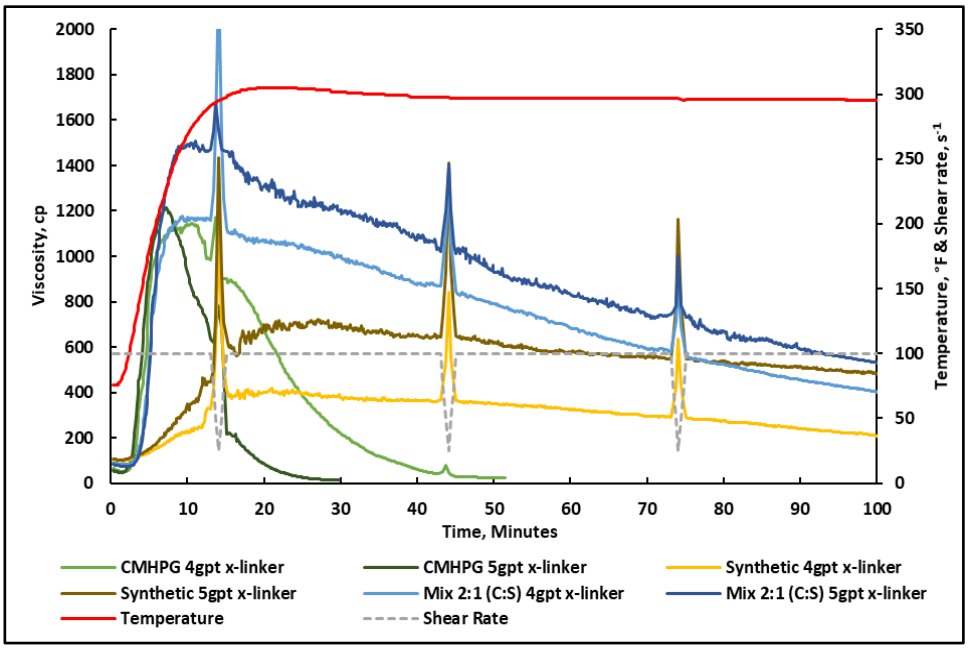

Fig. 2-20 Viscosity at 40 lb/1,000 gal 2:1 (CMHPG:Synthetic) dual polymer, 4-5 gpt crosslinker, pH 5 and 300°F.

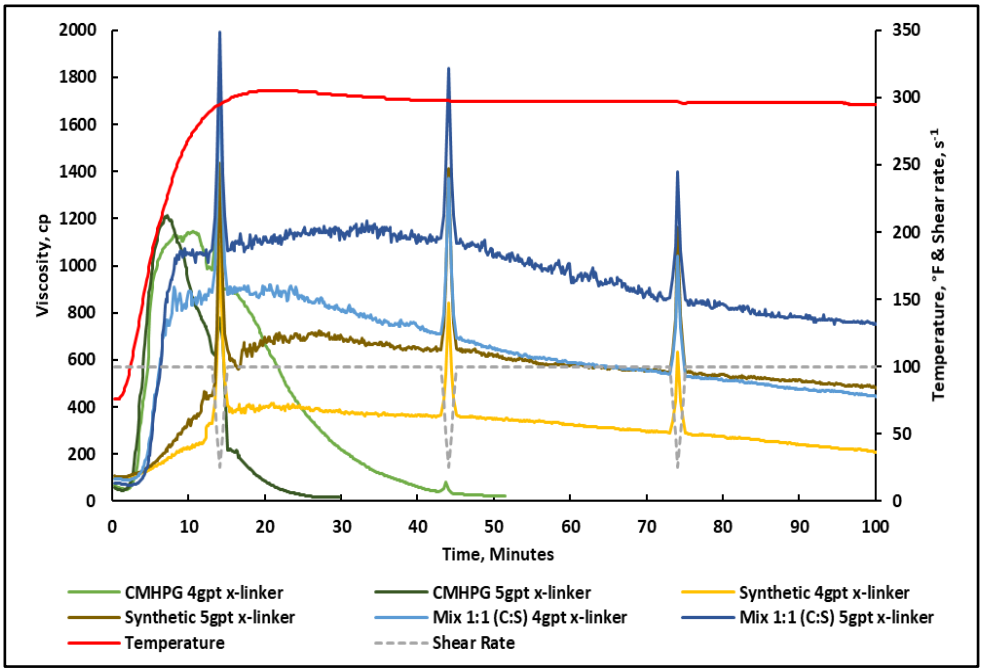

Fig. 2-21 Viscosity at 40 lb/1,000 gal 1:1 (CMHPG:Synthetic) dual polymer, 4-5 gpt crosslinker, pH 5 and 300°F.

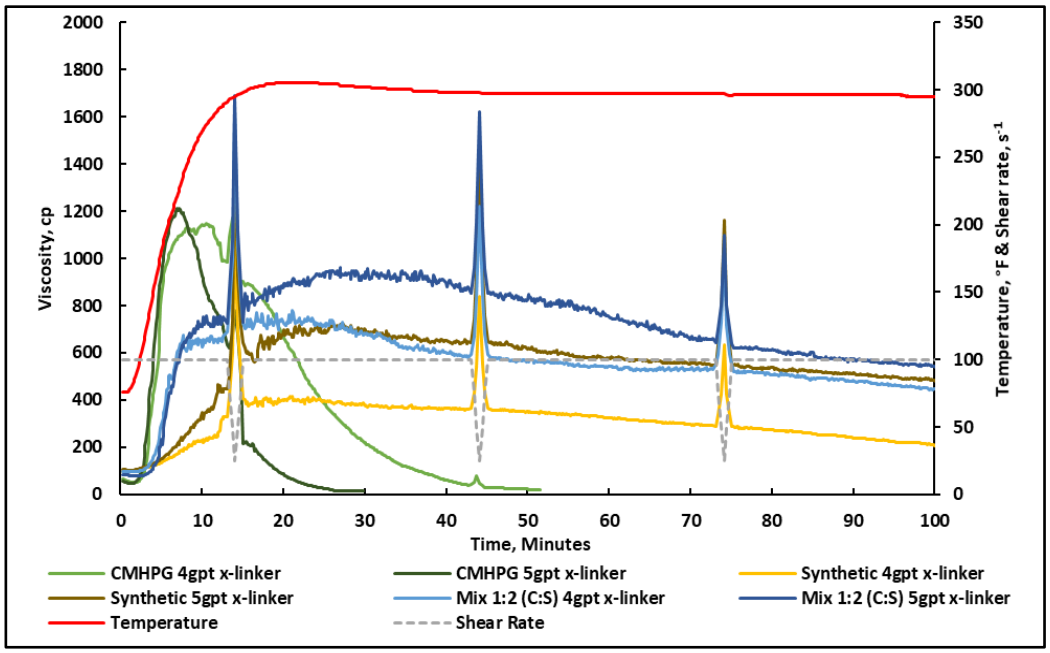

Fig. 2-22 Viscosity at 40 lb/1,000 gal 1:2 (CMHPG:Synthetic) dual polymer, 4-5 gpt crosslinker, pH 5 and 300°F.

Fig. 2-23 compares the 2:1 (CMHPG:Synthetic) dual polymer at 20, 30 and 40 lb/1,000 gal. The influence of crosslinker to polymer ratio is related to both the content of synthetic polymer and CMHPG in the mixtures. High concentration is required to overlap the polymers and crosslink them. CMHPG has a lower MW than synthetic polymer. Due to these factors, the 20 lb/1,000 gal 2:1 dual polymer fluid does not overlap sufficiently to allow the generation of a good crosslinking network. The 30 and 40 lb/1,000 gal 2:1 dual polymer provides better performance because it contains a higher content of polymers in solution that can overlap easier.

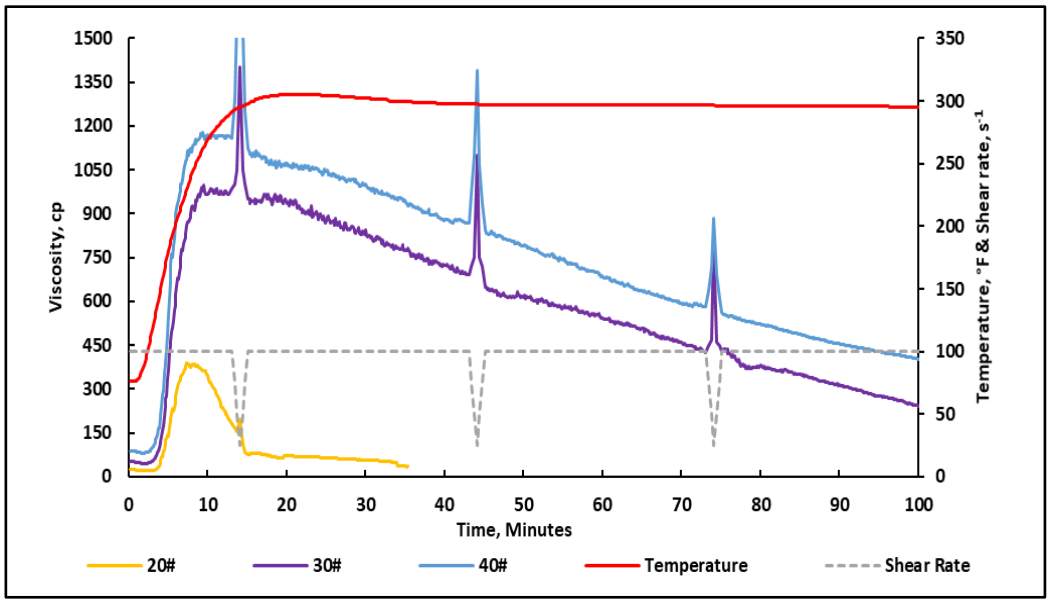

Fig. 2-23 Viscosity at 20, 30 and 40 lb/1,000 gal 2:1 (CMHPG:Synthetic) dual polymer, 4 gpt crosslinker, pH 5 and 300°F.

Fig. 2-24 compares the 1:1 (CMHPG:Synthetic) dual polymer at 20, 30 and 40 lb/1,000 gal at 300°F. These ratios contain a higher concentration of synthetic polymer than that in Fig. 22, and shows a drastic improvement in the performance of the 20 lb/1,000 gal solution. The viscosity of the 30 lb/1,000 gal dual polymer system also improves and surpasses the viscosity of the 40 lb/1,000 gal system. These improvements are due to the dual polymer systems having a more optimized crosslinking network with a greater proportion of synthetic polymer.

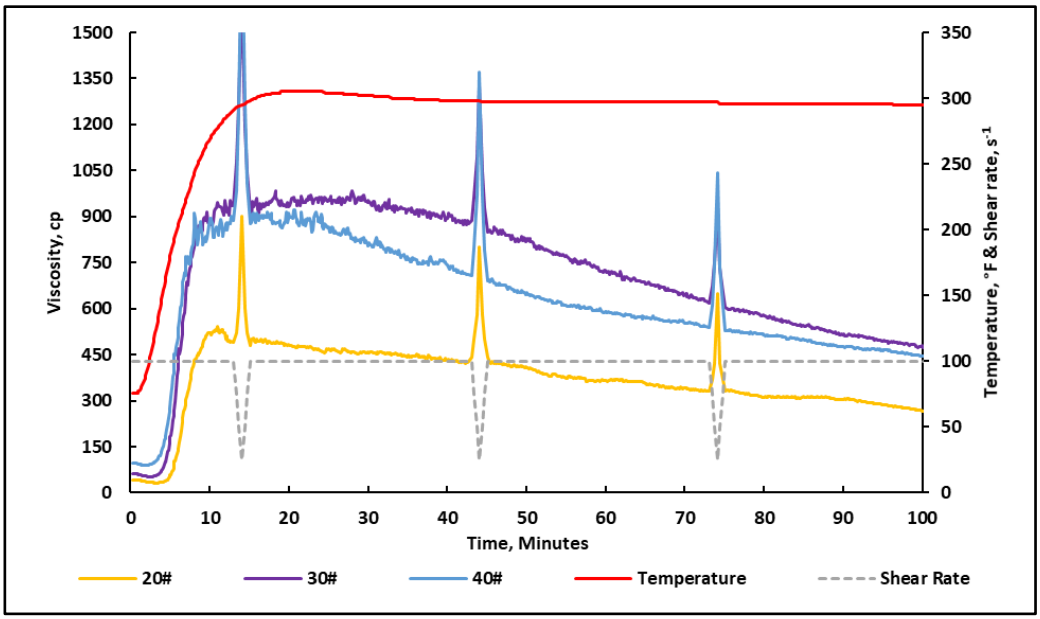

Fig. 2-24 Viscosity at 20, 30 and 40 lb/1,000 gal 1:1 (CMHPG:Synthetic) dual polymer, 4 gpt crosslinker, pH 5 and 300°F.

The performance of the 1:2 (CMHPG:Synthetic) dual polymer at 20, 30 and 40 lb/1,000 gal at 300°F is shown in **Fig. 2-25**. The further increase in the proportion of synthetic polymer in the system is shown to allow the 20 lb/1,000 gal dual polymer system to perform on par with the 30 and 40 lb/1,000 gal systems. This further highlights the importance of synthetic polymer on the crosslinked network.

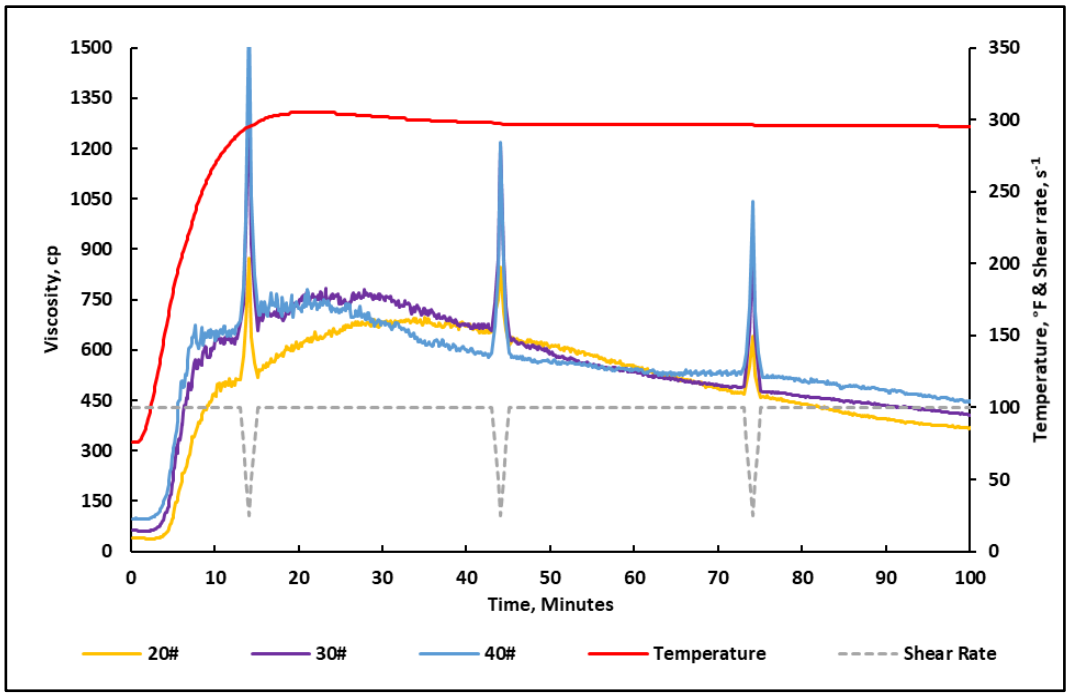

Fig. 2-25 Viscosity at 20, 30 and 40 lb/1,000 gal 1:2 (CMHPG:Synthetic) dual polymer, 4 gpt crosslinker, pH 5 and 300°F.

Figs. 2-26 and **2-27** highlight the lower loading possibilities of the dual polymer system by comparing 20 and 30 lb/1,000 gal dual polymer fracturing fluid performance to 40 lb/1,000 gal individual polymer fracturing fluids at 300°F. The synthetic polymer and CMHPG exhibit multiple intermolecular bonding opportunities in the form of hydrogen bonding. The dual polymer fracturing fluid observed an enhancement in performance could be due to changes in the polymer conformation in solution (Venugopal and Abhilash 2010). This occurs due to differences in hydrogen bonding interactions between individual fracturing fluid systems of water/CMHPG and water/Synthetic compared to the dual polymer system interactions of water/CMHPG/Synthetic (Khokhlov et al. 1993). This allows for a more optimized crosslinking network capable of generating higher viscosities at lower polymer loadings.

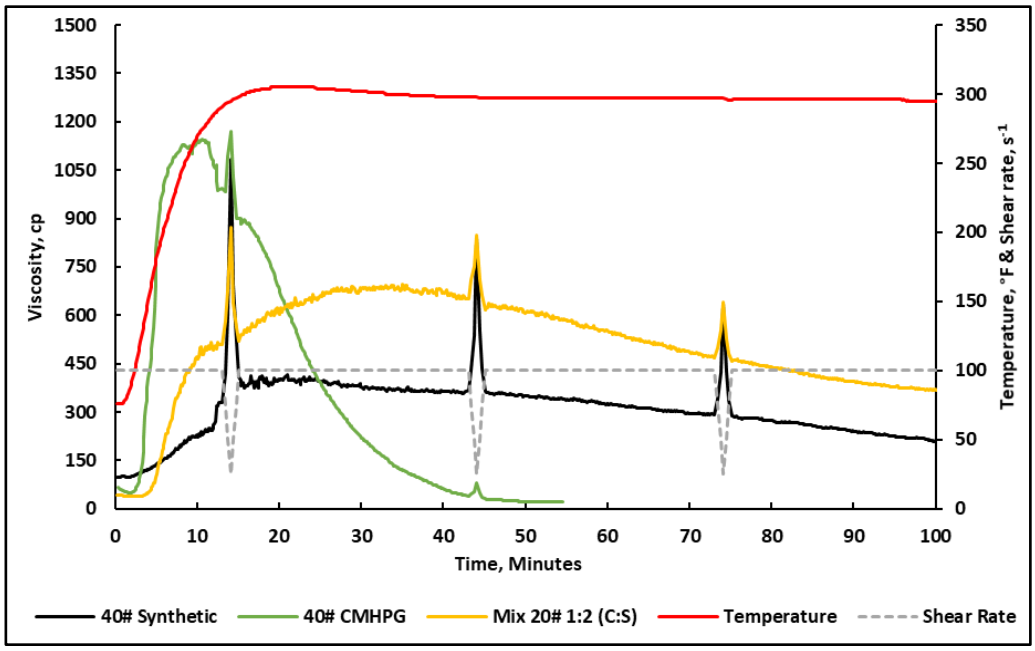

Fig. 2-26 Viscosity at 20 lb/1,000 gal 1:2 (CMHPG:Synthetic) dual polymer compared to 40 lb/1,000 gal individual polymer fracturing fluid, 4 gpt crosslinker, pH 5 and 300°F.

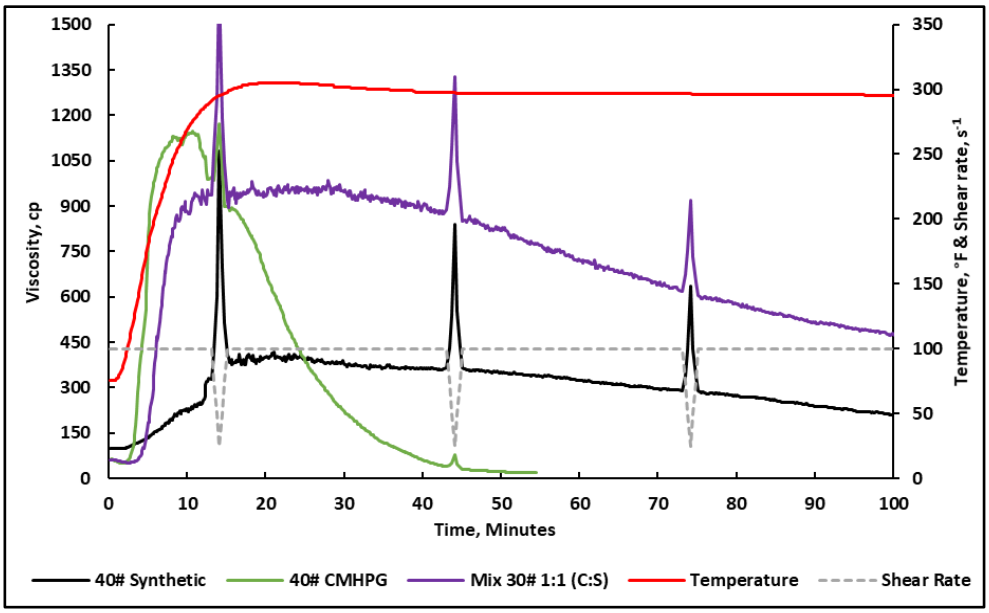

Fig. 2-27 Viscosity at 30 lb/1,000 gal 1:2 (CMHPG:Synthetic) dual polymer compared to 40 lb/1,000 gal individual polymer fracturing fluid, 4 gpt crosslinker, pH 5 and 300°F.

2.4.1. Elasticity Results

To measure the proppant carrying properties, solutions of 40 lb/1,000 gal CMHPG, synthetic, and dual polymer (1:1, CMHPG:Synthetic) fracturing fluids were crosslinked and tilted to assess the lipping characteristics at room temperature. The fluids looked viscous, very elastic, and a combination in between for CMHPG, synthetic, and dual polymer fracturing fluids, respectively, **Fig. 2-28**.

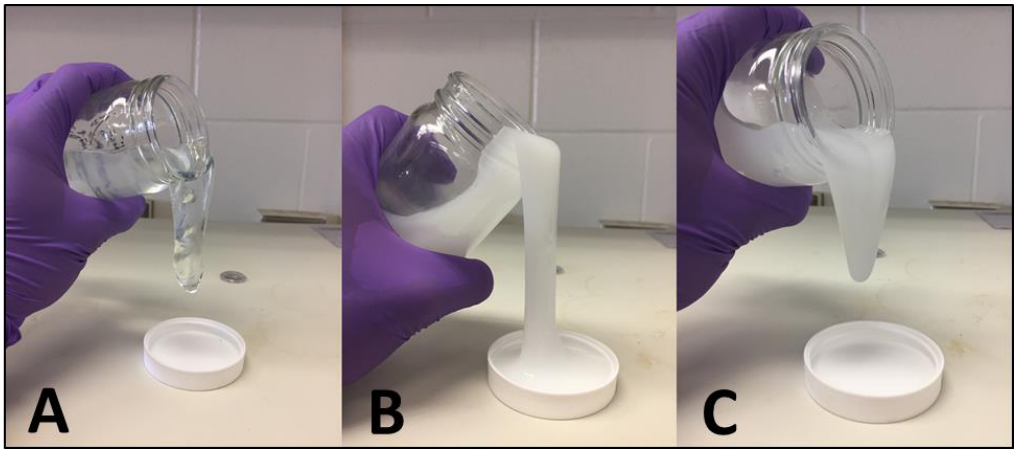

Fig. 2-28 Lipping behavior of (A) CMHPG, (B) Synthetic, and (C) dual polymer (1:1, CMHPG:Synthetic) crosslinked fracturing fluid, 4 gpt crosslinker, heated for 1 hour at 300°F to crosslink, lipped at room temperature.

The rheometer was also used to test elasticity and proppant carrying properties at high temperatures. **Fig. 2-29** compares the storage modulus measurements at 20, 30 and 40 lb/1,000 gal crosslinked CMHPG. The graph shows that the storage modulus is not stable, which is an indication of an unstable crosslinked structure. The unstable crosslinked structure could be due to over-crosslinking the polymer at pH 5.

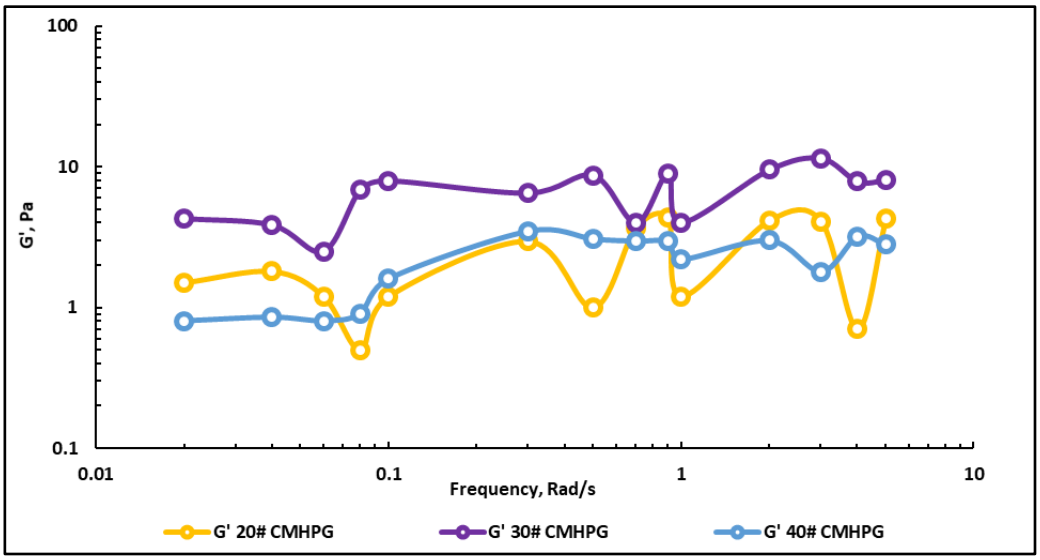

Fig. 2-29 Storage modulus at 20, 30 and 40 lb/1,000 gal CMHPG, 4 gpt crosslinker, pH 5 and 300°F.

Fig. 2-30 compares the storage modulus at 20, 30 and 40 lb/1,000 gal crosslinked synthetic polymer. The graph shows that the storage modulus is very stable, which is an indication of a good 3D crosslinked structure. Due to the higher crosslinker to polymer ratio at 20 lb/1,000 gal compared to 30 and 40 lb/1,000 gal, the storage modulus at 20 lb/1,000 gal achieves close values to the 40 lb/1,000 gal fluid.

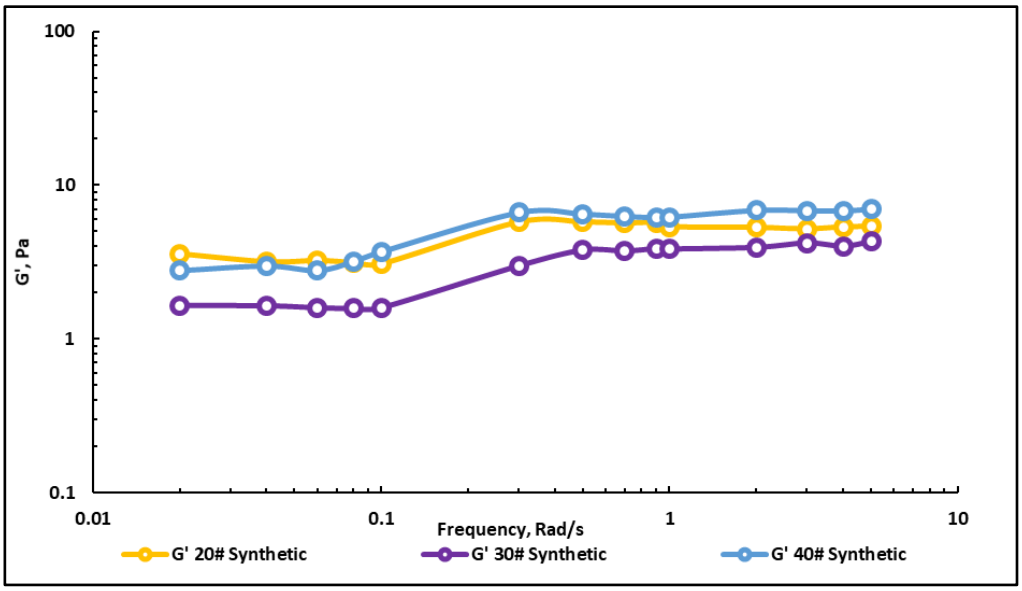

Fig. 2-30 Storage modulus at 20, 30 and 40 lb/1,000 gal synthetic polymer, 4 gpt crosslinker, pH 5, and 300°F.

Fig. 2-31 shares the storage modulus measurements at 20, 30 and 40 lb/1,000 gal 1:1 (CMHPG:Synthetic) crosslinked dual polymer. These results show that the dual polymer fracturing fluid storage modulus is higher than those of individual polymer and stable at the tested frequencies. This is an indication of a strong 3D crosslinked network that is able to carry proppant effectively at 300°F.

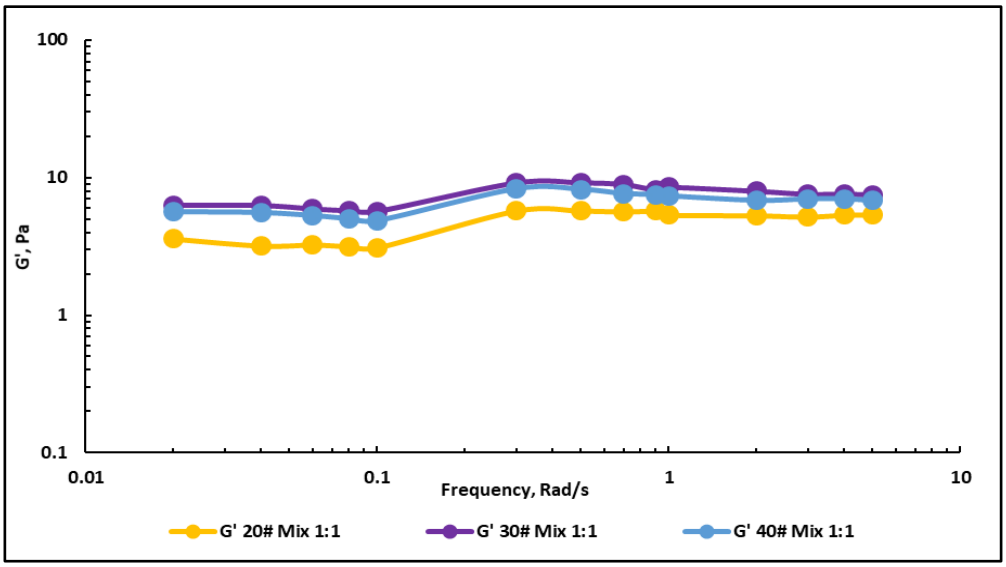

Fig. 2-31 Storage modulus measurements at 20, 30 and 40 lb/1,000 gal 1:1 (CMHPG:Synthetic) dual polymer, 4 gpt crosslinker, pH 5, and 300°F.

2.4.2. Proppant Settling

Fig. 2-32 shows proppant settling results for a 40 lb/1,000 gal 1:1 (CMHPG:Synthetic) dual polymer fracturing fluid at room temperature. The fluid can carry and suspend proppant (4 ppg- 40/70 Ottawa sand) for over 24 hours at these conditions. Similar behavior occurred with the 2:1 and 1:2 mixtures (CMHPG:Synthetic) at these conditions.

Fig. 2-32 Stable proppant suspension at 40 lb/1,000 gal dual polymer fracturing fluid, 4 gpt crosslinker, pH 5, and 77°F for 24 hours.

Results at room temperature might not perform the same way at high temperatures. The HP/HT see-through cell is one way to visualize proppant suspension under high-temperature conditions. This type of proppant test is static and representative of the weakest gel state where no additional pumping force is assisting in carrying proppant.

Fig. 2-33 shows the 40 lb/1,000 gal dual polymer fracturing fluid HP/HT see-through cell results. At 300°F the 40 lb/1,000 gal dual polymer fracturing fluids are stable. All tested dual polymer ratios can suspend over 90% of the proppant (4 ppg- 40/70 Ottawa sand) under these conditions. This is due to the highly elastic nature and strong polymer network that forms within the dual polymer fracturing fluid and allows for excellent proppant transport for the duration of pumping (1-2 hours).

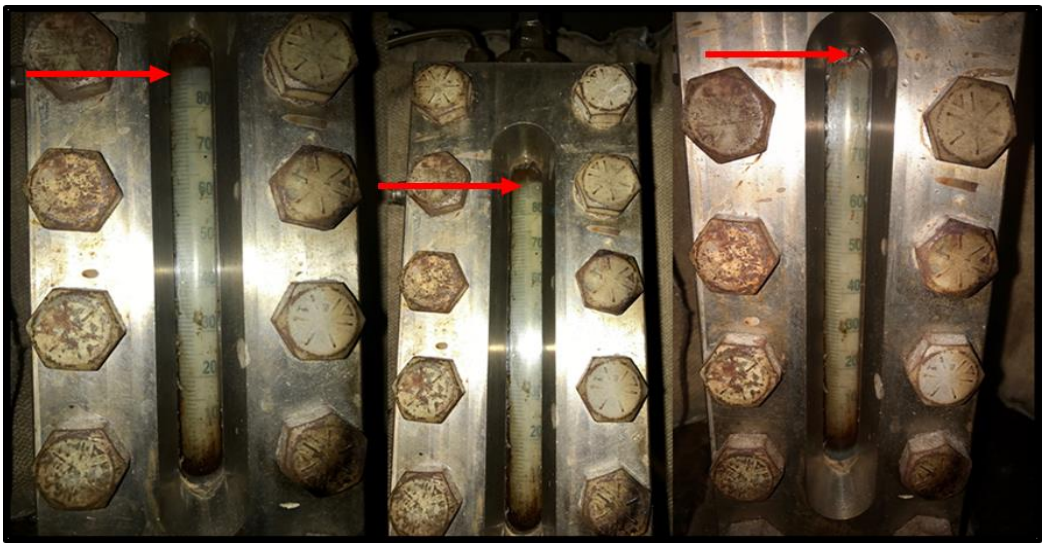

Fig. 2-33 Proppant settling at 40 lb/1,000 gal dual polymer fracturing fluid (left to right) 2:1, 1:1, and 1:2 (CMHPG:Synthetic), 4 gpt crosslinker, pH 5, and 300°F for 2 hours.

2.5. Conclusions

The hybrid dual polymers fracturing fluid exhibits a synergetic interaction between CMHPG and a synthetic polymer that enhances rheological performance beyond single polymer systems. The major benefit of this dual polymer system is to lower polymer loading, which reduces material cost, eases field applications, and potentially reduces damage in the generated fractures.

Based on the laboratory results we conclude the following for the dual polymer system examined:

1. The polymer interactions are mainly due to hydrogen bonding between the polymers; which influences the polymers conformation in solution and enables it to achieve higher viscosities at lower polymer loadings.

2. The dual polymer system was able to maintain a stable viscosity at 20 lb/1,000 gal and temperatures reaching 300°F.

3. The crosslinked dual polymer network provides sufficient energy to suspend and transport proppant at polymer concentrations as low as 20 lb/1,000 gal.

4. The crosslinked fluid can be broken with sodium bromate oxidizer.

5. The synergy between synthetic polyacrylamide-based polymers and CMHPG can be extended to other polysaccharide polymers with similar functional side groups (i.e. guar and HPG).

6. The synergy was also observed in the non-crosslinked form, which provides potential dual polymer applications in slickwater fracturing, drilling, and EOR.

2.6. Recommendations

Dual polymer fracturing fluid can achieve outstanding performance at 300°F. The lowest loading recommended is 20 lb/1,000 gal at a ratio of 1:2 (CMHPG:Synthetic). The loading recommended for optimum performance is 30 lb/1,000 gal at a ratio of 1:1 (CMHPG:Synthetic).

The field mixing recommendation is to provide 2 hydration units to fully hydrate the polymers individually. Following that, the hydrated polymers should be mixed to achieve homogeneity to initiate the interactions. Another field mixing approach would be to develop an invert emulsion pre-hydrated stock fluid including both polymers adjusted to the intended ratio which can then be pumped on the fly or prepared utilizing a single hydration unit. It is not recommended to add a polymer to an already hydrated polymer solution, as the second polymer hydration will take significantly longer.

2.7. Cost

As of writing this study, the cost of the used synthetic polymer is almost 10 times the cost of CMHPG. As seen from the results, a pure synthetic polymer system can handle the test conditions easily whereas a pure CMHPG system can not. To generate a successful pure CMHPG system for these conditions, the polymer loading has to be increased significantly which would produce formation damage concerns. The dual polymer system is an alternative solution with material cost priced lower than a pure synthetic polymer system while still being able to handle the test conditions.

2.8. Acknowledgements

The authors would like to thank Dwight Romanovicz (Cellular and Molecular Biology Department at UT Austin) for his innovative attempts with Cryo-SEM. Salar Afra helped with the FTIR tests is also much appreciated. Hamidreza Samouei's (Chemistry Department at Texas A&M), Leiming Li (Aramco Service Company), Joseph Baker's, and Tan Zhang's (Material Science and Engineering Department at Texas A&M) continuous discussion and questioning were extremely beneficial to this research. The authors are also grateful to Amanda Myatt's and Marry Beth Monroe's (Biomedical Engineering at Texas A&M) assistance in running all the lyophilizer tests.

2.9. References

Agoub, A., Smith, A., Giannouli, P. et al. 2007. Melt-in-the-mouth gels from mixtures of xanthan and konjac glucomannan under acidic conditions: A rheological and calorimetric study of the mechanism of synergistic gelation. *Carbohydrate Polymers* **69** (1): 713–724.

Almubarak, T., AlKhaldi, M., Panda, S. et al. 2015. Insights on Potential Formation Damage Mechanisms Associated with Hydraulic Fracturing. Presented at the International Petroleum Technology Conference, 6-9 December, Doha, Qatar. IPTC-18401-MS. https://doi.org/10.2523/IPTC-18401-MS.

Al-Muntasheri, G. 2014. A Critical Review of Hydraulic-Fracturing Fluids for Moderate to Ultralow Permeability Formations Over the Last Decade. *SPE Prod & Oper* **29** (4): 243–260. SPE-169552-PA. https://doi.org/10.2118/169552-PA.

Alquraishi, A. and Alsewailem, F. 2011. Adsorption of Guar, Xanthan and Xanthan-Guar Mixtures on High Salinity, High Temperature Reservoirs. Presented at the 10th Offshore Mediterranean Conference and Exhibition, Ravenna, Italy, 23-35 March.

Behera, B. and Das, P. 2018. Blue- and Red-Shifting Hydrogen Bonding: A Gas Phase FTIR and AB Initio Study of RR'CO···DCCl3 and RR'S···DCCl3 Complexes. *J. Phys. Chem. A* **122** (18): 4481-4489. https://doi.org/10.1021/acs.jpca.7b11962.

Cai, S., He, X., Liu, K. et al. 2017. Macromolecular Interactions and Synergy in Xanthan/HPAM Aqueous Solutions. *RSC J.* **7**: 41630–41639. https://doi.org/10.1039/c7ra05542k.

Clark, P., Halvaci, M., Ghaeli, H. et al. 1985. Proppant Transport by Xanthan and Xanthan-Hydroxypropyl Guar Solutions: Alternatives to Crosslinked Fluids. Presented at the SPE/DOE Low Permeability Gas Reservoirs Symposium, Denver, Colorado, 19-22 March. SPE-13907-MS. https://doi.org/10.2118/13907-MS.

Constien, V., Hawkins, G., Purd'homme, R. et al. 2000. In Reservoir Stimulation. Third edition. Editors: Economides, M. J. and Nolte, K. G., Chichester, London: Wiley, **8**-24.

Copetti, G., Grassi, M., Lapasin, R. et al. 1997. Synergistic gelation of xanthan gum with locust bean gum: A rheological investigation. *Glycoconjugate J.* **14** (1): 951-961.

Das, A., Chauhan, G., and Ojha, K. 2017. Improving Unconventional Reservoir Fracturing Using a Hybrid Surfactant-Polymer Gel System. Presented at the 79th EAGE Conference and Exhibition, Paris, France, 12-15 June.

Dogsa, I., Tomsic, M., Orehek, J. et al. 2014. Amorphous Supramolecular Structure of Carboxymethyl Cellulose in Aqueous Solution at Different pH Values as Determined by Rheology, Small Angle X-Ray and Light Scattering. *Carbohydrate Polymers* **111** (1): 492-504.

Dumaz, S. and Okay, O. 2000. Acrylamide/2-Acrylamido-2-Methylpropane Sulfonic Acid Sodium Salt-Based Hydrogels: Synthesis and Characterization. *Polymer* **41** (10): 3693-3604. https://doi.org/10.1016/S0032-3861(99)00558-3.

Economides, M. and Nolte, K. 2000. Reservoir Stimulation, Third Edition. John Wiley and Sons. Chichester, England, Wiley.

Fischer, C., Navarrete, R., Constien, V. et al. 2001. Novel Application of Synergistic Guar/Non-Acetylated Xanthan Gum Mixtures in Hydraulic Fracturing. Presented at the SPE International Symposium on Oilfield Chemistry, Houston, Texas, 13-16 February. SPE-65037-MS. https://doi.org/10.2118/65037-MS

Funkhouser, G. and Norman, L. 2003. Synthetic Polymer Fracturing Fluid for High-Temperature Applications. Presented at the SPE International Symposium on Oilfield Chemistry, Houston, Texas, 5–7 February. SPE-80236-MS. https://doi.org/10.2118/80236-MS.

Gall, B. and Raible, C. 1985. Molecular Size Studies of Degraded Fracturing Fluid Polymers. Presented at the SPE Oilfield and Geothermal Chemistry Symposium, Phoenix, Arizona, 9-11 March. SPE-13566-MS. https://doi.org/10.2118/13566-MS.

Gdanski, R. 2001. Impact of Clay Acidity on the pH of Invading Fluids. Presented at the SPE International Symposium on Oilfield Chemistry, Houston, Texas, 13-16 February. SPE-64983-MS. https://doi.org/10.2118/64983-MS.

Gdanski, R. 2002. High-pH Clay Instability Rating. Presented at the SPE International Symposium and Exhibition on Formation Damage Control, Lafayette, Louisiana, 20-21 February. SPE-73730-MS. https://doi.org/10.2118/73730-MS.

Gidley, J. L., Holditch, S. A., Dale, N. E. et al. 1989. *Recent Advances in Hydraulic Fracturing*. First edition. Richardson, Texas: Henry L. Doherty Memorial Fund of AIME, SPE.

Guo, J., Lu, H., Zhou, B. et al. 2012. A New Fracturing Fluid of Low Concentration. Presented at the SPE IADC/SPE Asia Pacific Drilling Technology Conference and

Exhibition, Tianjin, China, 9-11 July. SPE-155970-MS. https://doi.org/10.2118/155970-MS.

Habibpour, M. and Clark, P. 2017. Drag reduction behavior of hydrolyzed polyacrylamide/xanthan gum mixed polymer solutions. *J. Pet. Sci.* **14** (2): 412–423. https://doi.org/10.1007/s12182-017-0152-7.

Haque, Md. A., Kurokawa, T., and Gong, J. P. 2012. Super tough double network hydrogels and their application as biomaterials. *Polymer* **53** (1): 1805–1822. https://doi.org/10.1016/j.polymer.2012.03.013.

Harris, P., Morgan, R., and Heath, S. 2005. Measurement of Proppant Transport of Frac Fluids. Presented at the SPE Annual Technical Conference and Exhibition, Dallas, Texas, 9-12 October. SPE-95287-MS. https://doi.org/10.2118/95287-MS.

Holtsclaw, J., Galindo, G., and Chopade, P. 2017. Next-Generation Boron-Crosslinked Fracturing Fluids: Breaking the Lower Limits on Polymer Loadings. *SPE Prod & Oper* **32** (4): 440-448. SPE-174988-PA. https://doi.org/10.2118/174988-PA.

Hornof, V., Neale, G., and Chaaraoui, A. 1983. Viscosity of Surfactant-Polymer Solutions. Presented at the SPE Oilfield and Geothermal Chemistry Symposium, Denver, Colorado, 1-3 June. SPE-11775-MS. https://doi.org/10.2118/11775-MS

Huang, W. 2015. Drag Reduction in Pipeline by Polymer-Surfactant and Polymer-Polymer Mixtures. *Master of Applied Science Thesis*. Department of Chemical Engineering, University of Waterloo, Ontario, Canada.

ISO 13503-1, 2011. Petroleum and natural gas industries-completion fluids and materials-Part 1, Measurement of viscous properties of completion fluids, second edition. Geneva, Switzerland: ISO.

Jamshidi, H. and Rabiee, A. 2014. Synthesis and Characterization of Acrylamide-Based Anionic Copolymer and Investigation of Solution Properties. *Advances in Materials Science and Engineering* Article ID 728675. https://doi.org/10.1155/2014/728675.

Janson, J. 1998. Protein Purification: Principles, High-Resolution Methods, and Applications. Second Edition. John Wiley and Sons. Chichester, England, Wiley.

Khokhlov, A., Starodubtzev, S., Vasilevskaya, V. 1993. Conformational Transitions in Polymer Gels: Theory and Experiment. Responsive Gels: Volume Transitions I. *Advances in Polymer Science* **109**: 123-171. Springer, Berlin, Heidelberg. https://doi.org/10.1007/3-540-56791-7_3.

Khouryieh, H. 2006. Rheological Characterization of Xanthan-Guar Mixtures in Dilute Solutions. *Doctoral Dissertation.* College of Agriculture, Kansas State University, Manhattan, Kansas.

Legemah, M., Guerin, M., Sun, H. et al. 2014. Novel High-Efficiency Boron Crosslinkers for Low-Polymer-Loading Fracturing Fluids. *SPE J.* **19** (4): 737-743. SPE-164118-PA. https://doi.org/10.2118/164118-PA .

Legemah, M., Sun, H., Carman, P. et al. 2015. A Novel Approach to Crosslink Delay of Low-pH Fracturing Fluid. Presented at the International Symposium on Oilfield Chemistry, The Woodlands, Texas, USA, 13-15 April. SPE-173752-MS. https://doi.org/10.2118/173752-MS.

Lei, C. and Clark, P. E. 2007. Crosslinking of Guar and Guar Derivatives. *SPE J.* **12** (3): 316-321. SPE-90840-PA. https://doi.org/10.2118/90840-PA.

Liang, F. and Al-Muntasheri, G., Ow, H. et al. 2017. Reduced-Polymer-Loading, High-Temperature Fracturing Fluids by Use of Nanocrosslinkers. *SPE J.* **22** (2): 622-631. SPE-177469-PA. https://doi.org/10.2118/177469-PA.

Loveless, D., Holtsclaw, J., Saini, R. et al. 2011. Fracturing Fluid Comprised of Components Sourced Solely from the Food Industry Provided Superior Proppant Transport. Presented at the SPE Annual Technical Conference and Exhibition, Denver, Colorado, 30 October-2 November. SPE-147206-MS. https://doi.org/10.2118/147206-MS.

Loveless, D., Holtsclaw, J., Weaver, J. et al. 2014. Multifunctional Boronic Acid Crosslinker for Fracturing Fluids. Presented at the International Petroleum Technology Conference, Doha, Qatar, 19-22 January. SPE-17404-MS. https://doi.org/10.2523/IPTC-17404-MS.

Malik, A., Bolarinwa, S., Leal, J. et al. 2013. Successful Application of Metal-Crosslinked Fracturing Fluid with Low-Polymer Loading for High Temperature Proppant Fracturing Treatments in Saudi Arabian Gas Fields - Laboratory and Field Study. Presented at the SPE Middle East Oil and Gas Show and Conference, Manama, Bahrain, 10-13 March. SPE-164338-MS. http://doi.org/10.2118/164338-MS.

Nikonenko, N., Buslov, D., Sushko, N. et al. 2000. Investigation of Stretching Vibrations of Glycosidic Linkages in Disaccharides and Polysaccharides with use of IR Spectra

Deconvolution. *Biopolymers* **57** (4): 257-62. https://doi.org/10.1002/1097-0282(2000)57:4<257::AID-BIP7>3.0.CO;2-3.

Nová, L., Uhlík, F., Košovan, P. 2017. Local pH and Effective pKa of Weak Polyelectrolytes Insights from Computer Simulation. *Phys. Chem.* **19** (22): 14376-14387.

Paradossi, G., Chiessi, E., Barbiroli, A. et al. 2002. Xanthan and Glucomannan Mixtures: Synergistic Interactions and Gelation. *Biomacromolecules J.* **3** (1): 498-504.

Parris, M., MacKay, B., Rathke, J. et al. 2008. Influence of Pressure on Boron Cross-Linked Polymer Gels. *Macromolecules* **41** (21): 8181–8186. https://doi.org/10.1021/ma801187q.

Pettitt, D. J. 1970. Guar Gum-Polyacrylamide Compositions. US Patent No. 3,658,734.

Rosa, F., Bordado, J., and Casquilho, M. 2003. Hydrosoluble Copolymers of Acrylamide-(2-acrylamido-2-methylpropanesulfonic acid) Synthesis and Characterization by Spectroscopy and Viscometry. *J. Appl. Polym. Sci.* **87** (2): 192-198. https://doi.org/10.1002/app.11325.

Simeoni, M. 2016. Experimental Evaluation of Biopolymer and Synthetic Polymer Drag Reduction in Industrial Scale Facilities. *Doctoral Dissertation,* Environmental and Energy Engineering Sciences, University of Udine, Udine, Italy.

Sun, H. and Qu, Q. 2011. High-Efficiency Boron Crosslinkers for Low-Polymer Fracturing Fluids. Presented at the SPE International Symposium on Oilfield Chemistry, The Woodlands, Texas, USA, 11-13 April. SPE-140817-MS. https://doi.org/10.2118/140817-MS.

Thompson, R., Walker, M., Siebert, A. et al. 2016. An Introduction to Sample Preparation and Imaging by Cryo-Electron Microscopy for Structural Biology. *Methods* **100** (1): 3-15. https://doi.org/10.1016/j.ymeth.2016.02.017.

Todica, M., Stefan, R., Pop, C. 2015. IR and Raman Investigation of Some Poly(acrylic) Acid Gels in Aqueous and Neutralized State. *Acta Physica Polonica.* **128** (1): 128-135. https://doi.org/10.12693/APhysPolA.128.128.

Venugopal, K. and Abhilash, M. 2010. Study of Hydration Kinetics and Rheological Behavior of Guar. *International J. Pharma Sciences and Research* **1** (1): 28-39.

Vidal, R., Fagundes, F., de Menezes, S. et al. 2005. Solution Properties of Partially Hydrolysed Polyacrylamide and Chitosan Mixed Solutions. *Macromol. Symp:* 118–126.

Wang, K., Wang, Y., Ren, J. et al. 2017. Highly Efficient Nano Boron Crosslinker for Low-Polymer Loading Fracturing Fluid System. Presented at the SPE/IATMI Asia Pacific Oil & Gas Conference and Exhibition, Jakarta, Indonesia, 17-19 October. SPE-186943-MS. https://doi.org/10.2118/186943-MS.

Wiercigroch, W., Szafraniec, E., Czamara, K. et al. 2017. Raman and Infrared Spectroscopy of Carbohydrates: A Review. *Molecular and Biomolecular Spectroscopy* **185**: 317-335. https://doi.org/10.1016/j.saa.2017.05.045.

Williams, N., Kelly, P., Berard, K. et al. 2012. Fracturing Fluid with Low-Polymer Loading Using a New Set of Boron Crosslinkers: Laboratory and Field Studies. Presented at the SPE International Symposium and Exhibition on Formation Damage

Control, Lafayette, Louisiana, 15-17 February. SPE-151715-MS. https://doi.org/10.2118/151715-MS.

Yang, J., Cui, W., Guan, B. et al. 2016. Supramolecular Fluid of Associative Polymer and Viscoelastic Surfactant for Hydraulic Fracturing. *SPE Prod & Oper* **31** (4): 318-324. SPE-175762-PA. https://doi.org.ezproxy.library.tamu.edu/10.2118/175762-PA.

Zhang, L., Zhou, J., and Hui, P. 2005. A Comparative Study on Viscosity Behavior of Water-Soluble Chemically Modified Guar Gum Derivatives with Different Functional Lateral Groups. *J. Sci. Food Agric* **85** (15): 2638-2644. https://doi.org/10.1002/jsfa.2308.

3. NEW INSIGHTS INTO HYDRAULIC FRACTURING FLUIDS USED FOR HIGH-TEMPERATURE WELLS*

3.1. Abstract

Current interest in deep, low-permeability formations (< 10 md) demands accelerated development of high-temperature hydraulic fracturing technologies. Conventional guar systems break down above 300°F and require higher polymer loadings to maintain thermal stability. However, higher polymer loadings generate more residue and damage to the proppant pack and the formation. To resolve these problems, a variety of high-temperature stabilizers are added to enhance the thermal stability of these fracturing fluids at temperatures above 300°F. The focus of this work is to: (1) identify those additives that best enhance temperature stability of fracturing fluids and (2) study the rheological influence of incorporating these additives on the fracturing fluid systems.

The experimental fracturing-fluid solutions were prepared at a total polymer concentration of 30 and 40 lb/1,000 gal. Additives such as synthetic polymer, oxygen scavengers, crosslinkers, crosslinker delay additives, and pH buffers were examined in this work. Hydrated polymer solutions were crosslinked with a metallic crosslinker between 200-400°F. Viscosity measurements were carried out in a high-pressure/high-temperature (HP/HT) rheometer to evaluate rheology and thermal stability.

* Part of this chapter is modified with permission from "New Insights into Hydraulic Fracturing Fluids used for High-Temperature Wells" by Almubarak, T., Li, L., Ng, J. et al. 2021. Petroleum 7 (1): 70-79. Copyright 2021 by Elsevier.

Results show that adding a synthetic polymer and a crosslinker with the slowest reaction rate improves the fracturing fluid thermal stability. Of the three other additives tested, oxygen scavengers showed the greatest enhancement to thermal stability while pH buffers showed the least. Through the addition of high-temperature stabilizing additives, the fracturing fluid in this work was able to maintain a stable performance at temperatures up to 400°F.

Maintaining the thermal stability of fracturing fluids at a lower polymer loading remains a challenge in the industry. This work proposes techniques that can be used to enhance the thermal stability of fracturing fluids. Deeper knowledge about these different techniques will allow for better additive development and application in the field.

3.2. Introduction

Hydraulic fracturing fluids are pumped at high pressures to break down the rock and carry proppant inside the generated fractures. With the recent expansion of exploration technologies, many potential wells are located in high-temperature formations. As part of the fracturing fluids, polymers, crosslinkers, and other chemicals are added to the solution to generate the required elastic and viscous properties to carry the proppant downhole. For example, carboxymethyl hydroxypropyl guar (CMHPG) is a negatively charged polysaccharide-based biopolymer that is commonly used. CMHPG is produced by treating guar with both propylene oxide and chloroacetic acid, **Fig. 3-1** (Venkataiah and Mahadevan 1982; Pashaand Ngn 2008). Guar is derivatized to CMHPG to reduce impurities, increase pH tolerance, and improve temperature stability. These properties enable CMHPG to work as an excellent polymer for fracturing fluids in a variety of formations.

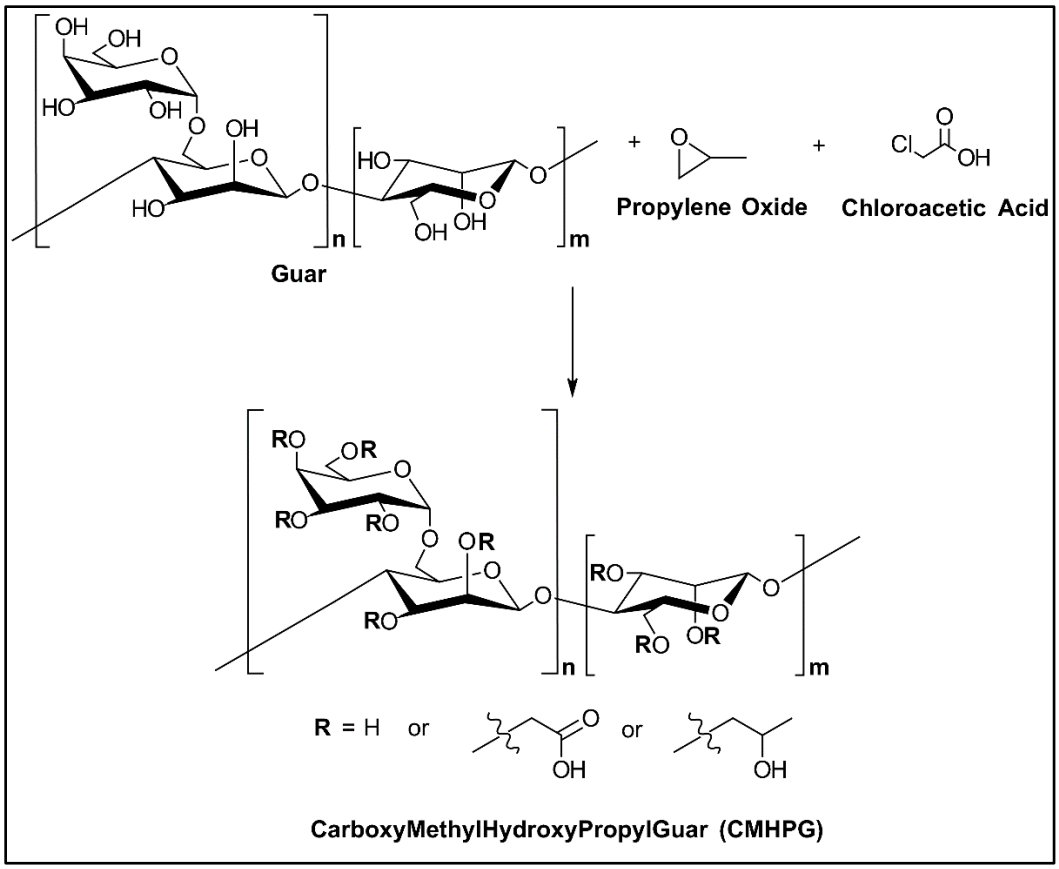

Fig. 3-1 Derivatization of guar to CMHPG.

At high temperatures (> 300°F), polymers, especially polysaccharides, thermally degrade, resulting in a loss of viscosity, which ultimately causes early proppant screen-out and failure in treatments. Therefore, measures must be taken to prevent the thermal degradation of the polymer. This loss in viscosity results from thermal degradation that occurs when polymer chains or the 3D crosslinked polymer structures break down. Thermal stability in polymers depends on the crosslinking bonds between the polymer and the crosslinker, and the bonds between the monomers in the backbone of the polymer chain. In the case of polysaccharides, the polymer backbone weakness resides in the glycosidic bonds linking mannose structures. Polysaccharide glycosidic (acetal) linkages

are susceptible to degradation through hydrolysis (Picout et al. 2001; Weaver et al. 2003; Vega-Cantu et al. 2006). At high temperatures, oxygen, free radicals, and protons accelerate the degradation of these bonds (Glass et al. 1983; Harms et al. 1984; Walker et al. 1995; Chetan and Songire 2015; Zhu et al. 2017). Some cases, such as the presence of hydrogen bonds, have shown an increase in the resistance of polymers to thermal oxidation by changing the conformation of polymers in solution (Glass et al. 1983).

For synthetic polyacrylamide-based polymers, specialty monomers such as 2-acrylamido-2-methylpropane sulfonic acid (AMPS) can be added to the chain to improve its thermal stability, salt resistance, and shear tolerance (Sigale and Omari et al. 1997). Several researchers have investigated this monomer using different terpolymers by incorporating AMPS at a concentration between 0-80%. Results published in the literature show that a concentration of 60% AMPS worked well in a polymer structure containing 0.5% acrylic acid, whereas a concentration of 80% AMPS performed worse (Funkhouser and Norman 2003). In some cases, depending on the other monomer choices, certain concentrations of AMPS did not produce a crosslinkable polymer structure. These results show that the concentration of AMPS has to be properly optimized in the polymer structure prior to any application. The addition of AMPS was also shown to enhance salt tolerance due to the position of the sulfonated molecule being a few atoms away from the polymer backbone structure, thus shielding the acrylic acid monomers from cations and giving them more freedom to crosslink with the intended crosslinker. Researchers have further shown the ability to use AMPS-containing polymers in solutions of 2 wt.% KCl where the similar polymer will readily precipitate in the absence of AMPS (Funkhouser

and Norman 2006; Holtsclaw and Funkhouser 2010). In addition, AMPS has been proven to provide delayed crosslinking behavior in water shut off treatment designs giving the fluid more time to go deep in theformation before crosslinking (Jayakumar and Lane 2013). The AMPS monomer also shows exemplary temperature-enhancement capabilities and shear tolerance by providing stiffness to the polymer structure due to the short branch generated by adding this monomer. The influence of AMPS was also studied over a range of temperatures up to 450°F with the addition of high-temperature stabilizers and exhibited a stable performance at these conditions (Funkhouser et al. 2013; Gupta and Carman 2011; Prakash et al. 2014; Song and Yang 2016).

The most common high-temperature stabilizers in the oil and gas industry are oxygen scavenging compounds. Oxygen scavengers such as chalcogen heterocyclic compounds protect the polymer at high temperatures from oxidation. They do so by donating electrons to reduce molecular oxygen to the -2 oxidation state (Gupta and Carman 2004). Examples of oxygen scavengers include methanol, sodium thiosulfate, and hydrosulfite. Care must be taken in selecting the appropriate oxygen scavenger, as the by-products formed by the scavenger must not interfere with the viscosity of the polymer. For this reason, oxygen scavengers should be tested with the treatment fluid to assess compatibility on a case-by-case basis. This is typically done using routine jar tests, rheometer, and fracture conductivity or coreflooding measurements (Jaffer et al. 2006; Fink 2013).

Buffers can also influence the thermal stability of polymers used in fracturing fluids. LaGrone et al. 1985 shows a positive correlation between basicity and the viscosity

of biopolymer solutions at high temperatures. At low pH, acid-catalyzed hydrolysis of the glycosidic bonds in polysaccharides occurs, causing a loss in viscosity. However, using high-pH fluids can result in formation damage and can negatively impact and limit the choice and subsequent performance of crosslinkers. Examples of buffersinclude amines, hydroxide, carbonate/bicarbonate solutions, and acetic acid/acetate solutions (Montgomery 2013).

Conventional fracturing fluids use borate-based crosslinkers due to their low cost, simplicity, and re-healing characteristic. Borate crosslinked systems may not perform well at high temperatures because of the changes in pH and the associated reduction of the concentration of monoborate ions (MBI) in solution (Harris 1993). Strong buffers are typically required to resolve this issue by maintaining a pH > 9 at these high temperatures. On the other hand, metallic crosslinkers form stronger bonds that are stable over awider range of conditions. Metallic crosslinkers are cheap, highly reactive with commonly used polymers, work well at pH ranges of 3-12, are stable at higher temperatures up to 450°F, can handle high salt concentrations, and have been successfully tested with produced waters (Putzig 2012; Hurnaus and Plank 2015, 2016; Prud'homme et al. 1988). However, metallic crosslinkers can be incompatible with other polymeric additives such as polymeric scale inhibitors and must be tested thoroughly (Almubarak et al. 2019a). They should be avoided when enzyme breakers are used because they can denature the enzymes (Li et al. 2009, 2010). Metallic crosslinkers are known to be shear sensitive, the crosslinking bonds can break due to mechanical shear, and the crosslinking bonds are irreparable once broken (Prud'homme et al. 1988, 1989).

To increase the resistance of the crosslinking bonds to the shear rate at high temperatures, the crosslinking reaction time with the polymer can be delayed. Delaying the crosslinking reaction reduces the number of crosslinked bonds formed initially and thus reduces the number of bonds that are irreversibly broken (Lord and Yaritz 1993). Crosslinker delayers can be incorporated through the manufacturing process of metallic crosslinkers by choosing the appropriate ligand combination (Harry et al. 1997, 1999; Moorhouse et al. 1998; Montgomery 2013; Sokhanvarian et al. 2019). By selecting the appropriate ligand-to-metal complex, the reaction rate of the metal crosslinkers can be controlled. Inaddition to the choice of crosslinker ligands, external additives such as polyols can be used to delaycrosslinking. Polyols such as sorbitol, fructose, and gluconic acid, and their related derivatives, act as high-temperature stabilizers by undergoing preferential crosslinking in place of the polymer (Back et al. 1979; Kaushik and Baht 1998).

Related advances in hydraulic fracturing include the ability to produce acceptable rheological properties with alternative water sources such as seawater and produced water (Almubarak et al. 2019a; Li et al. 2016a, 2016b). Other examples of innovation in this field include incorporating nanoparticles and nanocrosslinkers in fracturing fluids to enhance properties such as high-temperature stability and reducing polymer loading (Hurnaus and Plank 2015, 2016; Liang et al. 2017). However, there is still room for improvement in the area of high-temperature fracturing fluid application. This work quantifies the high-temperature limitations of conventional fracturing fluids and proposes multiple ways to resolve these issues by using high-temperature stabilizer additives such

as slow-reacting crosslinkers, crosslinker delayers, oxygen scavengers, and buffers. The work compares the performance of these additives to realize the impact and the possible combinations to develop more efficient high-temperature fracturing fluid solutions.

3.3. Experimental Procedures

3.3.1. Materials

CMHPG polymer powder and three zirconium crosslinkers with varying crosslinking reaction rates (slow: zirconium lactate and propylene glycol, medium: zirconium lactate and triethanolamine, and fast: zirconium lactate; all at 5.5-6 wt.% ZrO_2) were provided by a service company. The rheological behavior of these crosslinkers has been studied in detail (Almubarak et al. 2020). The slow-reacting crosslinker was used for the majority of the tests in this work. The medium- and fast-reacting crosslinkers were only used for comparison in the crosslinker choice experiments. The synthetic polyacrylamide-based polymer was provided in emulsion form (30 wt% active) and was used as received. The synthetic polymer is composed of acrylamide (AM), acrylic acid (AA), and AMPS (**Fig. 3-2**). Sodium thiosulfate pentahydrate and the crosslinking delay additives (sugar alcohol derivatives) were provided by a chemical company and used as received. Tetraethylenepentamine (TEPA) and acetic acid were provided at 99 wt% purity and used as received. Acetic acid and sodium acetate buffer was provided at 30 wt% and was used as received. Houston tap water (< 500 ppm) was used to mix all the systems.

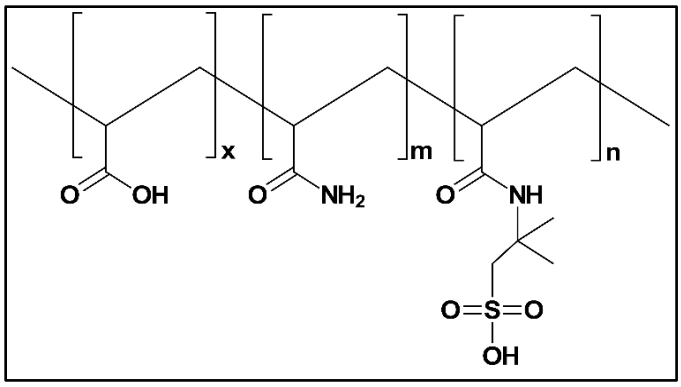

Fig. 3-2 Synthetic polymer composition (AA-AM-AMPS).

3.3.2. Fluid Preparation

The fracturing fluids were prepared, mixed, and tested within 12 hours; for that reason, no biocide was used. The 40 lb/1,000 gal fracturing fluid was prepared by adding 3.84 g of CMHPG powder to 800 cm^3 of tap water. The solution was mixed for 20 minutes at 800 RPM to achieve full hydration. For the experiment where synthetic polymer was incorporated, the fluids were prepared following the procedure in Almubarak et al. 2019b. After preparing the base gel, the fluid was transferred to the blender, and external high-temperature additives were added as needed and mixed thoroughly for 5 minutes at 200-400 RPM. The pH of the solution was adjusted by adding an appropriate amount of TEPA for the pH 10 tests, and acetic acid for the pH 5 tests. Zirconium crosslinkers were added last and mixed thoroughly for 30 seconds.

3.3.3. HP/HT Rheometer

An HP/HT rheometer was used to measure the apparent viscosity of the fracturing fluids at 200-400°F. The rheometer utilized R1/B5 bob and rotor combination, which requires a sample volume of 52 cm^3. The rheometer uses an electric jacket for heating; a

temperature sensor is mounted on the stator/bob to control sample temperature. A pressure of 350-500 psi was applied with nitrogen gas to prevent the boiling of the sample.

Viscosity measurements were taken under different shear rates to simulate the flow of the fracturing fluid through production tubular, perforations, and inside the created fracture. ISO13503-1 schedule was followed, where the shear rate schedule was set to 100 s^{-1} with short shear ramp spikes between 25 and 100 s^{-1}. The heater was preheated to 150°F before running the tests to ensure quick and consistent heating profiles. The fluid took 10-20 minutes to reach the testing temperature.

3.4. Results and Discussion

3.4.1. Fracturing Fluid Temperature Limits

The viscosity measurements of 40 lb/1,000 gal crosslinked CMHPG at 200-400°F and pH 5 is seen in **Fig. 3-3**. The results show that CMHPG can hold a stable viscosity performance up to 250°F with no additives at this pH. At temperatures above 250°F, the performance of CMHPG-based fracturing fluid deteriorates due to thermal and shear degradation. The performance of CMHPG was also found to vary proportionally with pH (**Fig. 3-4**). **Fig. 3-5** shows the influence of high temperature (300°F) on the crosslinked viscosity at 15, 20, 30, and 40 lb/1,000 gal of CMHPG.

CMHPG contains carboxymethyl groups that have a pKa of 3.5-4 at 77°F and partially deprotonate at pH 5 (Dogsa et al. 2014; Nová et al. 2017). The amount of intermolecular hydrogen bonding at pH 5 is influenced by the carboxymethyl content, which is typically low in industrial CMHPG (Szopinski et al. 2015). High-temperature and low-intermolecular hydrogen bonding influence the structural orientation of the

polymer (Finney and Soper 1994). This orientation could allow easier access for oxygen to attack the backbone. An attack on the polymer backbone would cleave the polymer chain and cause significant viscosity loss. Additionally, the polymer chains vibrate more at high temperatures, which becomes more pronounced at low polymer concentrations and weak hydrogen bonding (Bradley et al. 1988; Kök et al. 1999). This reduces viscosity and influences the thermal stability as well.

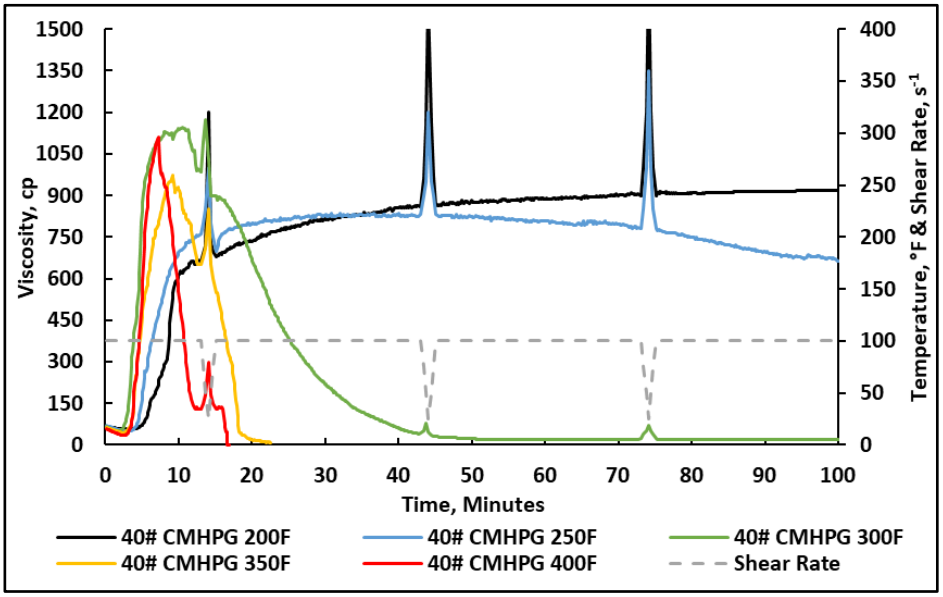

Fig. 3-3 Viscosity at 40 lb/1,000 gal CMHPG fracturing fluid, 4 gpt crosslinker, pH 5, 200-400°F.

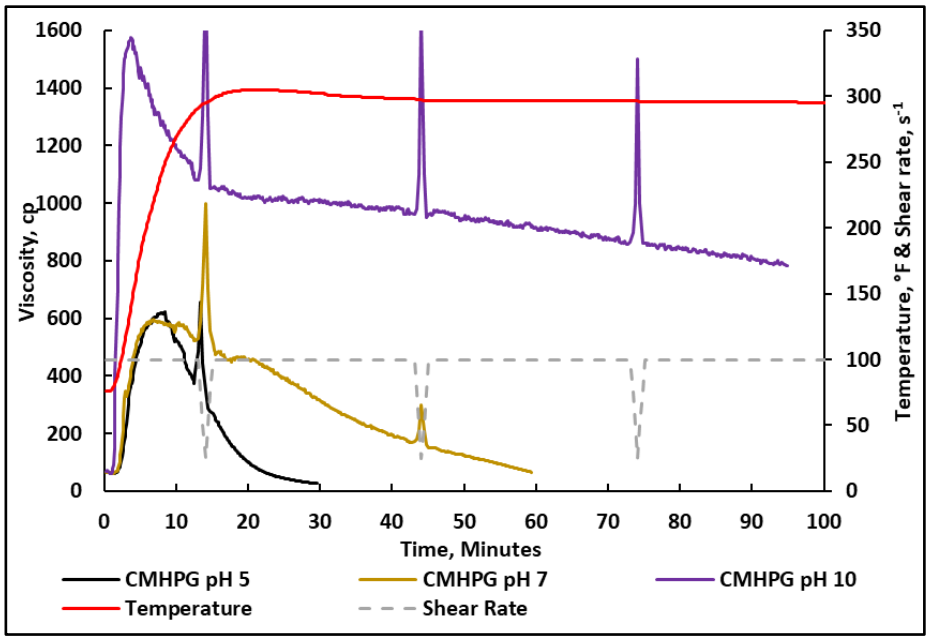

Fig. 3-4 Viscosity at 40 lb/1,000 gal CMHPG fracturing fluid, 2 gpt crosslinker, pH 5-10, 300°F (Almubarak et al. 2019b).

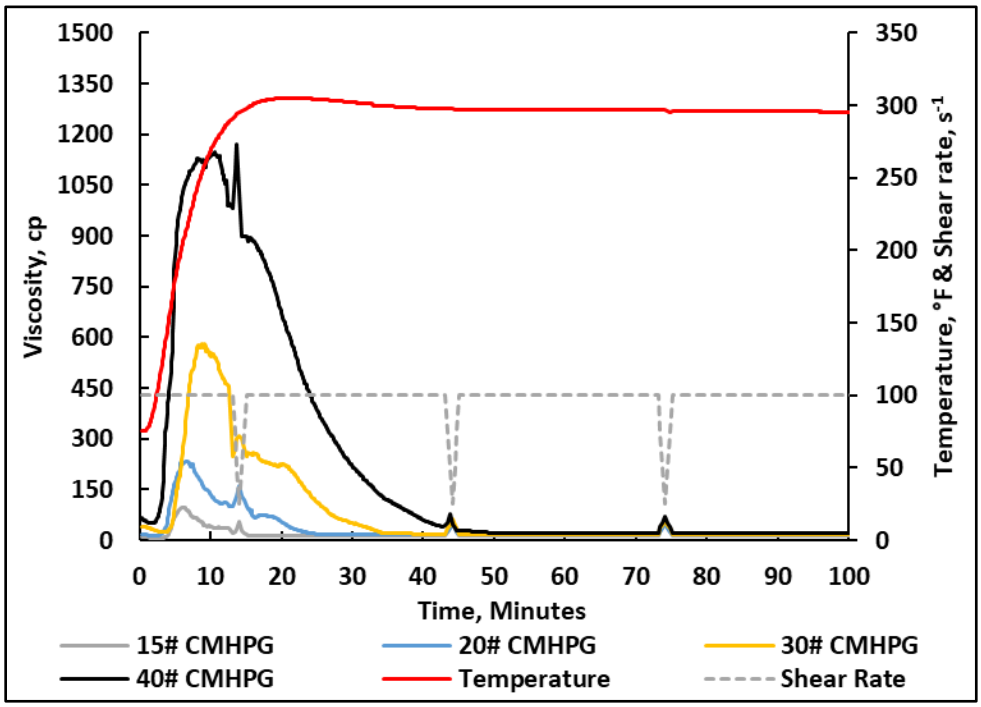

Fig. 3-5 Viscosity at 15, 20, 30, and 40 lb/ 1,000 gal CMHPG, 4 gpt crosslinker, pH 5, 300°F.

3.4.2. Addition of Sodium Thiosulfate

Sodium thiosulfate is commonly used as a high-temperature stabilizer. **Fig. 3-6** shows the effect of various concentrations of sodium thiosulfate on the thermal stability of CMHPG at 300°F. At this temperature, the performance of CMHPG alone is similar to those containing sodium thiosulfate. 40 ppt sodium thiosulfate was observed to have a negative impact on the solution. Sodium thiosulfate enhances the thermal stability of polymers by scavenging oxygen from the system, thereby preventing oxidation of the polymer backbone. However, sodium thiosulfate contains sodium ions that can screen the polymer negative charges. Under low pH and high-temperature conditions, it causes the collapse of the extended and deprotonated polymer conformation. Therefore, sodium thiosulfate does not improve rheological performance at these conditions (Khokhlov et al. 1993).

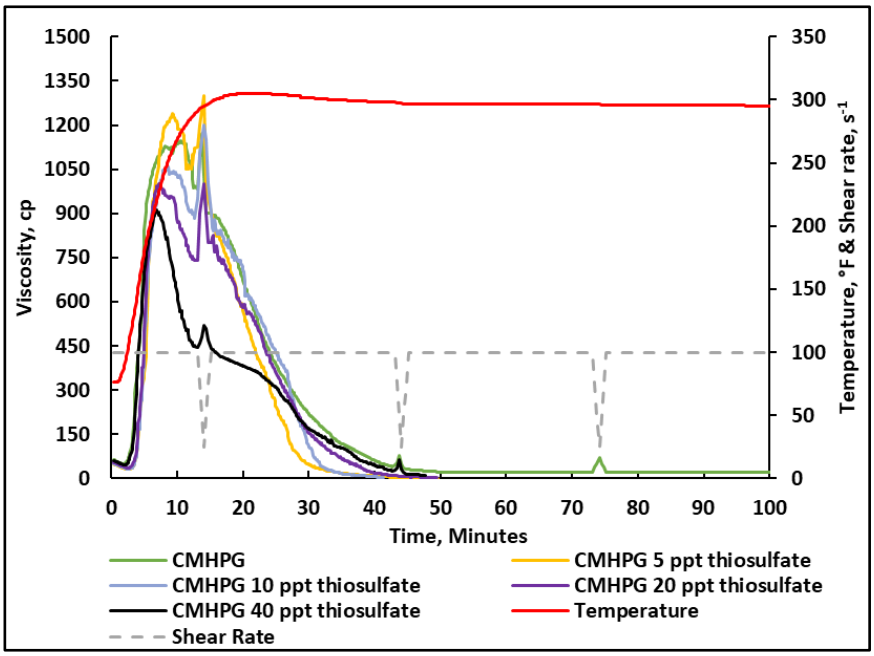

Fig. 3-6 Viscosity at 40 lb/1,000 gal to evaluate sodium thiosulfate HT stabilizer, 4 gpt crosslinker, pH 5, 300°F.

3.4.3. Addition of Synthetic Polymer

Synthetic polymer was added to CMHPG in the fracturing fluid to enhance the properties of CMHPG (Li 2009). **Fig. 3-7** shows the viscosity results for the 40 lb/1,000 gal crosslinked fracturing fluid viscosity. The addition of synthetic polymer increased the thermal stability of the fracturing fluid. The synthetic polymer increases the intermolecular hydrogen bonds, which would ultimately change the structural orientation of CMHPG in solution. Researchers proved the existence of hydrogen bonding between the two polymers through Fourier-transform infrared spectroscopy (FTIR) measurements (Almubarak et al. 2019b). Even if the glycosidic bond in CMHPG is cleaved, the intermolecular associations can hold the structure in shape and maintain viscosity for a longer time (Stokke et al. 1992).

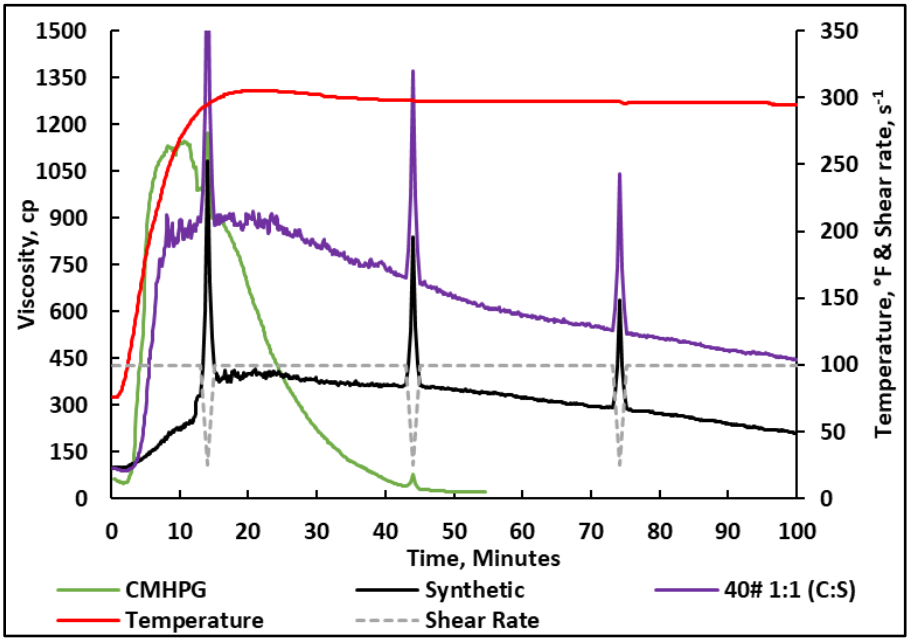

Fig. 3-7 Viscosity at 40 lb/1,000 gal fracturing fluid, 4 gpt crosslinker, pH 5, 300°F.

The acrylic acid monomer in the synthetic polymer has a pKa of 4-5 at 77°F (Ibarra-Montaño et al. 2015; Swift et al. 2016), while the AMPS monomer has a pKa of 1-2 (Kabiri et al. 2010; Atta et al. 2010). At pH 5 the polymer is sufficiently deprotonated. Even though the AMPS monomer is deprotonated, it does not contribute directly to the crosslinking reaction (Sigale and Omari 1997). These pH conditions allow for changes in the conformation of the polymer in solution, adding stiffness and thermal stability, as observed in **Fig. 3-8** (Jamshidi and Rabiee 2014). Therefore, the presence of the synthetic polymer eliminates the need for additional temperature stabilizers in the fracturing fluid systems at 300°F.

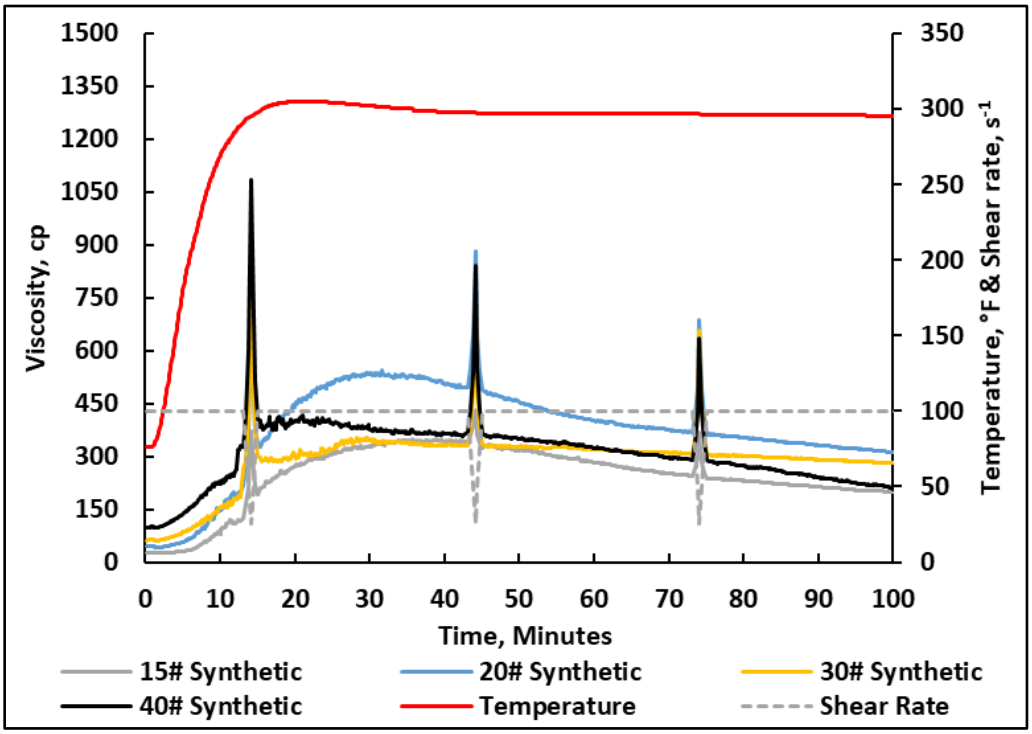

Fig. 3-8 Viscosity at 15, 20, 30, and 40 lb/ 1,000 gal synthetic polymer, 4 gpt crosslinker, pH 5, 300°F.

3.4.4. Effect of CMHPG: Synthetic Polymer Ratio

Fig. 3-9 compares the thermal stability for CMHPG: Synthetic ratios between 2:1 and 1:2 fracturing fluid systems at 30 and 40 lb/1,000 gal. A pronounced viscosity slope decline is seen when the ratio of CMHPG is dominant compared to when the synthetic polymer is dominant in the mixture. This decline results from the weak thermal stability of CMHPG at these conditions. The thermal stability of the fracturing fluid is improved when the synthetic polymer concentration is dominant in the mix.

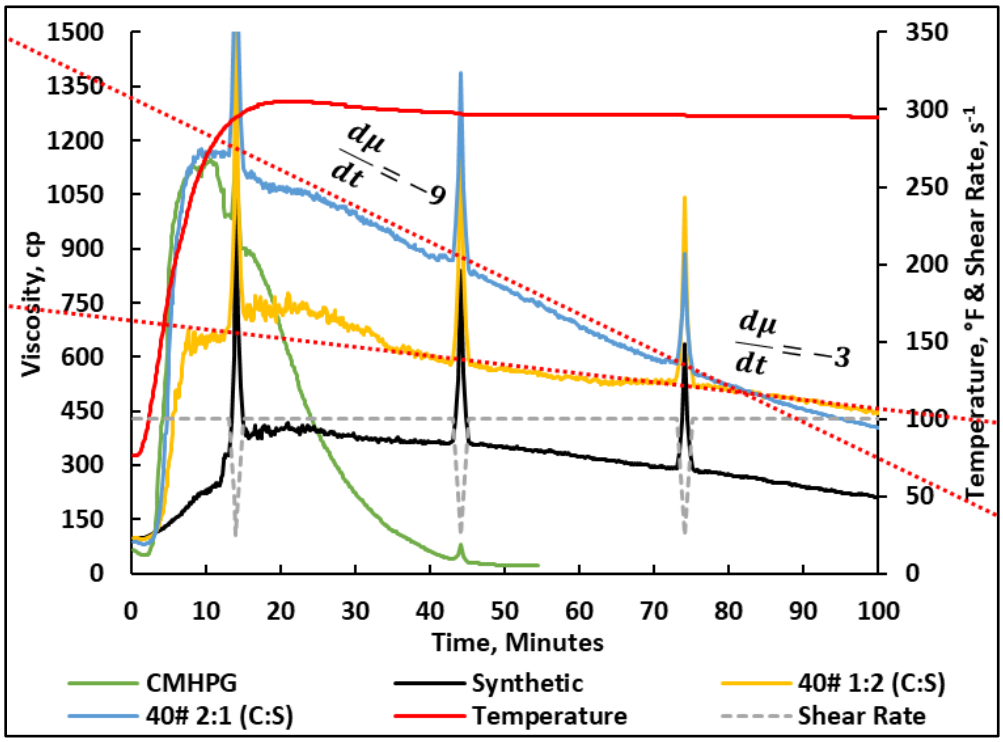

Fig. 3-9 Viscosity at 40 lb/ 1,000 gal 1:2 and 2:1 (CMHPG: Synthetic) fracturing fluid, 4 gpt crosslinker, pH 5, 300°F.

3.4.5. Performance above 300°F

Different ratios of the fracturing fluid were tested at temperatures above 300°F to assess its thermal stability limits. **Figs. 3-10** and **3-11** show the measured viscosity of 40

lb/1,000 gal 1:1 and 1:2 (CMHPG: Synthetic) fracturing fluid at temperatures between 300-400°F. Both ratios show a good performance up to 350°F. Beyond 350°F, a significant decrease in rheological performance is observed.

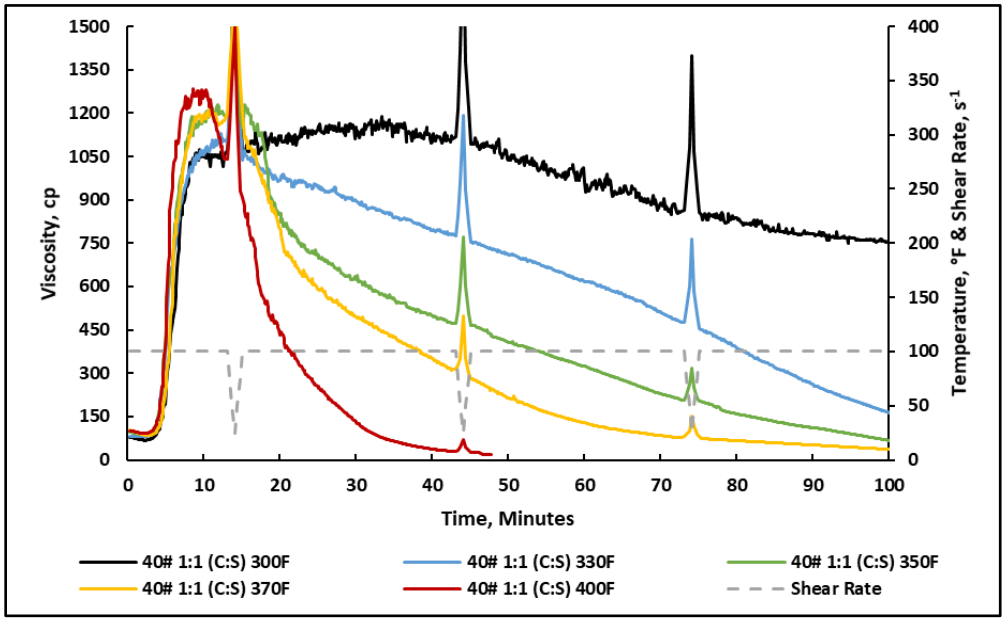

Fig. 3-10 Viscosity at 40 lb/1,000 gal 1:1 (CMHPG: Synthetic) fracturing fluid, 5 gpt crosslinker, pH 5, 300-400°F.

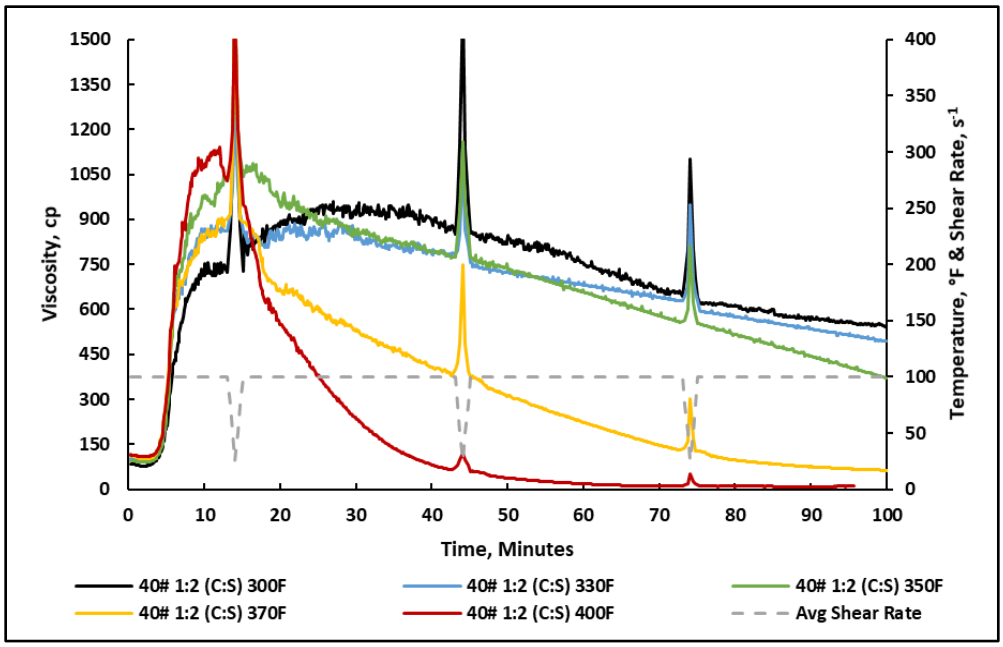

Fig. 3-11 Viscosity at 40 lb/1,000 gal 1:2 (CMHPG: Synthetic) fracturing fluid, 5 gpt crosslinker, pH 5, 300-400°F.

Figs. 3-12 and **3-13** compare the viscosity of 1:1 and 1:2 (CMHPG: Synthetic) fracturing fluid at 330 and 350°F, respectively. These results show that the 1:2 (CMHPG: Synthetic) fracturing fluid is more thermally stable than the 1:1 (CMHPG: Synthetic) ratio.

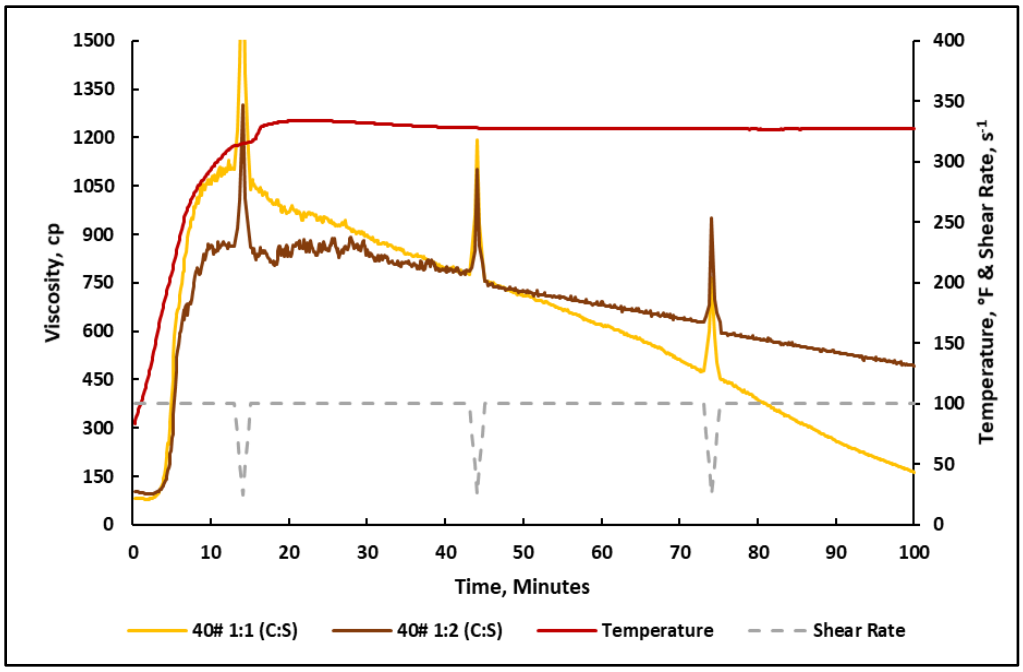

Fig. 3-12 Viscosity at 40 lb/1,000 gal 1:1 and 1:2 (CMHPG: Synthetic) fracturing fluid, 5 gpt crosslinker, pH 5, 330°F.

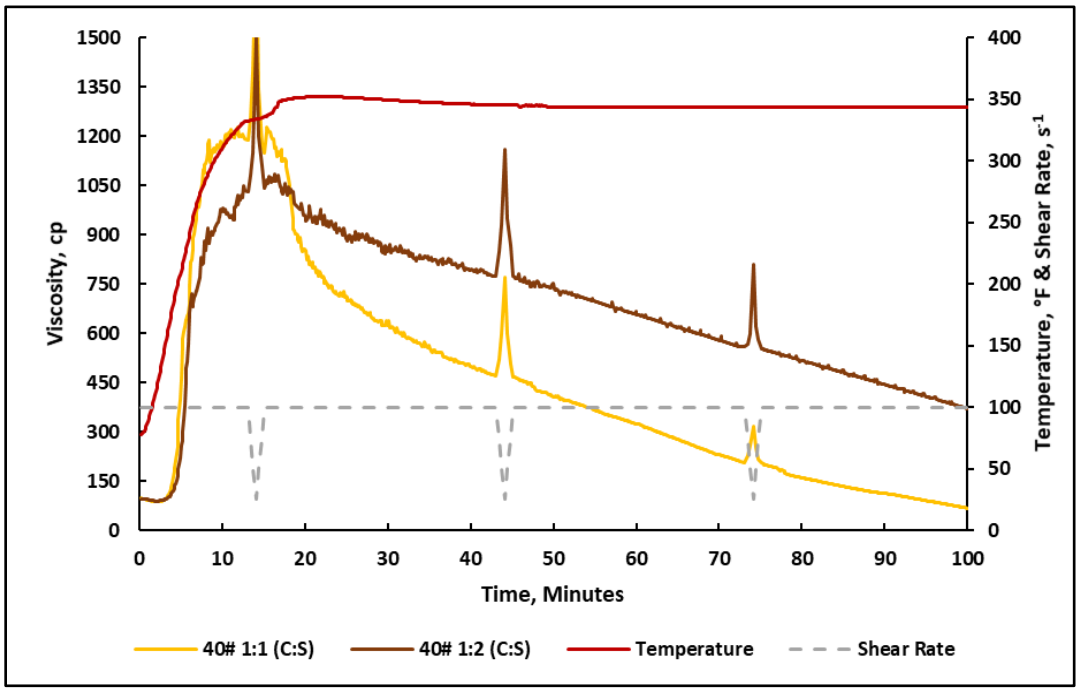

Fig. 3-13 Viscosity at 40 lb/1,000 gal 1:1 and 1:2 (CMHPG: Synthetic) fracturing fluid, 5 gpt crosslinker, pH 5, 350°F.

3.4.6. Polymer Loading Reduction above 300°F

To reduce the damage from polymers, a lower loading of a 30 lb/1,000 gal fracturing fluid was tested. The 1:2 (CMHPG: Synthetic) ratio fluid was able to maintain good viscosity and, similar to the 40 lb/1,000 gal, was thermally stable up to 350°F, as shown in **Fig. 3-14**.

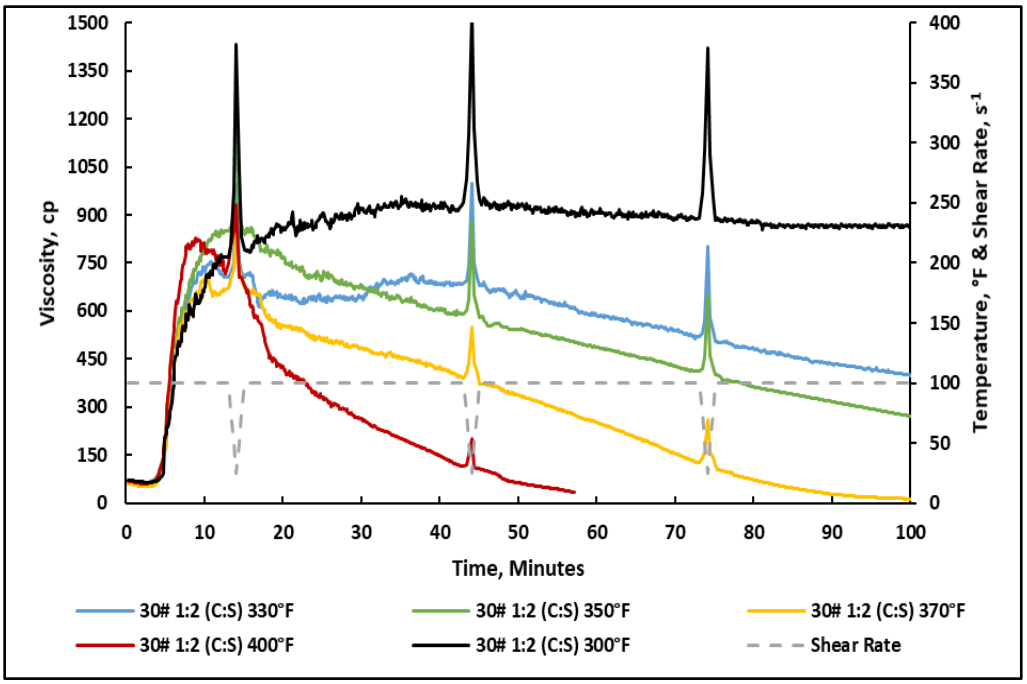

Fig. 3-14 Viscosity at 30 lb/1,000 gal 1:2 (CMHPG: Synthetic) fracturing fluid, 6 gpt crosslinker, pH 5, 300-400°F.

3.4.7. Other Additives to Enhance Thermal Stability

Polymer thermal stability in crosslinked fracturing fluids depends on two types of bonds (Prakash et al. 2014) that include the following: 1) The crosslinking bonds between the polymer and the crosslinker, and 2) The monomer to monomer bonds in the polymer backbone structure.

The thermal stability in the fracturing fluid can be enhanced by reducing the damage to these two main types of bonds. Many additives can be categorized as HT stabilizers; however, the different functions of these additives, at a proper combination, can be used to protect multiple bond types and, therefore, enhance the performance at temperatures above 350°F.

3.4.7.1. Crosslinkers

The crosslinking bond can be protected against shear to some degree by using a slow-reacting crosslinker. The reaction rate of crosslinkers can be controlled by using ligands that generally consist of lactate, triethanolamine, propylene glycol, etc. The order, type, and the number of ligands in the crosslinker composition can influence the crosslinking reaction rate and high viscosity generation. **Figs. 3-15** and **3-16** show the viscosity measurements using three types of crosslinkers that vary in the crosslinking reaction rate crosslinkers (slow, medium, and fast), measured at 370 and 400°F, respectively. The results show that a slow-reacting crosslinking will enhance thermal stability by minimizing shear degradation.

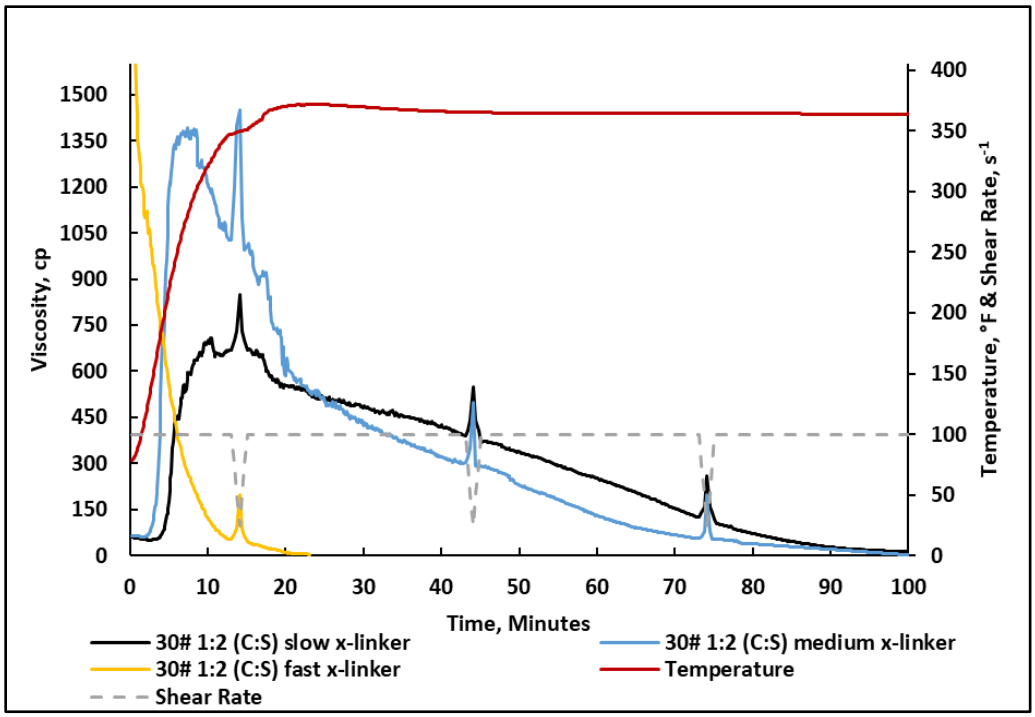

Fig. 3-15 Zirconium crosslinker type comparison on 30 lb/1,000 gal 1:2 (CMHPG: Synthetic) fracturing fluid viscosity, equivalent Zr to 6 gpt crosslinker, pH 5, 370°F.

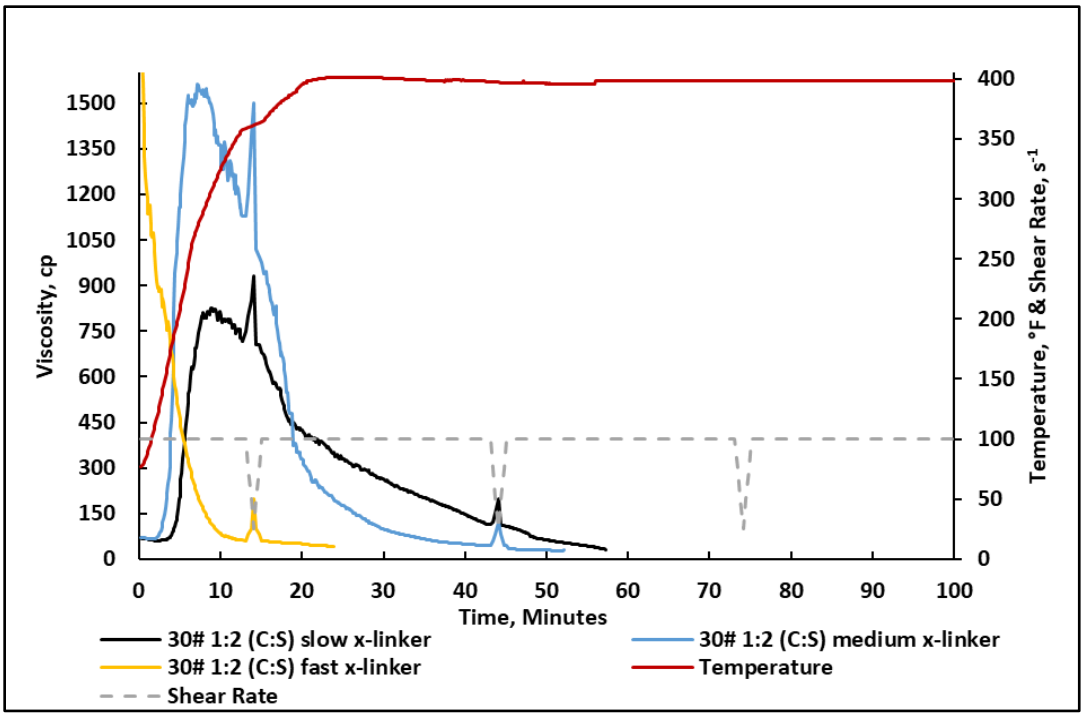

Fig. 3-16 Zirconium crosslinker type comparison on 30 lb/1,000 gal 1:2 (CMHPG: synthetic) fracturing fluid viscosity, equivalent Zr to 6 gpt crosslinker, pH 5, 400°F.

3.4.7.2. Crosslinking Delay Additives

To protect the crosslinking bond further, an external delay additive can be used. This additive contains similar functional groups to the fracturing fluid polymer and is engineered to favorably bond with the crosslinker. Delay additives would, therefore, restrict the amount of the crosslinker interacting with the polymer, and they would break or release the crosslinker to the fracturing fluid polymer over a longer period of time, to maintain a stable viscosity performance. **Figs. 3-17** and **3-18** show the viscosity measurements of the slow-releasing crosslinker base case compared to a slow-releasing crosslinker with the external crosslinking delay additive at 370 and 400°F, respectively. With the external crosslinking delay additive, the initial crosslinking is suppressed, resulting in lower initial fluid viscosity. This delay, in turn, places the crosslinking bonds

under less shear damage and increases the long-term stability of the fluid's viscosity. The results show that the external delay additive will enhance thermal stability performance by controlling the crosslinking reaction and minimizing shear degradation to a greater extent. The tested delay additive showed a slightly higher initial viscosity profile at 400 compared to 370°F, showing that the controlled release is weakened at higher temperatures.

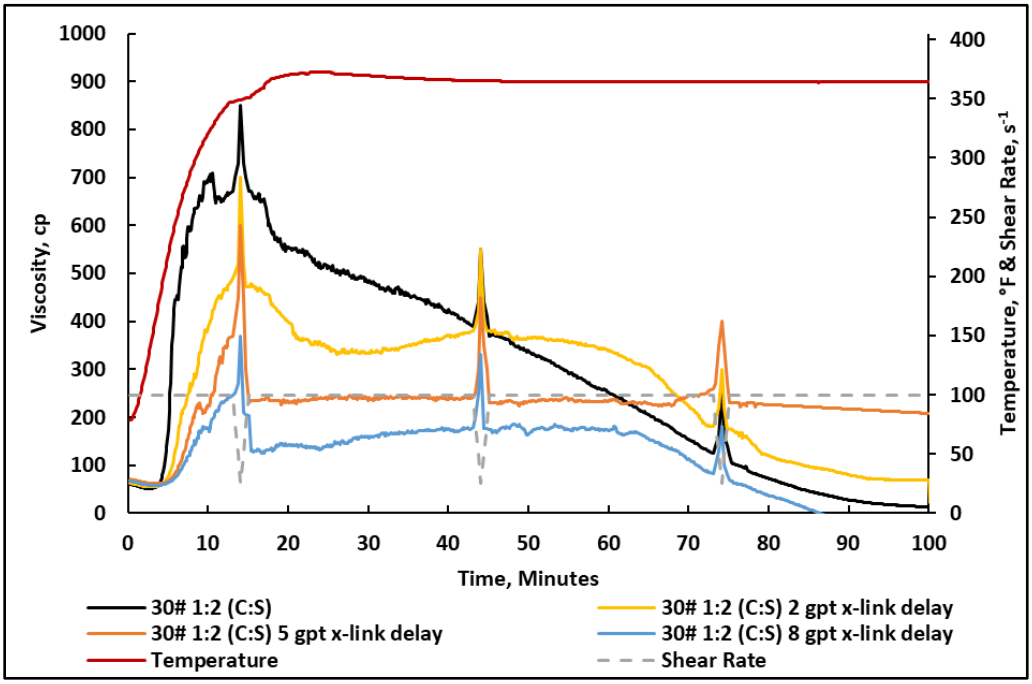

Fig. 3-17 Crosslinker delayer influence on 30 lb/1,000 gal 1:2 (CMHPG: Synthetic) fracturing fluid viscosity, 6 gpt crosslinker, pH 5, 370°F.

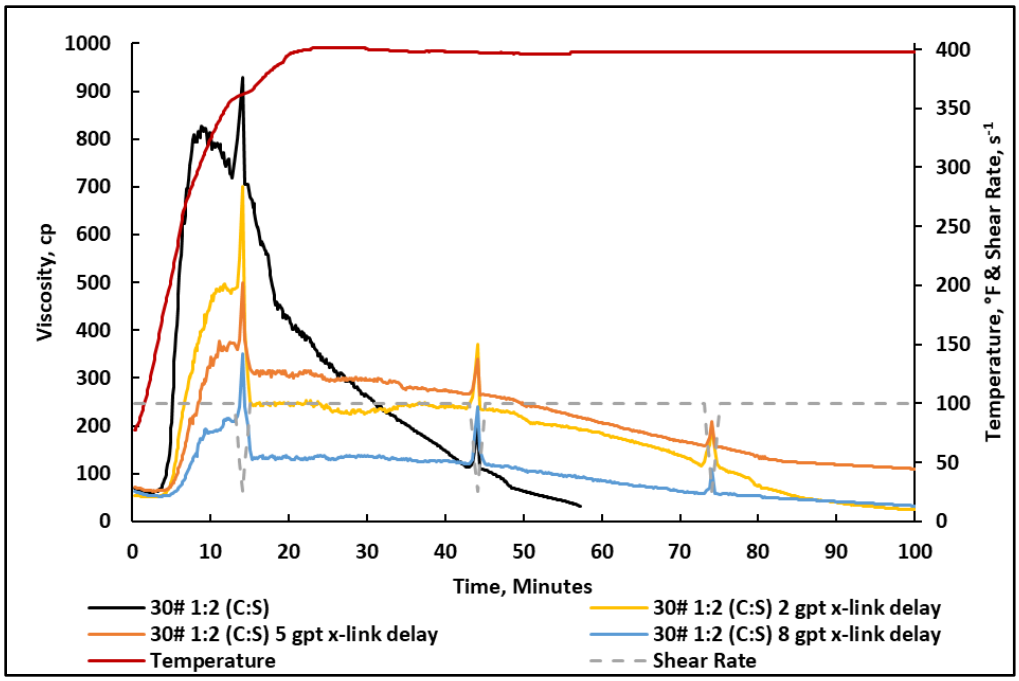

Fig. 3-18 Crosslinker delayer influence on 30 lb/1,000 gal 1:2 (CMHPG: Synthetic) fracturing fluid viscosity, 6 gpt crosslinker, pH 5, 400°F.

3.4.7.3. Oxygen scavengers

Dissolved oxygen in solution breaks down the polymer backbone bonds by undergoing several reactions that generate reactive radicals that can influence polymers in solution (Grollmann and Schnabel 1982; Kök 2007; Duan and Kasper 2011; Xiong et al. 2018). In addition, the polysaccharide molecular structure is thermally weak and can be easily cleaved at the glycosidic bond (Economides and Nolte 2000). To protect the polymer backbone bonds, reducing dissolved oxygen becomes important. Thiosulfate is a typical additive used to reduce oxygen in the solution. **Figs. 3-19** and **3-20** show the results of adding a sodium thiosulfate oxygen scavenger at 370 and 400°F, respectively.

The use of Sodium thiosulfate has some downsides such generating a notable concentration of H_2S at temperatures greater than 350°F (Ogunsanya and Li 2018). More

importantly, sodium thiosulfate will scavenge oxygen generated from the oxidizer breakers used and will interact with several other additives. These interactions have been observed to cause precipitation at 300°F (Almubarak et al. 2015). For that reason, the combination of thiosulfate high-temperature stabilizer and fracturing fluid additives must be thoroughly tested before field application.

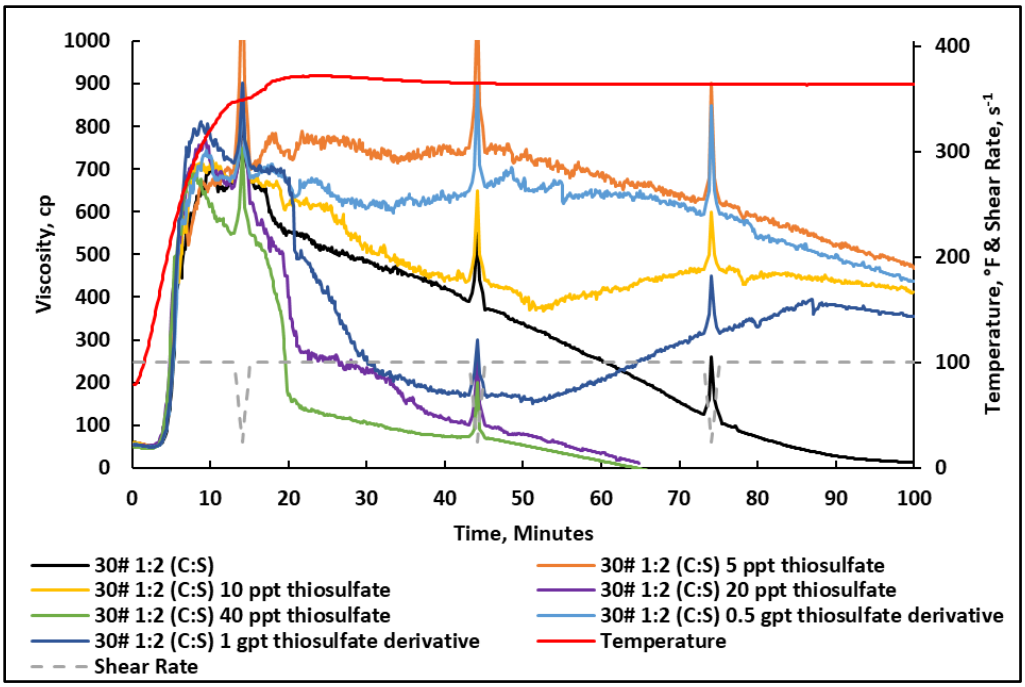

Fig. 3-19 Effect of oxygen scavenger on 30 lb/1,000 gal 1:2 (CMHPG: Synthetic) fracturing fluid viscosity, 6 gpt crosslinker, pH 5, 370°F.

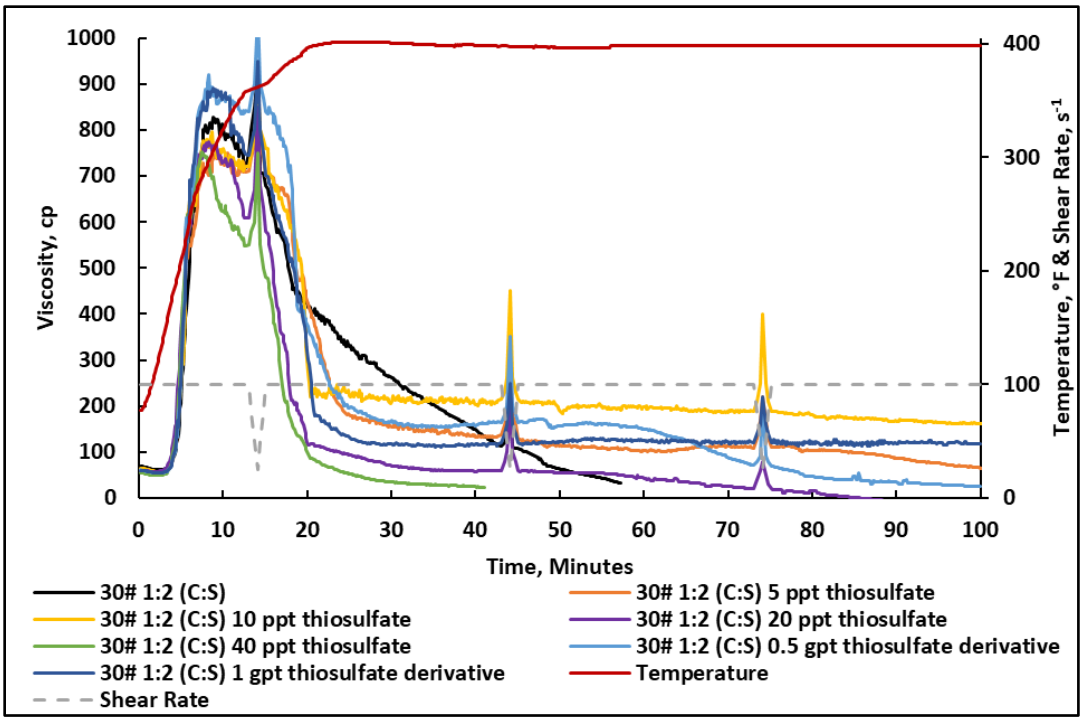

Fig. 3-20 Influence of oxygen scavenger on 30 lb/1,000 gal 1:2 (CMHPG: Synthetic) fracturing fluid viscosity, 6 gpt crosslinker, pH 5, 400°F.

3.4.7.4. pH Buffers

At high temperatures, the pH of the system is reduced because of a shift in the equilibrium of water dissociation (Langelier 1946). The pH change can influence the performance of many additives, including the reaction rate of crosslinkers. In addition, as the pH drops, the concentration of H+ in solution increases, and that can initiate hydrolysis reactions that would break the polymer backbone bonds and eventually reduces viscosity (Wolfenden et al. 1998). High pH systems are typically used to overcome this issue. However, lower pH fracturing fluid systems are frequently desired to reduce damage due to clays in the formation (Gdanski 2001, 2002), reduce hydroxide precipitation, and for compatible applications in acidic fracturing treatments. To maintain a stable viscosity at

lower pH, a pH buffer can be used. **Figs. 3-21** and **3-22** show the improved measured viscosity results with an acetic acid/acetate buffer at 370 and 400°F, respectively.

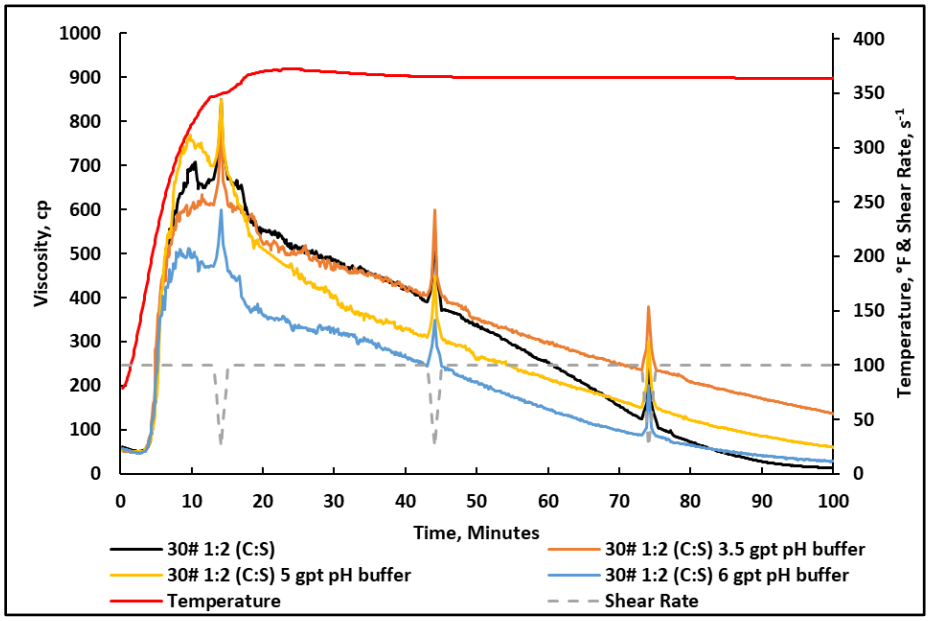

Fig. 3-21 pH buffer influence on 30 lb/1,000 gal 1:2 (CMHPG: Synthetic) fracturing fluid viscosity, 6 gpt crosslinker, pH 5, 370°F.

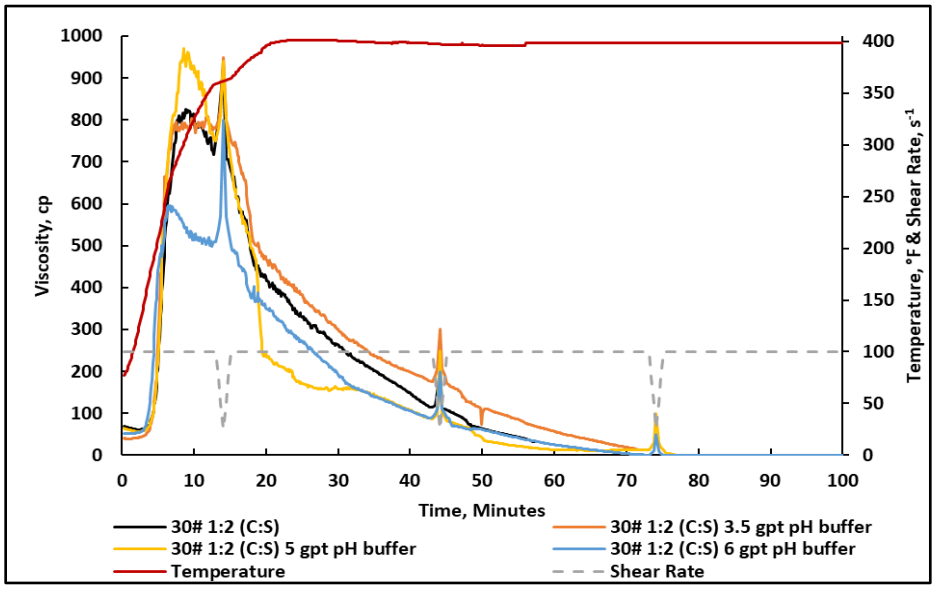

Fig. 3-22 pH buffer influence on 30 lb/1,000 gal 1:2 (CMHPG: Synthetic) fracturing fluid viscosity, 6 gpt crosslinker, pH 5, 400°F.

3.5. Conclusions

The main bonds that can influence the thermal stability of fracturing fluids are the polymer backbone bonds and the crosslinker-to-polymer bonds. This work presents different chemical techniques to enhance thermal stability in fracturing fluids. The tested fracturing fluid's thermal stability was enhanced by utilizing additives such as a synthetic polymer, slow-reacting crosslinkers, oxygen scavengers, crosslinking delay additives, and pH buffers.

The results of this research lead to the following conclusions:

1. Adding synthetic polymer (AA-AM-AMPS) to CMHPG can generate a stable 30 lb/1,000 gal fracturing fluids up to a temperature of 350°F.

2. The crosslinker-to-polymer bond can be protected at temperatures > 350°F by using a slow-reacting zirconium crosslinker.

3. The crosslinker-to-polymer bond can be further protected at temperatures > 350°F by adding an external crosslinking delay additive (sugar alcohol derivative).

4. Sodium thiosulfate can enhance thermal stability at temperatures > 350°F.

5. Acetic acid/acetate pH buffer adds minimal thermal stability at temperatures > 350°F.

6. Sodium thiosulfate does not add thermal stability in a 40 lb/1,000 gal pure CMHPG fracturing fluid system at pH ~5 and temperatures ≥ 300°F.

3.6. Recommendations

This work supports the combination of a slow-reacting crosslinker (Zr-lactate and propylene glycol) and an external crosslinking delay additive (sugar alcohol derivatives)

to achieve optimal shear tolerance and higher temperature stability performance at temperatures above 300°F for all polymer-based fracturing fluids.

Although the addition of oxygen scavengers showed excellent thermal stability, caution should be exercised in the addition of sodium thiosulfate pentahydrate in combination with pH buffers such as acetic acid/sodium acetate at pH 5 conditions because of the salt sensitivity of some polymers. This work further supports the addition of sodium thiosulfate pentahydrate at a maximum concentration of 10 ppt for pH 5 and 40 ppt for pH 10 conditions.

3.7. Acknowledgements

The authors thank Gia Alexander for editorial assistance in preparing this manuscript.

3.8. References

Almubarak, T., AlKhaldi, M., Ng, J. H. et al. 2019a. Design and Application of High-Temperature Raw-Seawater-Based Fracturing Fluids. *SPE J.* **24** (04): 1,929 - 1,946. SPE-195597-PA. https://doi.org/10.2118/195597-PA.

Almubarak, T., Ng, J. H., Nasr-El-Din, H. A. et al. 2019b. Dual-Polymer Hydraulic-Fracturing Fluids: A Synergy Between Polysaccharides and Polyacrylamides. *SPE J.* **24** (06): 2,635 - 2,652. SPE-191580-PA. https://doi.org/10.2118/191580-PA.

Almubarak, T., AlKhaldi, M., Panda, S. et al. 2015. Insights on Potential Formation Damage Mechanisms Associated with Hydraulic Fracturing. Presented at the International Petroleum Technology Conference, Doha, Qatar, 6-9 December. IPTC-18401-MS. https://doi.org/10.2523/IPTC-18401-MS.

Almubarak, T., Ng, J., Nasr-El-Din, H.A. et al. 2020. Zirconium Crosslinkers: Understanding Performance Variation In Crosslinked Fracturing Fluids. Presented at Offshore Technology Conference Asia, Virtual, 2 – 6 November, OTC-30381-MS.

Atta, A., Abd El Wahab, Z., ElShafey, Z. et al. 2010. Characterization and Evaluation of Acrylic Acid Co-2-Acrylamido-2-Methylpropane-1-Sulfonic Acid Hydrogel for Uranium Recovery. *J Dispersion Science & Technology* **31** (10): 1415-1422.

Back, J., Oakenfull, D., and Smith, M. 1979. Increased Thermal Stability of Proteins in the Presence of Sugars and Polyols. *Biochemistry* **18** (23): 5191-5196. https://doi.org/10.1021/bi00590a025.

Bradley, T., Ball, A., Harding, S. et al. 1988. Thermal Degradation of Guar Gum. *Carbohydrate Polymers* **10** (3): 205-214. https://doi.org/10.1016/0144-8617(89)90012-X.

Card, R., Nimerick, K., Marberry, J., et al. 1991. On-the-fly Control of Delayed Borate-Crosslinking of Fracturing Fluids US 5,877,127A.

Chetan, P. and Songire, S. 2015. A Sulfur-Free and Biodegradable Gel Stabilizer for High Temperature Fracturing Applications. Presented at the SPE North Africa Technical Conference and Exhibition, Cairo, Egypt, 14-16 September. SPE-175786-MS. https://doi.org/10.2118/175786-MS.

Dogsa, I., Tomsic, M., Orehek, J. et al. 2014. Amorphous Supramolecular Structure of Carboxymethyl Cellulose in Aqueous Solution at Different pH Values as Determined by Rheology, Small Angle X-Ray and Light Scattering. *Carbohydrate Polymers* **111** (1): 492-504.

Duan, J. and Kasper, D. 2011. Oxidative Depolymerization of Polysaccharides by Reactive Oxygen/Nitrogen Species. *Glycobiology* **21** (4): 401-409. https://doi.org/10.1093/glycob/cwq171.

Economides, M. and Nolte K. 2000. *Reservoir Stimulation*, Third Edition. John Wiley and Sons. Chichester, England.

Fink, J. 2013. Hydraulic Fracturing Chemicals and Fluids Technology, Gulf Professional Publishing.

Finney, J. and Soper, A. 1994. Solvent Structures and Perturbation in Solutions of Chemical and Biological Importance. *Chem. Soc. Rev.* **23** (1): 1-10. https://doi.org/10.1039/CS994230000.

Funkhouser, G. P. and Norman, L. R. 2003. Synthetic Polymer Fracturing Fluid for High-Temperature Applications. Presented at the International Symposium on Oilfield Chemistry, Houston, Texas, 5-7 February. SPE-80236-MS. https://doi.org/10.2118/80236-MS.

Funkhouser, G., Norman, L. 2006. Methods of Fracturing Subterranean Zones Penetrated by Well Bores and Fracturing Fluids Therefor, US Patent No. 6,986,391 B2.

Funkhouser, G., Saini, R., and Mukherjee, A. 2013. High Temperature Fracturing Fluids and Methods. US Patent No. 8,450,252 B2.

Gdanski, R. 2001. Impact of Clay Acidity on the pH of Invading Fluids. Presented at the SPE International Symposium on Oilfield Chemistry, Houston, Texas, 13-16 February. SPE-64983-MS. https://doi.org/10.2118/64983-MS.

Gdanski, R. 2002. High-pH Clay Instability Rating. Presented at the SPE International Symposium and Exhibition on Formation Damage Control, Lafayette, Louisiana, 20-21 February. SPE-73730-MS. https://doi.org/10.2118/73730-MS.

Glass, J., Soules, D., Ahmed, H. et al. 1983. Viscosity Stability of Aqueous Polysaccharide Solutions. Presented at the SPE California Regional Meeting, Ventura, California, 23-25 March. SPE-11691-MS. https://doi.org/10.2118/11691-MS.

Grollmann, U. and Schnabel, W. 1982. Free Radical-Induced Oxidative Degradation of Polyacrylamide in Aqueous Solution. *Polymer Degradation and Stability* **4** (3):203-212. https://doi.org/10.1016/0141-3910(82)90027-1.

Gupta, D. and Carman, P. 2004. Methods of Treating a Well with a Gel Stabilizer. US Patent No. 7,767,630 B2.

Gupta, D. and Carman, P. 2011. Fracturing Fluid for Extreme Temperature Conditions Is Just as Easy as The Rest. Presented at SPE Hydraulic Fracturing Technology Conference, The Woodlands, Texas, 24-26 January. SPE-140176-MS. https://doi.org/10.2118/140176-MS.

Harms, S., Goss, M. and Payne, K. 1984. New Generation Fracturing Fluid for Ultrahigh-Temperature Application. Presented at the SPE Formation Damage Control Symposium, Bakersfield, California, 13-14 February. SPE-12484-MS. https://doi.org/10.2118/12484-MS.

Harris, P. 1993. Chemistry and Rheology of Borate-Crosslinked Fluids at Temperatures to 300°F. *J Pet Technol* **45** (3): 264-269. SPE-24339-PA. https://doi.org/10.2118/24339-PA.

Harry, D., Moorhouse, R., Matthews, L. et al. 1997. Rheological Responses to Variations in Aqueous-Based Zirconium Crosslinker Chemistry. Presented at the International Symposium on Oilfield Chemistry, Houston, Texas, 18-21 February. SPE-37280-MS. https://doi.org/10.2118/37280-MS.

Harry, D., Putzig, D., Moorhouse, R. et al. 1999. Chemical Structures of Group 4 Metal Crosslinkers for Polygalactomannans. Presented at the SPE International Symposium

on Oilfield Chemistry, Houston, Texas, 16-19 February. SPE-50731-MS. https://doi.org/10.2118/50731-MS.

Holtsclaw, J. and Funkhouser, G. P. 2010. A Crosslinkable Synthetic-Polymer System for High-Temperature Hydraulic-Fracturing Applications. *SPE Drill & Compl* **25** (04): 555 - 563. SPE-125250-PA. https://doi.org/10.2118/125250-PA.

Hurnaus, T. and Plank, J. 2015. Crosslinking of Guar and HPG Based Fracturing Fluids Using ZrO_2 Nanoparticles. Presented at the SPE International Symposium on Oilfield Chemistry, The Woodlands, Texas, 13-15 April. SPE-173778-MS. https://doi.org/10.2118/173778-MS.

Hurnaus, T. and Plank, J. 2016. An ITC Study on the Interaction Energy between Galactomannan Biopolymers and Selected MO_2 Nanoparticles in Hydrogels. *Chemistry Select* **1** (8): 1804-1809.

Ibarra-Montaño, E., Rodríguez-Laguna, N., Sánchez-Hernández, A. et al. 2015. Determination of pKa Values for Acrylic, Methacrylic and Itaconic Acid by 1H and 13C NMR in Deuterated Water. *Journal of Applied Solution Chemistry and Modeling* **4** (1): 7-18.

ISO13503-1, 2011. *Petroleum and Natural Gas Industries-Completion Fluids and Materials-Part 1, Measurement of Viscous Properties of Completion Fluids*, Second Edition. Geneva, Switzerland: ISO.

Jaffer, A., Fulmer, D., Ensslen, J. 2006. Recent Developments in Organic Oxygen Scavenger Technology, NACE.

Jamshidi, H. and Rabiee, A. 2014. Synthesis and Characterization of Acrylamide-Based Anionic Copolymer and Investigation of Solution Properties. *Advances in Materials Science and Engineering*, Article ID 728675. doi:10.1155/2014/728675.

Jayakumar, S. and Lane, R. H. 2013. Delayed Crosslink Polymer Gel System for Water Shutoff in Conventional and Unconventional Oil and Gas Reservoirs. Presented at the SPE International Symposium on Oilfield Chemistry, The Woodlands, Texas, USA, 8-10 April. SPE-164046-MS. https://doi.org/10.2118/164046-MS.

Kabiri, M., Zohuriaan-Mehr, M., Mirzadeh, H. et al. 2010. Solvent, Ion and pH-Specific Swelling of Poly(2-Acrylamido-2-Methylpropane Sulfonic Acid). *J. Polym. Res*. **17** (2): 203-212.

Kaushik, J. and Baht, R. 1998. Thermal Stability of Proteins in Aqueous Polyol Solutions: Role of the Surface Tension of Water in the Stabilizing Effect of Polyols. *J Physical Chemistry B* **102** (36): 7058–7066. https://doi.org/10.1021/jp981119l.

Khokhlov, A., Starodubtzev, S., and Vasilevskaya, V. 1993. Conformational Transitions in Polymer Gels: Theory and Experiment. Responsive Gels: Volume Transitions I. *Advances in Polymer Science* **109**: 123-171. https://doi.org/10.1007/3-540-56791-7_3.

Kök, M. 2007. Understanding factors affecting depolymerisation of galactomannans at elevated temperatures; using rheological measurements. *Annual Transactions of the Nordic Rheology Society* **15** (1): 1-6.

Kök, M., Hill, S., and Mitchel, J. 1999. Viscosity of Galactomannans during High Temperature Processing: Influence of Degradation and Solubilisation. *Food Hydrocolloids* **13** (6): 535-542. https://doi.org/10.1016/S0268-005X(99)00040-5.

LaGrone, C., Baumgartner, S., and Woodroof Jr., R. 1985. Chemical Evolution of a High Temperature Fracturing Fluid. *SPE J.* **25** (5): 623-628. SPE-11794-PA. https://doi.org/10.2118/11794-PA.

Langelier, W. F. 1946. Effect of Temperature on the pH of Natural Waters. *American Water Works Association* **38** (2): 179-185.

Li, L. 2009. High Temperature Fracturing Fluids and Methods of Use. US20090145607A1.

Li, L., Al-Muntasheri, G., and Liang, F. 2016a. Nanomaterials-Enhanced High-Temperature Fracturing Fluids Prepared with Untreated Seawater. Presented at the SPE Annual Technical Conference and Exhibition, Dubai, UAE, 26-28 September. SPE-181283-MS. https://doi.org/10.2118/181283-MS.

Li, L., Al-Muntasheri, G., Liang, F. 2016b. A Review of Crosslinked Fracturing Fluids Prepared with Produced Water. *Petroleum* **2** (4): 313-323. http://dx.doi.org/10.1016/j.petlm.2016.10.001.

Li, L., Eliseeva, K. E., Eliseev, V. et al. 2009. Well Treatment Fluids Prepared with Oilfield Produced Water. Presented at the SPE Annual Technical Conference and Exhibition, New Orleans, Louisiana, 4-7 October. SPE-124212-MS. https://doi.org/10.2118/124212-MS.

Li, L., Ezeokonkwo, C. I., Lin, L. et al. 2010. Well Treatment Fluids Prepared With Oilfield Produced Water: Part II. Presented at the SPE Annual Technical Conference and Exhibition, Florence, Italy, 19-22 September. SPE-133379-MS. https://doi.org/10.2118/133379-MS.

Liang, F., Al-Muntasheri, G., Ow, H. et al. 2017. Reduced-Polymer-Loading, High-Temperature Fracturing Fluids by Use of Nanocrosslinkers. *SPE J.* **22** (2): 622-631. SPE-177469-PA. https://doi.org/10.2118/177469-PA.

Lord, D. and Yaritz, J. 1993. Delayed Crosslink Fracturing Fluid Rheology Influenced by Thermal and Shear History. Presented at the SPE International Symposium on Oilfield Chemistry, New Orleans, Louisiana, 2-5 March. SPE-25210-MS. https://doi.org/10.2118/25210-MS.

Montgomery, C. 2013. Fracturing Fluids Components. In *Effective and Sustainable Hydraulic Fracturing*, eds. Bunger, A. P., McLennan, J., and Jeffrey, R., Chap. 2, 25-45. InTech. http://dx.doi.org/10.5772/56422

Moorhouse, R., Harry, D., Matthews, L. et al. 1998. Inter-Relationships between Polymer/Crosslinker Chemistry and Performance. Presented at the SPE India Oil and Gas Conference and Exhibition, New Delhi, India, 17-19 February. SPE-39531-MS. https://doi.org/10.2118/39531-MS.

Nová, L., Uhlík, F., and Košovan, P. 2017. Local pH and Effective pKa of Weak Polyelectrolytes Insights from Computer Simulation. *Phys. Chem. Chem. Phys*. **19** (22): 14376-14387.

Ogunsanya, T. and Li, L. 2018. Safe Boundaries of High-Temperature Fracturing Fluids. Presented at the SPE/IADC Drilling Conference, Amsterdam, The Netherlands, 27 February-1 March. SPE-67743. https:// doi.org/10.2118/190029-MS.

Pasha, M. and Ngn, S. 2008. Derivatization of guar to sodium carboxymethyl hydroxypropyl derivative: Characterization and evaluation. *Pakistan J Pharmaceutical Sciences* **21**: 40-44.

Picout, D. R., Ross, Errington, N. et al. 2001. Pressure Cell Assisted Solution Characterization of Polysaccharides. 1. Guar Gum. *Biomacromolecules* **2** (4): 1301-1309. https://doi.org/10.1021/bm010118n.

Prakash, C., Achalpurkar, M., and Uppuluri, R. 2014. Performance Evaluation of High-Temperature Fracturing Fluid. Presented at the Abu Dhabi International Petroleum Exhibition and Conference, Abu Dhabi, UAE, 10-13 November. SPE-171710-MS. https://doi.org/10.2118/171710-MS.

Prud'homme, R., Ellis, S., Constien, V., et al. 1988. Reproducible Rheological Measurements on Crosslinked Fracturing Fluids. Presented at the SPE Annual Technical Conference and Exhibition, Houston, Texas, 2-5 October. SPE-18210-MS. https://doi.org/10.2118/18210-MS.

Prud'homme, R., Constien, V., and Knoll, S. 1989. The Effects of Shear History on the Rheology of Hydroxypropyl Guar Gels. *Advances in Chemistry* **223** (6): 89-112. https://doi.org/10.1021/ba-1989-0223.ch006.

Putzig, D. 2012. Zirconium-Based Cross-linker Compositions and Their Use in High pH Field Applications. US Patent No. 8236739 B2.

Sigale, K. and Omari, A. 1997. Aspects of crosslinking sulfonated polyacrylamides from rheological studies on their gels, *Journal of Applied Polymer Science* **64** (6): 1067-1072. https://doi.org/10.1002/(SICI)1097-4628(19970509)64:6<1067::AID-APP5>3.0.CO;2-J.

Sokhanvarian, K., Nasr-El-Din, H., and Harper, T., 2019. Effect of Ligand Type Attached to the Zirconium-Based Crosslinkers and the Effect of a New Dual Crosslinker on the Properties of Crosslinked Carboxymethylhydroxypropylguar. *SPE J*. Preprint. SPE-194204-PA. https://doi.org/10.2118/194204-PA.

Song, L. and Yang, Z. 2016. Synthetic Polymer Fracturing Fluid for Ultrahigh Temperature Applications. Presented at the International Petroleum Technology Conference, Bangkok, Thailand, 14-16 November. IPTC-18597-MS. https://doi.org/10.2523/IPTC-18597-MS.

Stokke, B., Christensen, B., and Smidsrod, O. 1992. Degradation of Multistranded Polymers: Effect of Interstrand Stabilization in Xanthan and Sclroglucan Studied by a Monte Carlo Method. *Macromolecules* **25** (8): 2209-2214. https://doi.org/10.1021/ma00034a023.

Swift, T., Swanson, L., Geoghegan, M. et al. 2016. The pH-Responsive Behaviors of Poly(Acrylic Acid) in Aqueous Solution is Dependent on Molar Mass. *Soft Matter* **9** (1): 2542-2549.

Szopinski, D., Kulicke, W., and Luinstra, G. 2015. Structure-Property Relationships of Carboxymethyl Hydroxypropyl Guar Gum in Water and a Hyperentanglement Parameter. *Carbohydrate Polymers* **119**: 159-166.

Vega, Hauge, R. H., Norman, L. R. et al. 2006. Effect of Magnesium and Iron on the Hydration and Hydrolysis of Guar Gum. *Biomacromolecules* **7** (2): 441-445. https://doi.org/10.1021/bm050569y.

Venkataiah, S. and Mahadevan, E. 1982. Rheological properties of hydroxypropyl- and sodium carboxymethyl-substituted guar gums in aqueous solution, *Journal of Applied Polymer Science* **27** (5): 1533-1548. https://doi.org/10.1002/app.1982.070270512.

Walker, M. L., Shuchart, C. E., Yaritz, J. G. et al. 1995. Effects of Oxygen on Fracturing Fluids. Presented at the SPE International Symposium on Oilfield Chemistry, San Antonio, Texas, 14-17 February. SPE-28978-MS. https://doi.org/10.2118/28978-MS.

Weaver, J., Gdanski, R. and Karcher, A. 2003. Guar Gum Degradation: A Kinetic Study. Presented at the International Symposium on Oilfield Chemistry, Houston, Texas, 5-7 February. SPE-80226-MS. https://doi.org/10.2118/80226-MS.

Wolfenden, R., Lu, X., and Young, G. 1998. Spontaneous Hydrolysis of Glycosides. *J. Am. Chem. Soc.* **120** (27): 6814-6815. https://doi.org/10.1021/ja9813055.

Xiong, B., Loss, R., Shields, D. et al. 2018. Polyacrylamide Degradation and its Implications in Environmental Systems. *Clean Water* **1** Article 17. https://doi.org/10.1038/s41545-018-0016-8.

Zhu, C., Krumm, C., Facas, G. et al. 2017. Energetics of cellulose and cyclodextrin glycosidic bond cleavage, *Reaction Chemistry & Engineering*. **2**: 201-214. https://doi.org/10.1039/C6RE00176A.

4. ZIRCONIUM CROSSLINKERS: UNDERSTANDING PERFORMANCE VARIATIONS IN CROSSLINKED FRACTURING FLUIDS*

4.1. Abstract

Borate crosslinkers are the most commonly used crosslinker in fracturing fluids. However, they exhibit lower performance at high temperature, high pressure, high water salinity, and low pH applications. Consequently, zirconium crosslinkers are utilized to address these limitations. Zirconium crosslinking chemistry is complex and depends on many factors such as pH, metal to ligand ratio, ligand order, ionic strength, and type of polymer used, which in turn influence the delay time, thermal stability and shear resistance performance.

This work evaluates the rheological performance of four different zirconium crosslinkers with a biopolymer and a synthetic polymer. The tested crosslinkers are manufactured in different chemical structures. The two polymers tested are 40 lb/1,000 gal CMHPG and 40 lb/1,000 gal synthetic polymer. The rheological performance was measured through HPHT rheometer (100 s^{-1} shear rate) at 200-400°F for 2 hours. The shear tolerance performance was also evaluated under a custom shear rate schedule (100-1000 s^{-1}).

* Part of this chapter is modified with permission from "Influence of Zirconium Crosslinker Chemical Structure and Polymer Choice on the Performance of Crosslinked Fracturing Fluids" by Almubarak, T., Ng, J., Nasr-El-Din, H.A. et al. 2021. The Canadian Journal of Chemical Engineering. Copyright 2021 by Wiley Online Library.

The results show significant variation in crosslinking performance due to the changes in crosslinker chemical structure and type of polymer used. Zirconium lactate and propylene glycol crosslinker shows the highest enhancement in shear and thermal stability with CMHPG based fracturing fluids. Surprisingly, the same crosslinker performed the least with synthetic polymer-based fracturing fluids. However, Zirconium triethanol amine and lactate showed significant enhancements in shear and thermal stability with synthetic polymer-based systems. The results also show and discuss the influence of systematically changing crosslinker ligand order in CMHPG and synthetic polymer-based fracturing fluids.

The work studies the influence of the zirconium crosslinker chemical structure on the rheological properties of both biopolymer and synthetic polymer-based fracturing fluids. The performance evaluation shows that delay time, shear and thermal stability can be enhanced by manufacturing the appropriate crosslinker chemical structure, thus reducing additional additives required used and saving cost.

4.2. Introduction

The name zirconium is taken from the name of the mineral zircon (from the Persian word zargun, which means gold-like metal). Zirconium (Zr) is a transition metal that is located in the fourth group and the fifth period of the periodic table and belongs to the titanium subgroup in which hafnium is also placed. Zr has an atomic number of 40, contains four valence electrons, and thus exists as Zr^{4+} in its ionic state. Zr occurs naturally in the form of five isotopes (^{90}Zr, ^{91}Zr, ^{92}Zr, ^{94}Zr, and ^{96}Zr) with ^{90}Zr making up ~51% of all Zr. Zr is primarily obtained from zircon ($ZrSiO_4$) along with hafnium; Baddeleyite (ZrO_2), another Zr containing ore, is a distant second source (Hedrick 1999). In 2015, the United States Geological Survey (USGS) reported that the production of zirconium was 1.52 million tons worldwide with Australia and South Africa accounting for 66% of the supply apart from the United States (Bedinger 2015).

Zr has seen a variety of applications across industries ranging from nuclear to electronics. When used as an alloying material, Zr provides good mechanical properties at high temperatures and imparts corrosion resistance to the metal. Oxides of Zr are also widely used in ceramics and scratch-proof coatings due to their resistance to crack propagation and their thermal insulation properties (Garvie et al. 1975; Milošev and Frankel 2018). They are also used as heterogeneous or homogeneous catalysts or as crosslinkers to enhance the viscoelastic properties of polymer solutions.

In the oil and gas industry, crosslinking is generally used to generate high viscosity and elasticity for applications such as hydraulic fracturing and water shut-off. To achieve this, tri-valent and tetra-valent cations are added to the polymer solution. Commonly used

elements include boron, aluminum, titanium, and zirconium (Hurnaus and Plank 2015, 2016). Boron is typically used to crosslink guar and its derivatives and is typically applied above pH 9 conditions for optimal crosslinking (Sun and Qu 2011). Compared to the above-mentioned metallic crosslinkers, borate crosslinked fluids are more shear tolerant and exhibit re-healing properties. This is due to the short life time of borate/polymer interaction (~ 1 millisecond) (Prud'homme et al. 1989). However, the performance of borate fluids can be severely impacted by factors including high temperature, and high pressure, pH, and water salinity. (Moorhouse et al. 1998; Parris et al. 2008; Sokhanvarian et al. 2019). Metallic crosslinkers seek to address the problems faced by borate-based fluids.

The crosslinking mechanism of metallic ions differs from those of borate-based crosslinkers. The latter interacts with the cis-hydroxyl functional side-groups of polysaccharides by first hydrolyzing to form tetrahydroxyborate anions (Bishop 2004, Sun and Qu 2011). On the other hand, metallic crosslinkers have been found to polymerize into oxide nanoparticles to facilitate crosslinking (Hurnaus and Plank 2015, 2016). These nanoparticles bond with the polymer through multiple hydrogen bonds to form a highly viscous fluid as shown in **Fig. 4-1**. However, unlike borate-polymer bonds, the bonds between the metallic crosslinker and the polymer bonds do not re-heal. Therefore, it becomes necessary to control the release of metallic crosslinkers by using the appropriate ligands (Harry et al. 1997; Moorhouse et al. 1998; Harry et al. 1999; Mirakyan et al. 2009; Sokhanvarian et al. 2019; Zhang et al. 2019).

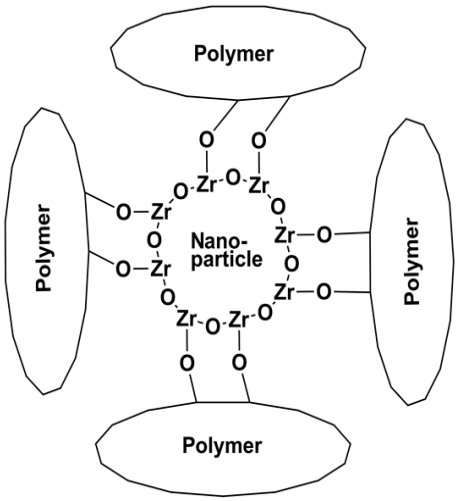

Fig. 4-1 Crosslinking of guar and derivatives through metallic crosslinkers (adapted from Kramer et al. 1988; Harry et al. 1999).

Ligands are molecules that form coordinate bonds to a central metal ion in solution and play an important role in stabilizing nanoparticles in solution. During the synthesis of Zr nanoparticles, ligands are used to prevent the precipitation of Zr oxides and to limit the growth of Zr nanoparticles beyond a desired particle size (Kragten and Parczewski 1981; Demkowicz 2001; Rose et al. 2001; Mizuno et al. 2006; Zhou et al., 2007; Harper et al. 2010). The ligands do so by covering the surface of the nanoparticle through the formation of chemical bonds with its surface oxygens or by chelating Zr (Chatry et al. 1994; Mizuno et al. 2006; Zhou et al. 2007). The stabilization of the nanoparticles is important for applications such as polymer nanocomposites and thin dielectric films (Chen et al. 2005; Cheema and Garnweitner 2014).

The type of ligands used also determines the reactivity and behavior of the Zr system and should be selected depending on the desired application of the Zr system (Bhatt et al. 2018). In catalytic chemistry, the choice of ligand can influence the reaction and the final product in many ways including stereochemistry, catalytic activity, reaction

selectivity, molecular weight and tacticity (of polymers), yield, and catalyst lifespan (Coates 2000; Zuckerman et al. 2000; Kobayashi and Ishitani 2000; Kobayashi et al. 2000; Millward et al. 2000; Cano Sierra et al. 2003; Bradley et al 2003, 2004; Luconi et al. 2010; Despagnet-Ayoub et al. 2013; Pacheco and Davis 2014). In medical imaging, ligands are selected in order to impart kinetic inertness or enhanced metal-binding rates (Wadas et al. 2010).

In the oil and gas industry, the effect of different ligands on the performance of polymers crosslinked by metallic crosslinkers has only been studied by a few authors. Moorhouse et al. (1998) tested a variety of carboxylate ligands with Zr and showed a significant difference in viscosity between the crosslinker formulations. Sokhanvarian et al. (2019) investigated the effect of lactate, lactate with propylene glycol, and lactate with triethanol amine on the performance of Zr crosslinkers and showed that strong bonding ligands lead to a slow viscosity buildup of the crosslinked polymer.

In addition, the size and electropositivity of the nanoparticle have also been observed to affect the characteristics of the crosslinked solution. Hurnaus and Plank (2016) compared the crosslinking of TiO2, SnO2, and SiO2 with guar and hydroxypropyl guar. From their tests, they reasoned that the efficacy of crosslinking improved with the electropositivity of the metal ion and that a large gain in entropy occurs during crosslinking. They also showed that crosslinking only occurred with nanoparticles below a certain size and that hydroxypropyl guar was able to crosslink with larger particle sizes than guar.

In this work, three different zirconium based crosslinkers are evaluated. The tests highlight the influence of temperature, shear rate, polymer type, and ligand type and ligand order on the performance of zirconium crosslinkers used in fracturing fluids. A final segment of the study will go into some details about zirconium crosslinker chemistry.

4.3. Experimental Procedures

4.3.1. Materials

The synthetic polymer used is in an emulsion form (30 wt.% active) and is composed of acrylamide (AM), acrylic acid (AA), and 2-acrylamido-2-methylpropane sulfonic acid (AMPS), **Fig. 4-2**. CMHPG (**Fig.4-3**), and zirconium crosslinkers with various ligands: 1) Zirconium lactate (Zr-La), 2) Zirconium lactate and triethanol amine (Zr-La-TEA), 3) Zirconium triethanol amine and lactate (Zr-TEA-La), and 4) Zirconium lactate and propylene glycol (Zr-La-PG) (all as 5.5-5.7 wt.% ZrO_2) were provided by a chemical company and were used as received, **Fig. 4-4**. Tetraethylenepentamine (TEPA) and acetic acid were provided at 99 wt.% concentration and were used as received. Houston tap water (< 500 ppm) was used to prepare all the systems.

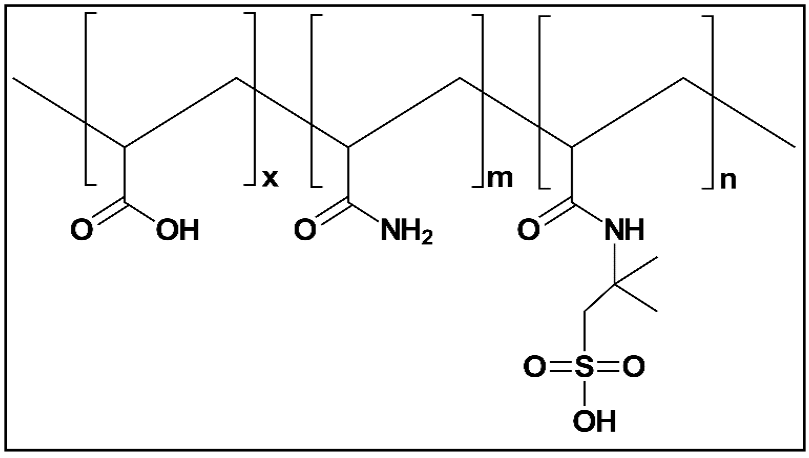

Fig. 4-2 Synthetic polymer (AA-AM-AMPS).

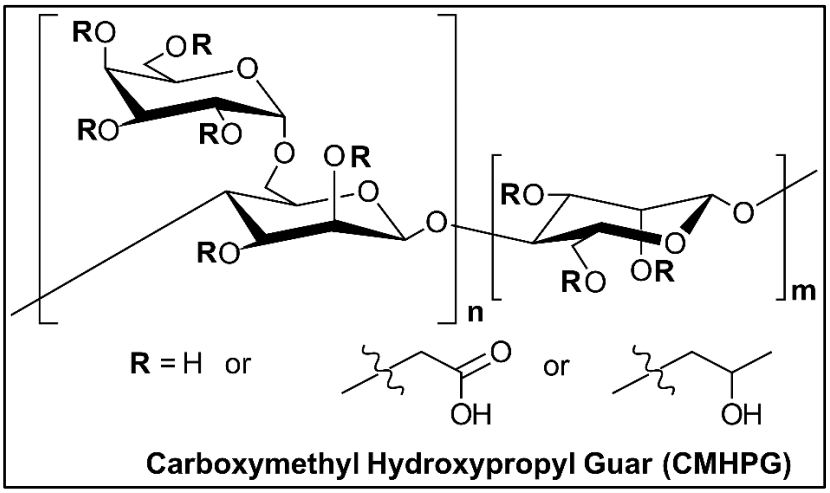

Fig. 4-3 Carboxymethylhydroxypropyl Guar (CMHPG).

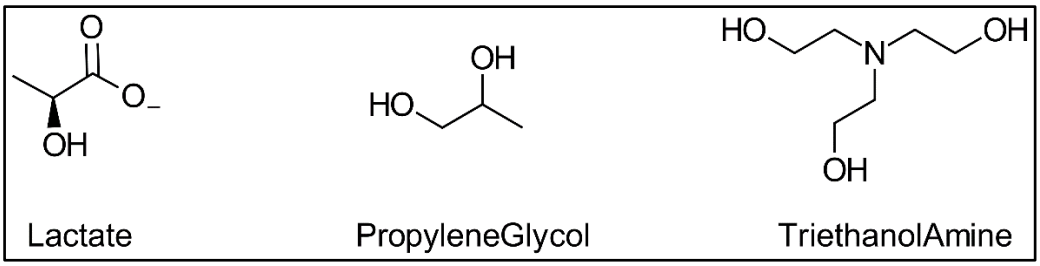

Fig. 4-4 Structure of ligands in zirconium crosslinkers.

4.3.2. Fluid Preparation

The fluids were prepared and tested on the same day; therefore, no biocide was used. Also, no surfactants, HT stabilizers, or external crosslinking delay agents were used to facilitate direct evaluation of the interactions between the crosslinker and polymer.

A solution of 40 lb/1,000 gal synthetic polymer was prepared by adding 6.4 cm^3 of the synthetic polymer to 400 cm^3 of tap water (16 gpt) in a Waring blender under rapid agitation (800+ RPM) for 15 s. Subsequently, the mixer speed was reduced to 200-400 RPM to generate a vortex and mixed for 15 minutes to fully hydrate the polymer in solution. Acetic acid was used to adjust the pH to 5. Crosslinker was added last and mixed thoroughly for 30 s.

A solution of 40 lb/1,000 gal CMHPG was prepared by adding 3.84 g of polymer to 800 cm^3 of tap water in a Waring blender maintaining a visible vortex for 15 minutes (200-800 RPM). The pH of the solution was then adjusted by adding an appropriate amount of TEPA for the pH 10 tests, and acetic acid for the pH 5 tests. Crosslinker was added last and mixed thoroughly for 30 s.

4.3.3. HP/HT Rheometer

An HP/HT rheometer was used to measure the apparent viscosity of the prepared fracturing fluids at 200-400°F. The rheometer utilized R1/B5 bob and rotor combination, which required a sample volume of 52 cm^3. The rheometer had an electric jacket for heating; a temperature sensor was mounted on the stator/bob to control sample temperature. A pressure of 350-500 psi was applied with nitrogen gas to prevent boiling of the sample.

Viscosity measurements were performed under different shear rates to simulate the flow of the fracturing fluid through production tubular, perforations, and inside the created fracture. ISO13503-1 was followed for the majority of the tests, where the shear rate schedule was set to 100 s^{-1} with short shear ramp spikes between 25 and 100 s^{-1}. The heater temperature was preheated to 150°F before starting the tests. This was done to ensure quick and consistent heating profiles. The fluid took 10-15 minutes to reach the testing temperature.

To study the influence of shear rate on the crosslinkers performance, a 200°F testing schedule was custom created. The customized schedule was set to 100 s^{-1} with short ramp spikes at 1000 s^{-1}. Also, to further understand the behavior at 250-300°F, a constant 40 s^{-1} shear rate schedule was utilized.

4.4. Results and Discussion

Carboxymethylhydroxypropyl guar is a cleaner derivative of guar that is functional in a variety of pH environments. The difference in functionality can be seen in **Fig. 4-5**, which shows the rheological performance of crosslinked CMHPG at pH 5, 7, and 10 using Zr-La-PG at 300°F. While CMHPG has been shown to be able to crosslink at all these pH levels, it has the weakest rheological stability at pH 5 (Almubarak 2018a, 2018b). Despite CMHPG's weaker rheological properties at pH 5, it should be noted that low pH environments yield a cleaner fracturing fluid treatment. This is due to minimizing damage to clays and precipitations of metal hydroxides that appear at higher pH levels (Gdanski 2001, 2002). For this reason and to consistently compare it with the synthetic polymer-based fracturing fluid, the crosslinking environment in this work was limited to a pH of 5.

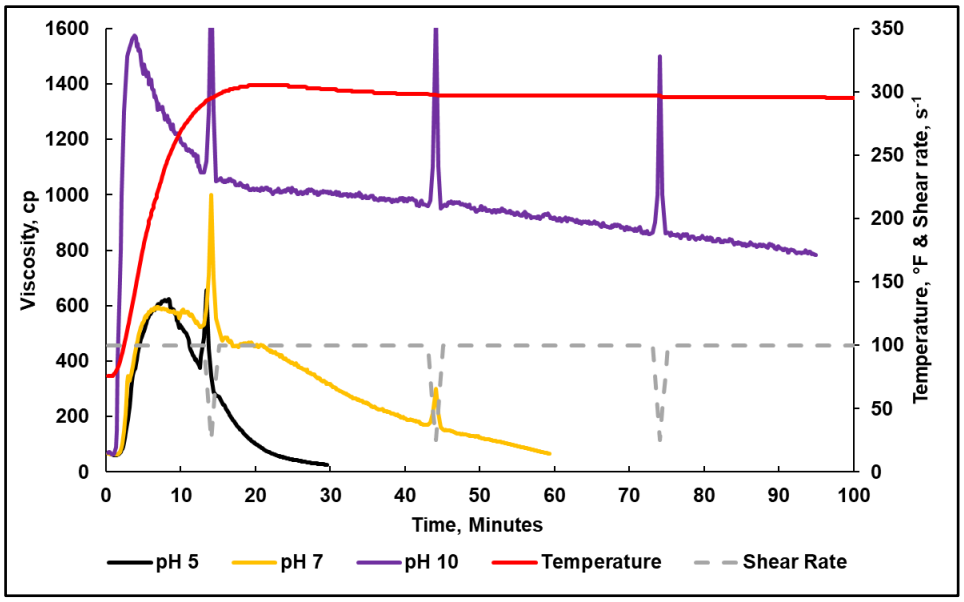

Fig. 4-5 40 lb/1,000 gal CMHPG, 2 gpt Zr-lactate and propylene glycol crosslinker, pH 5-10, 300°F (Almubarak et al. 2018a, 2018b).

4.4.1. Influence of Temperature

The first stage of this project consisted of testing the zirconium crosslinkers in a 40 lb/1,000 gal CMHPG based fracturing fluid system at pH 5 and between temperatures of 200-400°F. Fig. 4-6 shows that all three zirconium crosslinkers exhibit delayed crosslinking (>2 minutes), were able to crosslink CMHPG at 200°F, and generated sufficient thermal and rheological stability that indicate the ability to successfully carry proppant (≥100 cp). The graph also shows that Zr-La exhibits a faster crosslinking rate compared to the other two crosslinkers. The fast crosslinking rate results in an early crosslinked viscosity peak that is unstable and deteriorated in performance as the test continued. Zr-La-TEA exhibits a medium speed reaction, while Zr-La-PG resulted in the slowest generation of viscosity at these conditions.

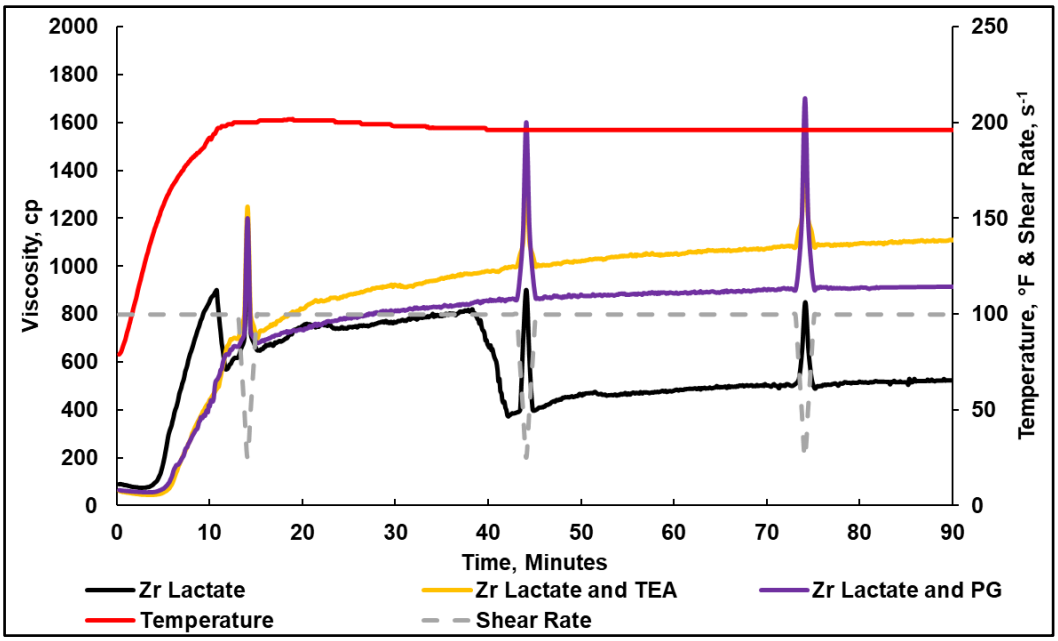

Fig. 4-6 40 lb/1,000 gal CMHPG based fracturing fluids, 4 gpt crosslinker, pH 5, 200°F.

The crosslinkers were further tested at 250°F. **Fig. 4-7** shows that CMHPG crosslinked with Zr-La-PG outperformed both fluids crosslinked with Zr-La and Zr-La-TEA at this temperature. This occurred because of the slow viscosity generation by Zr-La-PG and thus able to prevent early viscosity build-up and early shear degradation. The viscosity buildup and early shear degradation can be seen when the other crosslinkers are used.

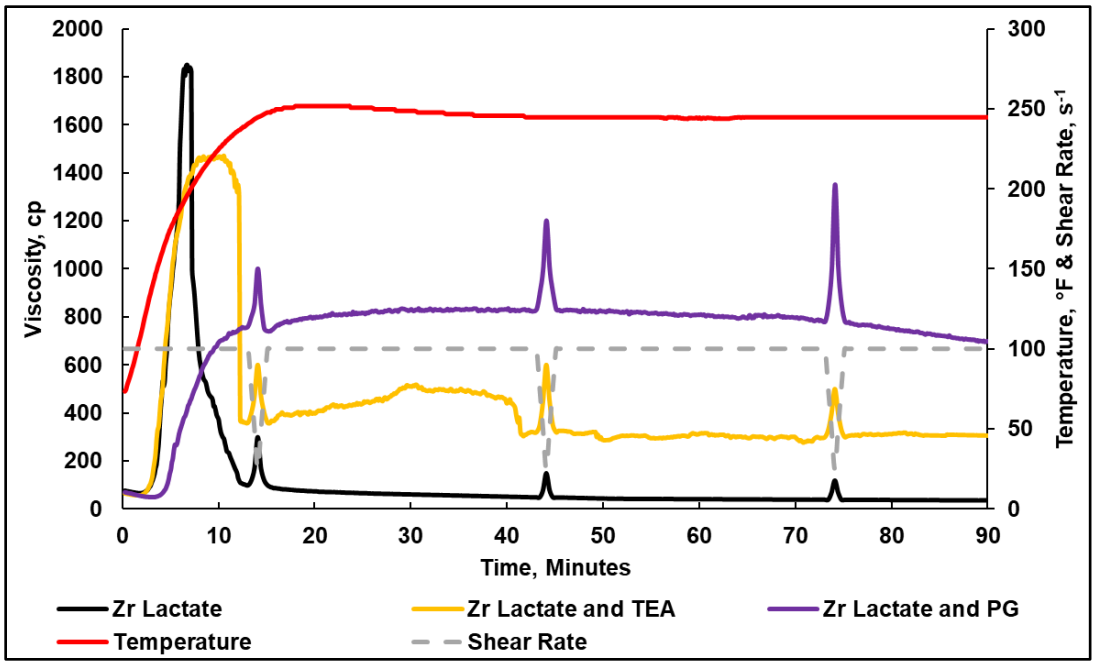

Fig. 4-7 40 lb/1,000 gal CMHPG based fracturing fluids, 4 gpt crosslinker, pH 5, 250°F.

The crosslinkers were also tested at 300, 350, and 400°F. **Figs. 4-8**, **4-9** and **4-10** show the results of the viscometer tests at these temperatures. The graphs show poor thermal stability of the fracturing fluid as the fluid viscosities drop below 100 cP in less than 1 hour. This is due to the thermal degradation of the polymer and the thermal instability of the crosslinker; the latter accelerates the crosslinking reaction and causes early shear degradation. Although the fluids fail to maintain thermal and shear stability for the duration of testing, the trend corresponds to that observed earlier at 200 and 250°F with Zr-La-PG being the most stable and Zr-La as the least stable crosslinker.

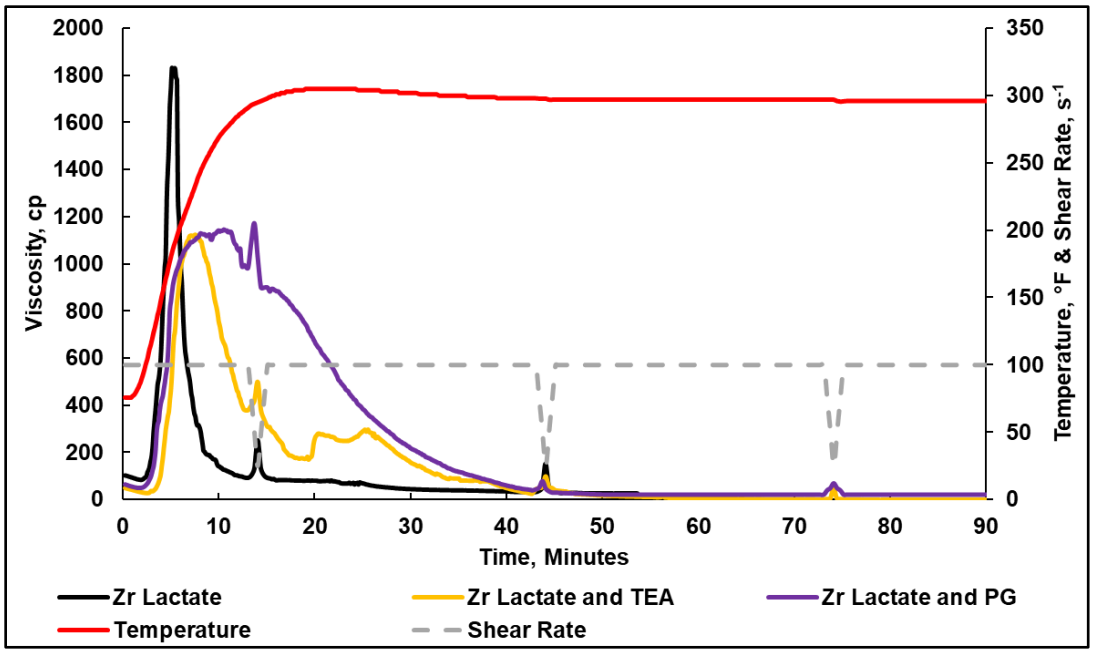

Fig. 4-8 40 lb/1,000 gal CMHPG based fracturing fluids, 4 gpt crosslinker, pH 5, 300°F.

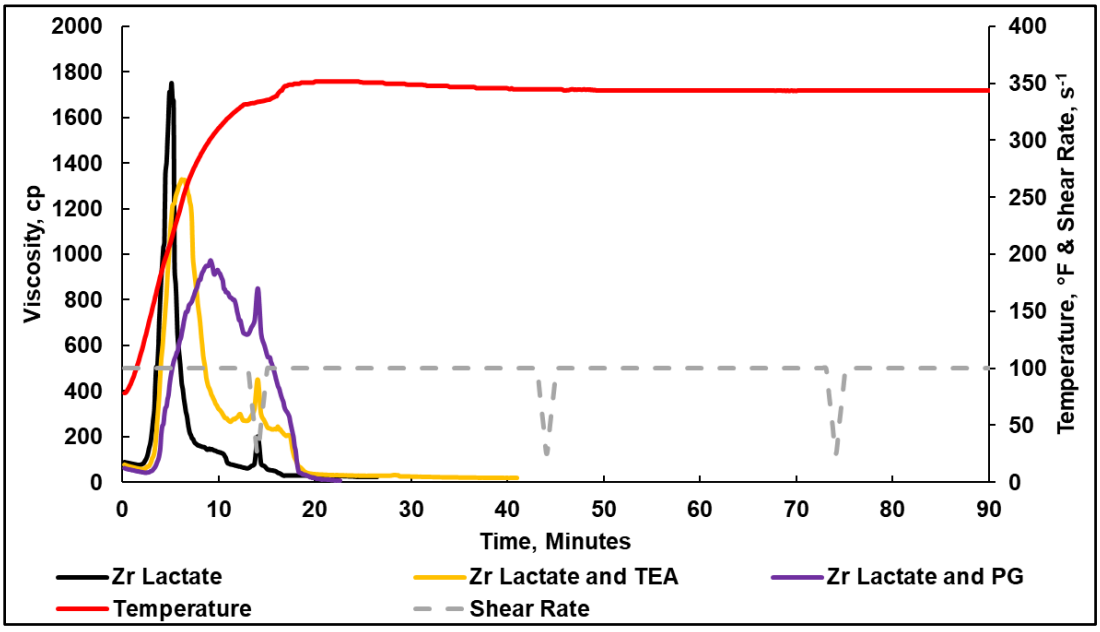

Fig. 4-9 40 lb/1,000 gal CMHPG based fracturing fluids, 4 gpt crosslinker, pH 5, 350°F.

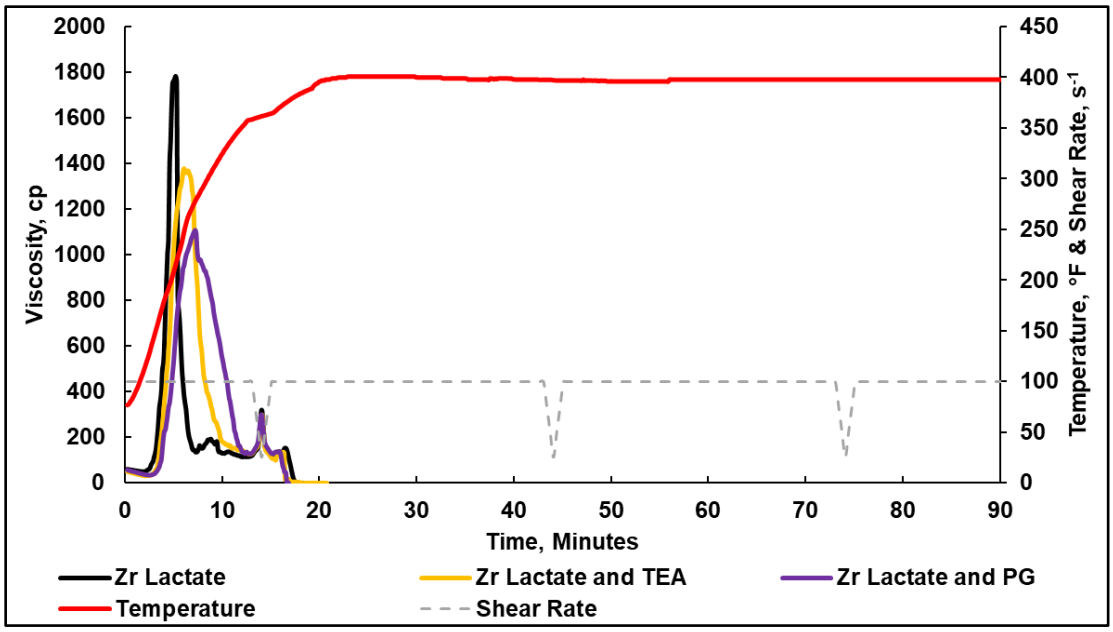

Fig. 4-10 40 lb/1,000 gal CMHPG based fracturing fluids, 4 gpt crosslinker, pH 5, 400°F.

4.4.2. Influence of Shear Rate

Fig. 4-11 and **Fig. 4-12** show the results of crosslinking CMHPG fracturing fluid with different crosslinkers under low shear rate (40 s^{-1}) conditions at 250 and 300°F respectively. At both conditions, Zr-La-PG was observed to be the best of the three crosslinkers while at 300°F, Zr-La and Zr-La-TEA were observed to have similar performances. This is expected as the lower shear conditions alleviate the need for shear tolerance provided by the crosslinker choice. However, despite the reduction in shear rate CMHPG still exhibits a thermal stability limit of 250°F. Therefore, while the choice of crosslinker is important, it is also necessary to note that the limitations posed by polymer thermal stability is independent of this choice. External high-temperature stabilizers such as oxygen scavengers must be added to prolong the rheological stability of the fluid when necessary.

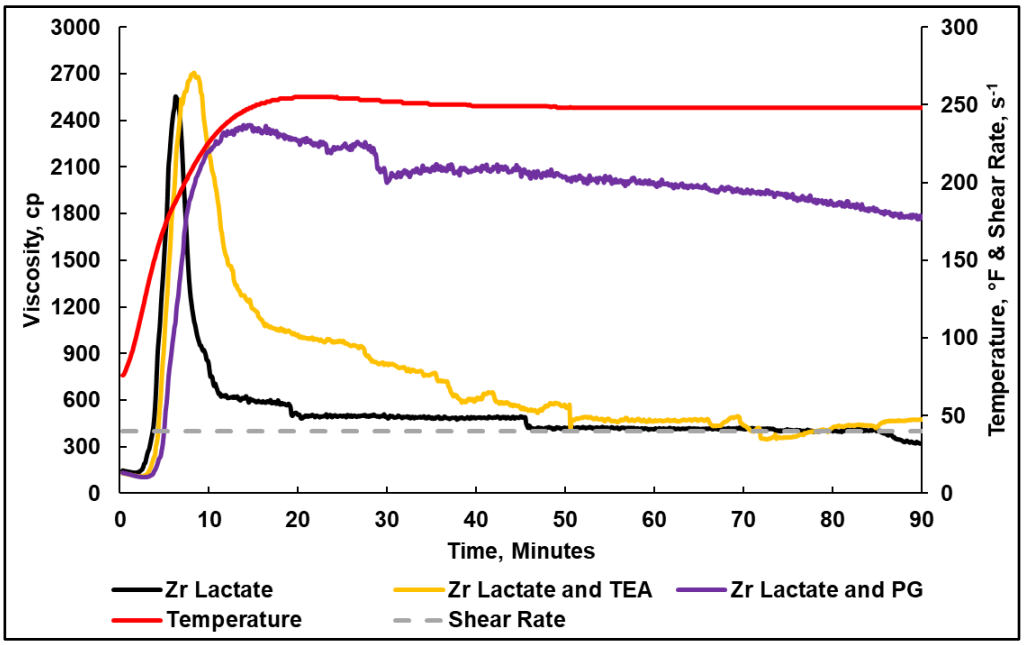

Fig. 4-11 40 lb/1,000 gal CMHPG based fracturing fluids, 4 gpt crosslinker, pH 5, 250°F, 40 s^{-1}.

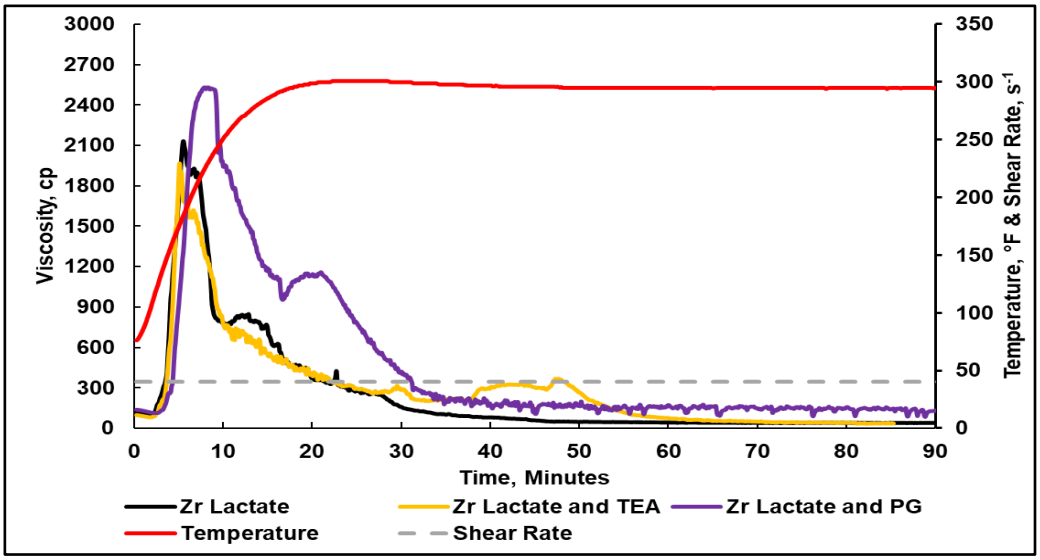

Fig. 4-12 40 lb/1,000 gal CMHPG based fracturing fluids, 4 gpt crosslinker, pH 5, 300°F, 40 s^{-1}.

To study the influence of shear degradation on the rheological properties, a special shear rate schedule using 100 s^{-1} shear rate with 1000 s^{-1} shear ramps was tested. The tests

were carried out at 200°F, and the results are shown in **Fig. 4-13**. This temperature was chosen to assess the crosslinkers by minimizing thermal degradation of the polymer. The results show that all crosslinkers exhibit clear shear degradation from the high shear ramps when compared to the viscosities generated at the same temperature with the normal ISO schedule in Fig. 6.

Of the three crosslinkers, Zr-La-PG appeared to be the least affected by each shear ramp whereas Zr-La and Zr-La-TEA both lost viscosity after the first two ramps and were subsequently unable to recover this lost viscosity. This is due to the consistent degree of growth and reactivity of the Zr-La-PG crosslinker. The quality of the manufactured zirconium crosslinkers is highly dependent on the source of zirconium used and the polydispersity index (PDI=Mw/Mn) of the manufactured ZrO_2 polymers. If the crosslinkers were manufactured with high PDIs, the response would show larger losses in viscosity after the shear ramps due to the large variations in molecular weights involved in the crosslinking.

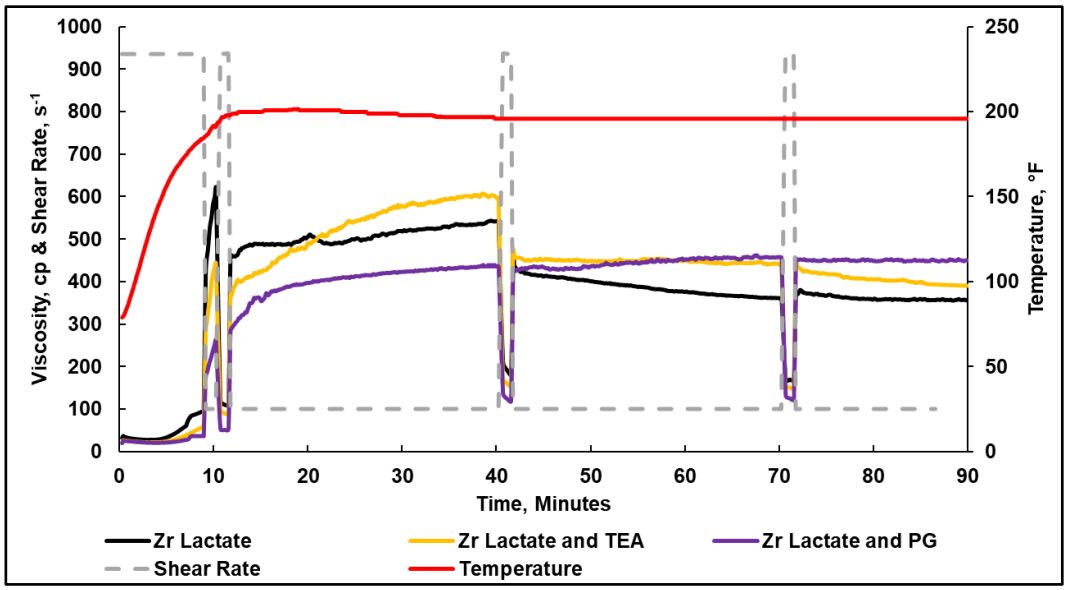

Fig. 4-13 40 lb/1,000 gal CMHPG based fracturing fluids, 4 gpt crosslinker, pH 5, 200°F, 100 s^{-1} with 1000 s^{-1} shear ramps.

4.4.3. Influence of Polymer Type

Polymers have specific conformations in solution which depend on the composition and purity. This can lead to variations in crosslinker interactions which in turn can alter viscosity, thermal stability and shear rate behavior. To determine the influence of the type of polymer used, synthetic polymer solutions were prepared and tested at the same conditions as CMHPG.

At temperatures between 200-350°F, the synthetic polymer was observed to have the best performance with Zr-La while Zr-La-PG performed the worst as shown in Figs. **4-14** to **4-16**. This is contrary to the tests with CMHPG that showed the best performance occurred with Zr-La-PG.

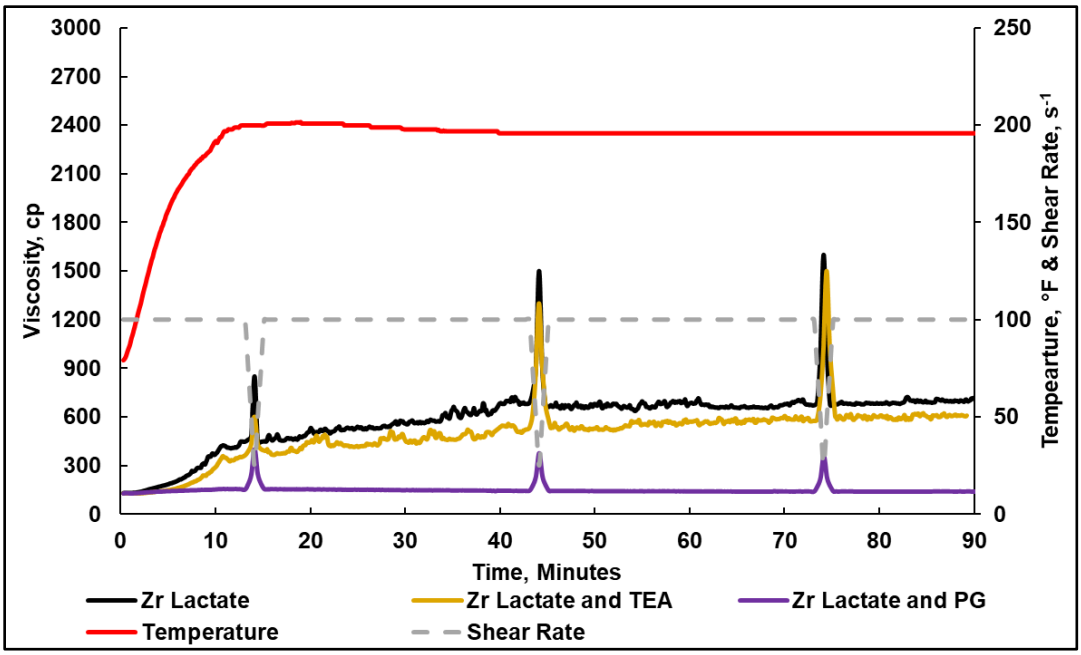

Fig. 4-14 40 lb/1,000 gal synthetic polymer-based fracturing fluids, 4 gpt crosslinker, pH 5, 200°F.

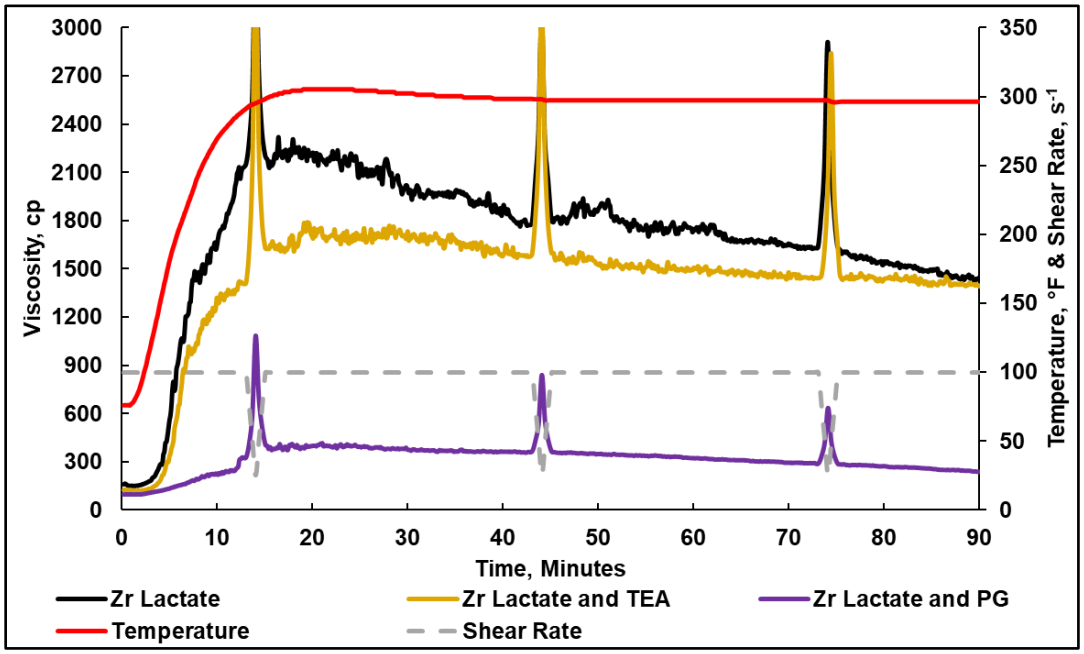

Fig. 4-15 40 lb/1,000 gal synthetic polymer-based fracturing fluids, 4 gpt crosslinker, pH 5, 300°F.

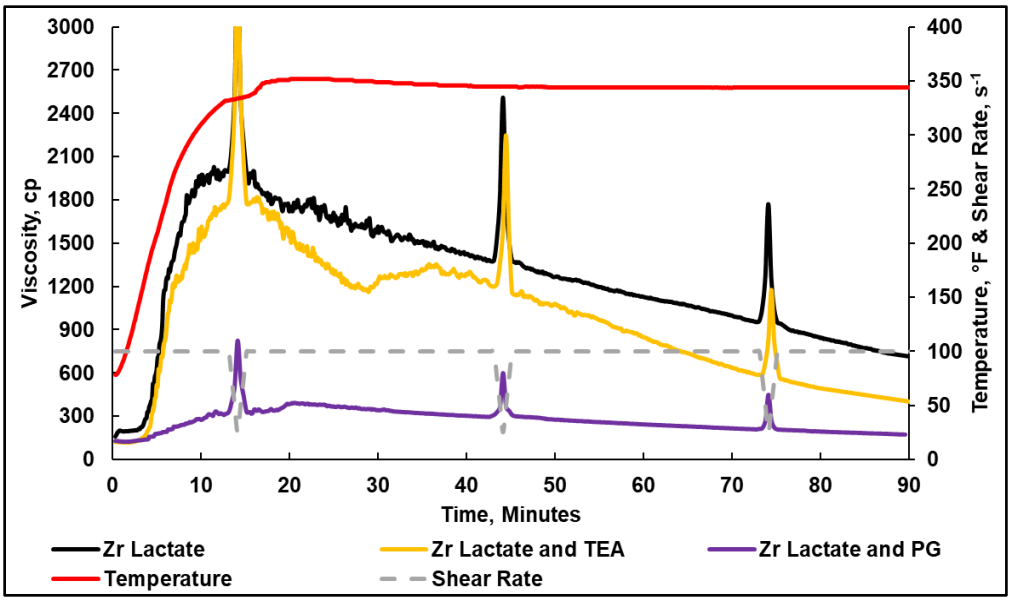

Fig. 4-16 40 lb/1,000 gal synthetic polymer-based fracturing fluids, 4 gpt crosslinker, pH 5, 350°F.

At 400°F, the synthetic polymer fluid crosslinked with Zr-La-TEA performed the best while Zr-La-PG generated the lowest viscosity as shown in **Fig. 4-17**. The poor performance of Zr-La-PG with synthetic polymer trends throughout all the tests. Fig. 4-16 also indicates that the polymer is reaching its thermal stability limits and high-temperature stabilizers are required to minimize the degradation.

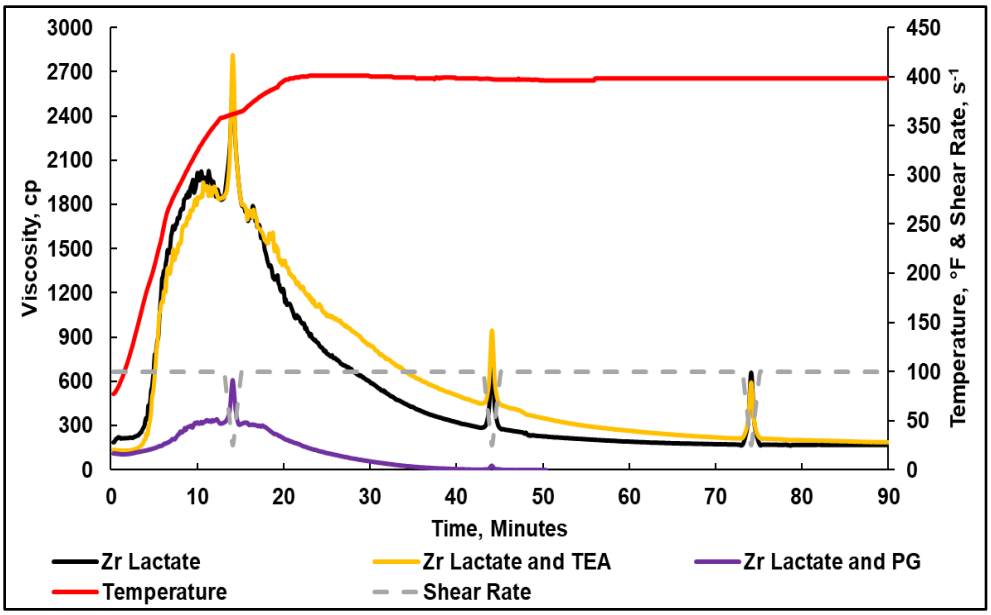

Fig. 4-17 40 lb/1,000 gal synthetic polymer-based fracturing fluids, 4 gpt crosslinker, pH 5, 400°F.

This difference in performance is due to the low reactivity by Zr-La-PG and was therefore unable to generate any significant viscosity with the synthetic polymer throughout the tests. To overcome this, higher concentrations of crosslinker is required as shown in **Fig. 4-18** where the synthetic polymer is crosslinked with 1-6 gpt Zr-La-PG at 300°F.

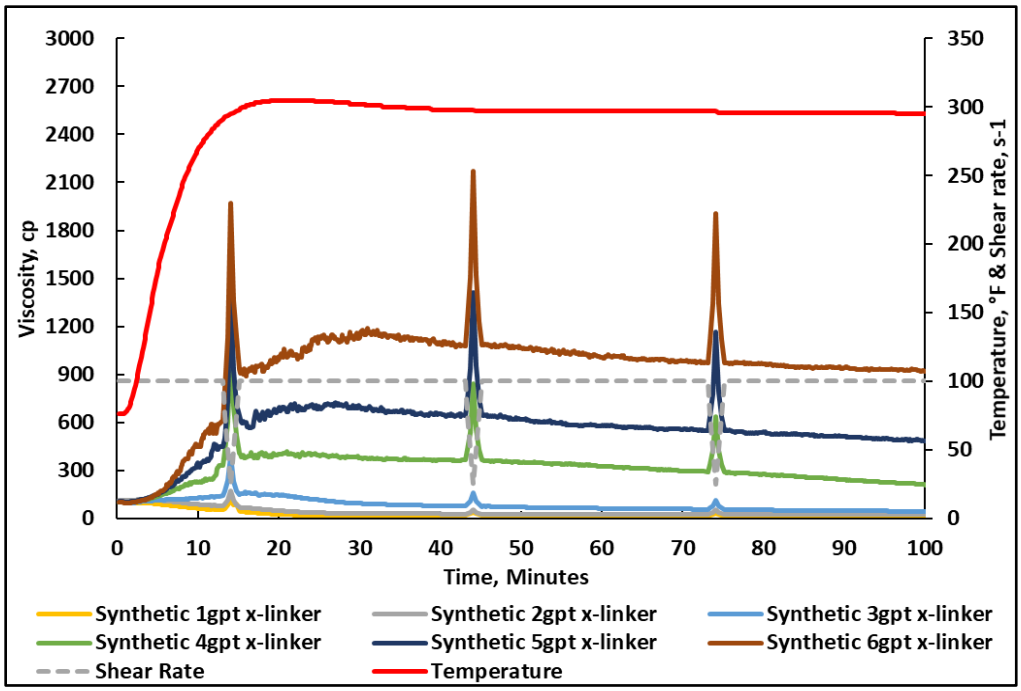

Fig. 4-18 40 lb/1,000 gal synthetic polymer, 1-6 gpt Zr-lactate and propylene glycol crosslinker, pH 5, 300°F.

This difference in behavior of the individual crosslinkers with synthetic polymer and CMHPG is due to the difference in shear tolerance of the two polymers. Incorporating certain concentration of AMPS monomer in the synthetic polymer structure adds stiffness, charge density, additional hydrogen bonding sites and provides a mix of hydrophobic and hydrophilic segments, which changes the hydrodynamic radius of the polymer in solution. These factors can enhance key properties such as shear resistance, salt tolerance and thermal stability of the polymer in solution (Sigale and Omari 1997; Jamshidi and Rabiee 2014).

4.4.4. Influence of Ligand Order

4.4.4.1. CMHPG Fracturing Fluid

In order to examine the influence of ligand order on the performance of the crosslinker with CMHPG, crosslinkers Zr-La-TEA, and Zr-TEA-La were chosen. The crosslinkers were added to a 40 lb/1,000 gal CMHPG fluid at pH 5 and tested at 200-400°F.

The viscosity performance results at 200 and 250°F can be seen in **Figs. 4-19** and **4-20**. The results show that although the crosslinkers contain the same type and content of ligands, the performance differs due to the order of ligands added in the zirconium crosslinkers. At 200°F, CMHPG crosslinked with Zr-TEA-La was observed to perform better than Zr-La-TEA. The same trend in performance is noticed at 250°F, although both crosslinker systems show a significant drop in viscosity at this temperature. This is due to both crosslinkers exhibiting high viscosity at 250°F which caused significant early shear degradation.

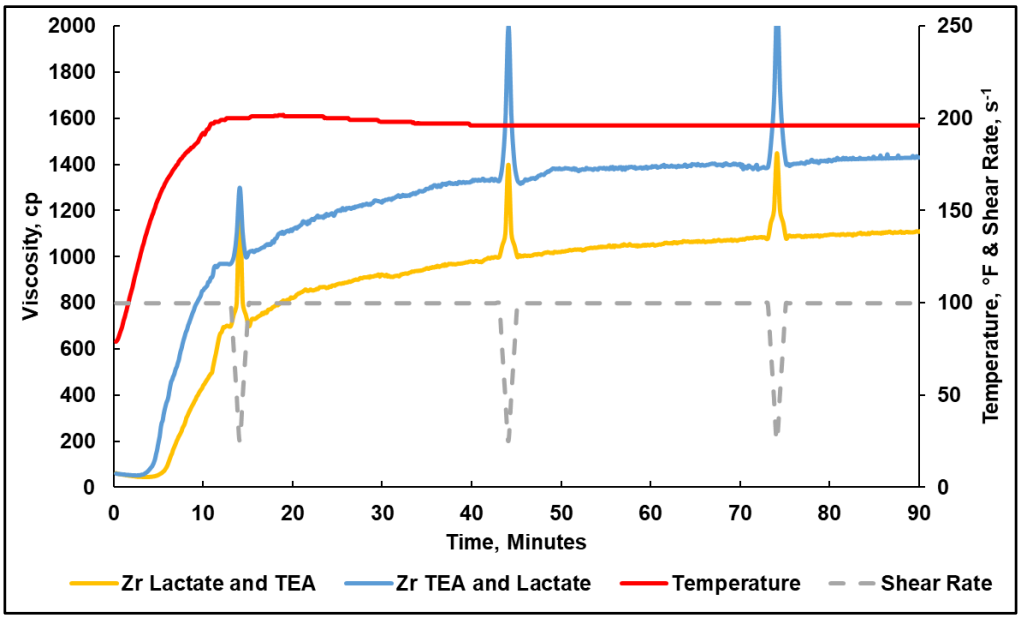

Fig. 4-19 40 lb/1,000 gal CMHPG based fracturing fluids, 4 gpt crosslinker, pH 5, 200°F.

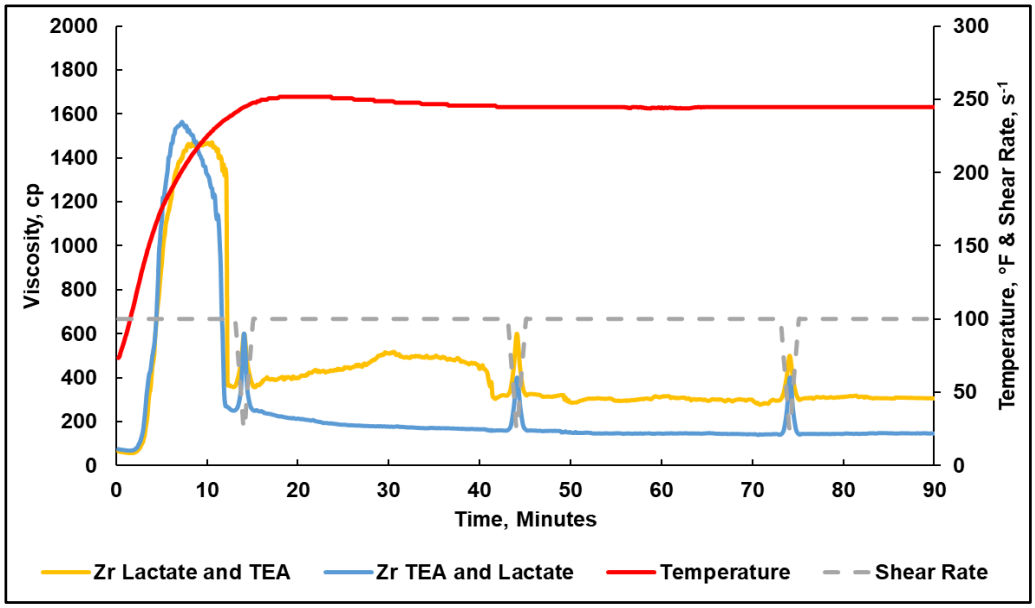

Fig. 4-20 40 lb/1,000 gal CMHPG based fracturing fluids, 4 gpt crosslinker, pH 5, 250°F.

The influence of shear rate on the two crosslinkers was also examined. **Fig. 4-21** shows the results of testing the CMHPG based fracturing fluid at 250°F using a constant

low shear rate schedule of 40 s^{-1}. The results show that both crosslinkers experience a quick drop in viscosity after an initial peak. This drop was also shown in Figs. 4-7 and 4-20, indicating that this occurrence is independent of ligand order.

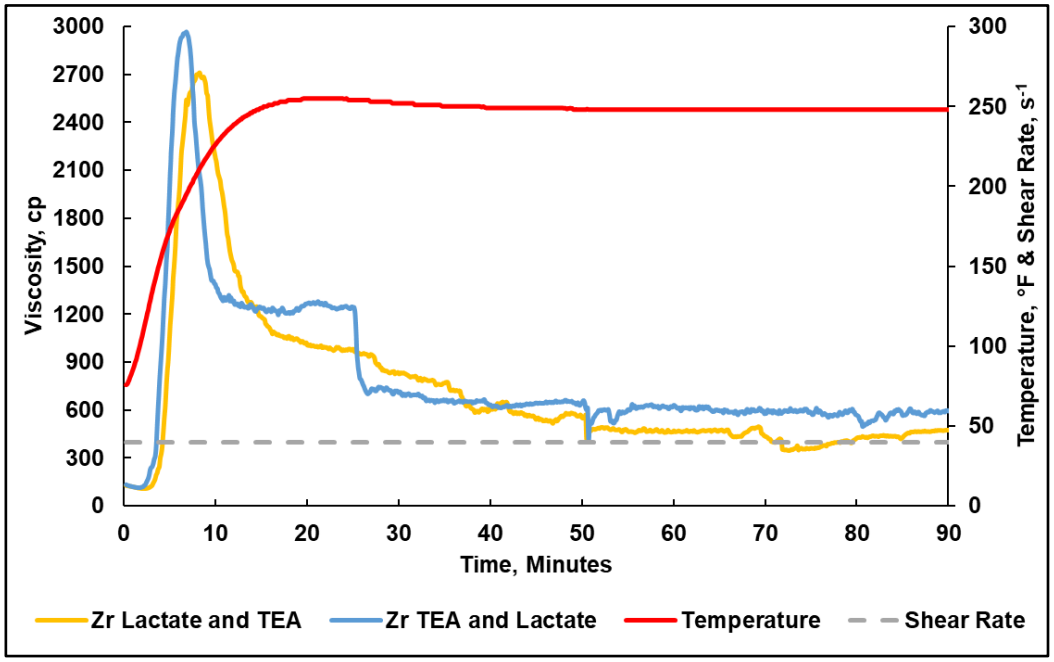

Fig. 4-21 40 lb/1,000 gal CMHPG based fracturing fluids, 4 gpt crosslinker, pH 5, 250°F, 40 s^{-1}.

Fig. 4-22 shows viscosity results at 300°F with a constant 40 s^{-1} shear rate schedule. The results are consistent with Fig. 4-12, and the viscosity drop is due to the weak thermal stability of CMHPG at these conditions. In addition, both crosslinkers show a viscosity hump (~25-50 minutes) with Zr-TEA-La being earlier than Zr-La-TEA. This indicates Zr-TEA-La has higher reactivity than Zr-La-TEA at these conditions.

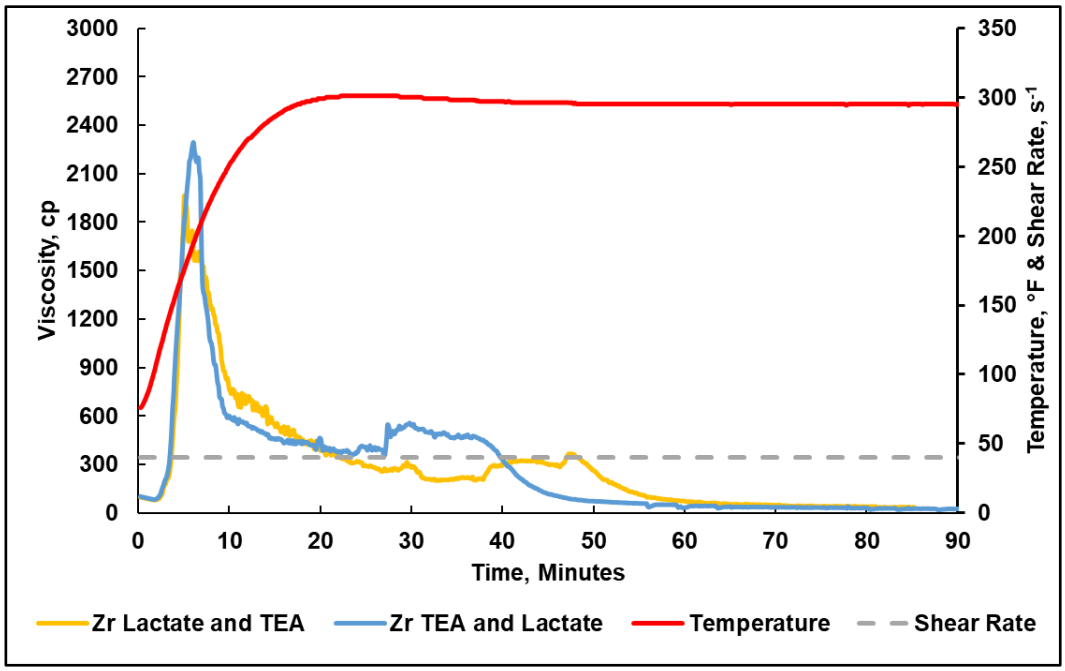

Fig. 4-22 40 lb/1,000 gal CMHPG based fracturing fluids, 4 gpt crosslinker, pH 5, 300°F, 40 s^{-1}.

Fig. 4-23 shows the results of the special shear rate schedule that contained shear ramps of 1000 s^{-1}. The tests were run at 200°F to minimize the influence of polymer thermal degradation on the results. The results show that both crosslinkers exhibit significant shear degradation after each ramp with Zr-TEA-La having lower viscosity of the two. This is in agreement with previous trends that show Zr-TEA-La has higher reactivity than Zr-La-TEA.

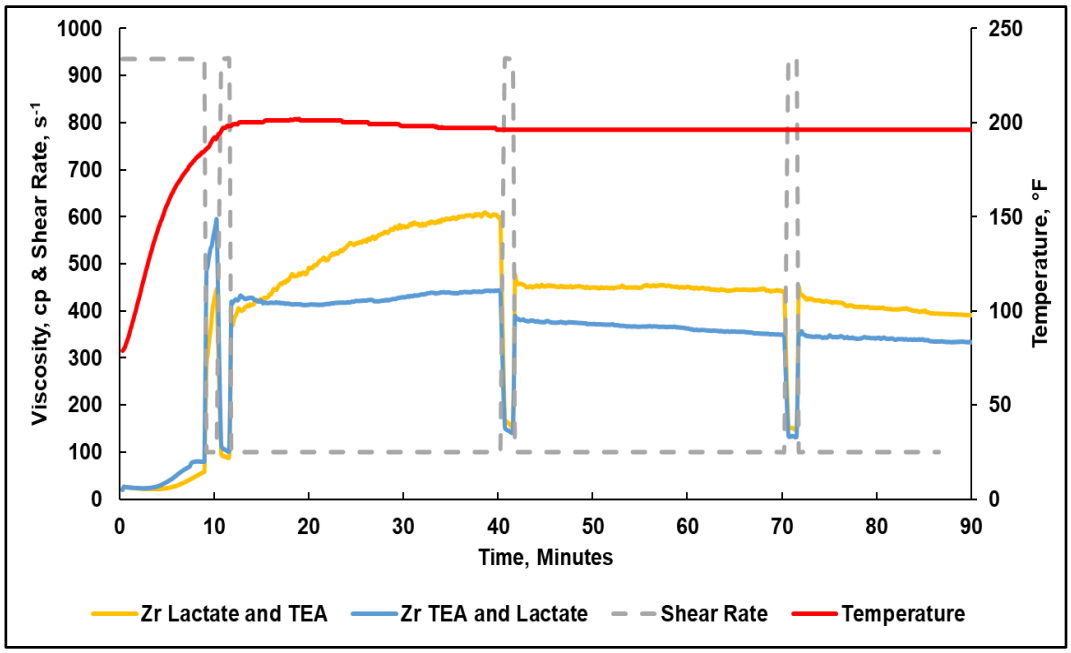

Fig. 4-23 40 lb/1,000 gal CMHPG based fracturing fluids, 4 gpt crosslinker, pH 5, 200°F.

4.4.4.2. Synthetic Polymer Fracturing Fluid

The same two crosslinkers (Zr-La-TEA and Zr-TEA-La) were tested with 40 lb/1,000 gal synthetic polymer-based fracturing fluids at temperatures between 200-400°F. **Figs. 4-24** to **4-27** show that Zr-TEA-La outperformed Zr-La-TEA when used with synthetic polymer fracturing fluid systems at all these temperature ranges.

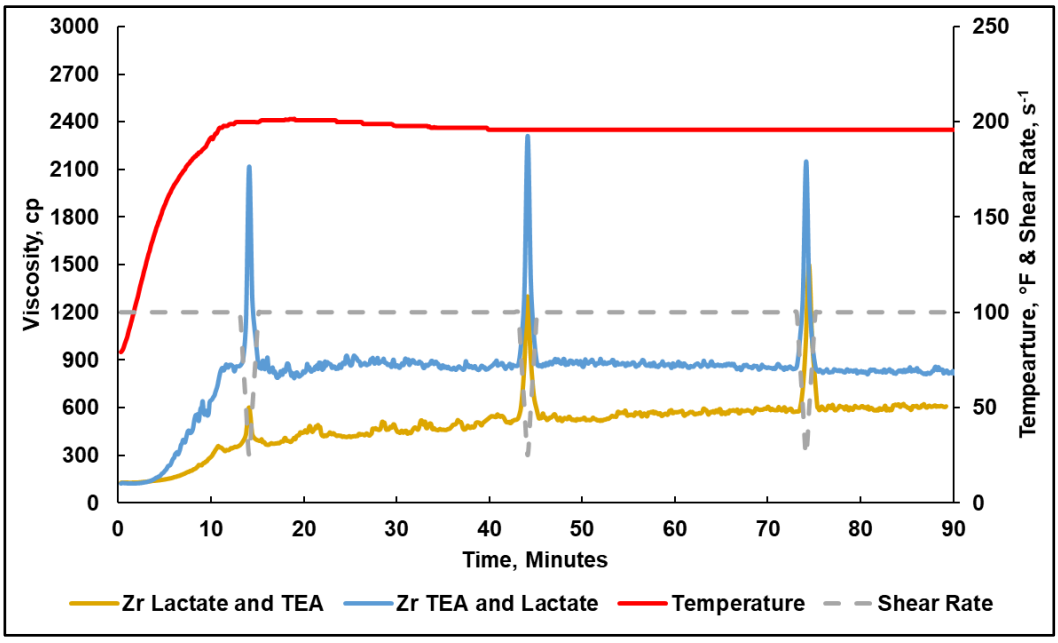

Fig. 4-24 40 lb/1,000 gal synthetic polymer-based fracturing fluids, 4 gpt crosslinker, pH 5, 200°F.

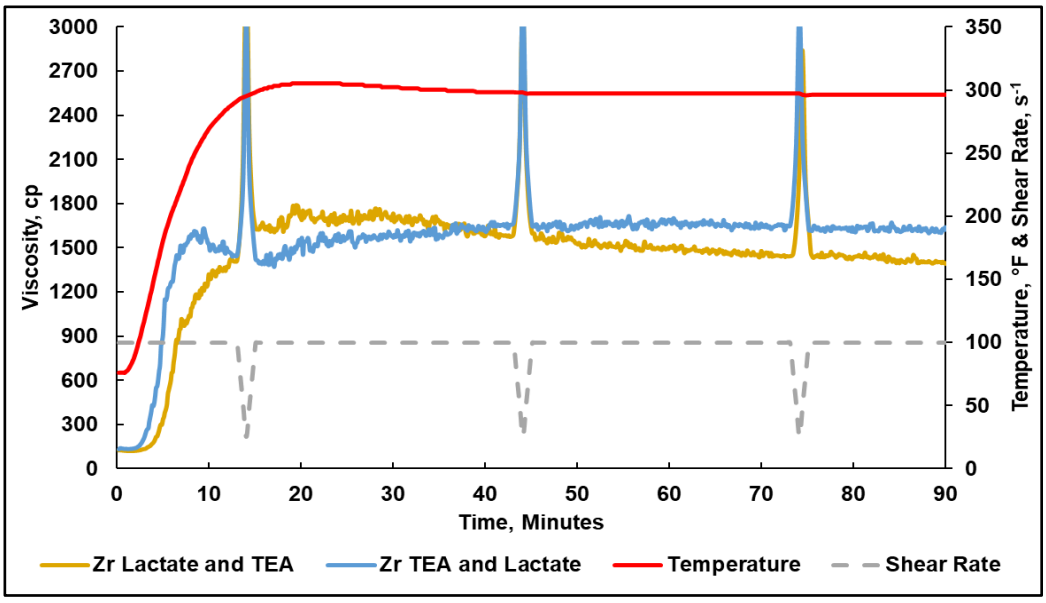

Fig. 4-25 40 lb/1,000 gal synthetic polymer-based fracturing fluids, 4 gpt crosslinker, pH 5, 300°F.

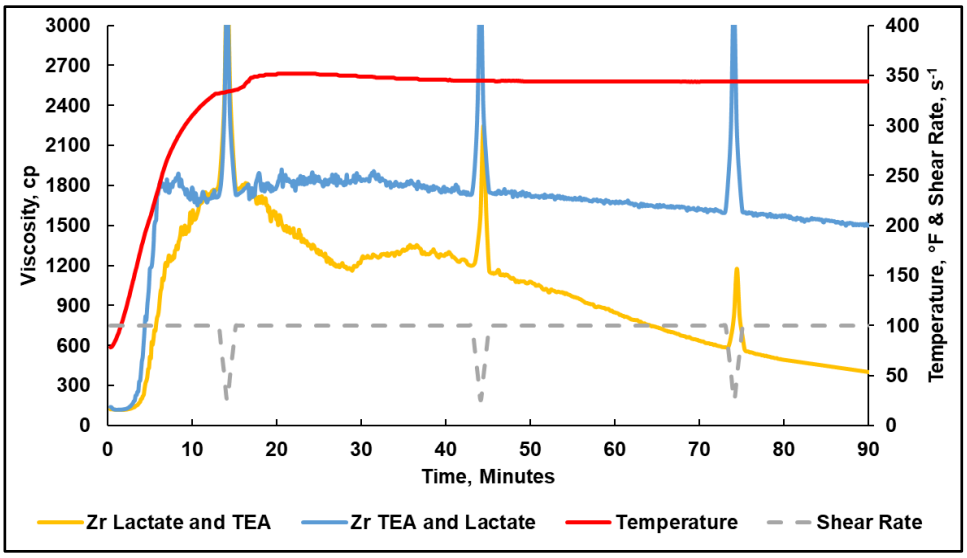

Fig. 4-26 40 lb/1,000 gal synthetic polymer-based fracturing fluids, 4 gpt crosslinker, pH 5, 350°F.

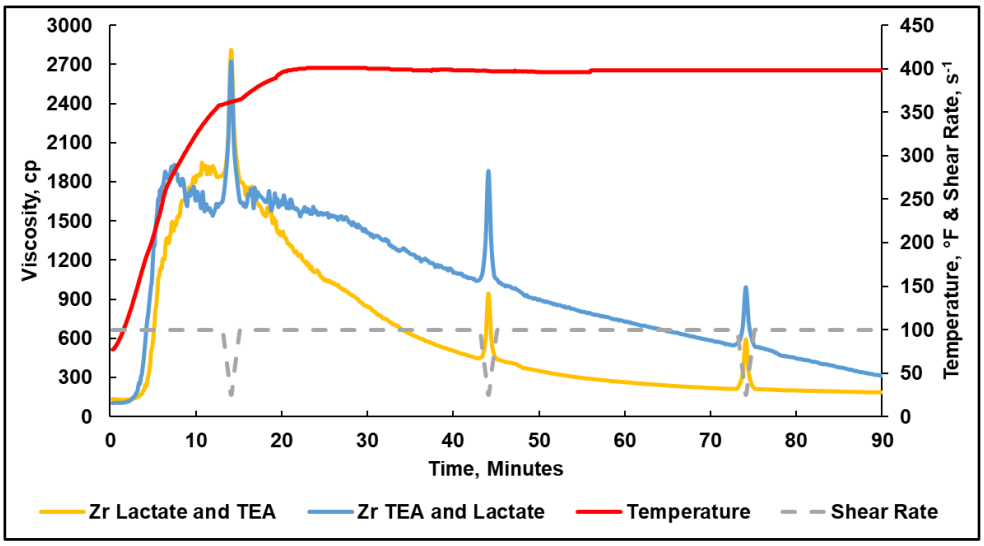

Fig. 4-27 40 lb/1,000 gal synthetic polymer-based fracturing fluids, 4 gpt crosslinker, pH 5, 400°F.

4.4.5. Zirconium Crosslinker Chemistry

Studies have shown that in the absence of strong ligands, zirconium hydrolyzes to form various mononuclear or monomeric species in solution, which form cyclic tetramers (Singhal et al. 1996; Kanazhevskiia 2001). Eventually, they continue to hydrolyze and the increase in the number of OH- groups around zirconium cations leads to the formation of $Zr\langle^{OH}_{OH}\rangle Zr$ linkages between tetramers and the formation of a polynuclear species, **Fig. 4-28**. As the degree of polymerization gradually increases and approaches the solubility limits, colloidal particles form and precipitate out of solution.

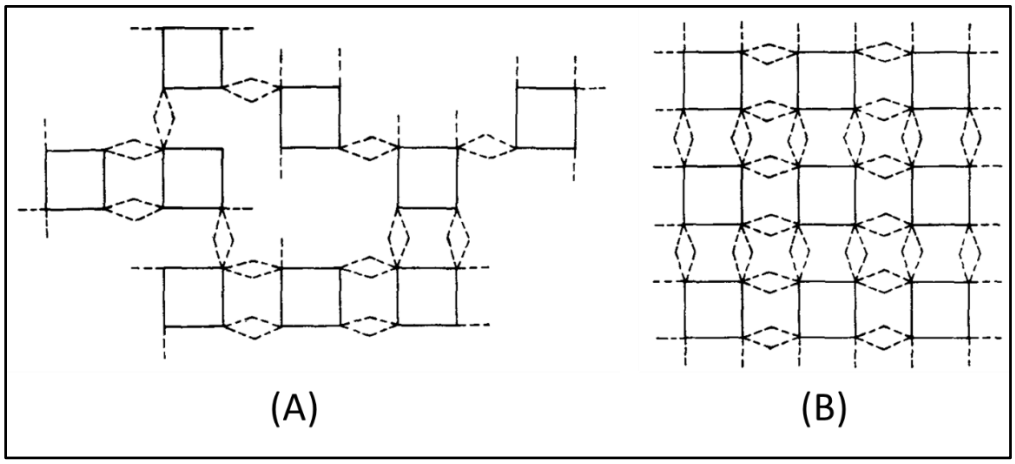

Fig. 4-28 Two-dimensional representation of polymeric species formed by the aqueous zirconium tetramers. The solid lines are the original tetrameric unit $Zr_4(OH)_8$. Dashed lines represent -OH groups formed by hydrolysis. Bent dashed lines represent a single hydroxyl group bonded to two metal atoms. (A) Randomly formed polymer. (B) Ordered polymer sheet (Clearfield 1990).

Ligands are added to the initial Zr solution to control the polymerization growth process and the interaction with the polymers. This is done to provide a delay in crosslinking viscosity to ease of pumping in fracturing fluid treatments. The presence of ligands can also influence the formation of polynuclear species as seen in **Fig. 4-29**.

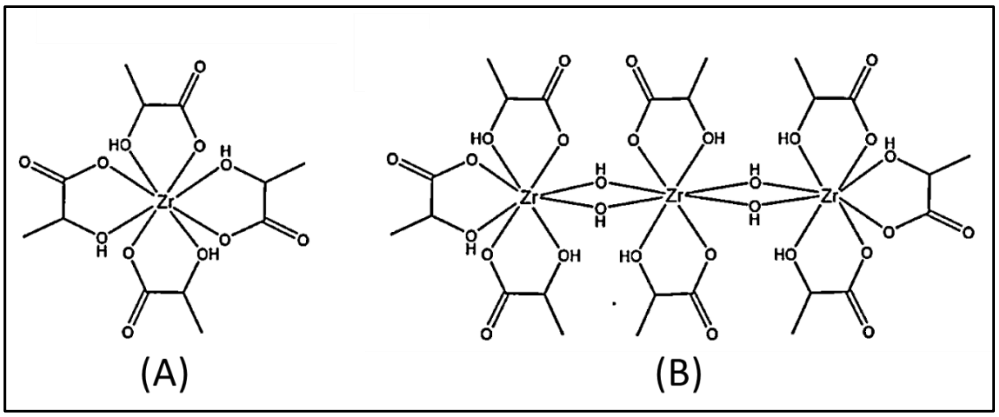

Fig. 4-29 (A) Proposed coordination of zirconium lactate. (B) Proposed polymeric structure of zirconium lactate (Demkowicz 2001).

As the ligands detach, water can interact with the polymeric species, causing zirconium species to undergo hydrolysis and polymerize into longer molecular weights. The larger polymeric species conform into globule shaped nanoparticles that can grow in size through hydrolysis (Kramer et al. 1988), **Fig. 4-30**. These particles are able to interact with the fracturing fluid polymer, **Fig. 4-31**.

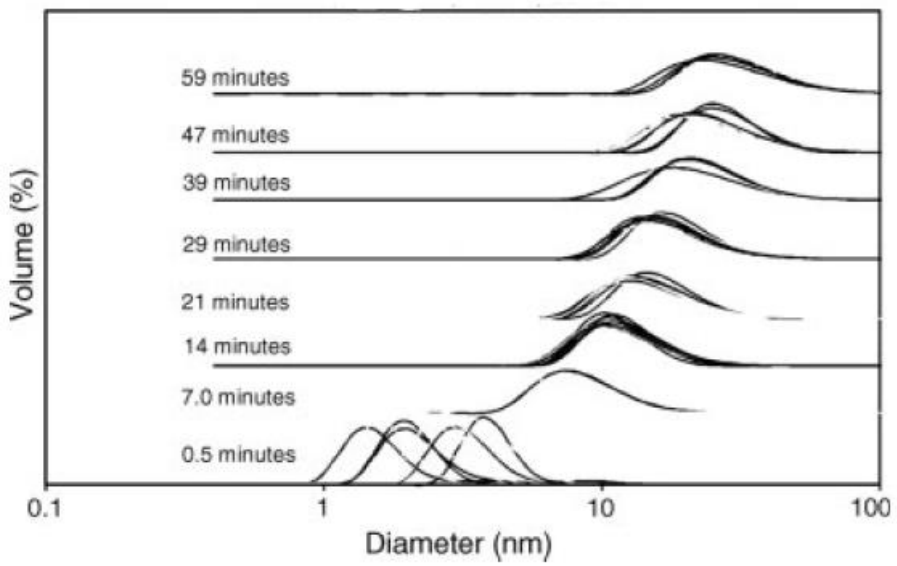

Fig. 4-30 Size Evolution of zirconium nanoparticles at 60°C after 1:1000 dilution in water, measured using dynamic light scattering (Ben, Y. et al. 2011).

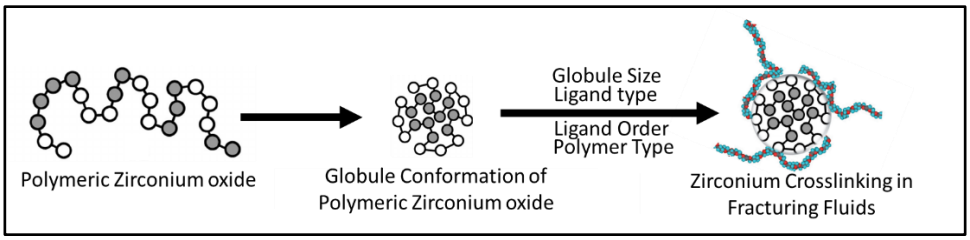

Fig. 4-31 A simplified schematic of polymeric zirconium oxide conformational change and interactions in fracturing fluids.

The size of colloidal particles in solution has been shown to influence the likelihood of achieving crosslinking viscosity. Hurnaus and Plank (2016) showed that the size of the colloidal particles required to crosslink guar is smaller than those required to crosslink HPG. In this work, the effect of ligands present in Zr crosslinkers have been shown to affect the crosslinker performance with synthetic polymer and CMHPG in different ways.

Some examples of ligands that are added to control the growth of Zr nanoparticles include lactate, phosphate, or 3-(trimethoxysilyl)propyl methacrylate (Demkowicz 2001; Rose et al. 2001; Zhou et al., 2007; Harper et al. 2010). These ligands function by forming a first coordination sphere around the Zr atom. Subsequently, additional ligands such as PG or ethylene glycol can be added to improve the stability of the Zr central atom (Kedzie 1955; Berger and Plechner 1956; Putzig 2008), which can still be easily hydrolyzed at high pH conditions (Demkowicz 2001). These ligands likely form a secondary coordination sphere as they are able to form hydrogen bonds with the ligands in the first coordination sphere, **Fig. 4-32**.

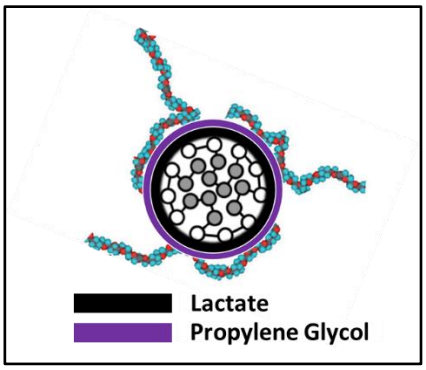

Fig. 4-32 A simplified representation of the proposed coordination spheres of Zr-La-PG crosslinker.

The polymer is crosslinked through the formation of hydrogen bonds or coordination bonds with the ZrO_2 nanoparticles. Rose et al. (2003) showed that lactate acts as a bidentate chelating agent that coordinates to the Zr central atom and that crosslinking with a polyacrylamide involved the replacement of coordinated lactate with an acrylate side group of the polymer in the first coordination sphere. Polyamides, on the other hand, have been found to crosslink via hydrogen bond formation (Jiang et al. 2017). Similar interactions can occur with the carboxylic acid and -OH side groups of CMHPG.

These interactions require the polymer side groups to enter either the first or second coordination sphere of the Zr colloidal species. This inevitably results in the replacement of the ligand in that sphere and therefore, the strength and type of ligand that occupies the corresponding coordination sphere plays an important role in determining the availability of the Zr for crosslinking.

The lack of a non-water ligand in the second coordination sphere of Zr-La allows for carboxylate groups on the synthetic polymer and CMHPG to interact with the Zr colloidal species simply through the replacement of the lactate ligand in the first coordination sphere. This results in the high initial viscosity observed with both polymers

with Zr-La. Due to the presence of PG and TEA in the second coordination sphere of the other two crosslinkers, the reactivity of the Zr-La-TEA and Zr-La-PG is lower than Zr-La, with Zr-La-PG having the slowest reaction rate.

This would imply that PG is more difficult to displace than TEA. This difficulty of displacement can be seen between the synthetic polymer and Zr-La-PG where very little viscosity increase is observed. PG contains a hydrophobic methyl group that influences its behavior in aqueous solutions (Rhys et al. 2016). Despite being hydrophobic, Rhys et al. (2016) also showed that hydrophobic hydration of the methyl group is possible. In CMHPG, it is likely that the hydroxyl groups can help in solvating PG, allowing for crosslinking between the polymers as observed in the results.

The effect of ligand order showed that the type of ligand present in each coordination sphere impacts the performance of the crosslinker and that neither ligand is able to replace the other in the first coordination sphere. This results in the observed difference in performance with both polymers.

4.5. Conclusions

Zirconium crosslinkers are the familiar choice when it comes to metallic crosslinkers. They have been used for many years providing much success to field operations world wide. Unfortunately, much ambiguity exists due to the lack of systematic studies in this area. The presented project is an initial attempt to understand the behavior of commercial zirconium crosslinkers. We hope that the work provides some insightful

knowledge towards the influence of ligand choice, ligand order, polymer choice, shear and temperature conditions on the performance of zirconium crosslinkers.

The tests conducted in this project produced the following conclusions:

- Zirconium lactate and propylene glycol crosslinker performed best with CMHPG based fracturing fluids at pH 5 and 200-400°F.
- Zirconium triethanol amine and lactate crosslinker performed best with synthetic polymer (AA-AM-AMPS) fracturing fluids at pH 5 and 200-400°F.
- Zirconium crosslinker reactivity in solution is directly related to the type and order of ligands attached.
- Zirconium Crosslinker reactivity in solution is influenced by the polymer type used.
- Polymer shear sensitivity can be reduced by using a slow releasing crosslinker for CMHPG and a faster releasing crosslinker for synthetic polymer (AA-AM-AMPS).

4.6. Acknowledgments

The authors would like to thank Leiming Li from Aramco Services Company for his assistance in the rheometer tests. The authors are also very grateful to Tom Harper from Maxflow Chemicals for providing the crosslinker samples and for his continuous discussion regarding this topic.

4.7. References

Almubarak, T., Li, L., Nasr-El-Din, H., et al. 2018a. Pushing the Thermal Stability Limits of Hydraulic Fracturing Fluids. Presented at the SPE Asia Pacific Oil and Gas Conference and Exhibition, Brisbane, Australia, 23-25 October. SPE-191920-MS. https://doi.org/10.2118/191920-MS.

Almubarak, T., Ng, J. H., Sokhanvarian, K., et al. 2018b. Improving Hydraulic Fracturing Fluids Through Dual Polymer Technology. Presented at the SPE Annual Technical Conference and Exhibition, Dallas, Texas, USA, 24-26 September. SPE-191580-MS. https://doi.org/10.2118/191580-MS.

Bedinger, G. M. 2015. Zirconium and Hafnium. *U.S. Geological Survey Minerals Yearbook* **1** (1): 86.1 – 86.6.

Ben, Y., Robb, I., Tonmukayakul, P. et al. 2011. Microgels for Oil Recovery. *Microgel Suspensions: Fundamentals and Applications*, First. Fernandez-Nieves, A., Wyss, H., Mattsson, J. et al., Chap. 16. 407-422. Germany: Wiley-VCH. https://doi.org/10.1002/9783527632992.ch16.

Berger, F. M. and Plechner, S. L. 1956. Zirconium containing anti-perspirant compositions. US2889253A.

Bhatt, N. B., Pandya, D. N., and Wadas, T. J. 2018. Recent Advances in Zirconium-89 Chelator Development. *Molecules* **23** (3): 638-662. https://doi.org/10.3390/molecules23030638.

Bishop, M., Shahid, A., Yang, J., et al. 2004. Determination of the Mode and Efficacy of the Cross-linking of Guar by Borate Using MAS 11B NMR of Borate Cross-linked

Guar in Combination with Solution 11B NMR of model systems. *Dalton Trans*. **17** (17): 2621–2634. https://doi.org/10.1039/b406952h.

Bradley, C. A., Flores-Torres, S., Lobkovsky, E., et al. 2004. Synthesis and Characterization of Zirconium and Iron Complexes Containing Substituted Indenyl Ligands: Evaluation of Steric and Electronic Parameters. *Organometallics **23*** (22), 5332-5346. https://doi.org/10.1021/om0495675.

Bradley, C. A., Lobkovsky, E., and Chirik, P. J. 2003. Synthesis of a Zirconium Sandwich Complex and Crystallographic Characterization of Its Adduct with Tetrahydrofuran. *J. Am. Chem. Soc*. **125** (27): 8110–8111. https://doi.org/10.1021/ja035594v.

Cano Sierra, J., Huerlander, D., Hill, M., et al. 2003. R. Formation of dinuclear titanium and zirconium complexes by olefin metathesis—Catalytic preparation of organometallic catalyst systems. *Chemistry* **9** (15): 3618–3622. https://doi.org/10.1002/chem.200304789.

Chatry, M., Henry, M., Livage, J. 1994. The role of complexing ligands in the formation of non-aggregated nanoparticles of zirconia. Journal of Sol-Gel Science and Technology 1 (3): 517-522. https://doi.org/10.1007/BF00486166.

Cheema, T. A. and Garnweitner, G. 2014. Phase-controlled synthesis of ZrO_2 nanoparticles for highly transparent dielectric thin films. *CrystEngComm* **16** (1): 3366-3375. https://doi.org/10.1039/C3CE42392A.

Chen, G., Zhou, S., Gu, G. et al. 2005. Effects of surface properties of colloidal silica particles on redispersibility and properties of acrylic-based polyurethane/silica

composites. *Journal of Colloid and Interface Science* **281** (2): 339-350. https://doi.org/10.1016/j.jcis.2004.08.100.

Clearfield, A. 1990. The Mechanism of Hydrolytic Polymerization of Zirconyl Solutions. J. Mater. Re. **5** (1): 161-162. https://doi.org/10.1557/JMR.1990.0161.

Coates, G. W. 2000. Precise Control of Polyolefin Stereochemistry Using Single-Site Metal Catalysts *Chem. Rev.* **100** (4): 1223-1252. https://doi.org/10.1021/cr990286u.

Demkowicz, P. A. 2001. Zirconium Complexes with Lactic Acid in the Solution and Solid State. Dissertation. University of Florida, Gainesville, Florida (May 2001).

Despagnet-Ayoub, E., Henling, L.M., Labinger, J.A., et al. 2013. Addition of a phosphine ligand switches an N-heterocyclic carbene-zirconium catalyst from oligomerization to polymerization of 1-hexene. *Dalton Trans.* **42** (44): 15544–15547. https://doi.org/10.1039/c3dt52342j.

Gdanski, R. 2001. Impact of Clay Acidity on the pH of Invading Fluids. Presented at the SPE International Symposium on Oilfield Chemistry, Houston, Texas, 13-16 February. SPE-64983-MS. https://doi.org/10.2118/64983-MS.

Gdanski, R. 2002. High-pH Clay Instability Rating. Presented at the SPE International Symposium and Exhibition on Formation Damage Control, Lafayette, Louisiana, 20-21 February. SPE-73730-MS. https://doi.org/10.2118/73730-MS.

Harper, T. L., Rosenberg, A., and Mehta, S. 2010. Stabilized aqueous aluminum zirconium solutions. US8124059B2.

Harry, D., D. Putzig, R. Moorhouse. et al. 1999. Chemical Structures of Group 4 Metal Crosslinkers For Polygalactomannans. Presented at the SPE International Symposium

on Oilfield Chemistry, 16-19 February, Houston, Texas. SPE-50731-MS. https://doi.org/10.2118/50731-MS.

Harry, D., R. Moorhouse, L. Matthews. et al. 1997. Rheological Responses to Variations in Aqueous-Based Zirconium Crosslinker Chemistry. Presented at the International Symposium on Oilfield Chemistry, 18-21 February, Houston, Texas. SPE-37280-MS.

Hedrick, J. B. 1999. Zirconium and Hafnium. *U.S. Geological Survey Minerals Yearbook* **1** (1): 87.1 – 87.6.

Hurnaus, T., and Plank, J. 2015. Crosslinking of Guar and HPG Based Fracturing Fluids Using ZrO. Presented at SPE International Symposium on Oilfield Chemistry, The Woodlands, Texas, 13-15 April. SPE-173778-MS. https://doi.org/10.2118/173778-MS.

Hurnaus, T., and Plank, J. 2016. An ITC Study on The Interaction Energy Between Galactomannan Biopolymers and Selected MO2 Nanoparticles in Hydrogels. Chemistry Select. 1: 1804-1809. https://doi.org/10.1002/slct.201600279

ISO 13503-1, 2011. Petroleum and natural gas industries-completion fluids and materials-Part 1, Measurement of viscous properties of completion fluids, second edition. Geneva, Switzerland: ISO.

Jamshidi, H. and Rabiee, A. 2014. Synthesis and Characterization of Acrylamide-Based Anionic Copolymer and Investigation of Solution Properties. *Advances in Materials Science and Engineering*. **2014** (1): 1-6. http://dx.doi.org/10.1155/2014/728675.

Jiang, H. Y., Zhang, G. Z., Feng, X. Q, et al. 2017. Room-temperature self-healing tough nanocomposite hydrogel crosslinked by zirconium hydroxide nanoparticles.

Composites Science and Technology **140** (1): 54-62. https://doi.org/10.1016/j.compscitech.2016.12.027.

Kanazhevskiia, V. V., Novgorodov, B. N., Shmachkova, V. P., et al. 2001. Structure of zirconium complexes in aqueous solutions. *Mendeleev Communications* **11** (6): 211-212. https://doi.org/10.1070/MC2001v011n06ABEH001509.

Kedzie, T. W. 1955. Propylene glycol soap gel stick anti-perspirant. US2857315A.

Kobayashi, S. and Ishitani, H. 2000. Novel binuclear chiral zirconium catalysts used in enantioselective strecker reactions. *Chirality* **12** (5-6): 540–543. https://doi.org/10.1002/(SICI)1520-636X(2000)12:5/6<540::AID-CHIR42>3.0.CO;2-P.

Kobayashi, S., Kusakabe, K., and Ishitani, H. 2000. Chiral catalyst optimization using both solid-phase and liquid-phase methods in asymmetric aza Diels-Alder reactions. *Org. Lett.* **2** (9): 1225–1227. https://doi.org/10.1021/ol005656b.

Kragten, J. and Parczewski, A. 1981. Photometric complex-formation titration of submicromolar amounts of zirconium. *Talanta* **28** (3): 149-155. https://doi.org/10.1016/0039-9140(81)80003-3.

Kramer, J., Prud'homme, R., Wiltzius, P. et al. 1988. Comparison of Galactomannan Crosslinking with Organotitanates and Borates. *Colloid and Polymer Science* **226** (1): 145-155.

Luconi, L., Giambastiani, G., Rossin, A., et al. 2010. Intramolecular σ-Bond Metathesis/Protonolysis on Zirconium(IV) and Hafnium(IV) Pyridylamido Olefin

Polymerization Catalyst Precursors: Exploring Unexpected Reactivity Paths. *Inorganic Chemistry* **49** (15): 6811–6813. https://doi.org/10.1021/ic100947q.

Millward, D.B., Sammis, G., and Waymouth, R.M. 2000. Ring-opening reactions of oxabicyclic alkene compounds: Enantioselective hydride and ethyl additions catalyzed by group 4 metals. *J. Org. Chem.* **65** (13): 3902–3909. https://doi.org/10.1021/jo991429f.

Milošev, I and Frankel, G. S. 2018. Review—Conversion Coatings Based on Zirconium and/or Titanium. *J. Electrochem. Soc.* **165** (3): C127-C144. https://doi.org/10.1149/2.0371803jes.

Mirakyan, A., Abad, C., Parris, M. et al. 2009. Rheological Characterization of Novel Delayed-Transition Metal Crosslinked Fracturing Fluids: Correlation with First Field Applications. Presented at the SPE Annual Technical Conference and Exhibition, New Orleans, 4–7 October. SPE-121757-MS. https://doi.org/10.2118/121757-MS.

Mizuno, M., Sasaki Y., Lee S. et al. 2006. High-Yield Sol−Gel Synthesis of Well-Dispersed, Colorless ZrO_2 Nanocrystals. *Langmuir* **22** (17): 7137-7140. https://doi.org/10.1021/la060774e.

Moorhouse, R., D. Harry, L. Matthews. et al. 1998. Inter-Relationships Between Polymer/Crosslinker Chemistry and Performance. Presented at the SPE India Oil and Gas Conference and Exhibition, 17-19 February, New Delhi, India. SPE-39531-MS. https://doi.org/10.2118/39531-MS.

Pacheco, J.J. and Davis, M.E. 2014. Synthesis of terephthalic acid via Diels-Alder reactions with ethylene and oxidized variants of 5-hydroxymethylfurfural. *Proc. Natl. Acad. Sci. USA* **111** (23): 8363–8367.

Parris, M. D., MacKay, B. A., Rathke, J. W. et al. 2008. Influence of Pressure on Boron Cross-Linked Polymer Gels. *Macromolecules* **41** (21): 8181-8186. https://doi.org/10.1021/ma801187q.

Prud'homme, R., Constien, V., and Knoll, S. 1989. The Effects Of Shear History On The Rheology Of Hydroxypropyl Guar Gels. *Advances in Chemistry*. **223** (6): 89-112. https://doi.org/10.1021/ba-1989-0223.ch006.

Putzig, D. E. 2008. Zirconium-based cross-linking composition for use with high pH polymer solutions. US20090227479A1.

Garvie, R. C., Hannink, R. H. and Pascoe, R. T. 1975. Ceramic steel? *Nature* **258** (1): 703–704. http://dx.doi.org/10.1038/258703a0.

Rhys, N. H., Gillams, R. J., Collins, L. E., et al. 2016. On the structure of an aqueous propylene glycol solution. *Journal of Chemical Physics* **145** (22): 1-12. https://doi.org/10.1063/1.4971208.

Rose, J., Chauveteau, G., Tabary, R. et al. 2001. Zirconium speciation in lactate solutions and polyacrylate gels. *Journal of Synchrotron Radiation* **8** (2): 686-688. https://doi.org/10.1107/S0909049500014631.

Rose, J., De Bruin, T. J. M., Chauveteau, G., et al. 2003. Aqueous Zirconium Complexes for Gelling Polymers. A Combined X-ray Absorption Spectroscopy and Quantum

Mechanical Study. *Journal of Physical Chemistry B.* **107** (13): 2910-2920. https://doi.org/10.1021/jp027114c.

Sigale, K. and Omari, A. 1997. Aspects of Crosslinking Sulfonated Polyacrylamides from Rheological Studies on Their Gels. *J Applied Polymer Science* **64** (6): 1067-1072. https://doi.org/10.1002/(SICI)1097-4628(19970509)64:6<1067::AID-APP5>3.0.CO;2-J.

Singhal, A., Toth, L. M., Lin, J. S., et al. 1996. Zirconium(IV) Tetramer/Octamer Hydrolysis Equilibrium in Aqueous Hydrochloric Acid Solution. *Journal of the American Chemical Society* **118** (46): 11529–11534. https://doi.org/10.1021/ja9602399.

Sokhanvarian, K., Nasr-El-Din, H. A., and Harper, T. 2019. Effect of Ligand Type Attached to Zirconium-Based Crosslinkers and the Effect of a New Dual Crosslinker on the Properties of Crosslinked Carboxymethylhydroxypropylguar. SPE J. SPE-194204-PA. https://doi.org/10.2118/194204-PA.

Sun, H. and Qu, Q. 2011. High-Efficiency Boron Crosslinkers for Low-Polymer Fracturing Fluids. Presented at SPE International Symposium on Oilfield Chemistry, The Woodlands, Texas, 11-13 April. SPE-140817-MS. https://doi.org/10.2118/140817-MS.

Wadas, T.J., Wong, E.H., Weisman, G.R., et al. 2010. Coordinating radiometals of copper, gallium, indium, yttrium, and zirconium for PET and SPECT imaging of disease. *Chem. Rev.* **110** (5): 2858–2902. https://doi.org/10.1021/cr900325h.

Zhang, K., Zhang, G., Li, Z. et al. 2019. Laboratory Evaluation of a Low pH and Low Polymer Concentration Zirconium-CMHPG Gel System for Hydraulic Fracturing. *Energy Fuels.* **33** (10): 9720-9735. https://doi.org/10.1021/acs.energyfuels.9b02419.

Zhou, S., Garnweitner, G., Niederberger, M. et al. 2007. Dispersion Behavior of Zirconia Nanocrystals and Their Surface Functionalization with Vinyl Group-Containing Ligands. *Langmuir* **23** (18): 9178–9187. https://doi.org/10.1021/la700837u.

Zuckerman, R.L., Krska, S.W., and Bergman, R.G. 2000. Zirconium-mediated metathesis of imines: A study of the scope, longevity, and mechanism of a complicated catalytic system. *J. Am. Chem. Soc.* **122** (5): 751–761. https://doi.org/10.1021/ja992869r.

5. INSIGHTS ON POTENTIAL FORMATION DAMAGE MECHANISMS ASSOCIATED WITH THE USE OF GEL BREAKERS IN HYDRAULIC FRACTURING*

5.1. Abstract

Hydraulic fracturing using water-soluble polymers has been extensively used to improve the productivity of oil and gas wells, especially in low-permeability formations. However, the production enhancement can be significantly reduced due to damage generated in the proppant pack or the fracture face. This work describes an approach to establish a suitable fracturing fluid cleanup process by analyzing the broken polymer residues generated from the use of different gel breaker types. In addition, this work studies the interactions of gel breakers with polymeric clay stabilizers, as well as the interactions of gel breakers with hydrogen sulfide (H_2S) in sour environments.

Several experiments were conducted to assess the effect of different gel breakers on a high-temperature fracturing fluid as a function of time. Commonly used gel breakers such as inorganic oxidizers (bromate and persulfate salts), specific enzymes, and acids were evaluated in this work. The influence of each gel breaker was examined using various techniques, such as Zeta Potential, Gel Permeation Chromatography (GPC), High-Pressure/High-Temperature (HP/HT) aging cells, H_2S compatibility tests and Environmental Scanning Electron Microscope/Energy Dispersive X-Ray Spectroscopy (ESEM/EDS).

* Part of this chapter is modified with permission from "Insights on Potential Formation Damage Mechanisms Associated with the Use of Gel Breakers in Hydraulic Fracturing" by Almubarak, T., Ng, J., AlKhaldi, M. et al. 2020. Polymers 12 (11): 2722. Copyright 2020 by MDPI.

All experiments were performed on a carboxymethyl hydroxypropyl guar (CMHPG) fracturing fluid with a polymer loading of 45 lb/1,000 gals at temperatures up to 300°F. The fracturing fluid also included a commonly used high-temperature stabilizer and a dual crosslinker (Boron/Zirconium).

The results obtained from this study have shown that the amount of residue and the size of the broken polymer chains were mainly dependent on the type of gel breaker used. Moreover, laboratory tests have revealed that some gel breaker types may negatively influence the performance of polymeric clay stabilizers. Additionally, this work showed damaging precipitations that can be generated due to the interactions of gel breakers with H_2S.

5.2. Introduction

Hydraulic fracturing treatments have been extensively used as one of the main stimulation techniques to enhance the productivity of oil and gas wells, especially in low-permeability fields (Clark 1949; Farris 1953; Al-Muntasheri 2014). These treatments have been applied in relatively shallow to deep hot formations with depth more than 20,000 ft (Yongjun et al. 1999; Ding et al. 2004). They have also been successfully applied using water salinities up to seawater and even produced water (Gupta et al. 2012; Li et al. 2016; Almubarak et al. 2019). One of the key factors that affect the success of hydraulic fracturing treatments is the selection of fracturing fluids and their additives. Optimum fracturing fluids have rheological properties such that it initially provides sufficient viscosity for fracture initiation and propagation, it is able to suspend proppant into the created fracture, and later it decomposes to a low viscosity fluid at the end of the treatment to allow for fracturing fluid cleanup and hydrocarbon production (Rae and Di Lullo, 1996).

There are several fracturing fluids that have been used in fracturing treatments. These fluids can be divided into two main groups, namely oil-based and water-based fracturing fluids. Oil-based fracturing fluids are gasoline gelled with aluminum carboxylates, soaps, viscous refined oils, phosphate esters or gelled crude emulsions (Howard and Fast 1970; Harms 1989; Maberry et al. 1997; Thompson et al. 2000; Taylor et al. 2010; Li et al. 2020). They were used to prevent damage to formations containing water-sensitive clays. With the introduction of clay stabilizers such as potassium chloride,

water-based fracturing fluids provided a safer, lower HSE (health, safety, and environment) footprint, and cheaper alternative to oil-based fracturing fluids.

A typical water-based fracturing fluid contains a polymer thickening agent, clay stabilizer, crosslinker, buffer system, and a gel breaker. Different polymers have been used as thickeners, such as starches and cellulose derivatives (Montgomery 2013; Azizov et al. 2015; Ming et al. 2016). However, the most common fracturing fluid polymers are guar gum and its two main derivatives hydroxypropyl guar (HPG) and carboxymethyl hydroxypropyl guar (CMHPG) due to their high performance, relatively low price and wide availability (White and Means 1975; Venkataiah and Mahadevan 1982; Weaver et al. 2003; Lei and Clark 2007; Pasha and Ngn 2008; Hu et al. 2015).

Guar gum and its derivatives provide sufficient rheological properties for proppant transport and leak-off control. These rheological characteristics can be reached with a lower concentration of guar gum when crosslinkers are used. There are two main types of crosslinkers: boron-based crosslinkers and metallic crosslinkers and they have been studied extensively by many authors throughout the years (Nickerson 1971; Kramer et al. 1987, 1988; Prud'homme et al. 1989; Brannon and Ault 1991; Dawson 1991; Kesavan et al. 1993; Harris 1993; Moorhouse et al. 1998; Parris et al. 2008; Almubarak et al. 2020). These two types of crosslinkers can be used individually or in combination to complement the weaknesses of each other (Yartiz et al. 1997; Driweesh et al. 2013).

Besides the fracturing fluid rheological properties, its chemical breakage and cleanup characteristics are critical for maintaining a high fracture conductivity. Gel breakers are used to reduce the viscosity of fracturing fluid either by cleaving polymer

molecules into smaller fragments or by de-crosslinking the network, which involves removal or rather chelation of the crosslinking molecules (Reddy 2014; Al-Muntasheri et al. 2018).

Gel breakers can be used in its “live” or encapsulated form. Breaker encapsulation technologies provide some control over the breaker active ingredient release rate. Therefore, the encapsulation provides a delayed activation especially at higher temperature conditions preventing aggressive reactions, early screen outs and corrosion to the tubular (Alterman and Chun 1976; Nolte 1985; Gulbis et al. 1992; Manalastas et al. 1992; Lo et al. 2002; Barati et al. 2012). Due to the many factors that can influence the encapsulated breaker release rate, “live” breakers with no encapsulation were used throughout this work to compare the gel breakers. To break the polymer molecule, three main gel breaker chemical families are typically used in the field: enzymes, oxidizers, and acids (Gall and Raible 1985; Brannon and Tjon-Joe-Pin 1994; Economides and Nolte 2000).

Enzymes are monomeric or oligomeric proteins that contain hundreds of amino acids. They can fold to form 3D structures that act as catalysts targeting specific bonds in the polymer, causing it to break into smaller fragments, thus, reducing the viscosity of the fracturing fluid. They only target specific chemical bonds in the polymer through a lock and key mechanism, posing a lower risk of side reactions with other additives or the tubular. They are also not consumed by breaking the polymer and will continue to act until they are denatured. Denaturing is the process where the enzyme loses its conformation and shape irreversibly, making it inactive and unable to function, commonly resulting in

precipitation. Enzyme denaturing can occur due to several reasons such as high temperature (>150°F), low or high pH conditions (pH < 4 or pH >10), extreme changes in salt concentrations, presence of solvents and the presence of transitional metals such as iron or zirconium (Gupta et al. 1992; Cabianco et al. 2007; Li et al. 2010). Some enzymes have also been known to reduce activity between 8 < pH < 10 or in the presence of calcium chelating agents (Elkatatny et al. 2017). However, there are many recent techniques that can be used to enhance the performance of enzymes under the harsh oil and gas field environments. These include the adaptation from organisms that live at a much higher temperature, use of specific ions such as calcium, enzyme mutation treatments (addition of disulfides bridges, increasing hydrogen bonding, increasing internal hydrophobicity), the use of organic additives, and increased pressure (Nelson et al. 1992; Samuel et al. 2010; Zhang et al. 2013).

Enzymes typically used to reduce the viscosity of crosslinked polysaccharides are from the glycoside hydrolase family. They catalyze the hydrolysis reaction of the β -1,4 glycosidic bond between the mannose molecules in the polysaccharide backbone to produce simple sugars such as monosaccharides or disaccharides that are soluble in water. Some examples of enzymes used in the oilfield include Amylase, Cellulase, Hemicellulase, Pectinase, and Mannanase (Al-Khaldi et al. 2011).

Oxidizers, on the other hand, work by producing active radicals that can randomly attack several hydrogens placed in the polymer structure, as seen with CMHPG in **Fig. 5-1**. The attack can result in either breaking the mannose backbone into soluble sugars or

breaking apart the galactose side chains producing insoluble residues (Brannon and Tjon-Joe-Pin 1994; Nasr-El-Din et al. 2007).

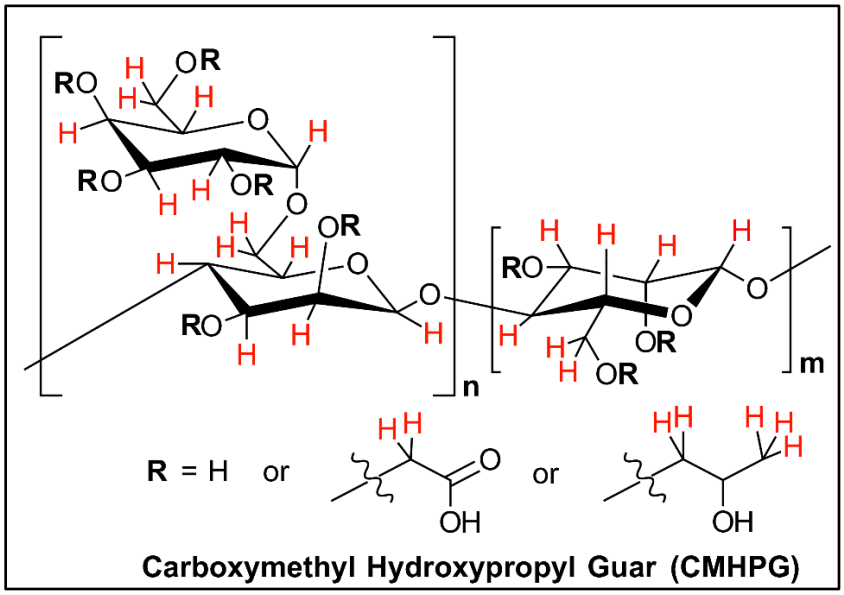

Fig. 5-1 Hydrogen atoms in red are sites on the polymer that can be attacked by oxidizer radical molecules (Adapted from Brannon and Tjon-Joe-Pin 1994).

These radicals are generated at specific temperature conditions. Persulfate salts are typical low-temperature gel breakers (120°F < T < 200°F) due to high reactivity at higher temperatures, whereas bromate salts are used for higher temperature applications (T > 200°F) (Economides and Nolte 2000). Unlike enzymes, the generated radicals are hard to control, limited in quantity, and will get consumed by the different additives in the fracturing fluid. They are also able to react with the tubular, causing corrosion. The most widely used oxidizers are persulfate salts.

Acid gel breakers work in a similar manner to oxidizers; they can break the polymer molecule through hydrolysis reactions in acidic conditions resulting in a variety of insoluble material. Acid gel breakers can also be used to de-crosslink borate-based

fracturing fluids by reducing the amount of monoborate ions (MBI) in solution due to the reduction in pH (Maley and O'Neil 2010).

Reinicke et al. (2012) provided a review of the potential formation and fracture damage processes that result from chemical, physical, and thermal interactions between fracturing fluids and formation components, including fluids and rock constituents. Optimal gel breakers must generate minimum unbroken gel residues to avoid causing any damage to the propped fracture (Almond and Bland 1984).

This work will provide 1) an overview of typical gel breaker analysis, 2) detailed polymer breakage analysis using GPC, 3) polymeric clay stabilizer performance analysis in the presence of gel breakers, and 4) gel breaker-induced precipitation in sour environments.

5.3. Experimental Procedures

5.3.1. Materials

The fluid used in this work is a 45 lb/1,000 gal CMHPG based fracturing fluid. The additives were mixed in the laboratory using typical concentrations used in the field. The fracturing fluid contained CMHPG polymer, high-temperature stabilizer, and a dual crosslinker (borate/zirconium), which were all provided by a service company and used as received, **Table 5-1**. Persulfate, bromate, enzyme, and acid “live” gel breakers were supplied by several service companies and were used as received for zeta potential, rheological measurements, GPC, and compatibility experiments. Two polymer clay stabilizers and KCl were supplied by several service companies and used as received for

the GPC and zeta potential tests. The composition of the tested additives used is shown in **Table 5-2**.

Chemical	Concentration
Polymer (CMHPG)	45 ppt
Gel stabilizer (Sodium Thiosulfate)	9 gpt
Zr- crosslinker (Zirconium Triethanolamine)	0.8 gpt
B- crosslinker (Potassium Metaborate)	0.1 gpt

Table 5-1 Fracturing fluid recipe.

Additive	Main Component
Acid breaker	Chlorous acid
Bromate gel breaker	Sodium bromate
Persulfate gel breaker	Diammonium peroxydisulfate
Enzyme gel breaker	Mixture of 1,6-α-D-galactosidase and endo-1,4-β-mannosidase
Polymeric clay stabilizer 1	Hydroxyalkyl alkylammonium chloride
Polymeric clay stabilizer 2	Polyquaternary amine
Salt clay stabilizer	KCl

Table 5-2 Additive composition.

5.3.2. Fluid Preparation

To prepare the 45 lb/1,000 gal crosslinked fracturing fluid, 4.32 g of CMHPG was added to 800 $cm^3$of tap water (< 500 ppm). The fluid was mixed at 400-800 RPM using a blender to create a visible vortex for 20 minutes. Following that, 7.2 cm^3 of the high-temperature stabilizer was added and mixed at 400-800 RPM for 5 minutes. Liquid gel breakers were added at this point as required (Acid: 2 gpt; Enzyme: 5 gpt), while solid gel breakers were added directly to the final crosslinked sample in the viscometer (Persulfate: 8 ppt; Bromate: 8 ppt). The pH was adjusted to 10 using NaOH. The crosslinkers were then included by adding 0.64 cm^3 of zirconium crosslinker followed by 0.08 cm^3 of borate crosslinker while shearing at 400-800 RPM. Samples of 52 cm^3 were used for the

viscometer tests, and samples of 250 cm^3 were used for the HP/HT aging cell tests that were further used for GPC analysis.

Zeta potential, H_2S tests, and specific additive compatibility tests did not include CMHPG or the dual crosslinkers; they were strictly between gel breakers and clay stabilizers, or gel breakers and H_2S.

5.3.3. Viscosity Measurements

An HP/HT rheometer was used to measure the apparent viscosity of the gelling samples under different shear rates and temperature ranges. This viscometer utilized standard R1/B5 bob and rotor combinations, which require a sample volume of 52 cm^3. The viscometer uses a sliding carbon block for dry heating, and the temperature sensor is mounted on the stator/bob to control sample temperature. A pressure of 1,000 psi was applied to prevent the boiling of the samples at high temperatures. Nitrogen gas was used because it is inert.

Viscosity measurements were performed under different shear rates to simulate the flow of the fracturing fluid through production tubular, perforations, and inside the created fracture following the ISO13503-1 testing schedule for a duration of 2.5 hours. The shear rate range was 100 s^{-1} with varying low shear ramps in the schedule, while the temperature was set at 300□F. Around 25 cm^3 of fracturing fluid was placed into the rheometer cup, followed by adding solid gel breakers (if required) in the middle, and the remaining 27 cm^3 of the fracturing fluid was then added. This method was used to ensure complete contact between the gel breakers and the fracturing fluid since the quantity of breakers used in each test is extremely low.

5.3.4. HP/HT Aging Cell

The HP/HT aging cells were mainly used to prepare the fracturing fluid samples for gel permeation chromatography analysis. The cells were also used to age fluids for the zeta potential tests. These experiments were carried out in 250 cm^3 glass bottles that were inserted to the HP/HT cells, pressurized by nitrogen to 400 psi and heated to 200-300°F for 0.5-48 hours.

5.3.5. Gel Permeation Chromatography

GPC is composed of different columns filled with porous beads of controlled porosity and particle size. The concept behind GPC is that the larger polymer molecules will not get trapped by the pores in the column and will appear early in the GPC results. The smaller molecules will take a longer time because they will get trapped in the column pores and would need to weave through the pores to get to the other end, which will cause them to appear later in the results. Based on this concept, the larger polymer fragments will appear earlier than the smaller polymer fragments. Also, the width of the peaks is representative of the polymer polydispersity index (PDI), **Fig. 5-2**. An analysis is further done using known molecular weight standards to determine the peak molecular weight of polymer fragments being measured. Jackson et al. (1996) showed that peak molecular weight (Mp) is a representation of the most abundant molecular weight in the sample. A curve fit can be done with the calibration points to extend the range beyond the standards being used. However, these values would not be as accurate as the values within the known standard values. For that reason, we only report values within the size of the standards used.

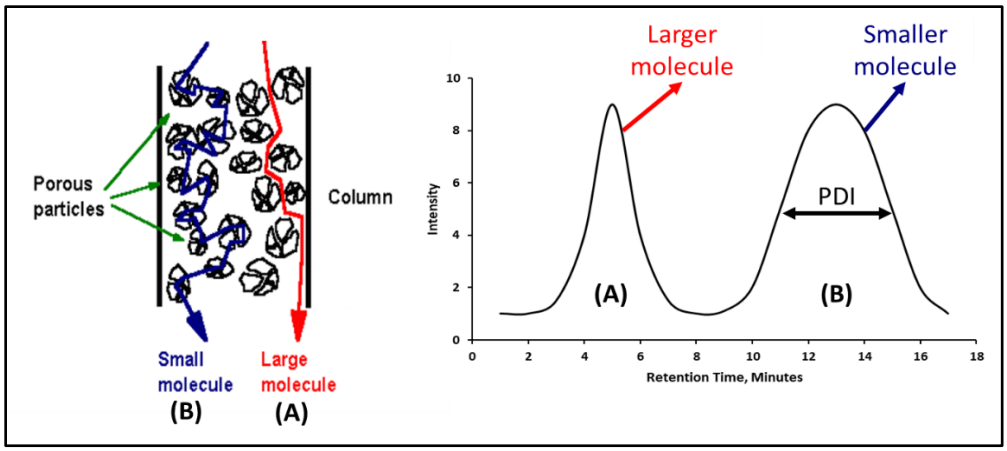

Fig. 5-2 Simplified GPC illustration and example showing that molecule A size > molecule B size, and molecule B PDI > molecule A PDI.

The developed aqueous gel permeation chromatography (GPC) method was applied to determine the Mp and the distribution profile of crosslinked 45 lb/1,000 gal polymer samples treated with gel breakers. About 150 mg of each sample was dissolved in 5 cm^3 of 0.05 M NaNO3. The diluted samples were shaken with a mixer at 300 rpm for 30 minutes. Then, the samples were directly injected into the GPC system. The standard solutions for calibration of the GPC column were prepared by dissolving 2 mg of each pullulan standard in 1 cm^3 of 0.05 M NaNO3 in separate vials. The standard solutions were dissolved for 1 hour to achieve complete dissolution of the polymer with occasional shaking. Eight pullulan calibration standards with the following peak molecular weights (Mp) values: 21,100; 47,100; 107,000; 194,000; 344,000; 708,000; 1,220,000 and 2,350,000 g/mol were used for the calibration of the column. All the GPC separations were carried out on a PL aquagel-OH MIXED-H (7.5 x 300 mm, 8 µm) column. The mobile phase was 0.05 M NaNO3. The flowrate throughout the separation was maintained at 0.8 cm^3/min.

A separate aqueous GPC method was developed to determine the peak molecular weight (Mp) and the distribution profile of heated and gel breaker-treated clay stabilizer polymer samples. All the treated samples were filtered through a 0.45 µm hydrophilic syringe filter before the analysis with GPC. Polyethylene glycol standards with a peak molecular weight (Mp) 106; 194; 282; 420; 610; 1,010; 1,480; 4,040; 7,830; 16,100; 21,300, 34,890, 47,100; 107,000; 194,000 and 344,000 g/mol were used for the calibration of the column. All samples were separated on a PSS NOVEMA Max (300 x 8 mm, 10 µ) 100 Å columns. The mobile phase was 0.05% formic acid, with a maintained flowrate of 0.8 cm^3/min.

All GPC separations for both sets of samples were carried out on an Agilent 1260 series high-performance liquid chromatography with a binary pump, a degasser, an auto-sampler, and a refractive index detector. Instrument control and GPC data analysis were performed through the OpenLAB and Cirrus software, respectively.

5.3.6. Zeta Potential

The zeta potential was measured by using micro electrophoresis. Changes in zeta potential were measured for illite crushed samples in solutions containing different clay stabilizers. Each sample was prepared by weighing out 1 gram of illite particles suspended in a total of 250 cm^3 of DI water (resistivity of 18 Ω.cm). Each of these suspensions were ultrasonicated for 30 minutes in a sonic bath. Following that, clay stabilizers and gel breakers were added to the samples (Persulfate: 8 ppt; Bromate: 8 ppt; Acid: 2 gpt; Enzyme: 5 gpt), shaken by hand, and aged for 24 hours at 200-300°F using aging cells as

required. After aging, the samples were shaken by hand and stood at room temperature (77°F) for another 24 hours to reach equilibrium prior to analysis.

The used electrode assembly was conditioned in 1 M NaCl using 350 cycles. This conditioning procedure produces a uniform black coating on the electrodes, which is vital for zeta potential analysis of suspensions in high ionic strength solutions.

The particle suspension was added as required to the cuvette at a 45° angle to avoid trapping air bubbles between the electrodes. Visual inspection for bubbles on the surface of the cuvette or between the electrodes is required to ensure proper measurements. Air bubbles can often be dislodged by gently tapping on a hard surface. The cuvette was then placed in the instrument and allowed to equilibrate to the measurement temperature of 25°C for a period of 5 minutes.

5.3.7. Sour Environment Compatibility Tests

Several tests were conducted to investigate the interaction of H_2S with different gel breakers at 77°F. The H_2S tests were conducted using a closed system loop. H_2S was generated by reacting 1 grams of iron sulfide (FeS) with 10 cm^3 of 10 wt% HCl in an Erlenmeyer flask, the generated H_2S gas was then diverted to a second flask containing a solution containing 200 cm^3 of DI water (resistivity of 18Ω.cm) and the gel breaker at the desired concentration (Persulfate: 8 ppt; Bromate: 8 ppt; Acid: 2 gpt; Enzyme: 5 gpt). After exposing the solution to H_2S gas, the H_2S was then diverted to a third flask containing 200 cm^3 of 5 wt.% of cadmium sulfate (CdSO4), where the unreacted H_2S was scavenged completely into solid cadmium sulfide (CdS). The setup is shown in **Fig. 5-3**. The H_2S experiments lasted 4 hours, and the middle flask solution was then filtered

through 0.2 µm filter paper and washed with DI water to determine if there was any precipitation. The same experimental procedure was conducted several times to assess the interaction of H2S with typical fracturing fluid gel breakers as a function of the gel breaker type.

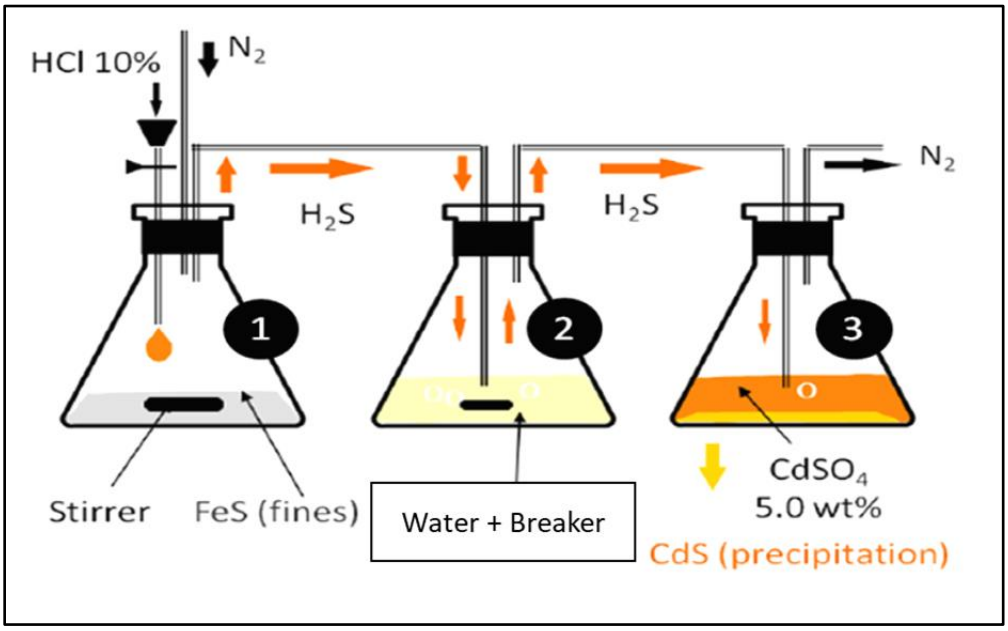

Fig. 5-3 H_2S compatibility experiment setup.

5.3.8. Environmental Scanning Electron Microscope

The environmental scanning electron microscope (ESEM) with integrated ultra-thin window energy dispersive X-ray detector was utilized to perform comprehensive compositional characterizations of the precipitation. The precipitation samples resulted from oxidizer gel breaker interactions in sour environments were first prepared by filtering the precipitation out of solution using a 0.2 µm filter paper. After that, the samples were dried at 60°C in the oven for 24 hours. The ESEM/EDS data are required to identify the

minerals in the sample. The primary goal in this test was to identify the main components of the precipitation resulting from gel breaker interactions in sour environments.

5.4. Results and Discussion

5.4.1. Fracturing Fluid Viscosity Tests

The fracturing fluid and gel breaker viscosity analysis were first conducted to determine the general effect of different gel breakers at 300ºF. The viscosity of the fracturing fluid without any gel breaker was averaging 350 cP after 2 hours at 300ºF and 100 s^{-1} shear rate. The fracturing fluid viscosity after 2.5 hours at the same temperature with bromate, acid, and enzyme gel breakers were 20, 50, 130 cP, respectively, **Fig. 5-4**. This test shows that all gel breakers are effective in breaking this fracturing fluid. The enzyme needed more time to fully activate and lower the viscosity of the fracturing fluid. Although the fracturing fluids containing bromate or acid were low and close in final broken viscosity values, when the fluids were taken out from the viscometer, the remaining effluents contained portions of the crosslinked fluid that were left unbroken. This has also been observed in several previous gel breaker evaluation tests that exhibited low viscosity while still containing a significant amount of unbroken fracturing fluid residue, **Fig. 5-5**. Further tests were conducted using GPC to understand the influence of each breaker type.

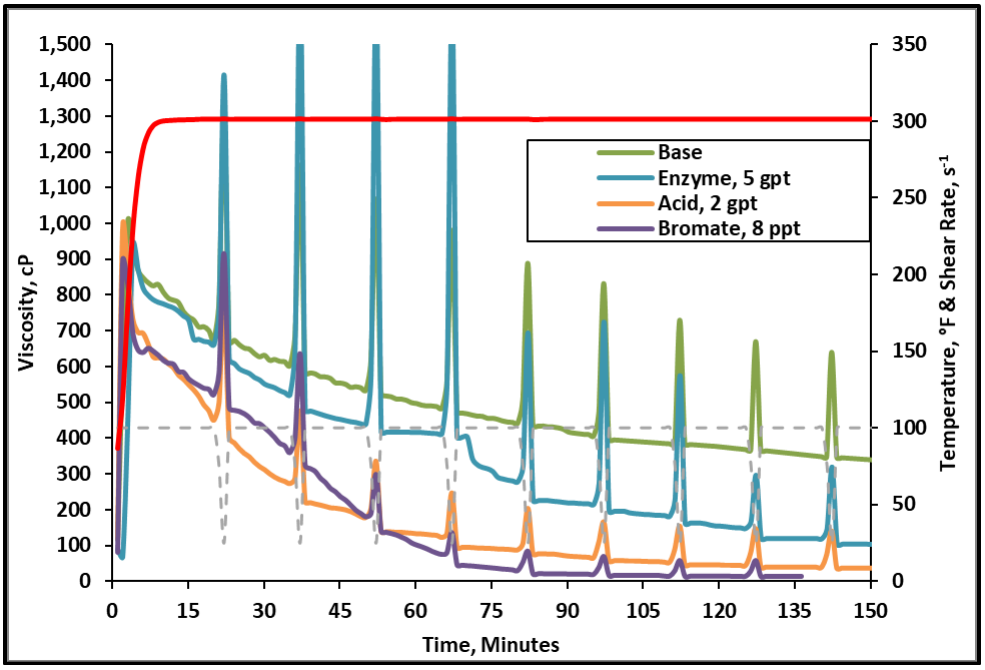

Fig. 5-4 Viscosity of 45 lb/1,000gal crosslinked fracturing fluid as a function of gel breaker type at 300°F.

Fig. 5-5 Unbroken polymer residue remaining after various breaker evaluation tests at 300°F (oxidizers and acids), yet they still exhibited low final viscosity (< 50 cp @ 100 s^{-1}).

5.4.2. Fracturing Fluid Polymer-Gel Breaker GPC Analysis

Several samples of the high temperature fracturing fluid were aged using HP/HT cell for 0.5, 2, 4, and 24 hours at 200°F with persulfate and at 300°F with bromate, acid, and enzymes. Visually, in the absence of gel breakers, the crosslinked samples remained crosslinked and showed no obvious reduction in the viscosity upon tilting after 24 hours. The samples that contained gel breakers showed a clear significant visual reduction in viscosity at all tested time periods.

After the crosslinker fracturing fluids were broken by the gel breakers, the samples were visually inspected for polymer residue. The fracturing fluid samples in the presence of bromate, persulfate or acid gel breaker that were tested for 24 hours were not homogenous. Clumps of polymer were separated from the less viscous water phase. The degree of residue and separation was highest in the samples containing acid gel breakers and the least in the enzyme gel breaker, **Fig. 5-6**.

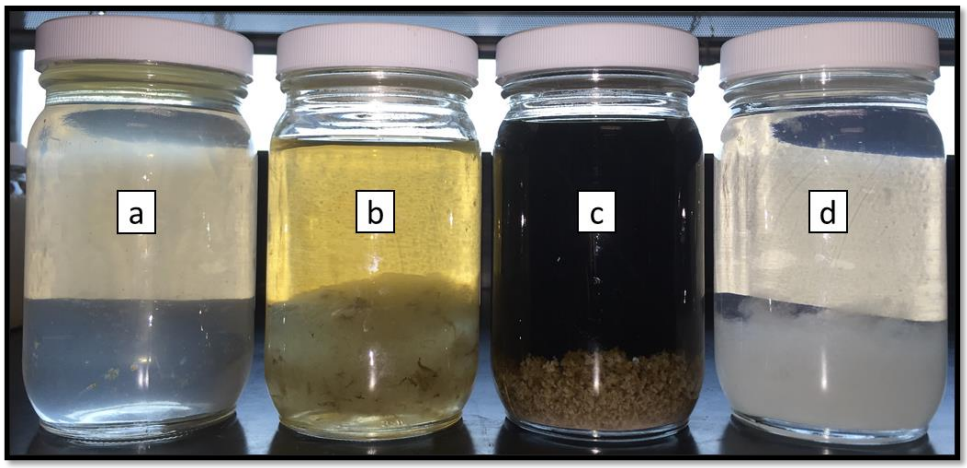

Fig. 5-6 Residual polymer in the broken crosslinked fracturing fluid samples after exposure to different gel breakers (a: enzyme -5 gpt, b: acid – 2 gpt, c: bromate – 8 ppt, d: persulfate - 8 ppt) after 24 hours at 200-300°F.

After completing the visual inspection, the samples were tested thoroughly using GPC to analyze and compare the effect of persulfate, bromate, acid, and enzyme gel breakers on the fracturing fluid polymer. The goal of this test was to compare the approximate broken polymer size in all gel breaker solutions at different time intervals. The polymer size in different gel breaker treated samples at 4 hours were from highest to lowest: enzyme, acid, persulfate, bromate, **Figs. 5-7, 5-8** and **5-9**. The samples that were aged for 24 hours showed that the polymer size comparison from highest to lowest was the following: acid, bromate, persulfate, enzyme, **Fig. 5-10**. It was noted that the bromate gel breaker reactions stopped after around 4 hours, as the molecular weight of the broken crosslinked polymer didn't change noticeably, whereas, the enzyme was fully functional after 24 hours and contributed to the lowest final molecular weight compared to all other gel breakers, **Fig. 5-11, Table 5-3**.

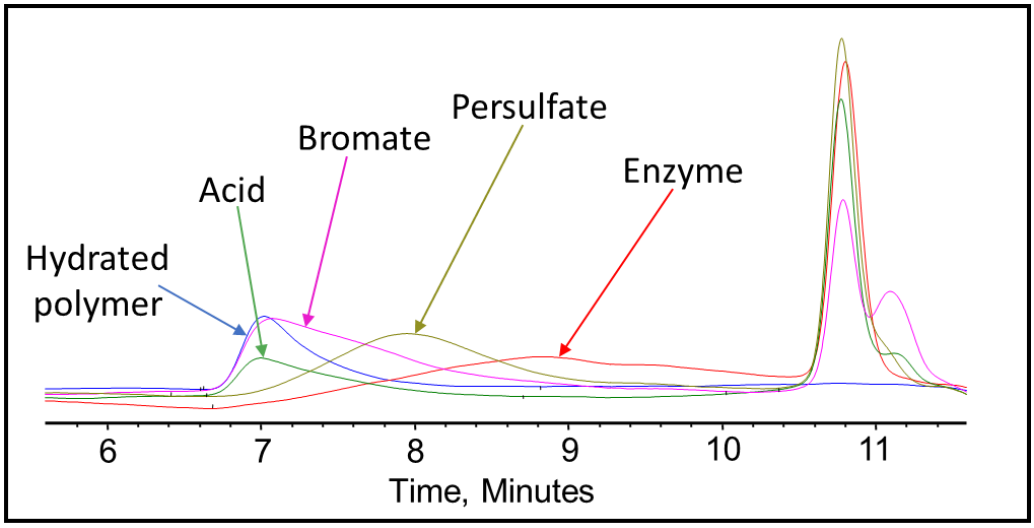

Fig. 5-7 GPC results of the 45 lb/ 1,000 gal crosslinked fracturing fluid exposed to different gel breakers (persulfate: 8 ppt, bromate: 8 ppt, acid: 2 gpt, enzyme: 5 gpt) after 0.5 hours at 200-300°F.

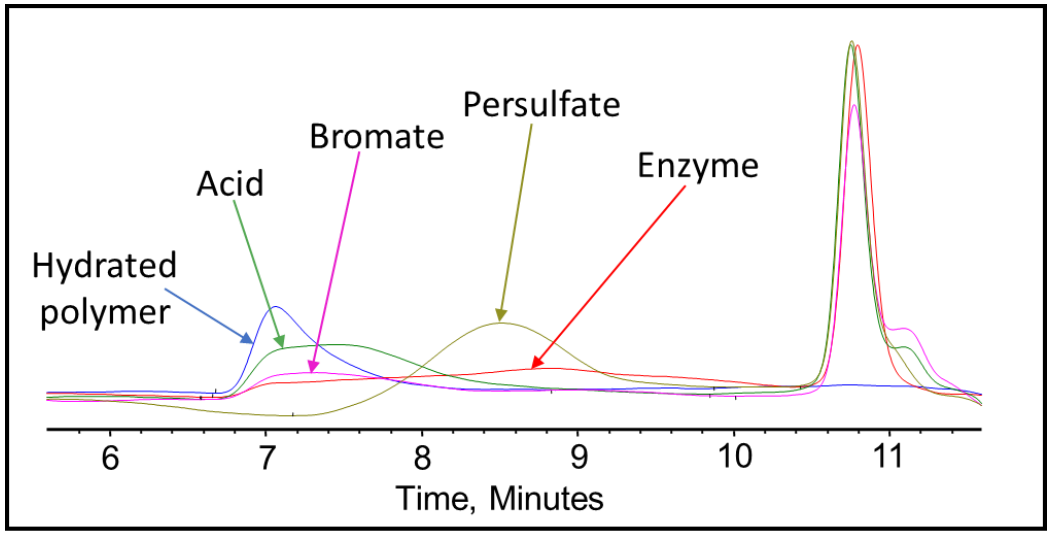

Fig. 5-8 GPC results of the 45 lb/ 1,000 gal crosslinked fracturing fluid exposed to different gel breakers (persulfate: 8 ppt, bromate: 8 ppt, acid: 2 gpt, enzyme: 5 gpt) after 2 hours at 200-300°F.

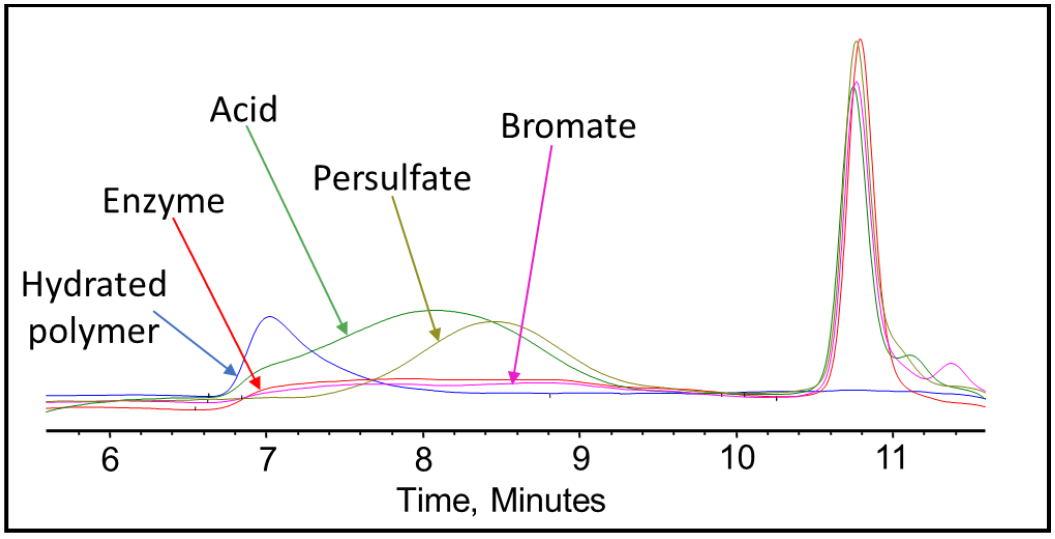

Fig. 5-9 GPC results of the 45 lb/ 1,000 gal crosslinked fracturing fluid exposed to different gel breakers (persulfate: 8 ppt, bromate: 8 ppt, acid: 2 gpt, enzyme: 5 gpt) after 4 hours at 200-300°F.

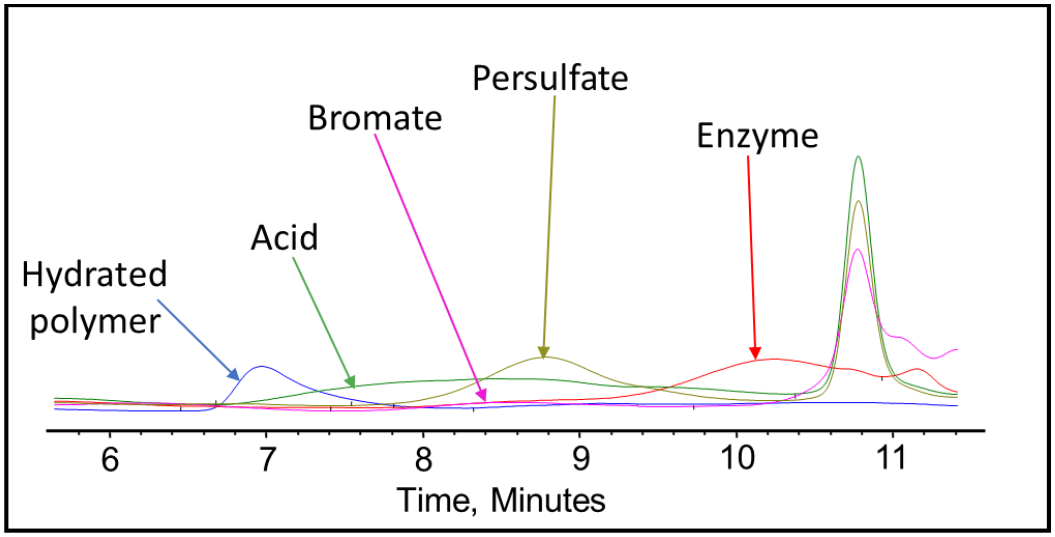

Fig. 5-10 GPC results of the 45 lb/ 1,000 gal crosslinked fracturing fluid exposed to different gel breakers (persulfate: 8 ppt, bromate: 8 ppt, acid: 2 gpt, enzyme: 5 gpt) after 24 hours at 200-300°F.

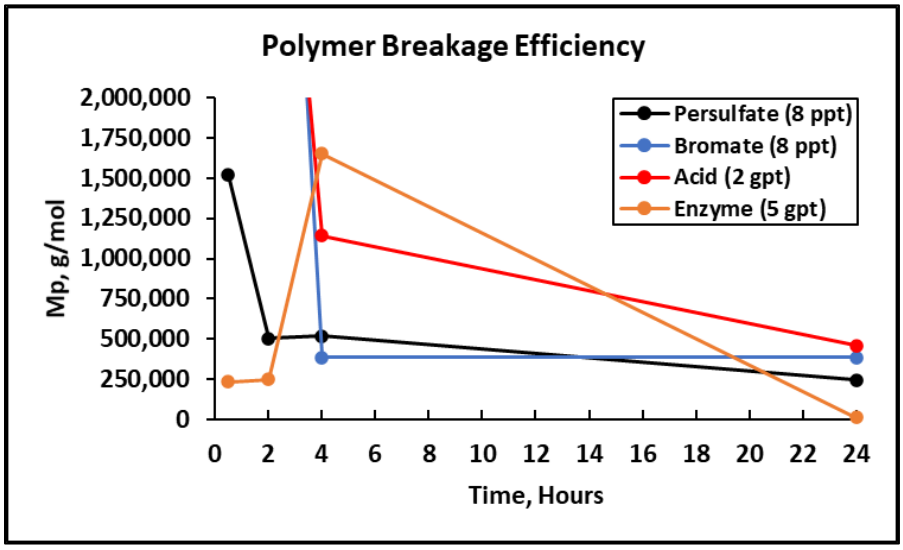

Fig. 5-11 Peak molecular weight values for the 45 lb/ 1,000 gal crosslinked fluid mixed with gel breakers at different time intervals at 200-300°F.

Sample, concentration	Mp 0.5 Hours (g/mol)	Mp 2 Hours (g/mol)	Mp 4 Hours (g/mol)	Mp 24 Hours (g/mol)
Persulfate gel breaker (8 ppt) @ 200°F	1,518,323	501,571	516,813	244,990
Bromate gel breaker (8 ppt) @300°F	>2,350,000	>2,350,000	386,069	383,142
Acid gel breaker (2 gpt) @300°F	>2,350,000	>2,350,000	1,142,500	458,188
Enzyme gel breaker (5 gpt) @ 300°F	234,276	248,669	1,651,134	12,428
Hydrated Polymer @ 77°F	>2,350,000			

Table 5-3 Peak molecular weight values of fracturing fluid polymer with gel breaker samples.

It was also noted that for the enzyme-treated sample, the peak molecular weight has shifted to a larger molecular range at 4 hours of the gel breaker treatment. This could be due to the method of enzyme attack. The enzyme attaches to a polymer strand while cleaving the glycosylic bonds and does not leave until the polymer is completely broken (Brannon and Tjon-Joe-Pin 1994). Therefore, in this case, the enzymes could have broken many long-chain polymers initially, which resulted in low peak molecular weight values at short aging periods. After 4 hours, the initially attacked polymers would have been

broken into a variety of sizes, leaving the majority of polymer remaining to be long-chained and relatively unbroken polymers. By the end of the 24 hours, the enzyme would have the time to break all the chains relatively equally into much smaller parts, which resulted in a very low peak molecular weight compared to the other gel breakers.

5.4.3. Zeta Potential

Zeta potential experiments were conducted to assess the fines migration tendency of illite clays in different solutions. Several experiments were initially conducted with and without the presence of clay stabilizers to determine their effect on illite clay particles zeta potential value in distilled water. Similar experiments were conducted in the presence of gel breakers at 77-300ºF. These experiments were mainly performed to determine the effect of different gel breakers on the performance of clay stabilizers.

The potential for fines migration is mainly dependent on the changes in the clay edge and surface charges. Measured zeta potential of any clay reflects the combined value for the surface and edge charge potentials (Chorom and Rengasamy 1995). When zeta potential becomes highly negative or positive (ζ-potential < -20 or ζ-potential > 20), it produces a significant repulsive force with similarly charged particles in solution. Sandstone formation rocks are negatively charged, and having a highly negative zeta potential value causes colloidal induced detachment of fines (Almubarak et al. 2015; Lee and Lee 2019). In other words, this highly negative value of zeta potential will increase the repulsive colloidal forces, which triggers the fines migration cases. **Figs. 5-12, 5-13, and 5-14** summarize the zeta potential results for solutions of illite in different clay stabilizer and gel breaker concentrations.

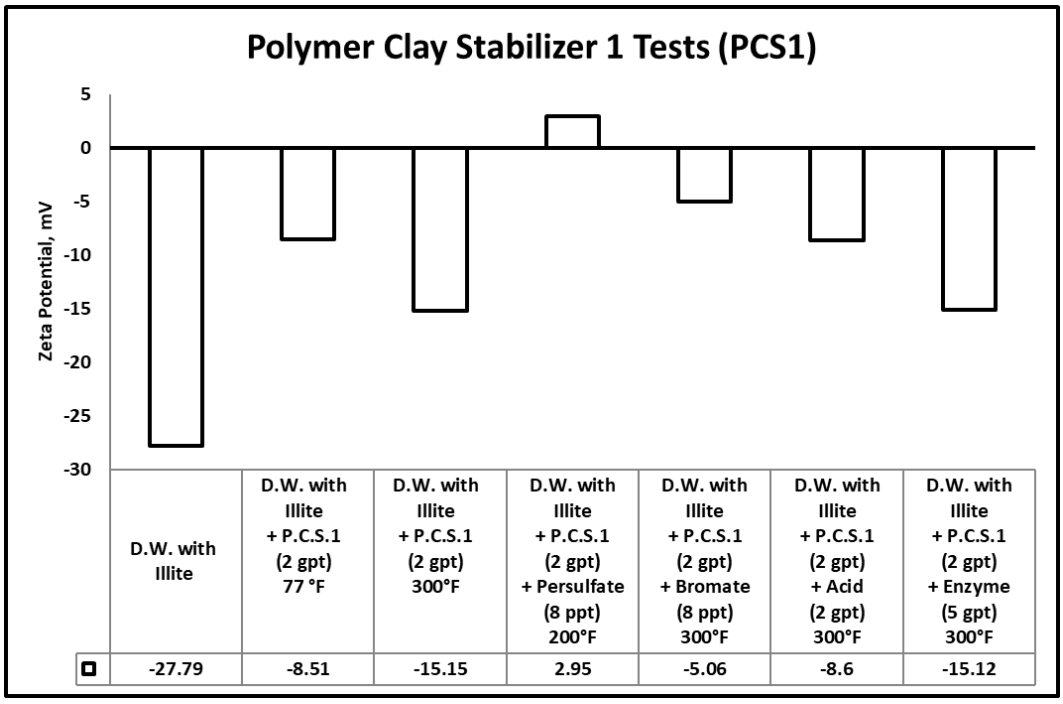

Fig. 5-12 Zeta potential test results for the tests involving gel breakers and polymeric clay stabilizer 1.

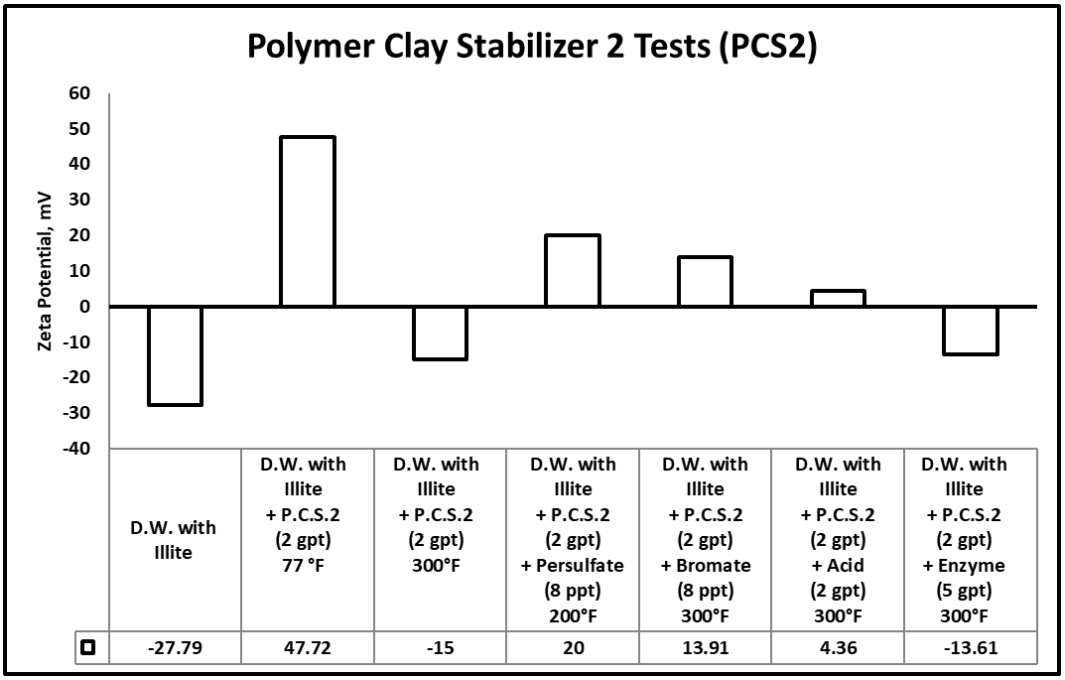

Fig. 5-13 zeta potential test results for the tests involving gel breakers and polymeric clay stabilizer 2.

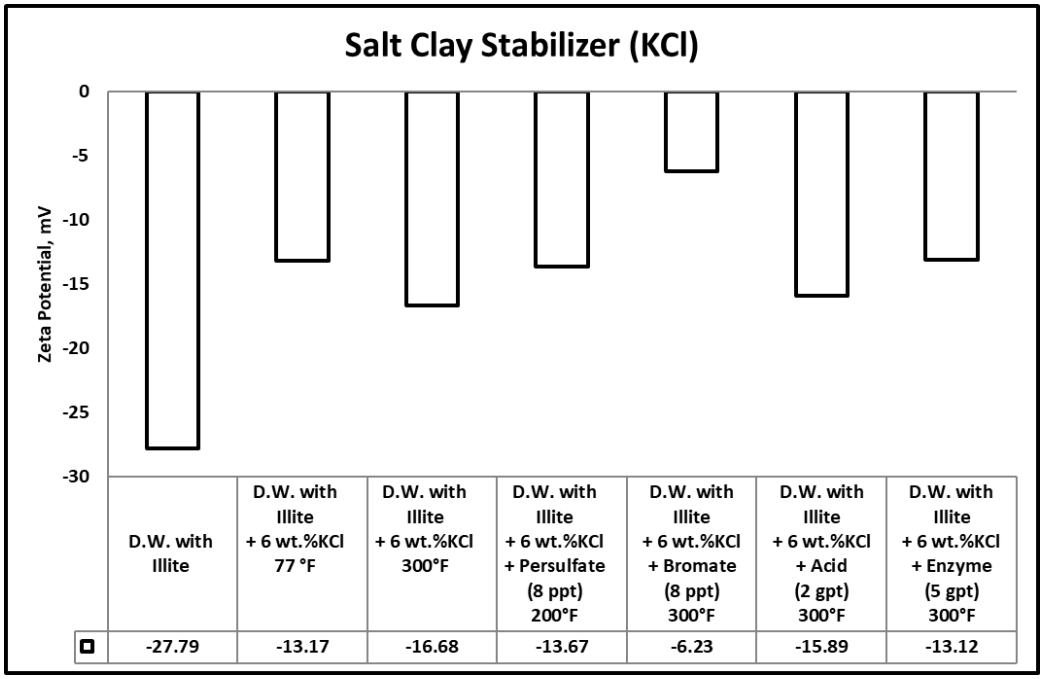

Fig. 5-14 Zeta potential test results for the tests involving gel breakers and KCl clay stabilizer.

The zeta potential value in the samples containing illite fine particles suspended in distilled water at room temperature (77°F) was -27 mV. This indicates the instability of the clays and the possibility of fines migration damage in the formation. The zeta potential values in samples containing illite fine particles suspended in distilled water with polymeric clay stabilizer 1, polymeric clay stabilizer 2 and 6 wt.% KCl at room temperature (77°F) were -8.5, 47, -13 mV, respectively. The values have increased compared to the base case where no clay stabilizer was used, indicating higher clay stability in the presence of either of the clay stabilizers.

Clay stabilizer 1 and 2 are polymeric clay stabilizers containing positive charges that allow them to attach and cover the different clays protecting them from exposure to fluids that can cause them to swell or migrate. Clay stabilizer 2 and illite solution zeta

potential value was highly positive, indicating that it is less likely to have chemically induced fines migrations. The difference between clay stabilizer 1 and 2 is the molecular weight; clay stabilizer 2 had a significantly higher molecular weight compared to clay stabilizer 1, producing more charges and explaining the difference in zeta potential results.

The zeta potential values of several samples were also measured after the addition of persulfate, bromate, acid, and enzyme gel breakers to solution of clay stabilizers and illite. The goal of the test was to check if there are any interactions between the gel breakers and polymeric clay stabilizers to determine if the polymeric clay stabilizers are still able to prevent clay problems during the treatment.

The zeta potential values of the samples containing illite fine particles suspended in a solution of distilled water and polymeric clay stabilizer 1 with persulfate, bromate, acid, or enzyme gel breakers after aging at 200-300ºF were 2.95, -5, -8.6 and -5.12 mV, respectively. These results show that the polymeric clay stabilizer 1 zeta potential values did not change significantly after exposure to the different gel breakers compared to the base case at room temperature (77°F), which had a value of -8.5 mV.

The zeta potential values of the samples containing illite fine particles suspended in a solution of distilled water and polymeric clay stabilizer 2 with persulfate, bromate, acid, or enzyme gel breakers after aging at 200-300ºF were 20, 14, 4.3 and -13.61 mV, respectively. This shows that the zeta potential value of the solution containing polymeric clay stabilizer 2 was reduced significantly compared to the base case at room temperature (77°F), which had a value of 47 mV. This indicates that the interactions with gel breakers at 300°F are reducing the performance of this typical polymeric clay stabilizer.

The zeta potential values of the samples containing illite fine particles suspended in a solution of distilled water and 6 wt.% KCl with persulfate, bromate, acid, and enzyme gel breakers after aging at 200-300ºF were -14, -10, -15 and -13 mV, respectively. The results show that the KCl clay stabilizer zeta potential value was relatively unaffected by the addition of the different gel breaker types and remained within the range of the base case at room temperature (77°F), which was -13 mV.

Polymeric clay stabilizer 2 solutions showed the largest reduction in the zeta potential value when exposed to all gel breakers at 300°F. Due to these results, a new set of tests was conducted to test the influence of aging at 300°F on all the tested clay stabilizers without the addition of gel breakers.

The zeta potential values of the samples containing illite fine particles suspended in a solution of distilled water with polymeric clay stabilizer 1, polymeric clay stabilizer 2 and 6 wt.% KCl, aged at 300ºF were -15, -15, -16 mV, respectively. From these results, it was found that the temperature has an impact on the polymeric clay stabilizer 1 and polymeric clay stabilizer 2 solution zeta potential value compared to the room temperature conditions (77°F), which previously produced values of -8.5 and 47 mV, respectively.

The use of the enzyme gel breaker did not change the solutions zeta potential values significantly when comparing the high-temperature zeta potential values for both polymeric clay stabilizers with and without enzyme gel breaker. This was expected given that the enzymes target specific bonds in guar and its derivatives and should not interfere with other additives used. On the other hand, the oxidizer and acid gel breakers still had an influence on both polymeric clay stabilizers. For example, in the absence of gel

breakers, polymeric clay stabilizer 2 solution zeta potential decreased from around 47 to -15 mV due to aging at 300ºF. However, when the solution prepared with clay stabilizer 2 was exposed to bromate and acid gel breakers at 300ºF, it decreased to 13.9 and 4.3, respectively. These results indicated that the gel breakers are affecting the polymeric clay stabilizers in addition to temperature playing a role. This clearly shows us that the polymeric clay stabilizers can be influenced by the presence of gel breakers and heat, and that can reduce the performance and prevent them from doing the intended job of stabilizing clays.

5.4.4. Polymeric Clay Stabilizer-Gel Breaker GPC Analysis

Further analysis was conducted using GPC to determine if the gel breakers had broken any of the polymeric clay stabilizers. Polymeric clay stabilizer 1 and 2 samples were aged using HP/HT aging cells for 24 hours/ The GPC results for the polymeric clay stabilizer 1 with persulfate at 200°F, as well as bromate, acid, enzyme gel breakers, and without any gel breaker at 300°F, are shown in **Fig. 5-15**. The peak molecular weights of polymeric clay stabilizer 1 are shown in **Table 5-4**. The results show that polymeric clay stabilizer 1 is not significantly affected by temperature due to the small decrease in peak molecular weight. It also shows that the acid had the most effect in reducing the polymeric clay stabilizer size by 30.5%. Despite these reductions to its peak molecular weight, polymeric clay stabilizer 1 showed largely similar zeta potential values, and therefore its clay stabilizing properties would not have been affected significantly.

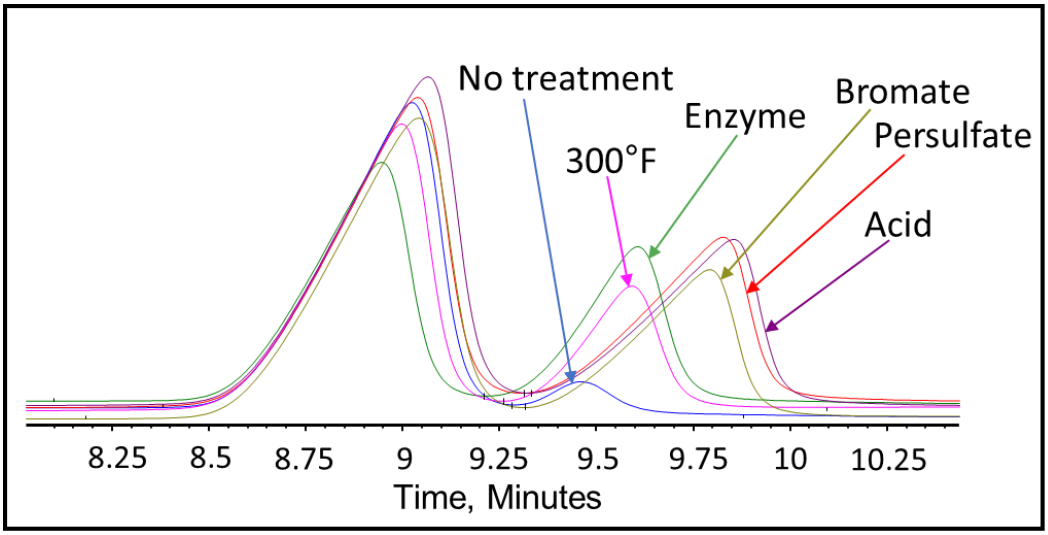

Fig. 5-15 GPC results of polymeric clay stabilizer 1 exposed to different gel breakers (persulfate: 8 ppt, bromate: 8 ppt, acid: 2 gpt, enzyme: 5 gpt) after 24 hours at 200-300°F.

Samples	Peak molecular weight (Mp) (g/mol)
PCS1 @ 77°F	5,786
PCS1 + Heat @300°F	5,085
PCS1 + Enzyme gel breaker (5 gpt) @ 300°F	4,950
PCS1 + Bromate gel breaker (8 ppt) @ 300°F	4,241
PCS1 + Persulfate gel breaker (8 ppt) @ 200°F	4,130
PCS1 + 2 gpt Acid gel breaker (2 gpt) @ 300°F	4,021

Table 5-4 Peak molecular weight values of polymeric clay stabilizer 1 with gel breaker samples after 24 hours.

Polymeric clay stabilizer 2 underwent the same gel breaker test as polymeric clay stabilizer 1, and the results for the GPC tests can be found in **Fig. 5-16.** The peak molecular weight of polymeric clay stabilizer 2 after each test can be found in **Table 5-5.** The results

show that temperature had the most effect on the reduction in the molecular weight of polymeric clay stabilizer 2, reducing it by 89.2%. This is significantly higher than the reduction in peak molecular weight in polymeric clay stabilizer 1. The presence of gel breakers also affects the extent of the reduction of the molecular size. However, in this case, it appears that polymeric clay stabilizer 2 is much more susceptible to temperature effects since at 200°F with persulfate, the molecular weight decreased the least at 56.4%. These changes in molecular weight clearly caused significant changes in zeta potential values for polymeric clay stabilizer 2 and affected its ability to stabilize clays. From these tests, it is important to determine the effect of gel breakers and temperature effects on the performance of polymeric clay stabilizers before applying them.

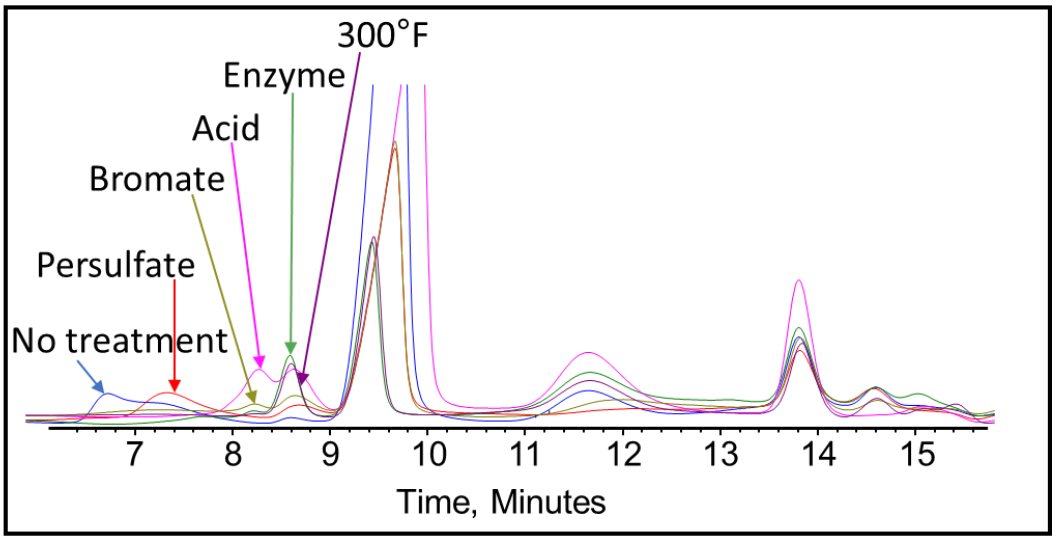

Fig. 5-16 GPC results of polymeric clay stabilizer 2 exposed to different gel breakers (persulfate: 8 ppt, bromate: 8 ppt, acid: 2 gpt, enzyme: 5 gpt) after 24 hours at 200-300°F.

Samples	Peak molecular weight (Mp) (g/mol)
PSC2 @ 77°F	107,594
PSC2 + Persulfate gel breaker (8 ppt) @ 200°F	46,810
PSC2 + Bromate gel breaker (8 ppt) @ 300°F	17,011
PSC2 + Acid gel breaker (2 gpt) @ 300°F	16,101
PSC2 + Enzyme gel breaker (5 gpt) @ 300°F	11,691
PSC2 + Heat @300°F	11,519

Table 5-5 Peak molecular weight values of polymeric clay stabilizer 2 with gel breaker samples after 24 hours.

5.4.5. H_2S-Gel Breaker Interactions

Sour environments are common in many formations throughout the world. In addition, some additives such as sodium thiosulfate (commonly used as a high-temperature stabilizer) can generate H_2S at high-temperature conditions (Ogunsanya and Li 2018). For that reason, checking additive compatibility with H_2S becomes important. Different types of gel breakers were analyzed to see if they had any negative interactions in the presence of H_2S. Enzyme and acid gel breakers showed no precipitation when exposed to H_2S gas, **Figs. 5-17** and **5-18**. On the other hand, bromate and persulfate gel breakers showed precipitation when exposed to H_2S gas, **Figs. 5-19** and **5-20**. H_2S can form a variety of species such as sulfate, sulfite, thiosulfate, and elemental sulfur in the presence of oxidants (Cadena and Peters 1988; Kotronarou and Hoffmann 1991; Parker 2010; Benchoam et al. 2019). The precipitation was later analyzed using the ESEM/EDS.

The results of the ESEM/EDS showed elemental sulfur as the main precipitation, **Fig. 5-21**. This is due to the oxidizer's reaction with H_2S that produces insoluble elemental sulfur, as seen in equations 5-1 and 5-2. The amount of sulfur was higher when persulfate gel breakers were used compared to bromate gel breakers.

$$8H_2S + 4O_2 \rightarrow S_8 + 8H_2O \quad (5\text{-}1)$$

$$8H_2S + 8Br_2 \rightarrow S_8 + 16HBr \quad (5\text{-}2)$$

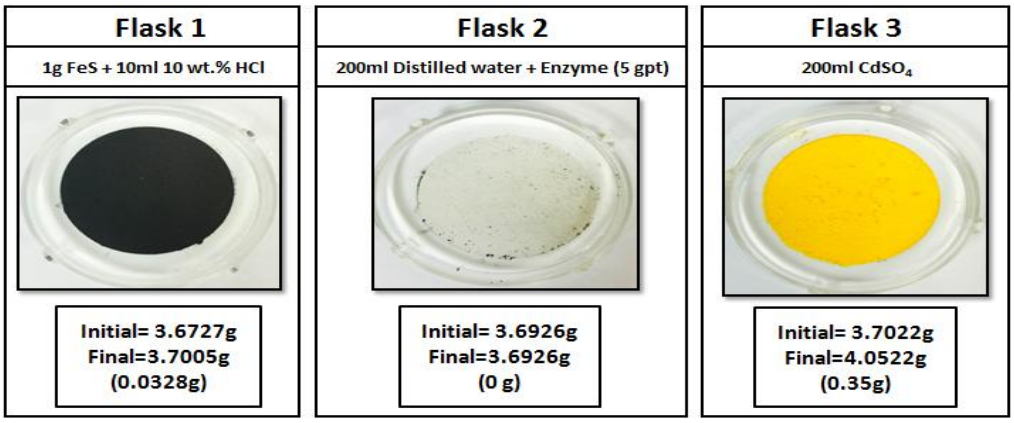

Fig. 5-17 Enzyme gel breaker interactions in a sour environment for 4 hours at 77°F.

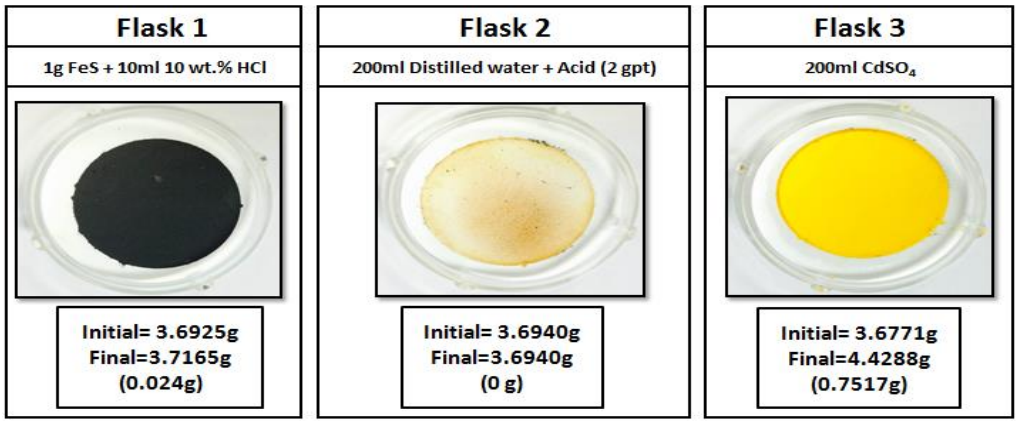

Fig. 5-18 Acid gel breaker interactions in a sour environment for 4 hours at 77°F.

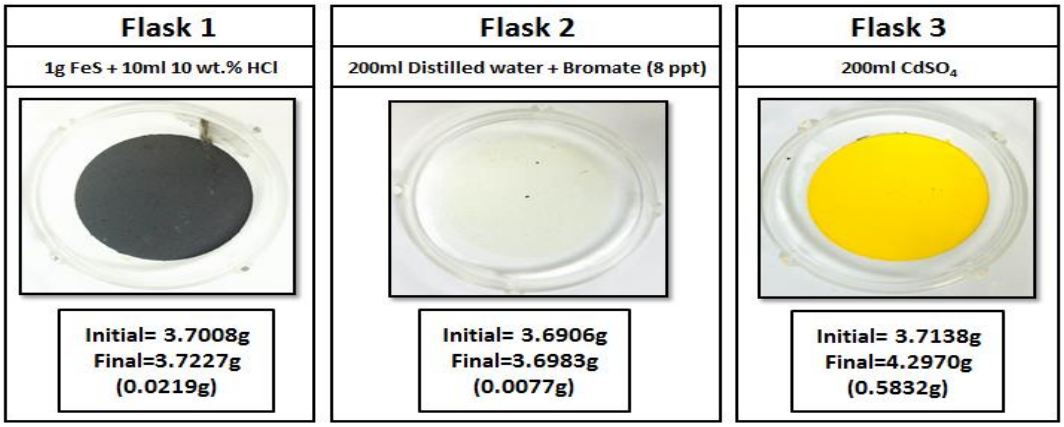

Fig. 5-19 Bromate gel breaker interactions in a sour environment for 4 hours at 77°F.

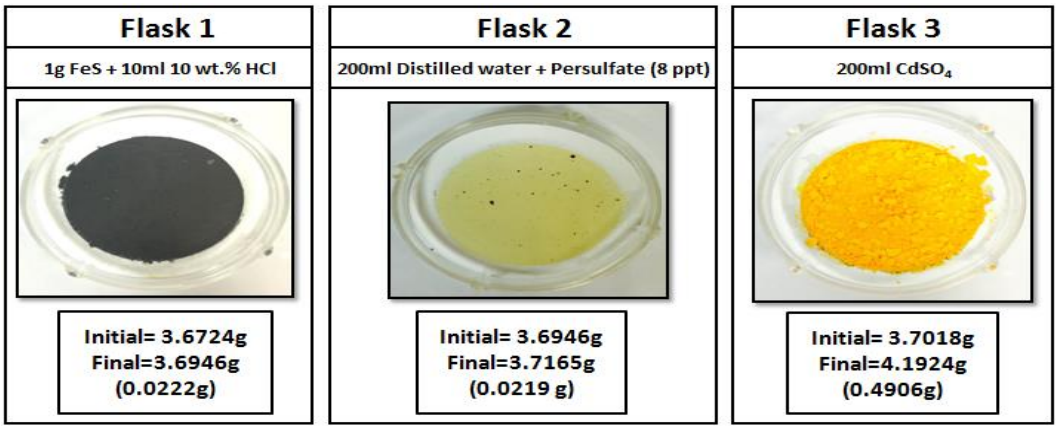

Fig. 5-20 Persulfate gel breaker interactions in a sour environment for 4 hours at 77°F.

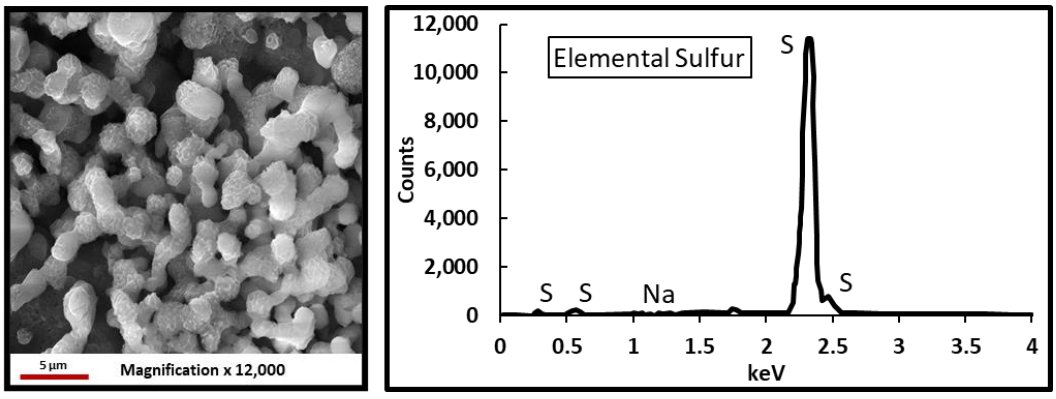

Fig. 5-21 ESEM analysis of the precipitation from oxidizer gel breaker interactions in a sour environment for 4 hours at 77°F.

5.5. Conclusions

This work utilized gel permeation chromatography to measure the size of broken polymer fragments in order to assess the effectiveness of each gel breaker type used in fracturing fluids. The influence of gel breakers on polymeric clay stabilizers and the interactions between gel breaker and H_2S were also evaluated.

From the lab tests, we can conclude the following:

1- The tested gel breakers were all effective in lowering the viscosity of the 45 lb/1,000 gal crosslinked fracturing fluid at 300°F.

2- The amount of visual polymer residue generated from the use of oxidizer and acid gel breakers is significant and may cause damage to the fracture conductivity.

3- The bromate gel breaker's intended reactions stopped after 4 hours at 300°F as the broken fracturing fluid polymer size remained constant.

4- Enzyme gel breakers took a longer duration to operate fully; however, they generated the smallest broken polymer fragments and the least residue in comparison to oxidizers and acid gel breakers after 24 hours at 300°F.

5- Heat (300°F) and gel breakers (acid, bromate) contributed to the break of polymeric clays stabilizers used in this work, the reduction in the size of polymeric clay stabilizers has negatively influenced its performance, which was evidenced by zeta potential measurements.

6- Elemental sulfur precipitation was observed when oxidizers were exposed to H_2S.

5.6. Recommendation

We highly recommend utilizing enzymes to break gelling polymers in fracturing fluids. Enzymes will continue to operate, generating the smallest polymer fragments which correlate directly to reducing damage in the proppant pack, fracture face, and the formation. In addition, enzymes are bond-specific and will not interact with other polymeric additives. We also recommend utilizing GPC for polymer-gel breaker analysis. The data obtained from the GPC technique will help in the optimization of time, temperature, gel breaker concentration, and polymer loading for the evaluation of each gel breaker used in field treatments.

5.7. Acknowledgements

We would like to extend special thanks to our colleagues in the formation damage and stimulation unit. Additional thanks go to Dr. Hameed AlBadairy, Hussain Al-Ibrahim, Abdulaziz AlGhamdi and Hassan AlHazzazi for their contribution to this project.

5.8. References

Al-Khaldi, M. H., Ghosh, B. and Ghosh, D. 2011. A Novel Enzyme Breaker for Mudcake Removal in High Temperature Horizontal and Multi-lateral Wells. Presented at the SPE Asia Pacific Oil and Gas Conference and Exhibition, Jakarta, Indonesia, 20-22 September. SPE-147863-MS. https://doi.org/10.2118/147863-MS.

Almond, S. and Bland, W. 1984. The Effect of Break Mechanism on Gelling Agent Residue and Flow Impairment in 20/40 Mesh Sand. Presented at the SPE Formation Damage Control Symposium, Bakersfield, California, 13-14 February. SPE-12485-MS. https://doi.org/10.2118/12485-MS.

Almubarak, T., AlDajani, O. and AlMubarak, M. 2015. A Collective Clay Stabilizers Review. Presented at the International Petroleum Technology Conference, Doha, Qatar, 6-9 December. IPTC-18394-MS. https://doi.org/10.2523/IPTC-18394-MS.

Almubarak, T., Alkhaldi, M., Ng, J. H. et al. 2019. Design and Application of High-Temperature Raw-Seawater-Based Fracturing Fluids. *SPE J.* **24** (04): 1,929 - 1,946. SPE-195597-PA. https://doi.org/10.2118/195597-PA.

Almubarak, T., Ng, J., Nasr-El-Din, H.A. et al. 2020. Zirconium Crosslinkers: Understanding Performance Variation In Crosslinked Fracturing Fluids. Presented at Offshore Technology Conference Asia, Kuala Lumpur, Malaysia, 17 – 19 August. OTC-30381-MS.

Al-Muntasheri, G. A. 2014. A Critical Review of Hydraulic-Fracturing Fluids for Moderate- to Ultralow-Permeability Formations Over the Last Decade. *SPE Prod & Oper* **29** (04): 243 - 260. SPE-169552-PA. https://doi.org/10.2118/169552-PA.

Al-Muntasheri, G. A., Li, L., Liang, F. et al. 2018. Concepts in Cleanup of Fracturing Fluids Used in Conventional Reservoirs: A Literature Review. *SPE Prod & Oper* **33** (02): 196 - 213. SPE-186112-PA. https://doi.org/10.2118/186112-PA.

Alterman, D. S., and Chun, K. W. 1976. Encapsulation Particles. U.S. Patent No. 3,983,254.

Azizov, E., Quintero, H. J., Saxton, K. et al. 2015. Carboxymethylcellulose a Cost Effective Alternative to Guar, CMHPG and Surfactant-Based Fluid Systems. Presented at the SPE/CSUR Unconventional Resources Conference, Calgary, Alberta, Canada, 20-22 October. SPE-175904-MS. https://doi.org/10.2118/175904-MS.

Barati, R., Johnson, S. Mccool, S. et al. 2012. Polyelectrolyte Complex Nanoparticles for Protection and Delayed Release of Enzymes in Alkaline pH and at Elevated Tempearature During Hydraulic Fracturing Oil wells. *J. of Appl. Polym. Sci.* **126** (02): 587-592. https://dx.doi.org/10.1002/app.36845.

Benchoam, D., Cuevasanta, E., Möller, M. et al. 2019. Hydrogen Sulfide and Persulfides Oxidation by Biologically Relevant Oxidizing Species. *Antioxidants*. **8** (2): http://dx.doi.org/10.3390/antiox8020048.

Borisov, I., Luksha, R., and Rashidova, S. 2015. Kinetic features of ammonium persulfate decomposition in aqueous medium. *Russian Chemical Bulletin* **64** (10): 2512-2513. http://dx.doi.org/10.1007/s11172-015-1185-y.

Brannon, H. and Ault, M. 1991. New, Delayed Borate-Crosslinked Fluid Provides Improved Fracture Conductivity in High-Temperature Applications. Presented at the SPE Annual Technical Conference and Exhibition, Dallas, Texas, 6-9 October. SPE-22838-MS. https://doi.org/10.2118/22838-MS.

Brannon, H., and Tjon-Joe-Pin, R. 1994. Biotechnological Breakthrough Improves Performance of Moderate to High-Temperature Fracturing Applications. Presented at the SPE Annual Technical Conference and Exhibition, New Orleans, Louisiana, 25-28 September. SPE-28513-MS. https://doi.org/10.2118/28513-MS.

Cadena, F. and Peters, R. 1988. Evaluation of Chemical Oxidizers for Hydrogen Sulfide Control. *Journal of Water Pollution Control Federation* **60** (07): 1259-1263. https://www.jstor.org/stable/25043633.

Chorom, M., Rengasamy, P. 1995. Dispersion and Zeta Potential of Pure Clays as Related to Net Particle Charge Under Varying pH, Electrolyte Concentration and Cation Type. *European Journal of Soil Science* **46** (04): 657-665. https://doi.org/10.1111/j.1365-2389.1995.tb01362.x.

Clark, J. 1949. A Hydraulic Process for Increasing the Productivity of Wells. *J Pet Technol* **1** (01): 1 - 8. SPE-949001-G. https://doi.org/10.2118/949001-G.

Cobianco, S., Albonico, P., Battistel, E. et al. 2007. Thermophilic Enzymes for Filtercake Removal at High Temperature. Presented at the European Formation Damage Conference, Scheveningen, The Netherlands, 30 May-1 June. SPE-107756-MS. https://doi.org/10.2118/107756-MS.

Dawson, J. 1991. A Thermodynamic Study of Borate Complexation with Guar and Guar Derivatives. Presented at the SPE Annual Technical Conference and Exhibition, Dallas, Texas, 6-9 October. SPE-22837-MS. https://doi.org/10.2118/22837-MS.

Ding, Y., Jiang, T., Wang, Y. et al. 2004. A Case Study of Massive Hydraulic Fracturing in An Ultra-deep Gas Well. Presented at the SPE Asia Pacific Oil and Gas Conference and Exhibition, Perth, Australia, 18-20 October. SPE-88613-MS. https://doi.org/10.2118/88613-MS.

Driweesh, S. M., Al-Atwi, M. A., Malik, A. R. et al. 2013. Successful Implementation of Zirconate Borate Based Dual Crosslinked Gel and Continuous Mixing System During Proppant Fracturing Treatment in a Complex High Temperature and High Pressure Sandstone Gas Reservoir in Saudi Arabia that Exceeded the Well Objective and Showed Substantial Increase in Operational Efficiency - A Case Study. Presented at the International Petroleum Technology Conference, Beijing, China, 26-28 March. IPTC-16664-MS. https://doi.org/10.2523/IPTC-16664-MS.

Economides, M. and Nolte, K. 2000. *Reservoir Stimulation*, third edition. Chichester, England: John Wiley and Sons.

Elkatatny, S., Mahmoud, M. and Shawabkeh, R. 2017. Investigating the Compatibility of Enzyme with Chelating Agents for Calcium Carbonate-Filter Cake Removal. Presented at the SPE Kingdom of Saudi Arabia Annual Technical Symposium and Exhibition, Dammam, Saudi Arabia, 24-27 April. SPE-187978-MS. https://doi.org/10.2118/187978-MS.

Farris, R.F. 1953. Fracturing Formations in Wells. U.S Patent No. 23,733.

Gall, B. and Raible, C. 1985. Molecular Size Studies of Degraded Fracturing Fluid Polymers. Presented at the SPE Oilfield and Geothermal Chemistry Symposium, Phoenix, Arizona, 9-11 March. SPE-13566-MS. https://doi.org/10.2118/13566-MS.

Gulbis, J., King, M., Hawkins, G. et al. 1992. Encapsulated Breaker for Aqueous Polymeric Fluids. *SPE Prod Eng* **7** (01): 9 - 14. SPE-19433-PA. https://doi.org/10.2118/19433-PA.

Gupta, D. S., Carman, P. S. and Venugopal, R. 2012. A Stable Fracturing Fluid for Produced Water Applications. Presented at the SPE Annual Technical Conference and Exhibition, San Antonio, Texas, USA, 8-10 October. SPE-159837-MS. https://doi.org/10.2118/159837-MS.

Gupta, D., Pakulski, M., Prasek, B. et al. 1992. High-pH-Tolerant Enzyme Breaker for Oilfield Applications. Presented at the Permian Basin Oil and Gas Recovery Conference, Midland, Texas, 18-20 March. SPE-23986-MS. https://doi.org/10.2118/23986-MS.

Harms, W. 1989. Application of Chemistry in Oil and Gas Well Fracturing. *Oil-Field Chemistry*. Borchardt, J. and Yen, T., Chap. 2. 55-100. Washington D.C.: American Chemical Society. https://doi.org/10.1021/bk-1989-0396.ch002.

Harris, P. C. 1993. Chemistry and Rheology of Borate-Crosslinked Fluids at Temperatures to 300F. *J Pet Technol* **45** (03): 264 - 269. SPE-24339-PA. https://doi.org/10.2118/24339-PA.

Howard, G.C. and Fast, C.R. 1970. *Hydraulic Fracturing*, . New York: Society of Petroleum Engineers of AIME.

Hu, Y. T., Chung, H. and Maxey, J. E. 2015. What is More Important for Proppant Transport, Viscosity or Elasticity?. Presented at the SPE Hydraulic Fracturing Technology Conference, The Woodlands, Texas, USA, 3-5 February. SPE-173339-MS. https://doi.org/10.2118/173339-MS.

ISO 13503-1, 2011. Petroleum and natural gas industries-completion fluids and materials-Part 1, Measurement of viscous properties of completion fluids, second edition. Geneva, Switzerland: ISO.

Jackson, C., Larsen, B., and McEwen, C. 1996. Comparison of Peak Molecular Weight Values as Measured for Polymer Molecular Weight Distribution by MALDI Mass Spectrometry and by Size Exclusion Chromatography. Presented at the International GPC symposium. Paper number 990662.

Kesavan, S., Prud'homme, R. and Parris, M. 1993. Crosslinked Borate HPG Equilibria and Rheological Characterization. Presented at the SPE International

Symposium on Oilfield Chemistry, New Orleans, Louisiana, 2-5 March. SPE-25205-MS. https://doi.org/10.2118/25205-MS.

Kolthoff, I. M. and Miller, I. K. 1951. The Chemistry of Persulfate. I. The Kinetics and Mechanism of the Decomposition of the Persulfate Ion in Aqueous Medium1. *J. Am. Chem. Soc.* **73** (7): 3055-3059. https://doi.org/10.1021/ja01151a024.

Kotronarou, A., and Hoffmann, M. 1991. Peroxymonosulfate: An Alternative to Hydrogen Peroxide for the Control of Hydrogen Sulfide. *Research Journal of the Water Pollution Control Federation* ***63*** (07): 965-970.

Kramer, J., Prud'homme, R., Norman, L. et al. 1987. Characteristics of Metal-Polymer Interactions in Fracturing Fluid Systems. Presented at the SPE Annual Technical Conference and Exhibition, Dallas, Texas, 27-30 September. SPE-16914-MS. https://doi.org/10.2118/16914-MS.

Kramer, J., Prud'homme, R., Wiltzius, P. et al. 1988. Comparison of galactomannan crosslinking with organotitanates and borates. *Colloid & Polymer Science* **266** (02): 145-155. http://dx.doi.org/10.1007/bf01452812.

Lee, K. S. and Lee, J. H. 2019. *Hybrid Enhanced Oil Recovery using Smart Waterflooding*, 1. New York, NY: Elsevier Science & Technology.

Lei, C. and Clark, P. E. 2007. Crosslinking of Guar and Guar Derivatives. *SPE J.* **12** (03): 316-321. SPE-90840-PA. https://doi.org/10.2118/90840-PA.

Li, L., Al-Muntasheri, G., Liang, F. 2016. A Review of Crosslinked Fracturing Fluids Prepared with Produced Water. *Petroleum* **2** (04): 313 - 323. https://doi.org/10.1016/j.petlm.2016.10.001.

Li, L., Lin, L., Ezeokonkwo, C. 2010. Treatment and Reuse of Oilfield Produced Water for Operations in a well. U.S. Patent No. 8,658,574.

Li, L., Ozden, A., Zhang, J. et al. 2020. Enhanced Gelled Hydrocarbon Well Treatment Fluids. *Petroleum* **6** (2): 177-181. https://doi.org/10.1016/j.petlm.2019.08.002.

Lo, S., Miller, M. J. and Li, J. 2002. Encapsulated Breaker Release Rate at Hydrostatic Pressure and Elevated Temperatures. Presented at the SPE Annual Technical Conference and Exhibition, San Antonio, Texas, 29 September-2 October. SPE-77744-MS. https://doi.org/10.2118/77744-MS.

Maberry, L., McConnell, S. and Hinkel, J. 1997. New Complexation Chemistry Provides Improved Continuous-Mix Gelled Oil. Presented at the International Symposium on Oilfield Chemistry, Houston, Texas, 18-21 February. SPE-37227-MS. https://doi.org/10.2118/37227-MS.

Maley, D. M. and O'Neil, B. J. 2010. Breaker Enhancer for Crosslinked Borates: Novel Self Generating Acid. Presented at the Canadian Unconventional Resources and International Petroleum Conference, Calgary, Alberta, Canada, 19-21 October. SPE-137490-MS. https://doi.org/10.2118/137490-MS.

Manalastas. P., Drake, E., Kresge, E. et al. 1992. Breaker Chemical Encapsulation with a crosslinked Elastomer Coating. U.S. Patent No. 5,110,486.

Ming, H., Lu, Y., Qiu, X. et al. 2016. Development and Field Application of a Novel Cellulose Fracturing Fluid. Presented at the SPE Asia Pacific Hydraulic Fracturing Conference, Beijing, China, 24-26 August. SPE-181778-MS. https://doi.org/10.2118/181778-MS.

Montgomery, C. 2013. Fracturing Fluid Components. *Effective and Sustainable Hydraulic Fracturing*. Jeffrey, R., Mclennan, J., Bunger, A., Chap. 2. 26 - 44. Intechopen. https://doi.org/10.5772/45724.

Moorhouse, R., D. Harry, L. Matthews. et al. 1998. Inter-Relationships Between Polymer/Crosslinker Chemistry and Performance. Presented at the SPE India Oil and Gas Conference and Exhibition, 17-19 February, New Delhi, India. SPE-39531-MS. https://doi.org/10.2118/39531-MS.

Nasr-El-Din, H. A., Al-Mohammed, A. M., Al-Aamri, A. D. et al. 2007. A Study of Gel Degradation, Surface Tension, and Their Impact on the Productivity of Hydraulically Fractured Gas Wells. Presented at the SPE Annual Technical Conference and Exhibition, Anaheim, California, U.S.A., 11-14 November. SPE-109690-MS. https://doi.org/10.2118/109690-MS.

Nelson, C., Schuppenhauer, M., Clark, Douglass. 1992. High-Pressure, High-Temperature Bioreactor for Comparing Effects of Hyperbaric and Hydrostatic Pressure on Bacterial Growth. *Applied and Environmental Microbiology* **58** (05): 1790-1793.

Nickerson, R. 1971. Thickening of Poly(vinyl alcohol) by Borate. *J. Appl. Polym. Sci.* **15** (01): 111-116. https://doi.org/10.1002/app.1971.070150110.

Nolte, K. G. 1985. Fracture Fluid Breaker System Which is Activated by Fracture Closure. U.S. Patent No. 4,506,734.

Ogunsanya, T. and Li, L. 2018. Safe Boundaries of High-Temperature Fracturing Fluids. Presented at the SPE Western Regional Meeting, Garden Grove, California, USA, 22-26 April. SPE-190029-MS. https://doi.org/10.2118/190029-MS.

Parker, M. 2010. Method for Removing Hydrogen Sulfide from Sour Gas and Converting it to Hydrogen and Sulfuric Acid. Dissertation. Stanford University, 06/2010.

Parris, M. D., MacKay, B. A., Rathke, J. W. et al. 2008. Influence of Pressure on Boron Cross-Linked Polymer Gels. *Macromolecules* **41** (21): 8181-8186. https://doi.org/10.1021/ma801187q.

Pasha, M., Ngn, S. 2008. Derivatization of guar to sodium carboxymethyl hydroxypropyl derivative: Characterization and evaluation. *Pakistan J Pharmaceutical Sciences* **21** (01): 40-44.

Prud'homme, R., Constien, V., and Knoll, S. 1989. The Effects Of Shear History On The Rheology Of Hydroxypropyl Guar Gels. *Advances in Chemistry* **223** (06): 89-112. https://doi.org/10.1021/ba-1989-0223.ch006.

Rae, P. and Lullo, G. D. 1996. Fracturing Fluids and Breaker Systems - A Review of the State-of-the-Art. Presented at the SPE Eastern Regional Meeting, Columbus. Ohio, 23-25 October, SPE-37359-MS, https://doi.org/10.2118/37359-MS.

Reddy, B. R. 2014. Laboratory Characterization of Gel Filter Cake and Development of Nonoxidizing Gel Breakers for Zirconium-Crosslinked Fracturing Fluids. *SPE J.* **19** (04): 662 - 673. SPE-164116-PA. https://doi.org/10.2118/164116-PA.

Reinicke, A., Blöcher, G., Zimmermann, G. et al. 2012. Mechanically Induced Fracture-Face Skin--Insights From Laboratory Testing and Modeling Approaches. *SPE Prod & Oper* **28** (01): 26 - 35. SPE-144173-PA. https://doi.org/10.2118/144173-PA.

Samuel, M., Mohsen, A. H., Ejan, A. B. et al. 2010. A Novel alpha-Amylase Enzyme Stabilizer for Applications at High Temperatures. *SPE Prod & Oper* **25** (03): 398 - 408. SPE-125024-PA. https://doi.org/10.2118/125024-PA.

Taylor, R. S., Fyten, G., Romanson, R. et al. 2010. Montney Fracturing-Fluid Considerations. *J Can Pet Technol* **49** (12): 28 - 36. SPE-143113-PA. https://doi.org/10.2118/143113-PA.

Thompson, J. E., DeVine, C. S. and Delorey, J. R. 2000. State-of-the-Art Nonphosphate Design Revolutionizes Hydrocarbon-Based Completion Technologies. Presented at the SPE Annual Technical Conference and Exhibition, Dallas, Texas, 1-4 October. SPE-63244-MS. https://doi.org/10.2118/63244-MS.

Venkataiah, S., Mahadevan, E. 1982. Rheological properties of hydroxypropyl- and sodium carboxymethyl-substituted guar gums in aqueous solution. *J. of Appl. Polym. Sci.* **27** (01): 1533-1548. https://doi.org/10.1002/app.1982.070270512.

Weaver, J., Gdanski, R. and Karcher, A. 2003. Guar Gum Degradation: A Kinetic Study. Presented at the International Symposium on Oilfield Chemistry, Houston, Texas, 5-7 February. SPE-80226-MS. https://doi.org/10.2118/80226-MS.

White, J. and Means, J. 1975. Polysaccharide Derivatives Provide High Viscosity and Low Friction at Low Surface Fluid Temperatures. *J Pet Technol* **27** (09): 1,067 - 1,073. SPE-4936-PA. https://doi.org/10.2118/4936-PA.

Yaritz, J., Stegent, N., Bailey, T. et al. 1997. Development of a Dual Crosslinker Fracturing Fluid System. Presented at the Latin American and Caribbean Petroleum Engineering Conference, Rio de Janeiro, Brazil, 30 August-3 September. SPE-38959-MS. https://doi.org/10.2118/38959-MS.

Yongjun, L., Yandong, C., Zhongyang, Z. et al. 1999. A Case Study of Boron Crosslinked Fracturing Fluid in Ultra-Deep Wall. Presented at the SPE International Symposium on Oilfield Chemistry, Houston, Texas, 16-19 February. SPE-50787-MS. https://doi.org/10.2118/50787-MS.

Zhang, B., Davenport, A. H., Whipple, L. et al. 2013. A Superior, High-Performance Enzyme for Breaking Borate Crosslinked Fracturing Fluids Under Extreme Well Conditions. *SPE Prod & Oper* **28** (02): 210 - 216. SPE-160033-PA. https://doi.org/10.2118/160033-PA.

6. DESIGN AND APPLICATION OF HIGH-TEMPERATURE RAW SEAWATER-BASED FRACTURING FLUID*

6.1. Abstract

Typically, water-based fracturing treatments consume a large volume of freshwater. Providing consistent freshwater sources is difficult and sometimes not feasible, especially in remote areas and offshore operations. Therefore, several seawater-based fracturing fluids have been developed in efforts to preserve freshwater resources. However, none of these fluids minimize fracture face skin and proppant conductivity impairment, which can be critical for unconventional well treatments.

Several experiments and design iterations were conducted to tailor raw seawater-based fracturing fluids. These fluids were designed to have rheological properties that can transport proppant under dynamic and static conditions. The optimized seawater-based fracturing fluid formulas were developed such that no scale forms when additives are mixed in or when the fracturing fluid filtrate is mixed with different formation brines. The tests were conducted using an HP/HT rheometer, coreflood, and aging cells at 250-300°F.

* Part of this chapter is modified with permission from "Design and Application of High-Temperature Raw-Seawater-Based Fracturing Fluids" by Almubarak, T., AlKhaldi, M., Ng, J. et al. 2019. SPE J **24** (4): 1929-1946. Copyright 2019 by Society of Petroleum Engineers.

The developed seawater-based fracturing fluids were optimized with an apparent viscosity above 100 cp at a shear rate of 100 s^{-1} and a temperature of 300°F for over 1 hour. The use of polymeric- and phosphonate- based scale inhibitors prevented the severe calcium sulfate scale formation in mixtures of seawater and formation brines at 300°F. Controlling the pH of fracturing fluids prevented magnesium and calcium hydroxide precipitation that occurs above a pH of 9.5. Most importantly, scale inhibitors had a negative impact on the viscosity of seawater fracturing fluid during testing due to their negative interaction with metallic crosslinkers. The developed seawater-based fracturing fluids were applied for the first time in an unconventional and a conventional carbonate well and showed very promising results; details of field treatments will be discussed in this work.

6.2. Introduction

Water-based hydraulic fracturing treatments in low permeability formations consume large volumes of freshwater. Low-volume hydraulic fracturing treatments can require 20,000 to 80,000 gallons of water (NYSDEC 1992). High-volume hydraulic fracturing treatments require volumes that could range between 3,000,000 to 5,000,000 gallons of water (Lee et al. 2011; Nicot and Scanlon 2012; Aminto and Olson 2012). Unconventional hydraulic fracturing treatments can use up to 13,000,000 gallons of water (Vengosh et al. 2014). Long horizontal multistage fracturing treatments can consume 600,000 gallons of water per stage (NYSDEC 2011). Replacing the use of fresh water with seawater is a critical task.

Using seawater as the treatment water raises many concerns of formation damage. Reinicke (2010) provided a general review of the potential formation and fracture damage processes that result from interactions between fracturing fluids and formation components including rock and fluid constituents, (**Fig. 6-1**). Scale formation during mixing seawater and formation brine is considered one of the main causes of fracture face skin and proppant conductivity impairment.

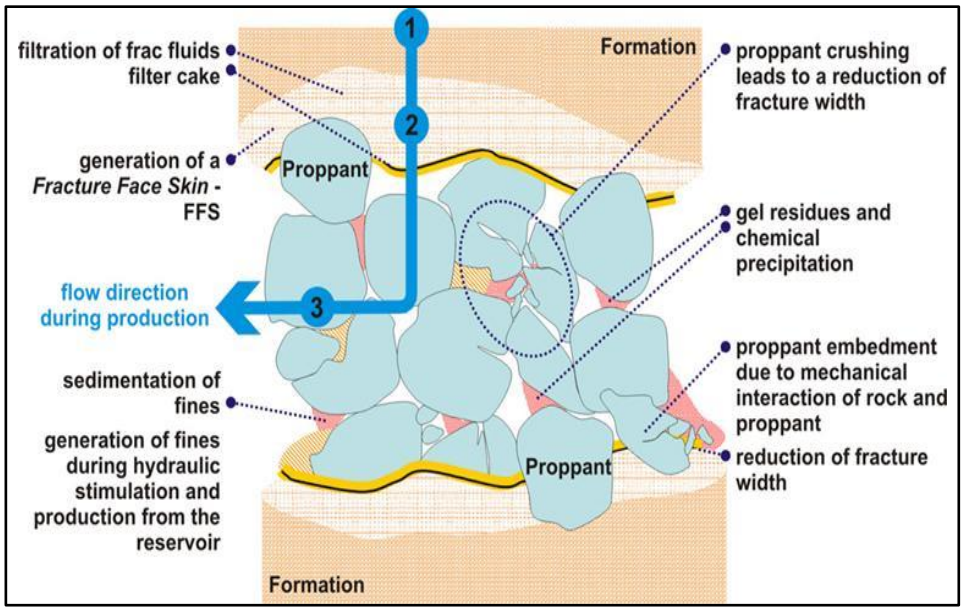

Fig. 6-1 Mechanisms of fracture face damage and proppant pack conductivity impairment (Reinicke 2010).

Some of the common seawater-based fracturing fluid approaches include chemically treating seawater to precipitate the ions of concern or physically filtering the ions using ion exchange membranes. The mentioned seawater treatments do not eliminate the cost of trucking to well locations (in the desert) and will not be practical offshore. Portable seawater treatment equipment can be used on site. However, it is very expensive and takes a very long time to generate sufficient volumes of mixing water. This delay can be an issue for unconventional multistage fracturing treatments that require large volumes of water to be readily available. Also, the portable equipment footprint is a concern on offshore platforms where space is limited.

The developed fracturing fluids should maintain minimum rheological performance while minimizing damage to the formation. Li et al. (2016) investigated many examples of formulating fracturing fluids using high salinity seawater and formation

brine up to 250°F. It becomes challenging at high-temperature (300°F) due to the weak thermal stability of commonly used fracturing fluids and severe scale precipitation (Alohaly et al. 2016; Abdulmajid et al. 2017; BinGhanim et al. 2017a, 2017b; Yamak et al. 2018; Elsarawy et al. 2018; Gupta et al. 2018). To overcome these issues, additives such as high-temperature stabilizers and scale inhibitors have to be incorporated. However, the rheological performance of fracturing fluids can be sensitive to any additive that is incorporated in the formula (Li et al. 2015).

6.2.1. Chemical Scaling

Seawater contains large amounts of sulfates (typically above 1,000 ppm, **Table 6-1**), whereas formation brine contains divalent cations such as calcium, barium, and strontium. When both brines come into contact, they tend to form an insoluble calcium sulfate scale. Calcium sulfate has a higher potential for scaling at bottom-hole conditions where its solubility limit decreases as the solution temperature increases above 100°F (Ramsdell and Partridge 1929; Bock 1961). Calcium sulfate scale exists in different forms depending on temperature. Examples of calcium sulfate scale are gypsum, anhydrite, or hemihydrate at < 108, 108-208, and 208-392°F, respectively (Moghadasi et al. 2003).

Component	Offshore Angola Sea (mg/L)	South China Sea (mg/L)	Mediterranean Sea (mg/L)	Gulf of Mexico (mg/L)	Danish North Sea (mg/L)	Arabian Gulf (mg/L)
Na^+	14,200	9,900	12,300	11,000	8,800	16,180
K^+	210	400	380	470	400	700
Ca^{2+}	300	420	500	650	420	650
Mg^{2+}	630	1,170	1,790	1,220	1,550	1,730
Sr^{2+}	5	7	N/A	10	6	N/A
Cl^-	15,000	18,000	22,000	19,700	22,000	31,000
HCO_3^-	95	110	140	90	140	N/A
CO_3^{2-}	N/A	N/A	N/A	40	N/A	N/A
SO_4^{2-}	1,400	2,500	2,900	3,310	3,300	4,020
TDS	31,850	32,500	40,010	36,500	36,600	54,000

Table 6-1 Composition of various seawaters near oilfields (Harris and van Batenburg 1999).

Scale inhibitors (SI) have been applied successfully to prevent the formation of different scales. They act as chelating agents to form a soluble complex, as threshold inhibitors that block the development of the supercritical nuclei, or as retarders of the growth of the scale crystals (Fan et al. 2010; Shen et al. 2012). Various types of calcium sulfate scale inhibitors have been used to mitigate calcium sulfate precipitation such as: polyphosphates, organophosphorus compounds, and polymeric inhibitors.

Polyphosphates scale inhibitors, such as sodium hexametaphosphate (HMP) (NaPO3)6, (**Fig. 6-2**), have limited applications in the oil industry. They are mainly used in boiler water treatments at low calcium concentrations (Fan et al. 2010; Shen et al. 2012; Farooqui et al. 2014).

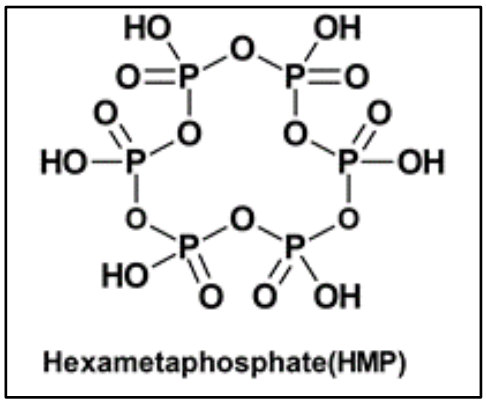

Fig. 6-2 Chemical structure of hexametaphosphate (HMP).

Another type of calcium sulfate scale inhibitors is organophosphorus compounds. Organophosphorus scale inhibitors are divided into two subgroups: phosphonates and phosphate esters. Compared to phosphonates, phosphate esters have lower thermal stability that can only reach 200°F with limited applications (Kelland 2014). For example, triethanolamine phosphate ester has a temperature limitation of 176°F due to hydrolysis (**Fig. 6-3**).

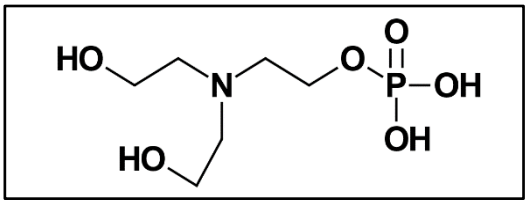

Fig. 6-3 Chemical structure of triethanolamine phosphate ester.

Phosphonate-based calcium sulfate scale inhibitors are reported to be effective when calcium sulfate scaling index < 1 (Fan et al. 2010; Lu et al. 2012). Most common phosphonate-based inhibitors are 1-hydroxyethane-1,1-diphosphonic acid (HEDP) and 2-phosphonobutane-1,2,4-tricarboxylic acid (PBTCA), (**Fig. 6-4**).

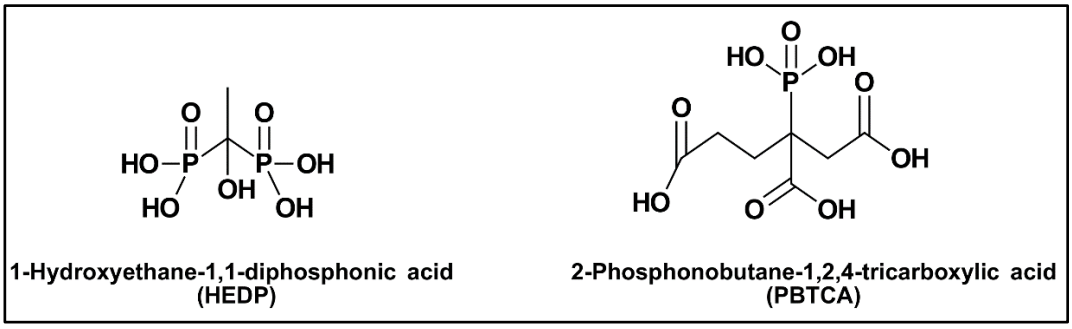

Fig. 6-4 Chemical structure of HEDP and PBTCA.

Introducing an amine group can enhance the inhibition ability of phosphonates, which will increase the metal binding ability of the phosphonate-based molecule (Almubarak et al. 2017). Examples of these aminophosphonates are aminotrimethylene phosphonic acid (ATMP), ethylenediaminetetramethylene phosphonic acid (EDTMP), hexamethylenediaminetetramethylene phosphonic acid (HMDTMP), and diethylenetriaminepentamethylene phosphonic acid (DTPMP) (**Fig. 6-5**).

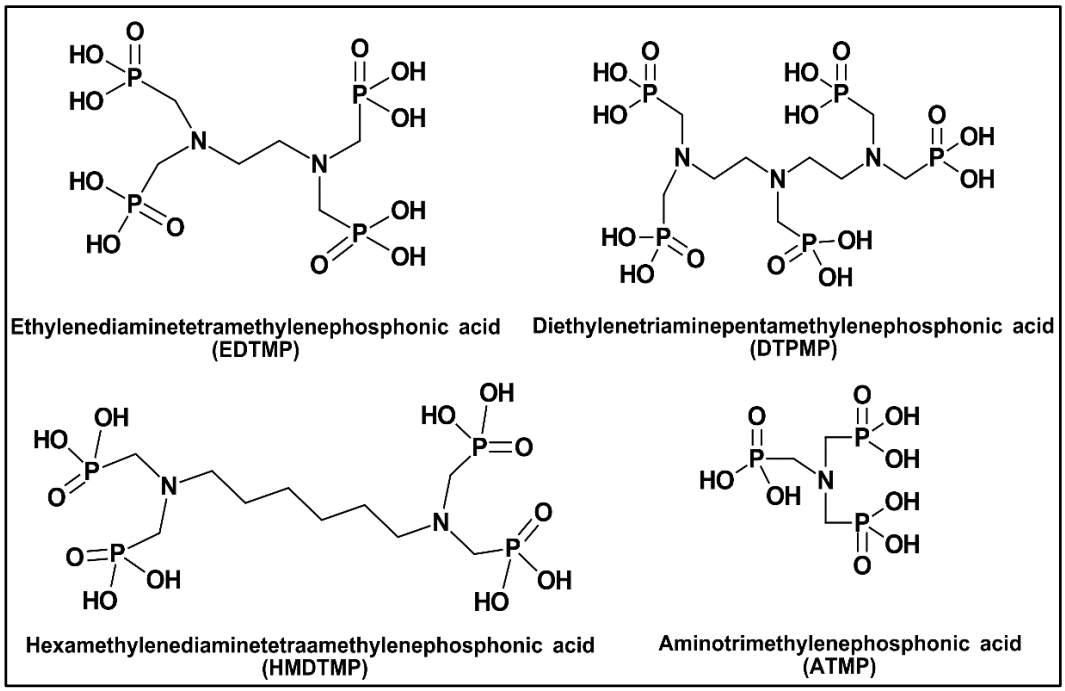

Fig. 6-5 Chemical structures of EDTMP, DTPMP, HMDTMP, and ATMP.

A study by Fan et al. (2010) has evaluated HMDTMP and DTMP phosphonate scale inhibitors at 392°F, and found that calcium sulfate is most effectively inhibited by HMDTMP at scaling index < 1. These phosphonate scale inhibitors were not effective at scaling index > 1 because they are not soluble enough in the presence of divalent cations.

In addition to phosphate and phosphonate inhibitors, polymeric inhibitors have been used extensively. These inhibitors are based on different functional groups such as polymaleic acid (PMA), polyacrylic acid (PAA), and polyphosphino carboxylic acid (PPCA) (**Fig. 6-6**). These scale inhibitors have high-temperature stability and higher tolerance for calcium ions (Tung et al. 2004; Bin Merdhah 2010; Lu et al. 2012; Farooqui et al. 2014).

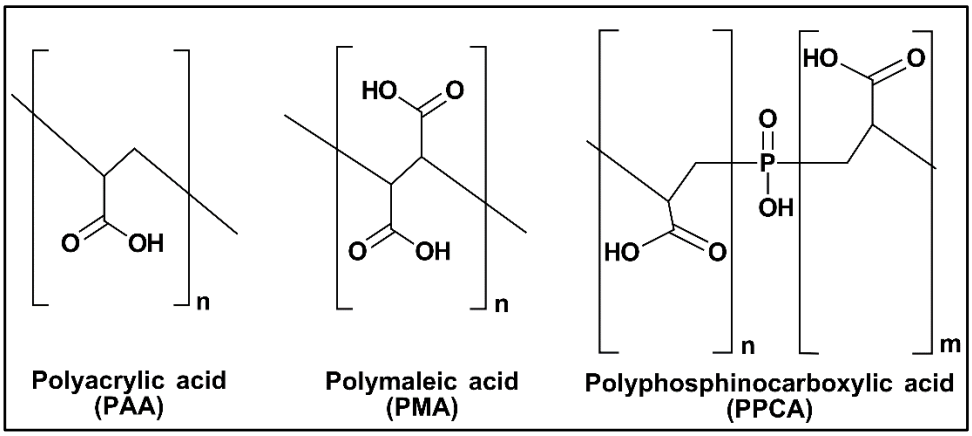

Fig. 6-6 Chemical structures of polymeric calcium sulfate scale inhibitors.

The objective of this study is to describe the development and field application of new seawater-based fracturing fluids, which are designed to be compatible with raw seawater and nearly scale-free when their filtrate is mixed with formation brines. The design of seawater-based fracturing fluids involved the modification of existing fracturing fluids to allow for control of polymer hydration, effective crosslinking, additive compatibility, and breaking performance at a temperature range of 250-300°F. Seawater-based fracturing fluid designs and field treatments are discussed to demonstrate the effective rheological and scale-free properties in both conventional and unconventional gas formations.

6.3. Experimental Procedures

6.3.1. Materials

Representative field samples of raw seawater, formation brines of conventional and unconventional wells were obtained and used to conduct lab experiments. Formation brine and seawater were later synthesized in the lab due to the large volume of tests. **Table**

6-2 gives the geochemical analysis of formation brines and seawater (at the field outlet); these concentrations were followed to prepare synthetic water samples.

Fluid	Na^+	Ca^{2+}	Mg^{2+}	SO_4^{2-}	Cl^-	HCO_3^-	TDS	pH
UNC Brine 1	28,400	14,000	1,100	1,030	71,000	60	115,690	4.3
UNC Brine 2	12,800	4,700	176	121	28,500	29	46,350	4.8
UNC Brine 3	10,286	42,970	3,203	144	113,495	554	170,700	5.9
CON Brine 1	62,700	22,000	1,180	25	139,000	0	224,995	4.3
Seawater	17,200	630	2,000	4,100	31,200	190	55,300	7.2

Table 6-2 Chemical analysis of seawater and different formation brines.

The initially proposed fracturing fluids for raw seawater application were two formulas commonly used by two different service companies (**Table 6-3)**. The formulas consisted of 50 lb/1,000 gal CMHPG, biocide, low pH buffer to aid hydration, surfactant to assist with flowback, clay stabilizer, HT stabilizer to help maintain thermal stability at 300°F, a strong base to adjust pH to 10, a dual crosslinker to overcome shear limitations while pumping (boron) and to remain stable at 300°F (zirconium). The first service company proposed one dual crosslinker additive and a bromate-based breaker (bromate has lower reactivity compared to persulfate at high temperatures (Al-Muntasheri 2014), while the other service company proposed two separate additives for the dual crosslinker and a chlorous acid-based breaker.

The adjustment and design of these gelling systems were conducted using raw seawater and chemical additives provided by the service companies to assure rapid implementation of the developed seawater-based fracturing fluid system in a field trial.

All chemical additives were used as received. No scale inhibitor was proposed in the initial formulas.

Fracturing Fluid 1	Additive	Fracturing Fluid 2	Additive
Linear gel	Seawater	Linear gel	Seawater
	Biocide		Biocide
	CMHPG		CMHPG
	Acetic acid/acetate		Acetic acid/acetate
	Surfactant		Surfactant
	Choline chloride		Hydroxyalkyl alkylammonium chloride
X-linker	Sodium thiosulfate	X-linker	Sodium thiosulfate
	NaOH (pH 10)		KOH (pH 10)
	Dual crosslinker (Triethanolamine, sodiumtetraborate, zirconium dichloride oxide)		Zr Triethanolamine
			Potassium metaborate
Breaker	Bromate breaker	Breaker	Chlorous acid breaker
	Encapsulated bromate breaker		

Table 6-3 Main chemical additives in the proposed raw seawater-based fracturing fluids.

Scale inhibitors A and B (supplied by chemical company 1), C, D, E (supplied by chemical company 2), F supplied by a service company, 1 and G supplied by chemical company 3 were used as received. Scale inhibitors A and B are a fully neutralized polyacrylate with low to medium molecular weight and thermal stability of up to 500°F. Scale inhibitors C, D, and E are short chained sulfonated copolymers that are thermally stable up to 300°F. Scale inhibitor F is polymeric with temperature stability up to 350°F. Scale inhibitor G is an aminophosphonate-based scale inhibitor with temperature stability up to 300°F. **Table 6-4** shows the physical properties of all these products. Scale inhibitors F and G were diluted by the service providers to ease the application in hydraulic fracturing operations.

	A	B	C	D		E	F	G
Appearance	Pale yellow liquid						Clear liquid	
Density, g/cm^3	1.3	1.3	0.96		0.96	0.96	1	0.98
Viscosity, cP	250	400	30-60		30-60	30-60	<15	<100

Table 6-4 Physical properties of tested scale inhibitors as received.

Coreflood or zeta potential tests were performed to determine clay sensitivity using representative cores of well-51, well-105, and well-320 from UNC 2 and UNC 3 formations. The selected cores from UNC 2 cores had a permeability of 1 - 2 md and a porosity of 7 – 15 vol%. X-ray diffraction (XRD) analysis showed that these cores contained 97 wt% quartz, 3 wt% kaolinite, and traces of illite (**Table 6-5**). UNC 3 cores had a permeability of < 0.1 md and a porosity of 8-10 vol%. X-ray diffraction (XRD) analysis showed that these cores contained 75 wt% calcite and 8 wt% clays (**Table 6-6**).

Mineral	Concentration, wt%
Quartz-SiO_2	97
Kaolinite- $Al_2Si_2O_5(OH)_4$	3
Microcline-$KAlSi_3O_8$	Traces
Albite-$NaAlSi_3O_8$	Traces
Pyrite-FeS_2	Traces
Clay Fraction	**Concentration, wt%**
Kaolinite- $Al_2Si_2O_5(OH)_4$	65
Illite-$KAl_2(Si_3Al)O_{10}(OH)_2$	4
Illite/Smectite-$KAl_4(SiAl)_8O_{10}(OH)_4.4H_2O$	3
Quartz-SiO_2	27
Gypsum-$CaSO_4.2H_2O$	1

Table 6-5 XRD bulk and clay analysis of formation core from UNC 2 formation.

Mineral	Concentration, wt%
Feldspar & Quartz-SiO_2	6.1
Calcite	75.9
Dolomite	4.3
Siderite	0.9
Pyrite-FeS_2	1.4
Anhydrite	1.5
Halite	1
Gypsum-$CaSO_4.2H_2O$	0.6
Kaolinite- $Al_2Si_2O_5(OH)_4$	2.6
Illite-$KAl_2(Si_3Al)O_{10}(OH)_2$	2.3
I/S-$KAl_4(SiAl)_8O_{10}(OH)_4.4H_2O$	1.8
Chlorite	1.6

Table 6-6 XRD bulk and clay analysis of formation core from UNC 3 formation.

6.3.2. Analytical Techniques

The formation rock samples were manually ground to a fine powder using a porcelain mortar and pestle. The fine powder was mounted into the XRD sample holder by back pressing. The XRD patterns of the sample powders were measured at 50 to 90°angles with a step size of 0.020. The patterns were compared to a database to find the best match to identify the phases.

Environmental Scanning Electron Microscopy (ESEM) and Energy Dispersive X-ray Spectrometry (EDS) analyses were used to identify all types of chemical scaling that occurred during the modification of seawater-based fracturing fluids. Samples of each mineral scale were placed on the ESEM sample holder. The ESEM was operated up to 15 kV, 0.23 Torr water vapor pressure and 10 mm working distance. Topographical backscattered images at magnifications ranging from 60 and 8,000 times together with EDS spectra were acquired from different areas of the sample.

6.3.3. Zeta Potential

The zeta potential was measured by using microelectrophoresis. Changes in zeta potential were measured for different crushed formation rocks in various solutions. Each sample was prepared by weighing 0.2 g of crushed core particles and suspending each sample in 50 cm^3 samples of distilled water, seawater, and fracture fluids.

Each of these suspensions was sonicated for 30 minutes and were allowed to stand for a minimum of 48 hours before analysis was conducted at room temperature. The used electrode assembly was then conditioned in 1M NaCl solution using 350 cycles. This conditioning procedure produces a uniform black coating on the electrodes for zeta potential analysis of suspensions in high ionic strength.

The core particle suspension was added as required to the plastic cuvette at a 45° angle to avoid trapping air bubbles between the electrodes. The cuvette was then placed in the instrument and allowed to equilibrate to the measurement temperature of 77°F for 5 minutes.

6.3.4. Compatibility and Scaling Tendency

Scale prediction used an Excel-based simulation program. It is based on Pitzer's theory of electrolytes (Pitzer 1977), and it can predict scale formation for common minerals. These predictions were conducted at a bottom-hole temperature, and pressure of 280-300°F and 1,000 psi, respectively, at different mixture ratios of seawater and formation brine.

Laboratory compatibility tests were conducted to investigate the scaling potential in mixtures of formation brine and seawater. These experiments were carried out at 270-300°F. HP/HT aging cells were used to conduct the compatibility testing at 400 psi (pressurized by nitrogen). Different ratios of formation brine were tested for scaling tendency over 24 hours of soaking time. At the end of the testing period, each brine was observed visually for precipitation.

6.3.5. Viscosity Tests

An HP/HT rotational rheometer was used to measure the apparent viscosity of the fracturing fluids under different shear rates and temperatures. This rheometer used a standard R1/B5 bob and rotor combinations, which require a sample volume of 52 cm^3. A pressure of 1,000 psi (using nitrogen) was applied to minimize evaporation of the sample.

Viscosity measurements were performed under shear ramps to simulate the flow of the fracturing fluid through production tubulars, in perforations, and inside the created fracture. The testing followed ISO 13503-1 schedule, where the shear rate range was between 25 and 100 s^{-1}, while the temperature ranged from 250 to 300°F. Samples of approximately 800 cm^3 were prepared each day as a linear gel (Tables 6-3) of which 250

cm^3 were crosslinked for each rheometer run. 52 cm^3 sample is added to the rheometer cup. For breaker tests, a sandwich method was applied, 25 cm^3 of the fracturing fluid sample was placed into the rheometer cup, followed by adding breakers directly in the cup, and covered with 27 cm^3 of the sample to achieve a total volume of ~ 52 cm^3.

6.3.6. Retained Permeability Using Coreflooding

Selected cores from UNC 2 formation (~1-2 md) were chosen to conduct core flood experiments. The length and the diameter of the cores were 3 and 1.5 in., respectively. Initially, each core was saturated with UNC 2 formation brine, and then it was loaded into the core holder. The temperature was maintained at 300°F. Back pressure and overburden pressure were fixed at 1,000 and 2,000 psi, respectively.

The cores were flooded using formation brine as the saturation fluid. During this stage, the injection flow rate was varied between 0.5 and 2.0 cm^3/min to eliminate the possibility of mechanically induced fines migration. Following that, Approximately 70 pore volumes (PV) of fracture fluid filtrate (seawater or distilled water) was injected into the core. The pressure drop across the core was recorded. Then, formation brine was injected to displace the injected fluids and the pressure drop across the core was measured. The pressure drop across the core before and after injection of fracturing fluid filtrate was used to assess the filtrate-rock interactions. Freshwater-fracturing fluid and seawater-fracturing fluid filtrate were compared. The goal was to investigate the need for a clay stabilizer in the formula.

6.4. Results and Discussion

Several design iterations were performed to develop the seawater-based formula such that it exhibited adequate rheological properties (> 100 cp at 100 s^{-1}) for fracturing applications in conventional and unconventional formations. Additionally, these optimized formulas were developed such that no scale formed when their filtrate was mixed with different formation brines. Initial design attempts focused on the prevention of different mineral scaling associated with the use of seawater.

6.4.1. Compatibility and Scaling Tendency

Initial compatibility experiments indicated that the seawater and formation brine are not compatible with the strong base additives initially proposed by the service companies in the seawater-based fracturing fluid formulas. It was observed that magnesium hydroxide $Mg(OH)_2$ precipitated after the addition of strong base additives (NaOH, KOH) to seawater (**Fig. 6-7**). The seawater contains nearly 2,000 ppm of magnesium ions (Mg^{2+}), which precipitate when free hydroxide ions (OH^-) are introduced by the fracturing fluid additive at pH above 9.5.

Similarly, calcium hydroxide precipitated after the addition of the same strong base additives to formation brine (**Fig. 6-8**). Formation brines contain a high concentration of calcium ions (Ca^{2+}), some up to 43,000 ppm, which precipitate at a pH above 9.5.

a)

b)

c)

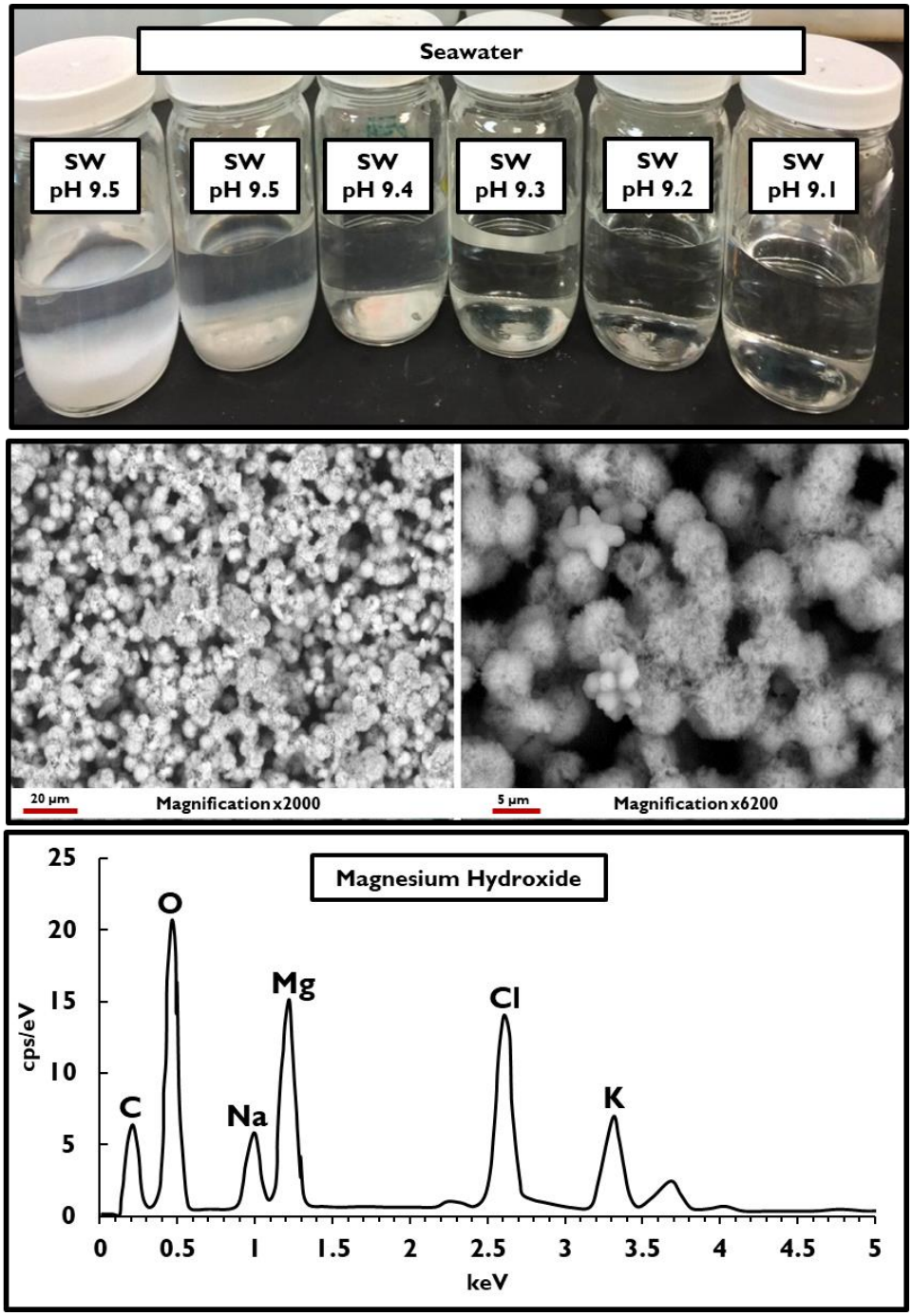

Fig. 6-7 a) Determining the pH of precipitation in seawater by using NaOH, b) Precipitation analyzed in ESEM, c) Precipitation is identified by EDS as mainly Mg(OH)2.

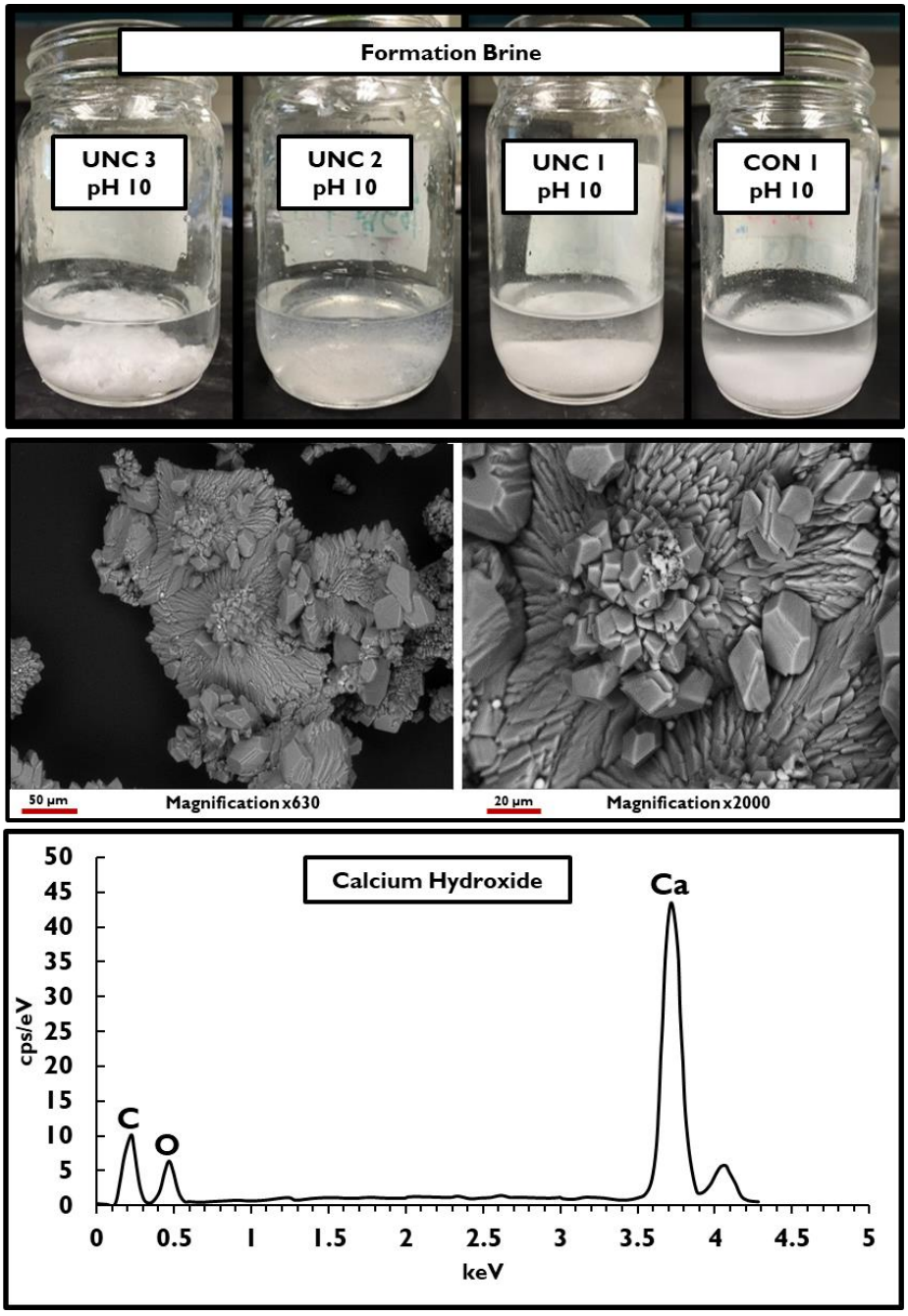

Fig. 6-8 a) Formation brines show precipitation at pH 10 (using NaOH), b) Precipitation analyzed using ESEM, and c) Precipitation is identified by EDS as mainly Ca(OH)2 with some CaCO3.

ESEM/EDS analysis indicated that formation brine precipitates at pH > 9.5 and yields mainly calcium hydroxide, while the precipitate in seawater at pH > 9.5 is mainly magnesium hydroxide. These hydroxides are insoluble at the originally proposed pH 10. This finding was one of the main bases for the development of the improved seawater-based fracturing fluid formulas.

In addition to hydroxide precipitation, calcium sulfate scale was also expected due to the presence of sulfate ions in the seawater, and calcium ions in formation brines (Table 6-2). Simulations were performed to determine the critical mixing ratio at which calcium sulfate scale occurs at 280-300°F. **Fig. 6-9** indicates that a mixing ratio of 60:40 by volume (seawater:formation brine) resulted in the highest amount of calcium sulfate precipitation. The peak concentrations of calcium sulfate in UNC 1, UNC 2, UNC 3, and CON 1 formations at 60:40 by volume (seawater:formation brine) were 1,500, 80, 3,500 and 2,500 ppm, respectively.

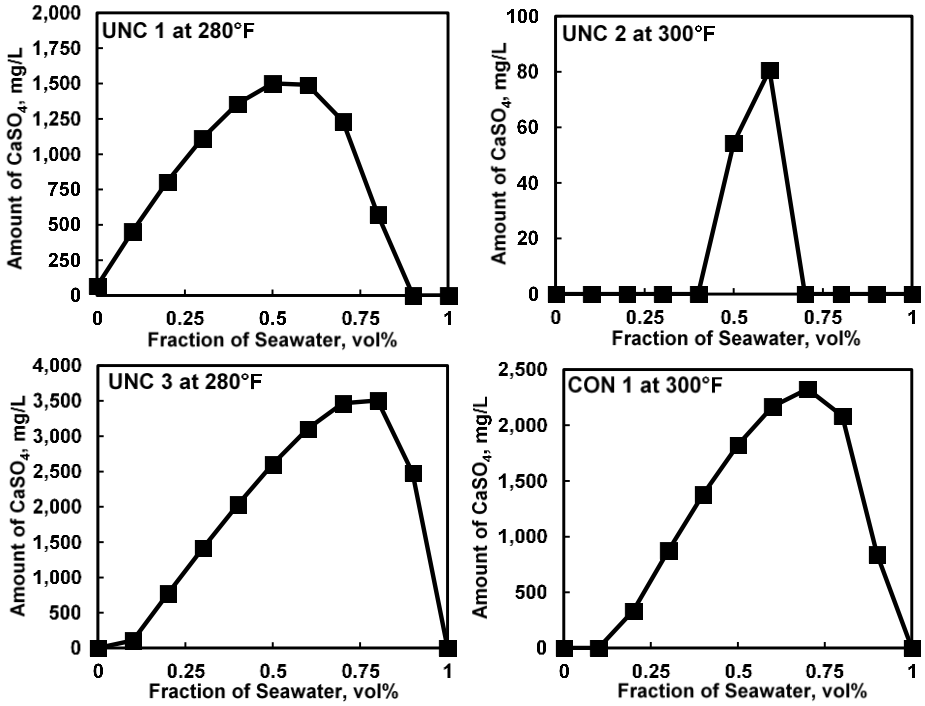

Fig. 6-9 Predictions of calcium sulfate scale precipitation for different ratios of seawater and formation brines at 280 and 300°F.

Laboratory static scaling experiments were conducted for different seawater mixtures with formation brines at 300°F. These experiments were conducted using a convection oven at 500 psi (N_2 pressure). Seawater in these mixtures varied between 10 and 90 vol%.

Following the soaking period, these mixtures were visually inspected for any precipitation. Calcium sulfate precipitation was observed in different seawater mixtures with formation brines, which occurred when seawater volume percentage was above 10 vol% in its mixtures with formation brines after 24 hours soaking time at each temperature (**Fig. 6-10**).

a)

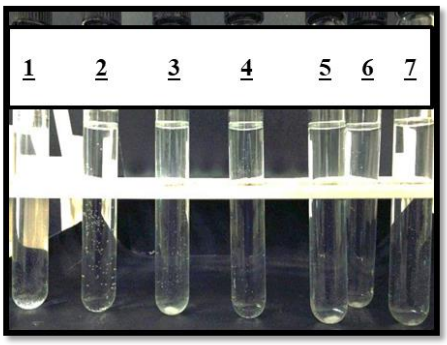

Tube#	UNC 1 Brine, vol%	Seawater, vol%	Observation
1	10	90	ppt
3	25	75	ppt
5	40	60	ppt
6	50	50	ppt
7	60	40	ppt
4	75	25	clear
2	90	10	clear

b)

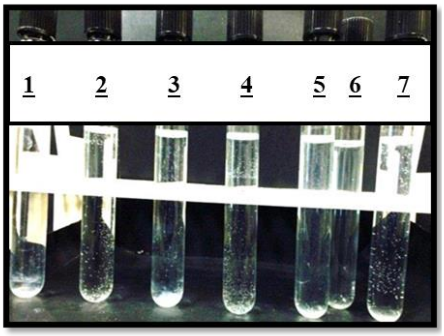

Tube#	UNC 2 Brine, vol%	Seawater, vol%	Observation
1	10	90	ppt
3	25	75	ppt
5	40	60	ppt
6	50	50	ppt
7	60	40	ppt
4	75	25	ppt
2	90	10	clear

c)

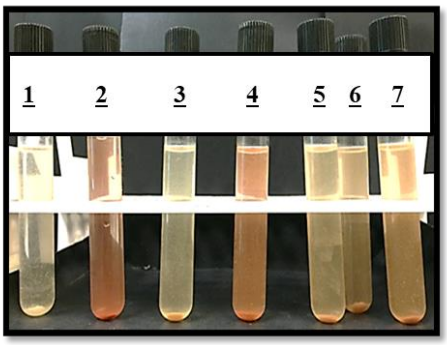

Tube#	UNC 3 Brine, vol%	Seawater, vol%	Observation
1	10	90	ppt
3	25	75	ppt
5	40	60	ppt
6	50	50	ppt
7	60	40	ppt
4	75	25	ppt
2	90	10	ppt

Fig. 6-10 Compatibility of seawater with: a) UNC 1 formation brine, b) UNC 2 formation brine, and c) UNC 3 formation brine. The red color indicates the presence of iron from field formation brine samples. The samples were soaked for 24 hours at 300°F.

Calcium sulfate scale precipitation was imaged through ESEM to observe the severity of scale as temperature increased from 200-300°F (**Fig. 6-11)**.

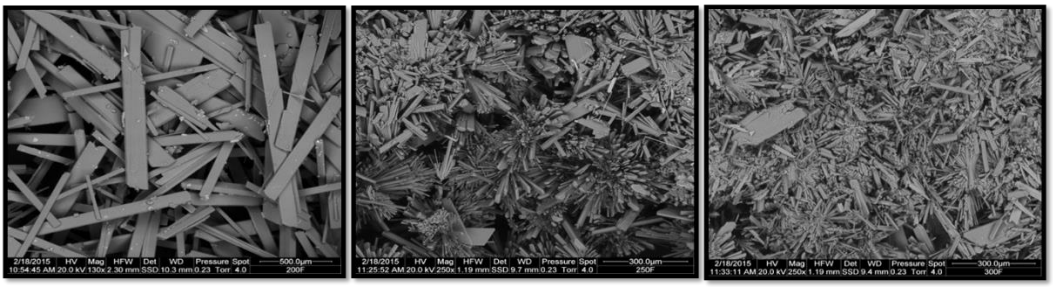

Fig. 6-11 Influence of temperature on calcium sulfate scale: the crystal size is smaller and more severe as temperature increases, at 60:40 volume ratio of seawater: formation brine.

These scaling experiments indicated that the use of seawater-based fracturing fluids in unconventional gas resource development would be associated with a high potential for fracture face skin and proppant conductivity impairment (Fig. 1). Therefore, extensive scale inhibition experiments were conducted and design the optimal scale inhibition package to prevent calcium sulfate precipitation.

The scale inhibitors (Table 6-4) were all assessed to prevent calcium sulfate precipitation in mixtures of seawater with formation brines at 300°F. The duration of scale inhibition experiments was 24 hours at 500 psi, using 60:40 by volume (seawater:formation brine).

Scale inhibitors A, B, C, D, and E failed in preventing calcium sulfate scale precipitation, while scale inhibitors F and G were effective in preventing calcium sulfate precipitation for at least 24 hours at 300°F. The minimum inhibition concentration (MIC) of scale inhibitors F and G were 3 and 0.5 gpt, respectively (**Fig. 6-12)**. These concentrations were higher than typical MIC due to the dilution of chemicals by the service providers.

a)

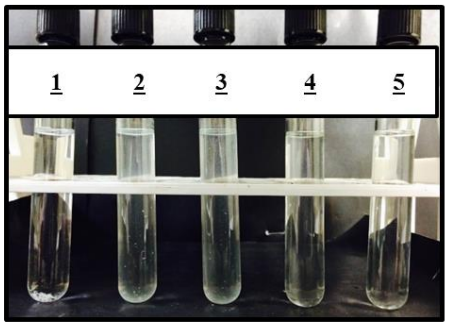

Tube#	Scale Inhibitor	Concentration, gpt	Observation
1	Blank	0	ppt
2	SI G	0.5	clear
3	SI G	0.3	clear
4	SI F	5	clear
5	SI F	3	clear

b)

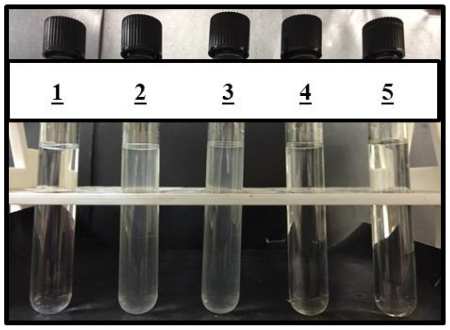

Tube#	Scale Inhibitor	Concentration, gpt	Observation
1	Blank	0	ppt
2	SI G	0.5	clear
3	SI G	0.3	clear
4	SI F	5	clear
5	SI F	3	clear

c)

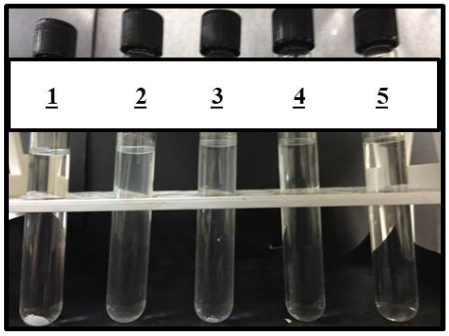

Tube#	Scale Inhibitor	Concentration, gpt	Observation
1	Blank	0	ppt
2	SI G	0.5	clear
3	SI G	0.3	ppt
4	SI F	5	clear
5	SI F	3	clear

Fig. 6-12 Compatibility of seawater with: a) UNC 1 formation brine, b) UNC 2 formation brine, and c) UNC 3 formation brine. The samples were left for 24 hours with scale inhibitors F and G (60:40 volume ratio of seawater:formation brine) at 300°F.

6.4.2. Viscosity Measurements

Prior to optimizing the rheological properties of the crosslinked seawater-based fracturing fluids, the hydration of their polymers in seawater was investigated. The CMHPG polymers (obtained in powder form) were added to 800 cm^3 of seawater at a

concentration of 45 lb/1000 gal, and they were mixed in a blender for 1 hour at a constant rotational speed of 800 RPM at 77°F. At 5 minute time intervals, 250 cm^3 were quickly transferred into the cup, and viscosity was measured using a rheometer at 300 RPM. The same procedure was followed when distilled water was used.

Fig. 6-13 shows the apparent viscosity of 45 lb/1000 gal CMHPG hydrating in seawater (SW) and distilled water (DW). CMHPG was fully hydrated in seawater, where it reached 44 and 46 cp in less than 10 minutes at 77°F for fracturing fluid formulas 1 and 2, respectively. The time it took to reach full hydration in distilled water was faster due to the absence of salts (Das et al. 2014). The difference in viscosity value between the two CMHPG is because the two service companies sourced CMHPG from two different manufacturers (Acartürk and Celkan 2009).

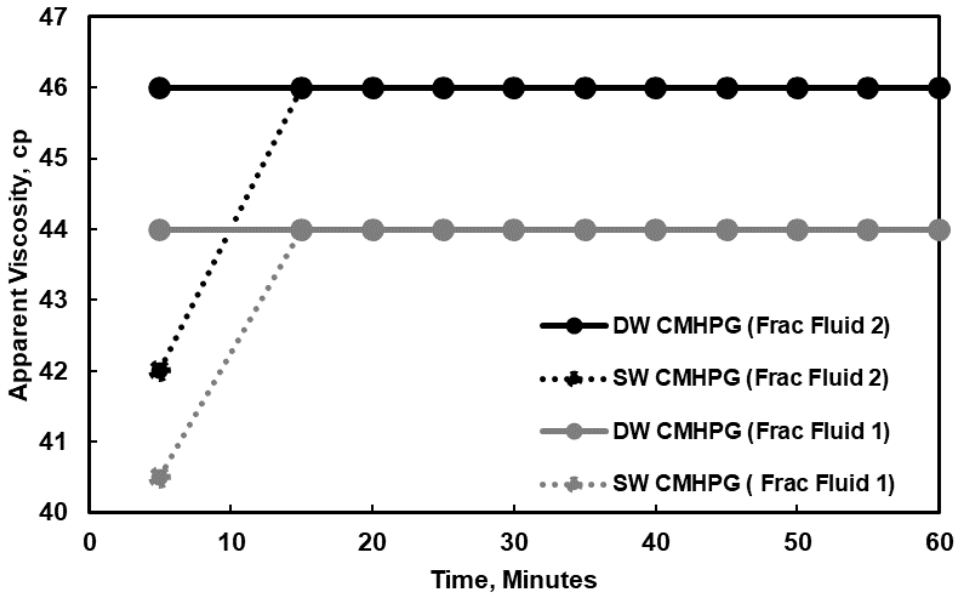

Fig. 6-13 Apparent viscosity of CMHPG at 45 lb/1000 gal in seawater (SW) and distilled water (DW), to test the ability to fully hydrate in seawater, 77°F, and 300 RPM.

After completing the evaluation of gelling agent hydration in seawater, extensive viscosity experiments were conducted to optimize the seawater-based fracturing fluids. The scaling test results indicated that scale inhibitors F and G at concentrations of 3 and 0.5 gpt, respectively, were able to prevent calcium sulfate scale from occurring when mixing seawater with formation brine at reservoir conditions. Also, the scaling tests also pointed out the need to replace the strong base additive and that the pH of the final fracturing fluids should be less than 9.5 to prevent calcium and magnesium hydroxide precipitation.

The fracturing fluids went through many trials to achieve acceptable rheological performance. The main adjustments included adding scale inhibitor to prevent calcium sulfate scaling, replacing strong bases with buffers, adding gel stabilizers, crosslinkers delayers, and HT stabilizers to maintain pH and thermal stability at 300°F. **Table 6-7** shows the final formulas for both seawater-based fracturing fluids. Fracturing fluid from service company 2 was able to achieve minimum rheological requirements with a fewer stabilizer additives. This could be due to the high quality of the initial CMHPG polymer or due to the choice of individual dual crosslinker additives.

Fracturing Fluid 1	Additive	Concentration	Fracturing Fluid 2	Additive	Concentration
Linear gel	Seawater		Linear gel	Seawater	
	Biocide	0.5 lb/1,000 gal		Biocide	0.3 lb/1,000 gal
	CMHPG	45 lb/1,000 gal		CMHPG	45 lb/1,000 gal
	Acetic acid/acetate	0.2 gal/1,000 gal		Acetic acid/acetate	0.2 gal/1,000 gal
	Surfactant	2.5 gal/1,000 gal		Surfactant	2 gal/1,000 gal
	SI G	0.5 gal/1,000 gal		SI G	0.5 gal/1,000 gal
X-linker	Sodium thiosulfate	10 gal/1,000 gal	X-linker	Sodium thiosulfate	9 gal/1,000 gal
	Triethanolamine	6 gal/1,000 gal		Potassium carbonate/bicarbonate	Adjust to pH 9.3
	Tetraethylenepentamine	Adjust to pH 9.4		Zr Triethanolamine	1.1 gal/1,000 gal
	Dual crosslinker (Triethanolamine, sodiumtetraborate, zirconium dichloride oxide)	4 gal/1,000 gal		Potassium metaborate	0.5 gal/1,000 gal
Breaker	Bromate breaker	1 lb/1,000 gal	Breaker	Chlorous acid breaker	1 gal/1,000 gal
	Encapsulated Bromate breaker	3 lb/1,000 gal			

Table 6-7 Main chemical additives of the final seawater-based fracturing fluids.

Experimental results indicate that the presence of scale inhibitors negatively affected the performance of the fracturing fluid. **Fig. 6-14** shows that the addition of scale inhibitor F to the seawater-based fracturing fluid 1 resulted in apparent viscosity after 30 mins decrease from 600 to 300 and 50 cp when its concentrations were 0, 3 and 5 gpt, respectively. Similarly, scale inhibitor G also reduced the apparent viscosity.

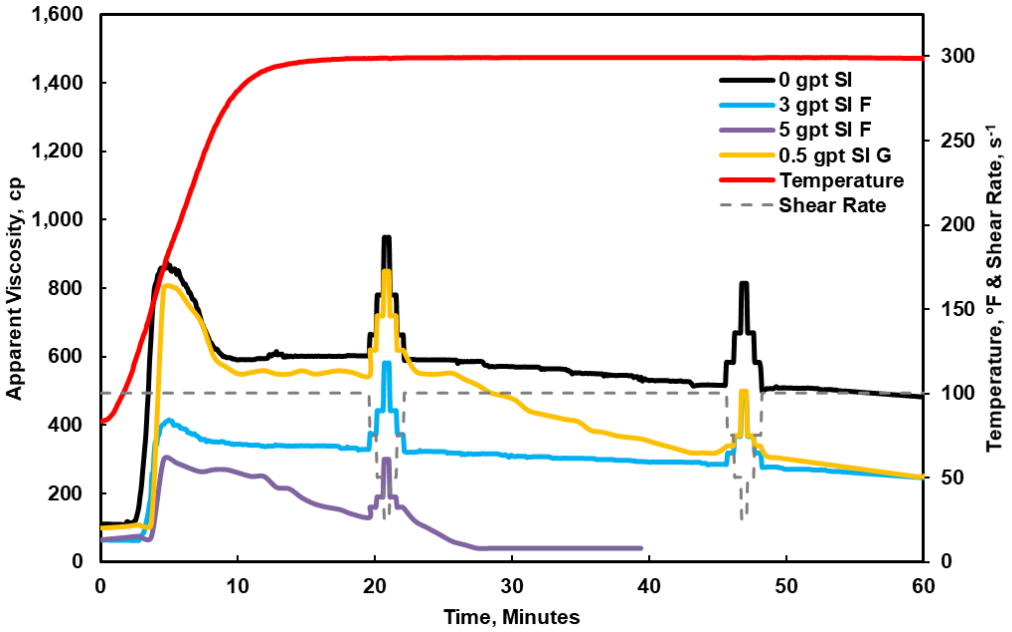

Fig. 6-14 Effect of scale inhibitors F and G on the apparent viscosity of seawater-based fracturing fluid 1.

Scale inhibitors and fracturing fluid are typically tested separately; for that reason, the difficulty of achieving a compatible crosslinker and scale inhibitor in the fracturing fluid formula is not well recognized. Once they are tested in combination, an obvious decline in both scale prevention and rheological performance is observed.

One solution is to pump prepad stages containing the scale inhibitor to minimize the viscosity drop in the wellbore and avoid a screen-out. Another solution is to add higher crosslinker concentrations to compensate for the viscosity drop (Levanyuk et al. 2012). The final solution includes going through a trial and error process to find an acceptable performance for both the scale inhibitor and crosslinker (Yue et al. 2014).

Wylde and Mahmoudkhani (2016) studied the interactions of scale inhibitors with zirconium crosslinkers and realized that the crosslinkers were causing a zirconium scale

to form. They concluded that this scale could influence the results of the traditional scale loop testing method. Alsaiari et al. (2016) did a thorough study with different polymeric and phosphonate based scale inhibitors using Green Laser Batch Experiments (GLBE). The tests indicated the formation of a zirconium scale that was identified as ZrO_2 nanoparticles in solution. They noted that the onset time for precipitation in solution varied depending on the scale inhibitor used.

Hurnaus and Plank (2015) showed that metallic crosslinkers generate metal oxide nanoparticles in solution (< 10 nm) and they are mainly what crosslinks the polymers, giving the viscosity increase. Based on all these studies, scale inhibitors can interact with crosslinkers and influence the size and dispersion properties of the generated ZrO_2 particles in solution, which in turn can influence the rheological performance. Alsaiary et al. (2016) also suggested that the scale inhibitors could perhaps adsorb on the generated particles temporarily, which could impair the intended function of the crosslinker and the scale inhibitor.

This information shows the importance of examining the scaling tendency of calcium sulfate scale with both the crosslinker and scale inhibitor additive in solution. **Fig. 6-15** highlights the scale inhibitor performance failure at 60:40 (seawater: UNC 3 formation brine) when soaked at 300°F. This test previously passed when the solution didn't include a crosslinker, however when it included crosslinker it could only prevent precipitation up to 270°F at SI concentration of 0.5 gpt.

a)

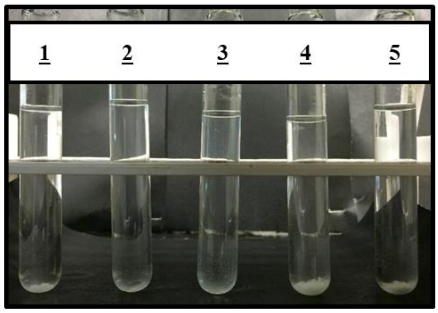

Tube #	Scale Inhibitor	Concentration, gpt	Observation
5	Blank	0	ppt
4	SI G	0.5	ppt
3	SI G	1	clear
2	SI F	5	clear
1	SI F	3	ppt

b)

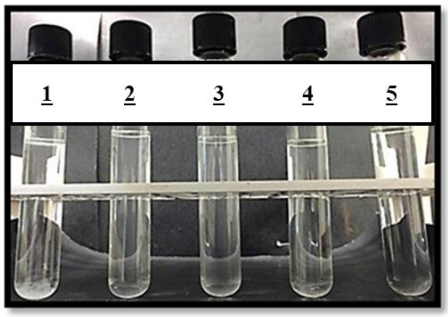

Tube #	Scale Inhibitor	Concentration, gpt	Observation
1	Blank	0	ppt
2	SI G	0.5	clear
3	SI G	1	clear
4	SI F	3	clear
5	SI F	5	clear

Fig. 6-15 Compatibility of seawater fracturing fluid (all additives except polymer) with UNC 3 formation brine at: a) 300 and b) 270°F. The tests were soaked for 24 hours with scale inhibitors F and G (60:40 seawater: formation brine).

Fig. 6-16 shows that the majority of the solutions remain scale free at 0.5 gpt SI G, 270-300°F, for 24 hours. Taking into consideration the cooling effect while pumping the fluids, this was acceptable (Agnew 1966). Following this, the finalized two formulas of seawater-based fracturing fluids were tested for rheological performance and maintained an apparent viscosity value above 100 cp at 100 s^{-1} for more than 1 hour at 250 and 300°F (**Figs. 6-17** to **6-21)**.

a)

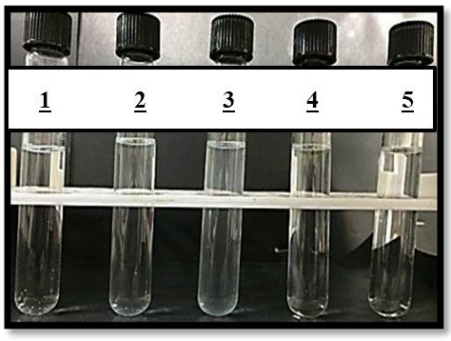

Tube#	Scale Inhibitor	Concentration, gpt	Observation
1	Blank	0	ppt
2	SI G	0.5	clear
3	SI G	1	clear
4	SI F	3	clear
5	SI F	5	clear

b)

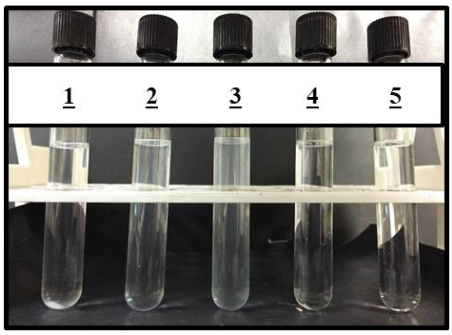

Tube#	Scale Inhibitor	Concentration, gpt	Observation
1	Blank	0	ppt
2	SI G	0.5	clear
3	SI G	1	clear
4	SI F	3	clear
5	SI F	5	clear

c)

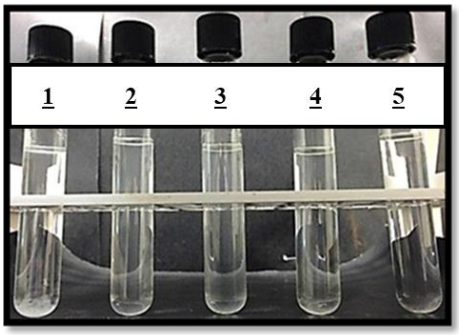

Tube#	Scale Inhibitor	Concentration, gpt	Observation
1	Blank	0	ppt
2	SI G	0.5	clear
3	SI G	1	clear
4	SI F	3	clear
5	SI F	5	clear

Fig. 6-16 Compatibility of seawater fracturing fluid (all additives except polymer) with: a) UNC 1 formation brine at 280°F, b) UNC 2 formation brine at 300°F, and c) UNC 3 formation brine at 270°F. The tests were left for 24 hours with scale inhibitors F and G (60:40 seawater: formation brine).

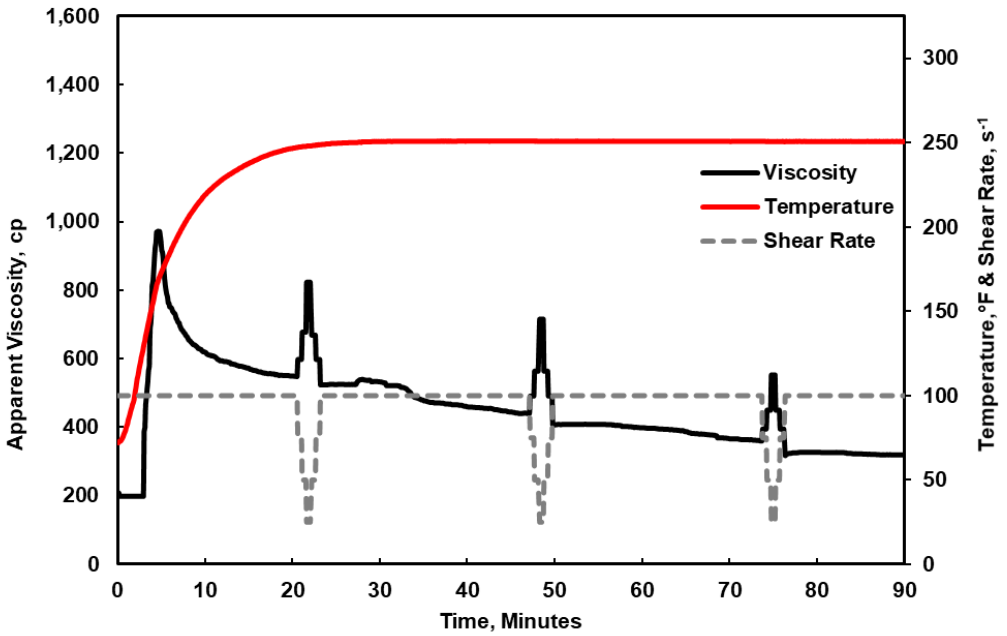

Fig. 6-17 Apparent viscosity of final seawater-based fracturing fluid 1 in the presence of 0.5 gpt SI G at 250°F.

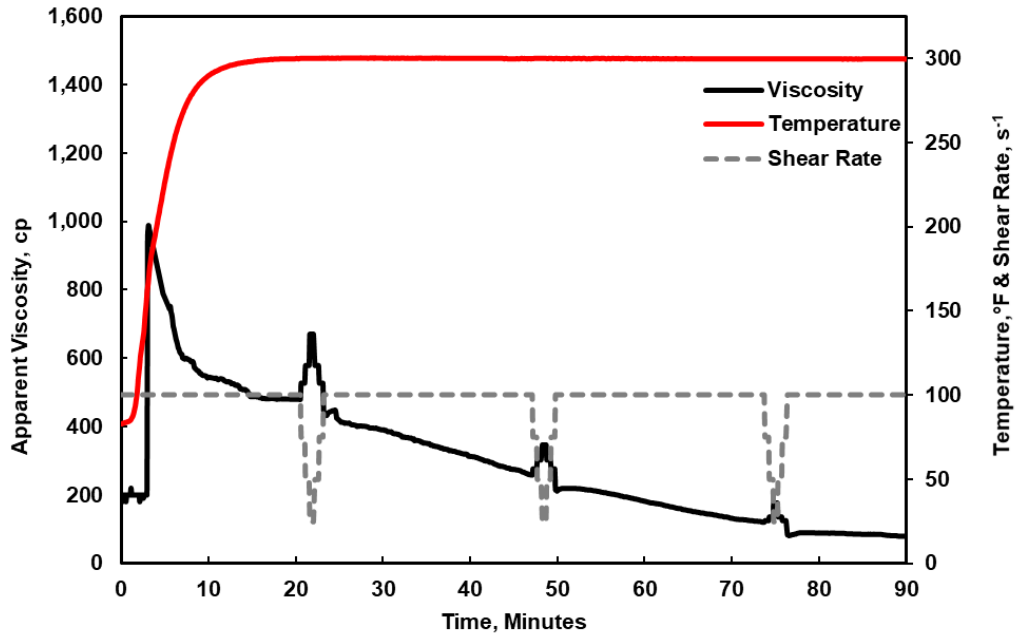

Fig. 6-18 Apparent viscosity of final seawater-based fracturing fluid 1 in the presence of 0.5 gpt SI G at 300°F.

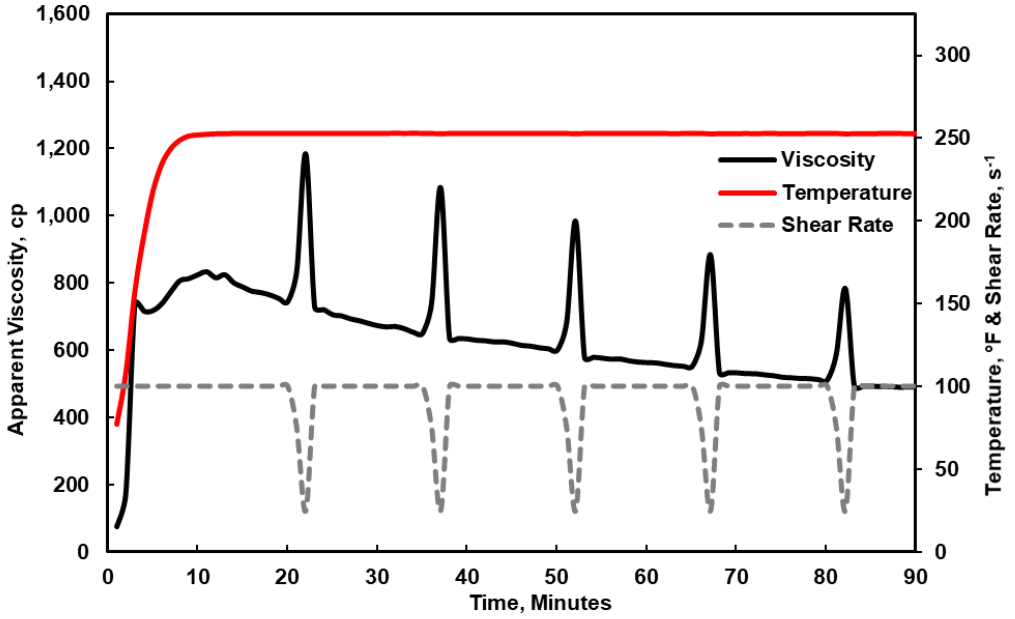

Fig. 6-19 Apparent viscosity of final seawater-based fracturing fluid 2 in the presence of 0.5 gpt SI G at 250°F.

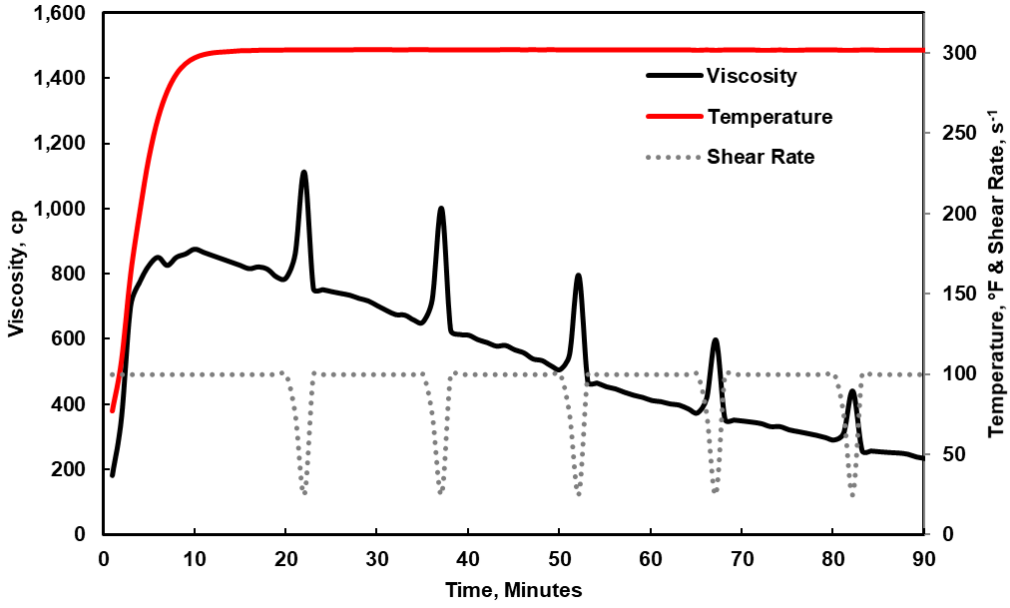

Fig. 6-20 Apparent viscosity of final seawater-based fracturing fluid 2 in the presence of 0.5 gpt SI G at 300°F.

Fig. 6-21 Seawater-based fracturing fluid 1: A) lipping at room temperature and B) lipping with 20/40 ceramic proppant loading of 5 ppg after heating at 200°F for 30 minutes.

These two systems were able to hold 5 lb/gal of 20/40 ceramic proppant at 200°F for nearly 30 minutes. Additionally, the apparent viscosity of both seawater-based fracturing fluid systems was determined in the presence of bromate breakers, (**Figs. 6-22** and **6-23)**. The apparent viscosity of broken seawater-based fracturing fluids 1 and 2 reached 50 cp after 70 and 110 minutes, respectively.

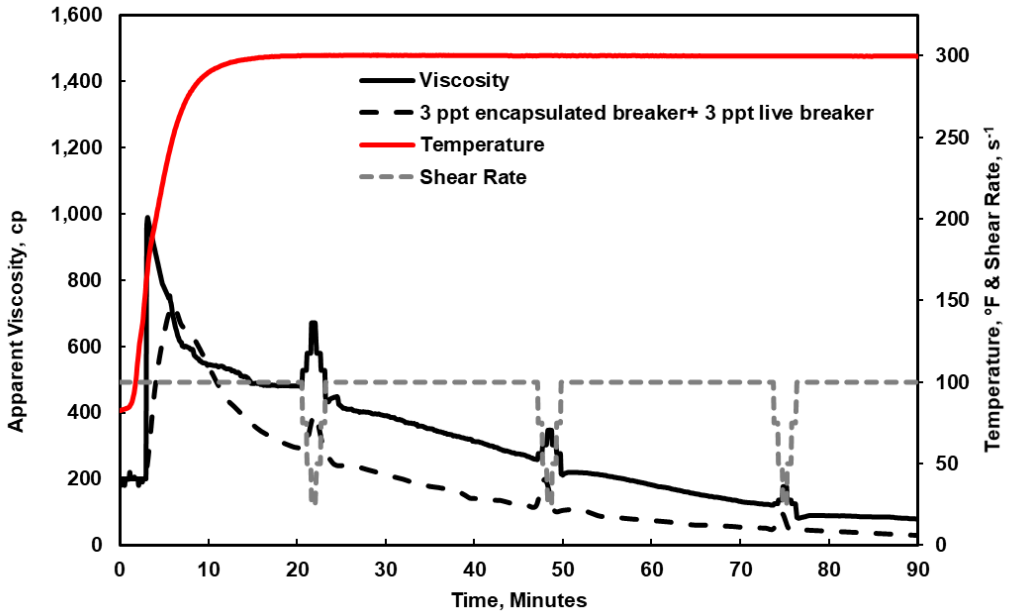

Fig. 6-22 Apparent viscosity of final seawater-based fracturing fluid 1 with bromate breakers at 300°F.

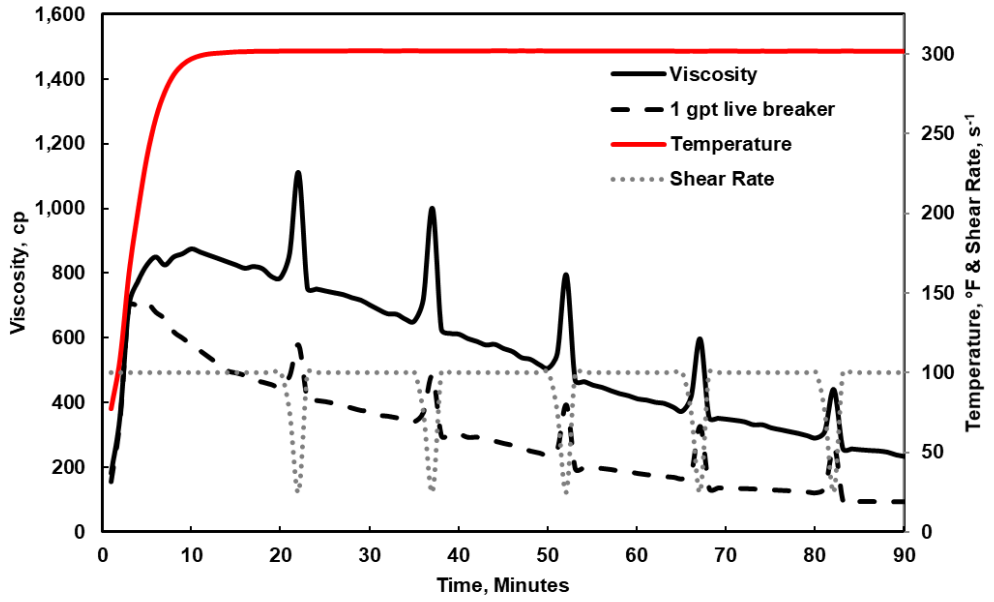

Fig. 6-23 Apparent viscosity profile of final seawater-based fracturing fluid 2 with bromate breaker at 300°F.

6.4.3. Zeta Potential and Retained Permeability

Zeta potential experiments were conducted to assess the fines migration tendency of clays present in core samples (Table 6-5 and 6-6). The potential for fines migration is mainly dependent on the changes in the clays' edge and surface charges. The measured zeta potential of any clay reflects the combined value for the surface and edge potentials. When zeta potential becomes high ($x < -20$) this change in the surface potentials produces a significant repulsive force, causing colloidal induced detachment of fines, also known as fines migration (Almubarak et al. 2015). In other words, increasing the zeta potential negatively at the particle surfaces will increase the repulsive colloidal forces, which triggers fines migration. **Fig. 6-24** shows the zeta potential of crushed core samples suspended in different water systems at 77°F.

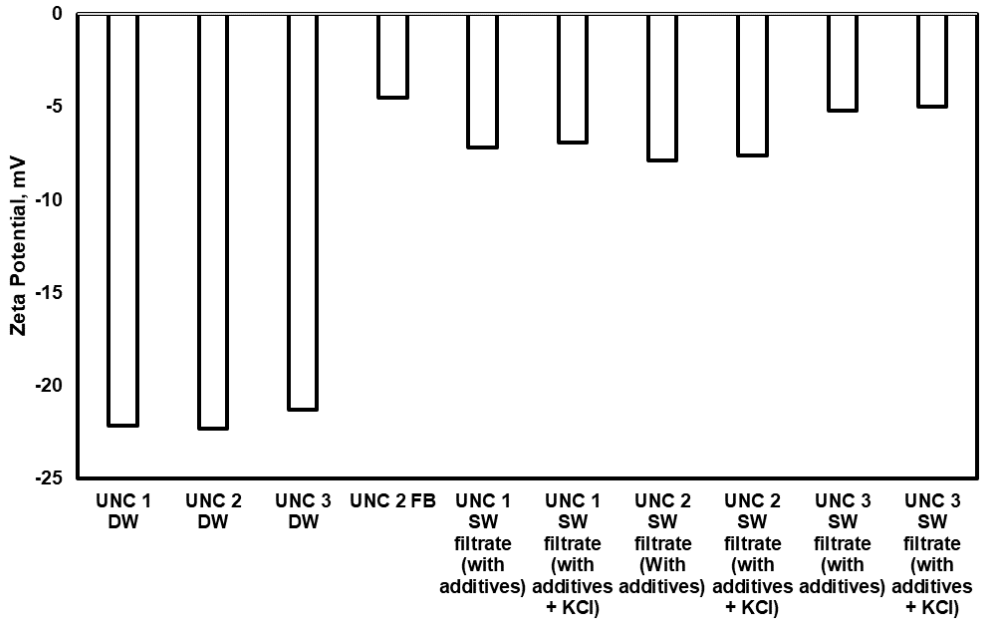

Fig. 6-24 Zeta potential of crushed core particles in DW: distilled water, FB: formation brine, SW: seawater, with all fracturing fluid additives (except polymer), and some with KCl (6 wt%) at 77°F.

The highest zeta potential was observed in the cores fine particles suspended in distilled water with values of nearly -23 mV, while the lowest zeta potential is observed in formation brine of -3 mV. Seawater-based fracturing fluid filtrate with and without clay stabilizer (6 wt% KCl) showed negative but close to neutral values which indicated clay charge stability.

One core from UNC 2 formation (Well-105 core plug #16) was injected with nearly 80 pore volumes of freshwater fracturing fluid filtrate (without clay stabilizer). As expected, the pressure drop across the core increased from nearly 13 to 20 psi due to lack of clay stabilizer, representing a permeability reduction of 35%, (**Fig. 6-25)**.

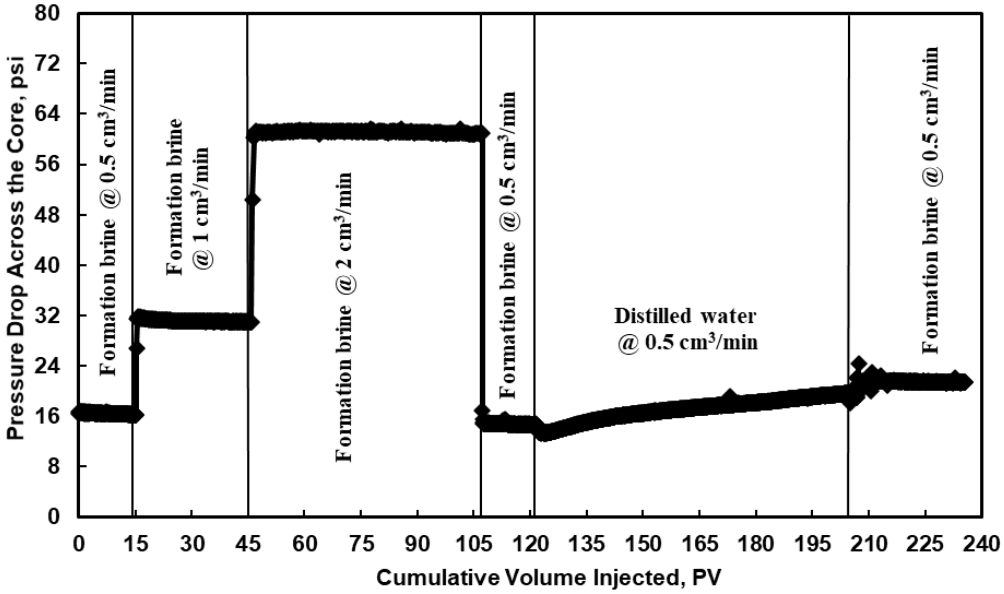

Fig. 6-25 Pressure drop across the core before and after distilled water injection at 300°F.

In contrast, 60 pore volumes of seawater-based fracturing fluid filtrate (without clay stabilizer) were injected into the core (well-51 core plug # 393), and no adverse effect

on permeability was observed. The pressure drop across the core remained at 16 psi before and after seawater injection (**Fig. 6-26)**.

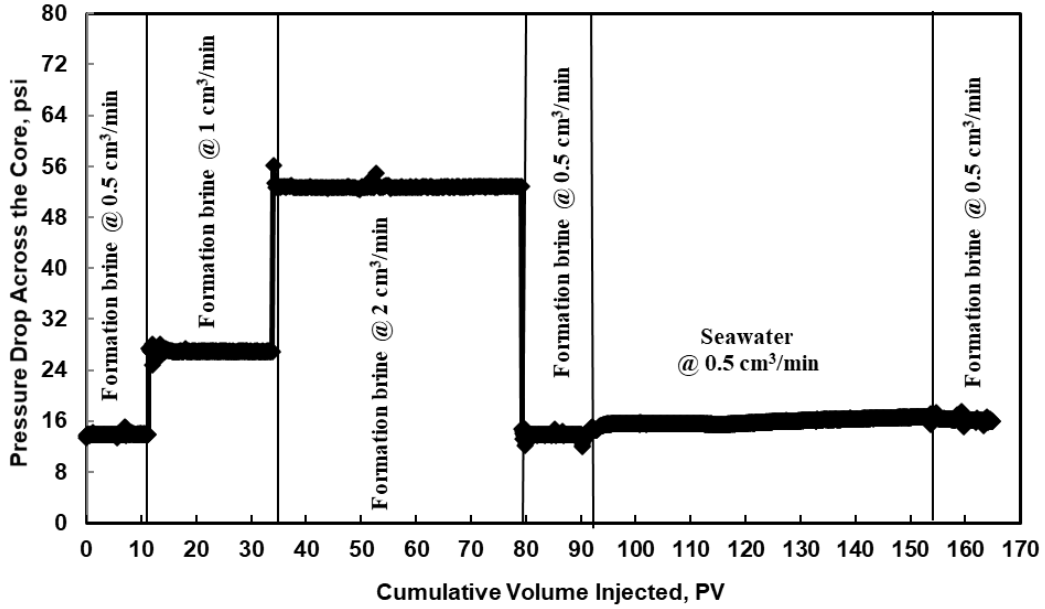

Fig. 6-26 Pressure drop across the core before and after seawater fracturing fluid filtrate injection at 300°F.

Based on the zeta potential and coreflood results, the salts available in seawater are sufficient to stabilize clays. For this reason, no clay stabilizer was included in the final formula.

6.4.4. Field Application

The above guidelines were followed in wells where high-temperature seawater fracturing fluid treatment was applied. The field operation included careful adjustments to the buffer additive volumes to ensure proper pH (~ 9.3 to 9.4) is achieved. Also, mixing the polymer was performed slowly and properly to prevent fish eyes.

The first raw seawater-based fracturing fluid treatment was applied in a multistage fracturing treatment consisting of 16 stages. The well was completed in an unconventional carbonate reservoir at 280°F (UNC 3), where the seawater-based fracturing fluid 1 formula (Table 6-7) was applied in the last stage. The fracturing fluid system was loaded with fiber and pumped with local 100 mesh sand in a highway fracturing pumping style. The treatment was risky due to the presence of fiber, which lowers the pH and weakens the gel strength. The treatment placed 230,000 lbs of sand, which was pumped at a maximum sand concentration of 4 ppg with no operational issues. The seawater fracturing fluid stage was evaluated and has shown an increase of about 8% in production compared to the fresh water stages in the same well. The seawater-based fluid was also able to carry 3% more proppant than the freshwater-based fluid due to the higher fluid density.

The raw seawater-based fracturing fluid formula was also applied in a single-stage acid fracturing job in a conventional carbonate formation at 300°F (**Fig. 6-27**). The treatment used the seawater fracturing fluid 2 formula (Table 6-7). The treatment consisted of 24 pumping stages, where the fracturing fluid was pumped first, followed by the emulsified acid, then a diverter. A closure fracture acid (CFA) was also used at the end of the treatment, followed by an overflush. The pumping rates ranged from 20-60 bpm as the stages progressed and was reduced to 10-15 bpm for the CFA and overflush. The pumping operation lasted 80 minutes with an average surface treating pressure of 6,500 psi and a maximum treating pressure of 11,500 psi. The operation was successful, and the results showed six times the expected production compared to similar wells treated with

freshwater-based fluids. Both field trials were successfully executed and paved the way for future raw seawater-based stimulation treatments.

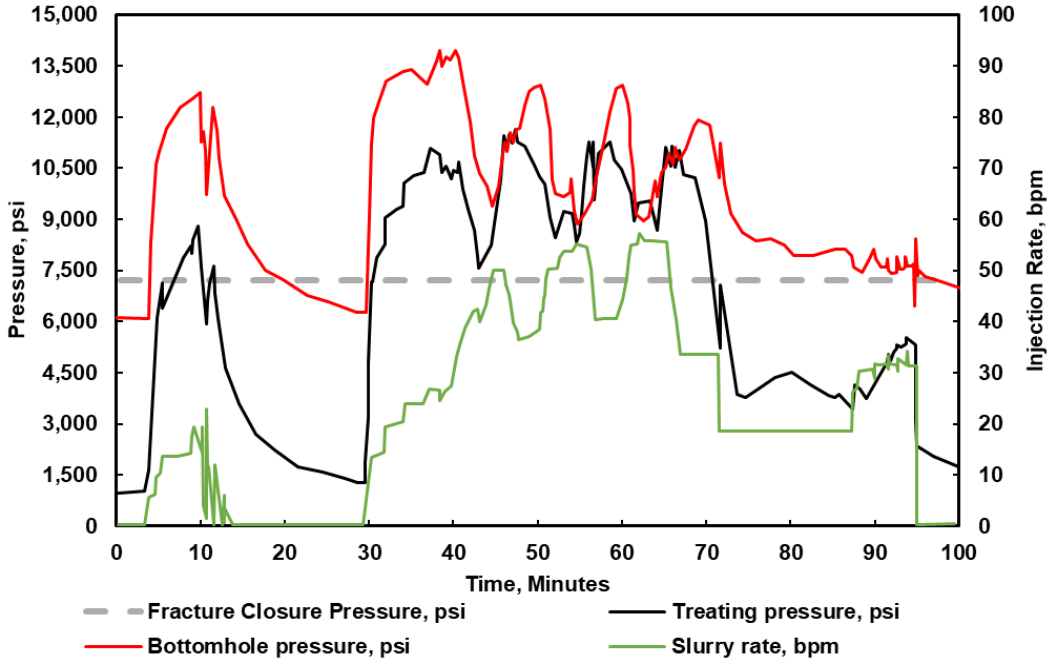

Fig. 6-27 Conventional carbonate well acid fracturing treatment pressure, bottomhole pressure, slurry rate recorded during the fracturing operation.

6.5. Conclusions

Several experiments, adjustments, and design iterations were conducted to tailor seawater-based fracturing fluids for field application. These fluids were designed to achieve rheological properties such that they can carry and transport proppant under dynamic and static conditions despite the direct incompatibility challenge between scale inhibitors and metallic crosslinkers. Also, these final formulas were developed such that no scale forms when the fracturing fluid filtrate is mixed with different formation brines. Most importantly, they were designed to utilize raw seawater pipelines without any further treatments.

Based on this study, the following conclusions were drawn:

1. The success of formulating a high temperature seawater-based fracturing fluid heavily relies on the compatibility between metal crosslinkers and scale inhibitors.

2. Calcium sulfate scale precipitation is severe at 300°F; scale inhibitors must be incorporated when seawater is used.

3. Strong base additives should be replaced by buffers at 300°F.

4. Seawater contains sufficient salts to keep up to 8 wt% clays stable, which eliminates the need for clay stabilizers at these conditions.

5. Differences between buffer additive types, gel stabilizers, crosslinking delay additives and high-temperature stabilizers require more attention; when properly understood, they can be used in various combination to further enhance the fracturing fluid thermal stability.

This work discusses the challenges associated with developing a scale-free raw seawater-based fracturing fluid, and provides the industry with the procedure to overcome these challenges and produce a successful fracturing fluid. Several field treatments utilized the newly developed seawater-based fracturing fluid formula, which resulted in successful field trials in an unconventional and a conventional carbonate formation.

6.6. Acknowledgements

The authors appreciate and thank Abdulaziz AlGhamdi for his hard work in all the compatibility tests. Also, the authors would like to thank Ibrahim Al-Hulail, Ibrahem Al Shomli, and Prasad Karadkar for their support in refining the developed recipes.

6.7. References

Abdulmajid, A., Hansen, J., Al-Dahlan, M. et al. 2017. Seawater Based Fracturing Fluid: A Game Changer in Hydraulic Fracturing Applications in Saudi Arabia. Presented at SPE Middle East Oil & Gas Show and Conference, 6-9 March, Manama, Kingdom of Bahrain, March 6-9. SPE-184015. http://doi:10.2118/184015-MS.

Acartürk, F. and Celkan, A. 2009. Comparison of Guar Gum from Different Sources for the Preparation of Prolonged-Release or Colon-Specific Dosage Forms. *Pharmaceutical Development & Technology*. **14** (3): 271-277. http://doi.org/10.1080/10837450802572375.

Agnew, B. 1966. Evaluation of Fracture Treatments with Temperature Surveys. *SPE J*. **18** (7): 892-898. SPE-1287-PA. http://doi.org/10.2118/1287-PA.

AlMubarak, T., AlDajani, O. and AlMubarak, M. 2015. A Collective Clay Stabilizers Review. International Petroleum Technology Conference, Doha, Qatar, 6-9 December. SPE-18394. http://doi.prg/10.2523/IPTC-18394-MS.

AlMubarak, T., Ng, J., and Nasr-El-Din, H. A. 2017. Chelating Agents in Productivity Enhancement: A Review. Presented at SPE Oklahoma Oil and Gas Symposium, Oklahoma City, OK, USA, March 27-31. SPE-185097-MS. http://doi.org/10.2118/185097-MS.

Al-Muntasheri, G. 2014. A Critical Review of Hydraulic-Fracturing Fluids for Moderate- to Ultralow-Permeability Formations over the Last Decade. *SPE Prod & Oper* **29** (4): 243-260. SPE-169552-PA. http://doi.org/10.2118/169552-PA.

Alohaly, M., BinGhanim, A., Rahal, R. et al. 2016. Seawater Fracturing Fluid Development Challenges: A Comparison between Seawater-Based and Freshwater-Based Fracturing Fluids Using Two Types of Guar Gum Polymers. Presented at SPE Kingdom of Saudi Arabia Annual Technical Symposium and Exhibition, Dammam, Saudi Arabia, April 25-28. SPE-182799. http://doi:10.2118/182799-MS.

Alsaiari, H., Al-Khaldi, M., Al-Taie, I. et al. 2016. Effect of Crosslinkers on the Performance of Calcium Sulfate Scale Inhibitors at High-Temperature: Impact of Zirconium. Presented at the SPE International Oilfield Scale Conference and Exhibition, Aberdeen, Scotland, UK, 11-12 May. SPE-179878-MS. http://doi.org/10.2118/179878-MS.

Aminto, A., and Olson, M. 2012. Four-Compartment Partition Model of Hazardous Components in Hydraulic Fracturing Fluid Additives. *J Natural Gas Science and Engineering* **7** (1): 16-21.

Bin Merdhah, A. 2010. Inhibition of Calcium Sulfate and Strontium Sulfate Scale in Waterflood. *SPE Prod & Oper* **24** (4): 545-552. SPE-141168-PA. http://doi.org/10.2118/141168-PA.

BinGhanim, A., Al-Hussain, A., Karadkar, P. et al. 2017. High-Temperature Fracturing Fluid Based on Nanofiltered Seawater. Presented at SPE Kingdom of Saudi Arabia Annual Technical Symposium and Exhibition, Dammam, Saudi Arabia, April 24-27. SPE-189048. http://doi:10.2118/189048-MS.

BinGhanim, A., Chen, T., Al-Ohaly, M. et al. 2017. Scale Mitigation Strategy for Fracturing Using Seawater-Based Fluid. Presented at SPE Kingdom of Saudi Arabia

Annual Technical Symposium and Exhibition, Dammam, Saudi Arabia, April 24-27. SPE-188029. http://doi:10.2118/188029-MS.

Bock, E. 1961. On the Solubility of Anhydrous Calcium Sulphate and of Gypsum in Concentrated Solutions of Sodium Chloride at 25°C, 30°C, 40°C, and 50°C. *Canadian J Chemistry* **39** (9): 174-175.

Das, P., Konale, S., and Kothamasu, R. 2014. Effect of Salt Concentration on Base-gel Viscosity of Different Polymers used in Stimulation Fluid Systems. Presented at the SPE/EAGE European Unconventional Resources Conference and Exhibition, Vienna, Austria, 25-27 February. SPE-167786-MS. http://doi.org/10.2118/167786-MS.

Elsarawy, A., Nasr-El-Din, H. and Cawiezel, K. 2018. Compatibility and Rheology of High-pH Borate Gels Prepared with Produced Water for Hydraulic-Fracturing Applications. *SPE Prod & Oper* **33** (2): 179-195. SPE-185983-PA. http://doi.org/10.2118/185953-PA.

Fan, C., Kan, A., Fu, G. et al. 2010. Quantitative Evaluation of Calcium Sulfate Precipitation Kinetics in the Presence and Absence of Scale Inhibitors. *SPE J.* **15** (4): 977-988. SPE-121563-PA. http://doi.org/10.2118/121563-PA.

Farooqui, N., Grice, A., Sorbie, K. et al. 2014. Polyphosphino Carboxylic Acid (PPCA) Scale Inhibitor for Application in Precipitation Squeeze Treatments: The Effect of Molecular Weight Distribution. Presented at the NACE International Corrosion Annual Conference and Exposition, San Antonio, TX, March 9-13. NACE-2014-4100.

Gupta, D., Carman, P., and Nguyen, S. 2018. Novel Chelation Opens the Door for Redeployment of Sea Water Based Fracturing Fluids in High Temperature Wells. Presented at SPE International Conference and Exhibition on Formation Damage Control, Lafayette, LA, USA, February 7-9. SPE-189543. http://doi.org/10.2118/189543-MS.

Harris, P., and van Batenburg, D. 1999. A Comparison of Freshwater- and Seawater-Based Borate-Crosslinked Fracturing Fluids. SPE International Symposium on Oilfield Chemistry, 16-19 February, Houston, Texas. SPE-50777-MS.

Hurnaus, T. and Plank, J. 2015. Crosslinking of Guar and HPG Based Fracturing Fluids Using ZrO_2 Nanoparticles. SPE International Symposium on Oilfield Chemistry, The Woodlands, TX, USA, 13-15 April. SPE-173778-MS. http://doi.org/10.2118/173778-MS.

ISO 13503-1, 2011. Petroleum and natural gas industries-Completion fluids and materials-Part 1, Measurement of viscous properties of completion fluids, second edition. Geneva, Switzerland: ISO.

Kelland, M. 2014. *Production Chemicals for the Oil and Gas Industry*, Second Edition, Chapman and Hall/CRC Press, Boca Raton, FL.

Lee, D., Herman, J., Elsworth, D. et al. 2011. A Critical Evaluation of Unconventional Gas Recovery from the Marcellus Shale, Northeastern United States. *K S C E J Civil Engineering* **15** (4): 679-687.

Levanyuk, O., Overin, A., Sadykov, A. et al. 2012. A 3-Year Results of Application a Combined Scale Inhibition and Hydraulic Fracturing Treatments using a Novel

Hydraulic Fracturing Fluid, Russia. Presented at the SPE International Conference on Oilfield Scale, Aberdeen, UK, 30-31 May. SPE-155243-MS. http://doi.org/10.2118/155243-MS.

Li, L., Al-Muntasheri, G., Lian, F. 2016. A Review of Crosslinked Fracturing Fluids Prepared with Produced Water. Petroleum. 2 (4): 313- 323. http://doi.org/10.1016/j.petlm.2016.10.001.

Li, L., Qu, Q., Sun, H. et al. 2015. How Extremely High-TDS Produced Water Compositions Affect Selection of Fracturing Fluid Additives. Presented at SPE International Symposium on Oilfield Chemistry, The Woodlands, TX, USA, 13-15 April. SPE-173746-MS. http://doi.org/10.2118/173746-MS.

Lu, H., Kan, A., Zhang, P. et al. 2012. Phase Stability of Calcium Sulfate in the System NaCl/Monoethylene Glycol/Water. *SPE J.* **17** (1): 187-197. SPE-130697-PA. http://doi.org/10.2118/130697-PA.

Moghadasi, J., Jamialahmadi, M., Müller-Steinhagen, H. et al. 2003. Scale Formation in Iranian Oil Reservoir and Production Equipment during Water Injection. Presented at the SPE International Symposium on Oilfield Scale, Aberdeen, UK, 29-30 January. SPE-80406-MS. http://doi.org/10.2118/80406-MS.

New York State Department of Environmental Conservation (NYSDEC). 1992. Chapter 9: Drilling Phase: Drilling, Casing and Completion Operations. Draft Generic Environmental Impact Statement on the Oil, Gas, and Solution Mining Regulatory Program. Albany, New York. 52 pages.

New York State Department of Environmental Conservation (NYSDEC). 2011. Preliminary Revised Draft Supplemental Generic Environmental Impact Statement on the Oil, Gas, and Solution Mining Regulatory Program. Well Permit Issuance for Horizontal Drilling and High-Volume Hydraulic Fracturing to Develop the Marcellus Shale and Other Low-Permeability Gas Reservoirs. Albany, New York. 1,095 pages.

Nicot, J., and Scanlon, B. 2012. Water use for Shale-gas Production in Texas, U.S. *Environmental Science and Technology* **46** (6): 3580-3586.

Pitzer, K. 1977. Electrolyte Theory-Improvements since Debye and Huckel. *Act. Chem. Res.* **10** (10): 371-377. http://doi.org/10.1021/ar50118a004.

Ramsdell, L. and Partridge, E. 1929. The Crystal Forms of Calcium Sulfate. *J American Mineralogist.* **14** (1): 59-74.

Reinicke, A., 2010. Mechanical and Hydraulic Aspects of Rock–Proppant Systems — Laboratory Experiments and Modelling Approaches. Doctoral Thesis, Universitat Potsdam, Potsdam, Germany.

Shen, D., Shcolnik, D., Perkins, R. et al. 2012. Evaluation of Scale Inhibitors in Marcellus High-Iron Waters. Oil and Gas Facilities, *SPE J* **1** (5): 34-42. SPE-141145-PA. http://doi.org/10.2118/141145-PA.

Tung, N., Phong, N., Long, B. et al. 2004. Scale Inhibitors for Co-Deposited Calcium Sulfate and Calcium Carbonate in Squeeze Process in White Tiger Oilfield. Presented at the SPE International Symposium on Oilfield Scale, Aberdeen, UK, May 26-27. SPE-87467-MS. http://doi.org/10.2118/87467-MS.

Vengosh, A., Jackson, R., Warner, N. et al. 2014. A Critical Review of the Risks to Water Resources from Unconventional Shale Gas Development and Hydraulic Fracturing in the United States. *Environmental Science and Technology*. ***48*** (15): 8334-8348.

Wylde, J. and Mahmoudkhani, A. 2016. Development of a Scale Inhibitor for Zr-Crosslinked Seawater Systems: A Case History of Successful Testing to Failure and Field Applications. Presented at the SPE International Oilfield Scale Conference and Exhibition, Aberdeen, Scotland, UK, 11-12 May. SPE-179881-MS. http://doi.org/10.2118/179881-MS.

Yamak, R., Nasr-El-Din, H., Rahim, S. et al. 2018. Rheology Studies of Crosslinked Fracturing Fluids Utilizing Seawater. Presented at SPE Kingdom of Saudi Arabia Annual Technical Symposium and Exhibition, Dammam, Saudi Arabia, April 23-26. SPE-192275. http://doi:10.2118/192275-MS.

Yue, Z., Fu, Q., Lang, N. et al. 2014. Liquid Scale Inhibitors for Metallic-Crosslinked Gel Fracturing Systems. SPE International Oilfield Scale Conference and Exhibition, Aberdeen, Scotland, 14-15 May. SPE-169806-MS. http://doi.org/10.2118/169806-MS.